INVESTIGATION AND OPTIMISATION OF COMMERCIAL REFRIGERATION CYCLES USING THE NATURAL REFRIGERANT CO_2

A thesis submitted for the degree of Doctor of Engineering

By

Jason Alexander Shilliday

Supervised by Professor Savvas Tassou

School of Engineering and Design, Brunel University

October 2012

Abstract

With tighter regulations on the use of Hydroflurocarbons (HFCs) due to their high GWP (Global Warming Potential), many supermarket operators are looking for alternative refrigerants. To contribute to this, the objectives of this thesis are to investigate the practicality, environmental benefits and economic viability of an all-CO_2 transcritical refrigeration system suitable for small supermarkets. Whilst the environmental benefits of using CO_2 as a refrigerant are clear, there is rather limited practical and technical knowledge on the design and operation of these systems.

In this work, simulation models of a transcritical 'booster' CO_2 refrigeration system have been developed to investigate and evaluate its performance against that of a traditional HFC system. The models were verified using test results from an experimental CO_2 system built at Brunel University. To evaluate the performance of the CO_2 refrigeration system in the field, energy data from a real supermarket employing a HFC refrigeration system was used for energy simulations. The results demonstrate that the annual energy consumption of the CO_2 refrigeration system in a small supermarket in Northern Ireland would be equivalent to that of a typical HFC refrigeration system. However, the low GWP of CO_2 will result in a 50% reduction in the combined direct and indirect CO_2 emissions over the operational life of the system assuming an annual leakage rate of 15%. Northern Ireland has a high number of small supermarkets due to its rural population, approximately 615. The CO_2 system presented in this research could replace the existing R404A systems in these small supermarkets resulting in emissions reduction of up to 188,752 tCO_2e.

This research has developed selection techniques and criteria to be considered by supermarket designers and operators when developing national strategies for the eventual phase-out of HFC refrigerants in all supermarket sizes. The validated simulation models developed in this research combined with the detailed geographical and refrigeration load ratio analysis presented, will provide valuable information that will assist system designers and operators in the efficient design and optimisation of CO_2 technology for small supermarkets.

Contents

List of Figures

List of Tables

Abbreviations

GWP	Global Warming Potential
ODP	Ozone Depletion Potential
COP	Coefficient of Performance
CFC	Chlorofluorocarbons
HCFC	Hydrochlorofluorocarbons
HFC	Hydrofluorocarbons
HC	Hydrocarbons
GHG	Green house gas
UNFCC	United Nations Framework on Climate Change
EES	Engineering Equation Solver
LT	Low temperature
MT	Medium temperature
HT	High Temperature

Refrigerants

R40	Methyl Chloride	CH_3Cl
R744	Carbon Dioxide	CO_2
R290	Propane	C3H8
R717	Ammonia	NH_3
R11	Trichlorofluoromethane	CCl_3F
R12	Dichlorodifluoromethane	CCl_2F_2
R22	Chlorodifluoromethane	$CHClF_2$
R32	Difluoromethane	CH_2F_2
R113	1,1,2-Trichlorotrifluoroethane	$C_2F_3Cl_3$
R114	1,2-Dichlorotetrafluoroethane	$C_2F_4Cl_2$
R125	Pentafluoroethane	C_2HF_5
R134a	1,1,1,2-Tetrafluoroethane	$C_2H_2F_4$
R407c	R-32/R-125/R-134a (23/25/52)	
R404a	R-125/R-143a/R-134a (44/52/4)	
R410a	R-32/R-125 (50/50)	

Nomenclature

Chapter 2

COP	Coefficient of performance	
h	Enthalpy	(kJ/kg)
Q	Cooling capacity	(kW)
W	Work input	(kW)

Chapter 3

α_o	Air side heat transfer coefficient	(W/m^2.K)
α_{do}	Dry out flow heat transfer coefficient	(W/m^2.K)
α_{mist}	Mist out flow heat transfer coefficient	(W/m^2.K)
α_r	Refrigerant side heat transfer coefficient	(W/m^2.K)
α_{tp}	Two phase flow heat transfer coefficient	(W/m^2.K)
ΔT_{lm}	Log mean temperature difference	(K)
ε	Void fraction	
η_{is}	Isentropic efficiency	
η_{IHX}	Internal heat exchanger efficiency	
η_o	Fin efficiency	
ρ	Density	(kg/m^3)
ρ_F	Liquid density	(kg/m^3)
ρ_V	Vapour density	(kg/m^3)
λ_t	Thermal conductivity of tube wall	(W/m^2.K)
A_i	Internal surface area	(m^2)
A_O	Outside surface area	(m^2)
Cp_a	Air specific heat capacity	(J/kg.K)
D_i	Internal diameter	(m)
D_o	Outside diameter	(m)
f	Friction factor	
f_L	Liquid phase friction factor	
f_V	Vapour phase friction factor	
F	Fin pitch	(m)
G	Mass flux	(kg/s.m^2)
G_a	Air mass flux	(kg/s.m^2)
h	Enthalpy	(kJ/kg)
h_{is}	Isentropic enthalpy compression	(kJ/kg)
h_{HPVin}	High pressure valve in enthalpy	(kJ/kg)

h_{HPVout}	High pressure valve out enthalpy	(kJ/kg)
h_r	Refrigerant enthalpy	(kJ/kg)
j	Colburn j-factor	
L	Length	(m)
$\dot{m}$	Refrigerant mass flow rate	(kg/s)
$\dot{m}_a$	Air mass flow rate	(kg/s)
$\dot{m}_{LT}$	Low temperature evaporator mass flow rate	(kg/s)
$\dot{m}_{LP}$	Low pressure compressor mass flow rate	(kg/s)
$\dot{m}_{HP}$	High pressure compressor mass flow rate	(kg/s)
$\dot{m}_{MT}$	MT evaporator mass flow rate	(kg/s)
N	Number of tubes	
P	Pressure	(bar)
P_{HPVin}	High pressure valve in pressure	(bar)
P_{HPVout}	High pressure valve out pressure	(bar)
P_{GCopt}	Optimum gas cooling pressure	(bar)
P_r	Receiver pressure	(bar)
Pr	Prandtl number	
q_{potn}	Maximum heat transfer capacity	(kW)
Q	Cooling capacity	(kW)
Q_{HT}	High temperature evaporator cooling capacity	(kW)
Q_{LT}	Low temperature evaporator cooling capacity	(kW)
Re	Reynolds number	
Re_{Dh}	Reynolds number based on hydraulic diameter	
T_a	Air temperature	(°C)
T_{amb}	Ambient temperature	(°C)
T_{GC}	Gas cooling temperature	(°C)
T_{GCapr}	Gas cooling approach temperature	(°C)
U	Overall heat transfer coefficient	($W/m^2.K$)
W_{HP}	High pressure compressor work input	(kW)
W_{LP}	Low pressure compressor work input	(kW)
X	Refrigerant vapour quality	
X_{di}	Refrigerant vapour quality at dry out inception	
X_{de}	Refrigerant vapour quality at dry out completion	

Chapter 4

N_{years}	Number of years	
m_{ref}	Mass of refrigerant in cycle	(kg)
α_{rec}	End of life refrigerant recovery	(%)

LE_{annual}	Annual refrigerant leakage rate	(%)
β	CO_2 emissions rate of electricity generation	(kg CO_2 / kWh)
E	Annual energy use	(kWh)

Chapter 6

$\dot{m}$	Refrigerant mass flow rate	(kg/s)
$\dot{V}_{swept}$	Swept volume	(m^3/h)
ρ_{suc}	Suction density	(kg/m^3)
η_{vol}	Volumetric efficiency	(kg/m^3)
$\dot{m}_r$	Refrigerant mass flow rate	(kg/s)
$\dot{m}_a$	Air mass flow rate	(kg/s)
h_a	Air enthalpy	(kJ/kg)
h_r	Refrigerant enthalpy	(kJ/kg)

Chapter 7

N_{years}	Number of years	
m_{ref}	Mass of refrigerant in cycle	(kg)
α_{rec}	End of life refrigerant recovery	(%)
LE_{annual}	Annual refrigerant leakage rate	(%)
β	CO_2 emissions rate of electricity generation	(kg CO_2 / kWh)
E	Annual energy use	(kWh)

Acknowledgements

Firstly I would like to thank my academic supervisor Professor Savvas Tassou for all his help and guidance throughout this project. I am very grateful and I hope to continue working with him and Brunel University on further industrial collaborations. I would also like to thank INyoman Suamir at Brunel University for all his help building and making adjustments to the experimental system. The experiments would not have been as successful without his excellent practical engineering abilities. I would also like to give a special thanks to Professor Maria Kolokotroni who initiated my interest in research at Brunel University during my MSc.

This research would not have been possible without the support from the industrial sponsor Shilliday refrigeration. In particular I would like to thank Norman Shilliday and Liam Walsh at Shillidays, whom without their initial vision, encouragement and support this research would not have been possible.

I would like to thank my wife Pier for all her support and in particular her patience during this project and also my parents Alex and Roberta for their support.

Finally I would like to thank all my friends who I have met during the modules at Brunel and Surrey, in particular Stafford, Carlos and Helen.

This research has been funded by the Engineering and Physical Sciences Research Council and Shilliday Refrigeration, to whom I would like to extend my gratitude and acknowledge their support.

Executive Summary

Introduction

Hydroflurocarbon (HFC) refrigerant leakages from supermarket refrigeration systems can have a detrimental effect on the environment due to their high global warming potential (GWP). Supermarket operators are under increasing environmental pressures through legislation such as the Kyoto and Montreal protocols to reduce this effect. While the leaks can be reduced by enforcing containment and regular leak checks, a better solution might be to replace the current HFC refrigerants with refrigerants that have a much lower GWP. CO_2 (Carbon Dioxide) has a GWP of 1 (BSI, 2010), which is much lower than the GWP of the common supermarket HFC refrigerant R404A which has a GWP of 3780 (BSI, 2010). CO_2 has also excellent thermo physical and heat transfer properties and a much higher vapour density than R404A resulting in a greater volumetric refrigeration effect. This offers the advantage of smaller and lighter equipment for a given refrigeration load. However, CO_2 operates at much higher pressures than HFC refrigerants and has a much lower critical temperature resulting in supercritical gas cooling when ambient temperatures approach its critical temperature of 31.1°C. This results in a transcritical cycle and provides significant design operation and control challenges. A way to avoid operation at transcritical conditions is to couple the CO_2 refrigeration system with a more conventional system in a cascade arrangement to provide the heat rejection. This introduces complexities, cost and the need to have different systems for chilled and frozen food applications. The preferred solution for smaller supermarkets and convenience stores might be a single system that can satisfy both the chilled and frozen food needs, a transcritical CO_2 system with a 'booster' compressor for Low Temperature (LT) refrigeration. The 'booster' compressor would be integrated into the existing Medium Temperature (MT) cycle so the whole system uses CO_2 as the refrigerant, avoiding the use of the complex and expensive cascade cycle for smaller systems. The integration of an LT 'booster' compressor into an existing MT transcritical CO_2 cycle would decrease the compression ratio of the LT compressor, increasing the efficiency of the MT and LT

combined cycle as a whole. This all-CO_2 cycle could offer a potential solution, as a replacement to high GWP HFC refrigeration systems for small supermarkets and will be investigated in this thesis.

This project aims to make a significant input in this international research and development effort on the design, investigation and development of efficient transcritical CO_2 systems for retail food applications.

To date, there have been numerous CO_2 installations, mainly in large supermarkets, where the additional cost of the systems can be more easily justified. There are however, a large number of smaller supermarkets where an economical and practical solution is still in its infancy. Other research in this area has detailed the high heat transfer coefficient of CO_2 at low vapour qualities and the use of single circuits in a CO_2 evaporator as opposed to multiple circuits. The optimisation of the evaporator circuitry and geometry specifically for CO_2 avoiding refrigerant mal-distribution could lead to increased heat transfer, simplifying the evaporator and reducing material use and costs. The reported high heat transfer of CO_2 at low vapour qualities could also be utilised by supplying a low quality vapour directly to the evaporator, increasing heat transfer. To date, supermarket installations have been using standard HFC evaporators, not optimised for CO_2.

Aims and Objectives

The aim of this research was to investigate the practicality, economic viability and environmental benefits achievable from the creation of an all CO_2 transcritical cycle, avoiding the use of the cascade cycle and HFCs, suitable for small supermarkets. The CO_2 booster cycle is a single circuit dual temperature transcritical CO_2 cycle which uses a traditional transcritical CO_2 cycle for the medium temperature load with a booster compressor for the low temperature load.

Whilst the environmental benefits of using CO_2 as a refrigerant are clear, there is a lack of both practical and technical knowledge on using and designing these refrigeration systems. This research aims to assist both supermarket operators and

design engineers in the uptake of CO_2, replacing HFCs as refrigerants used in supermarkets. To help meet this aim the following objectives have been set:

- Develop a numerical model to predict the annual electricity consumption and other operational parameters of a CO_2 refrigeration system and a R404A refrigeration system including pressures, temperatures and refrigerant flow rates. Compare and discuss the results of each model including the annual electricity consumption and direct and indirect CO_2 emissions.

- Develop a numerical model to predict the performance of an evaporator coil specifically designed and optimised for CO_2.

- Perform controlled tests on an experimental CO_2 refrigeration system. Use experimental test results to verify and optimise the numerical model of the CO_2 refrigeration system.

- Use the verified numerical model to investigate the performance of a CO_2 refrigeration system in a real small supermarket currently using a R404A refrigeration system.

- Test and compare the performance of the CO_2 refrigeration system at different locations around the UK with different refrigeration capacities. Compare both the environmental impact and annual electricity consumption of the refrigeration systems and identify the impact of the location and weather conditions as well as low temperature and medium temperature refrigeration loads on a CO_2 refrigeration system performance.

Summary of research

A review of the literature has revealed a resurgent interest in the use of CO_2 as a refrigerant in supermarket refrigeration systems. There has been a significant growth of CO_2 based systems in the UK with all of the major supermarkets having trialled systems and some planning a number of future installations. The large variety of commercial and experimental systems using CO_2 in a subcritical and transcritical

cycle were also reviewed. There have been many installations using CO_2 across the UK for the larger supermarkets and superstores but only a small number of installations in small supermarkets. An appropriate CO_2 refrigeration solution for the smaller supermarket sized stores would lead to a significant reduction in the environmental impact due to refrigerant leakages.

Early simulations of a CO_2 booster refrigeration system for a small supermarket showed an increase in annual electricity costs of 18% when compared to a traditional R404A system located in Northern Ireland. However the much lower GWP of CO_2 coupled with a refrigerant leakage rate of 15% of the system charge, resulted in a reduction in CO_2 emissions of 128 tCO_2 over a 10 year period.

A numerical model of a plate-finned tube evaporator coil was developed and different circuitry configurations and tube diameters were simulated using CO_2 as the refrigerant. The investigation found that by reducing the number of circuits from 3 to 1 increased the mass flux and the velocity of the refrigerant. The single-circuited evaporator reduced the length of pipe needed for complete evaporation, reducing the size of the evaporator required. The reduction in the number of circuits did increase the refrigerant pressure drop across the evaporator; however the pressure drop is small and had negligible impact on the compressor power consumption.

An experimental system was built to run controlled tests to verify the results of the numerical models and to investigate the operational performance of an experimental system. The tests revealed that the heat transfer performance of CO_2 had been underestimated when compared to a R404A system. The design temperature difference between the refrigerant condensing and ambient temperatures for a R404A system is usually 10 K. The means condenser rejects the heat from the superheated refrigerant to a temperature 10 K above the ambient temperature. The design figure of a 10 K temperature differential was used for the early simulations of the CO_2 system but the experimental results revealed that the condenser / gas cooler has the ability to reject heat from the superheated CO_2 to a temperature 2 K above the ambient temperature. CO_2 had the ability to reject more heat in the condenser / gas cooler than R404A. The numerical model was updated and optimised with the new

temperature differential of 2 K and the system was re-simulated and verified to agree well with the test results.

To compare the performance of the CO_2 booster system to the performance of a real small supermarket using a traditional R404A refrigeration system, a small supermarket in Northern Ireland was fitted with power logging equipment and a data recording system to record the state of the expansion valves so the hourly refrigeration loads could be calculated. Using hourly ambient temperatures the performance of the R404A system was simulated over a one year period so that the annual power consumption of the system could be calculated.

The results of these annual simulations showed that the CO_2 system did consume more power than the R404A at ambient temperatures above 13°C. This result agreed with other researchers (Ge and Tassou, 2011) that there was an optimum ambient temperature below which the CO_2 booster system performed most efficiently.

The TEWI calculation was used to measure and compare the environmental impact of both the R404A and CO_2 refrigeration systems. For the supermarket studied, a CO_2 booster refrigeration system would result in a 50% reduction in the environmental impact from direct and indirect emissions. Over a 10 year life cycle this equates to 361 tCO_2. The simulation model was also used to calculate the environmental impact of replacing existing small supermarket R404A refrigeration systems in Northern Ireland with the CO_2 booster system presented in this thesis. This would result in a reduction of 188,753 tCO_2 emissions over a 10 year period.

Further investigation of the power consumption of the CO_2 booster system and a traditional R404A system revealed that the CO_2 booster system became more efficient than the R404A when a lower ratio of medium temperature to low temperature refrigeration was used. A ratio analysis was preformed to calculate maximum ratios of medium temperature to low temperature refrigeration capacities. CO_2 booster systems installed using these ratios would equal the annual power consumption of a R404A system. CO_2 booster systems installed using ratios lower than the maximum ratios developed would outperform a traditional R404A system leading to lower annual power consumption.

This research has also led to a number of valuable contributions to knowledge which are detailed below.

Contributions to knowledge

1. A numerical model has been created specifically for this research and has been verified against results of tests performed on an experimental CO_2 booster system. CO_2 refrigeration booster systems are still relatively new, so no 'off the shelf software tools are available to accurately calculate the refrigerant flow rates and pressure drops for compressor and pipework selection in real supermarket installations. This software tool can be used by supermarket designers and engineers for this purpose.

2. The results from the tests on the experimental system showed that the performance of the CO_2 system was affected by heat transfer from the surroundings. This resulted in the low pressure compressor performing inefficiently due to a higher suction gas temperature from heat being transferred to the compressor suction line. The high rate of heat transfer also resulted in the refrigerant evaporating in the receiver and the distribution pipework lowering the cooling capacities of the evaporators. An insulated receiver should be specified on all CO_2 booster system receivers. Installing contactors should be made aware of the high levels of heat transfer of a CO_2 system compared to a R404A system. Contractors should also be made aware that the not insulating all suction lines correctly with high levels of insulation will lower the performance of a CO_2 system much more than would occur for a R404A system.

3. The numerical modelling has shown that a CO_2 booster refrigeration system has similar annual energy consumption as a R404A system in a small supermarket with refrigeration capacities of 46 kW medium temperature and 6 kW low temperature refrigeration loads.

4. This research has also shown that the performance of a CO_2 booster refrigeration system when compared with a traditional R404A system is not only a function of the ambient temperature but also a function of the ratio of medium temperature refrigeration load to low temperature refrigeration load. Lowering

the ratio increased the efficiency of the CO_2 system and at a ratio of 1:1 the CO_2 booster system can be 16% more efficient than a R404A system.

5. The validated simulation models developed in this research combined with the detailed geographical and refrigeration load ratio analysis presented, will provide valuable information that will assist system designers and operators in the efficient design and optimisation of CO_2 technology for small supermarkets. As a rule of thumb, the more northerly the location the more efficient the CO_2 booster system will be. The ratios presented in Table 7.4 of this thesis should be considered by designers when considering a CO_2 booster system for a small supermarket.

6. By comparing the capital and installation cost of the CO_2 booster system with that of the HFC systems this research has concluded that high capital cost is the main barrier to the widespread application of CO_2 booster technology to small supermarkets. The capital cost of the CO_2 booster system investigated in this thesis was 63% high than that of a traditional R404A system, currently used in small supermarkets. The research has also demonstrated the significant environmental benefits that can arise from the use of CO_2 as a refrigerant compared to HFC refrigerants. It is difficult to see any growth in the installation of CO_2 systems in these supermarkets without some form of Government led incentive.

Publications

Shilliday, J.A., Tassou, S.A., Shilliday, N. (2009) 'Comparative energy and exergy analysis of R744, R404A and R290 refrigeration cycles', *International Journal of low carbon technologies,* 4 pp. 104-111.

Shilliday, J.A., Tassou, S.A., Shilliday, N. (2010) 'Investigation of carbon dioxide as a refrigerant for supermarkets', *Engineering Doctorate Annual Conference,* Brunel University, UK, 7th January 2010

Shilliday, J.A., Tassou, S.A., (2010) 'Numerical analysis of a fin and tube evaporator using the natural refrigerant CO_2', 1st IIR Conference on sustainability and the cold chain, Cambridge, UK, March 2010.

Chapter 1 Introduction

In the UK, leakage of refrigerants from supermarket refrigeration systems containing Hydroflurocarbons (HFCs) in 2005 was equivalent to the release of 2 million tonnes of CO_2 (Lacros and Enviros, 2007). This is equivalent to a leakage of 512 tonnes of the HFC refrigerant R404A from supermarket refrigeration systems. In comparison, 2 million tonnes of CO_2 is released by the generation of 3.7 million kWh of electricity which is enough to power 765,931 households for 1 year. In the same year (2005) the total UK CO_2 emissions from power stations was 172.7 million tonnes (DECC, 2012). The leakage of HFCs from supermarket refrigeration system therefore accounted for approximately 1% of total CO_2 emissions.

The leakage rates of HFCs from supermarket refrigeration systems can be reduced by enforcing regular leak checks, but an alternative would be to use natural refrigerants with a low GWP such as CO_2 which has a Global Warming Potential (GWP) of 1 compared to 3780 for R404A. Refrigeration systems also have an indirect effect on the environment from the consumption of fossil fuels to generate electricity for their operation. Therefore a switch from HFCs to CO_2 should not increase the indirect environmental impact. This is a considerable challenge for engineers and designers and the motivation behind this thesis.

1.1 Refrigerants

The invention of synthetic refrigerants by Thomas Midgely Jr in 1928 (Midgley and Henne, 1930) enabled refrigeration devices to be used for domestic and commercial purposes. Prior to this, ammonia (R717), methyl chloride (R40), propane (R290) and sulphur dioxide (SO_2) were used as refrigerants but were highly toxic or flammable. This isolated their uses for industrial purposes at a safe distance from the general public after several fatal accidents occurred in the early 1900's from the leakage of

these highly toxic refrigerants from domestic and commercial refrigerators. Carbon Dioxide (R744) was used as a refrigerant as far back as 1889 (Thevenot, 1979) and was a preference onboard ships and in public places because of its non-flammability and non-toxicity. However, the refrigerant required large amounts of energy to compress as the gas to get a similar cooling rate as that of the other refrigerants. The compression of Carbon Dioxide required a much higher compression ratio as there was a higher differential between the evaporating and condensing absolute pressures. Section 2.8.1 of this thesis compares the properties of these refrigerants. The invention of synthetic refrigerants led to the creation of the refrigeration industry and the emergence of refrigeration as a necessity for the preservation of food. The safe operating characteristics of synthetic Chlorofluorocarbons (CFCs) enabled refrigeration systems to be used safely for commercial and domestic purposes.

The discovery of a 10% reduction in the atmospheric Ozone levels over the Antarctic by a British Antarctic survey team in 1985 confirmed the theory presented by Molina and Rowland (1974) that the release of chlorine from CFCs was causing a breakdown of Ozone, enabling the penetration of harmful ultraviolet (UV-B) radiation from the sun to the earth's surface. As soon as 1987 an international treaty, The Montreal Protocol on Substances that deplete the ozone layer was agreed by 23 nations and came into force on 1st January 1989 (UNEP, 1987). The treaty dictated the phase out of CFC production and use worldwide by 1996 for developed countries and 2010 for developing countries. With the restrictions and eventual ban of the use of CFCs the industry turned to the use of Hydrochlorofluorocarbons (HCFCs), which have a much lower Ozone Depletion Potential (ODP) than CFCs as a short term replacement. Revisions to the Montreal Protocol banned the use of virgin HCFCs from 2010 onward with a complete ban from 2015.

HFCs were developed as replacements for the banned CFCs and HCFCs as they had zero ODP and were not included in the Montreal Protocol. However, in 1997 the Kyoto Protocol included HFCs as one of the gases considered to be partly responsible for 'Global Warming' due to their high GWP. The Kyoto Protocol came into force in 2005 and as a result the EU established the F-Gas Regulations in 2006 aimed at reducing emissions of certain fluorinated gases, including HFCs. The

regulations set out policies for the labelling, reporting and recovery of fluorinated gases as well as certification and training programs for personnel involved in leakage inspections and the recovery, recycling, reclamation and destruction of fluorinated gases. Some EU member states have placed further restrictions on the use of HFCs. In 2007 Denmark banned the use of HFC refrigerants in refrigeration equipment having a total charge of more than 10 kg of HFCs. Austria has also banned HFCs in 2008 for use in domestic appliances and air conditioning while Norway placed a tax on the purchase of HFCs (Hekkenberg and Schoot-Uiterkamp, 2007).

1.2 Supermarkets

In 2006 there were approximately 6578 supermarkets in the UK. Around 2000 of these are superstores (Tassou *et al.*, 2010), with large refrigeration systems containing up to 1500 kg of HFC refrigerants. With reported UK leakage rates of up to 20% (Cowan *et al.*, 2009) environmentally friendly alternatives to HFC based supermarket refrigeration systems will lead to significant improvements in the protection of the environment. The many refrigerant shifts experienced by the refrigeration industry over the years has led supermarket operators to search for future proof refrigerants which are both environmentally sound and energy efficient. The use of the natural refrigerants Ammonia, Hydrocarbons or Carbon Dioxide could be a potential solution. All are naturally occurring chemicals with zero ODP and zero or extremely low GWP values. Ammonia has been used for many years in industrial refrigeration plant but its toxic and flammable properties require special safety precautions. This limited the use of Ammonia in the past to industrial plants or as a primary cascade refrigerant in commercial applications where the public health and fire risk of a gas leak is minimised as the pipes and plant are situated a safe distance from the public.

Hydrocarbons (HCs) such as Propane and Butane have good properties as refrigerants but are extremely flammable and pose a fire rise if a leak occurs. They have been used in domestic refrigeration for many years. The refrigerant charge of a

Propane system is 50% of that of an R22 system, which leads to a lower cost when compared to that of an HFC system (Riffat *et al.*, 1997). The public awareness of the use of HCs in commercial refrigeration is growing and with this also public confidence in the safety measures.

CO_2 was one of the earliest refrigerants used but engineers lost interest due to the high operating pressures and difficulty in containing the refrigerant inside the system due to the basic sealing technology available at that time. Recently CO_2 has gained in popularity because unlike Ammonia and HCs it is not flammable or toxic. Sealing technology nowadays is capable of withstanding the pressures inside a CO_2 system and the efficiency of newly designed systems has been reported to be similar to HFC systems (Sliva *et al.*, 2010; Austin-Davies and Da Ros, 2007). CO_2 also has excellent thermo physical and heat transfer properties as a refrigerant. It has a much higher vapour density than other refrigerants resulting in a greater volumetric refrigeration effect. The high vapour density of the refrigerant results in a lower swept volume requirement of the compressor compared to HFC systems. Equipment has the potential to be smaller, lighter and more efficient (Kim, *et al.*, 2004a).

CO_2 operates at much higher pressures than other refrigerants and has a much lower critical temperature resulting in supercritical gas cooling when at heat rejection temperatures above 31.1°C, as opposed to subcritical condensing in traditional HFC systems. The low critical point of CO_2 is a challenge for engineers due to the transcritical cycle at high ambient temperatures. This cycle leads to much higher pressures and higher energy consumption, so a high percentage of installations worldwide have avoided the transcritical cycle by using another refrigerant cascaded with CO_2 to keep it operating in a traditional subcritical cycle. The cascaded subcritical cycle is an expensive solution lending itself to larger supermarkets, where economies of scale exist.

There have been many large installations using CO_2 across the UK but only a small number of installations in small supermarkets. However, there is a much greater distribution of smaller supermarkets for which an appropriate CO_2 refrigeration solution has to be fully researched. An all-CO_2 cycle would operate transcritically at ambient temperatures approaching 31.1°C. Using a temperature differential for CO_2

of 10K, equivalent to that of a R404A system, the ambient temperature at which transcritical operation would occur would be 21.1°C. In Northern Ireland these high temperatures occur for only a fraction of the year if at all, Figure 1.1 (Met Office, 2012). The system could potentially operate subcritically with lower energy consumption for a high proportion of the year.

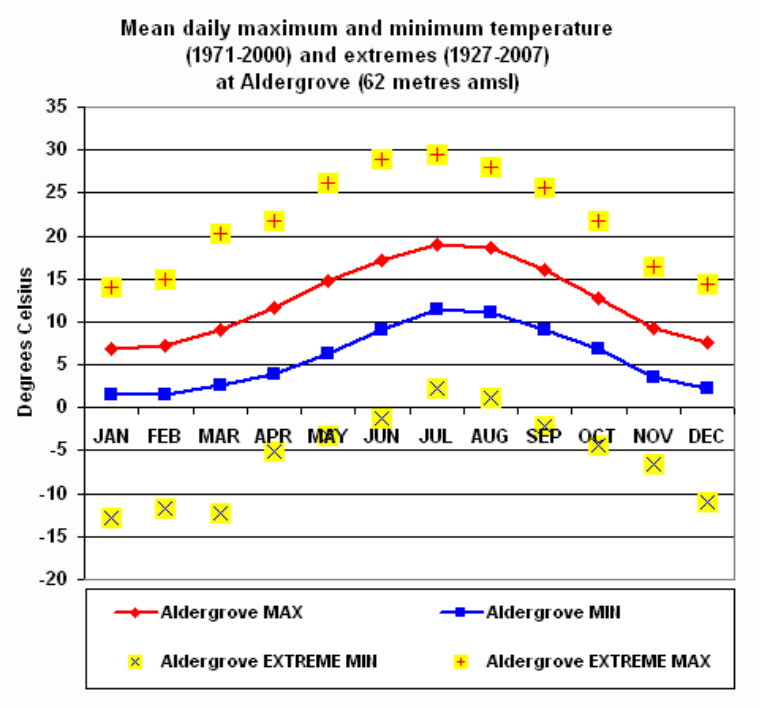

Figure 1.1 Annual average monthly minimum and maximum ambient temperature for Belfast (Met Office, 2012)

Supermarkets generally have two temperature levels of refrigeration; a medium temperature level (MT) for dairy and meat products and a low temperature (LT) level for frozen food. The low temperature refrigeration systems have high compression ratios due the high pressure difference between evaporating and condensing pressures. At high ambient temperatures a transcritical CO_2 cycle for LT refrigeration would be very inefficient. A method of increasing the efficiency of the LT side would be to add a 'booster' compressor to a transcritical MT CO_2 cycle; this would decrease the compression ratio of the LT compressor and increase the efficiency of the LT cycle and the efficiency of the MT and LT combined cycle as a whole. This all-CO_2 cycle could offer a potential solution, as a replacement to high

GWP HFC refrigeration systems for small supermarkets and will be investigated in this thesis. A schematic of the proposed 'booster' cycle is shown in Figure 1.2.

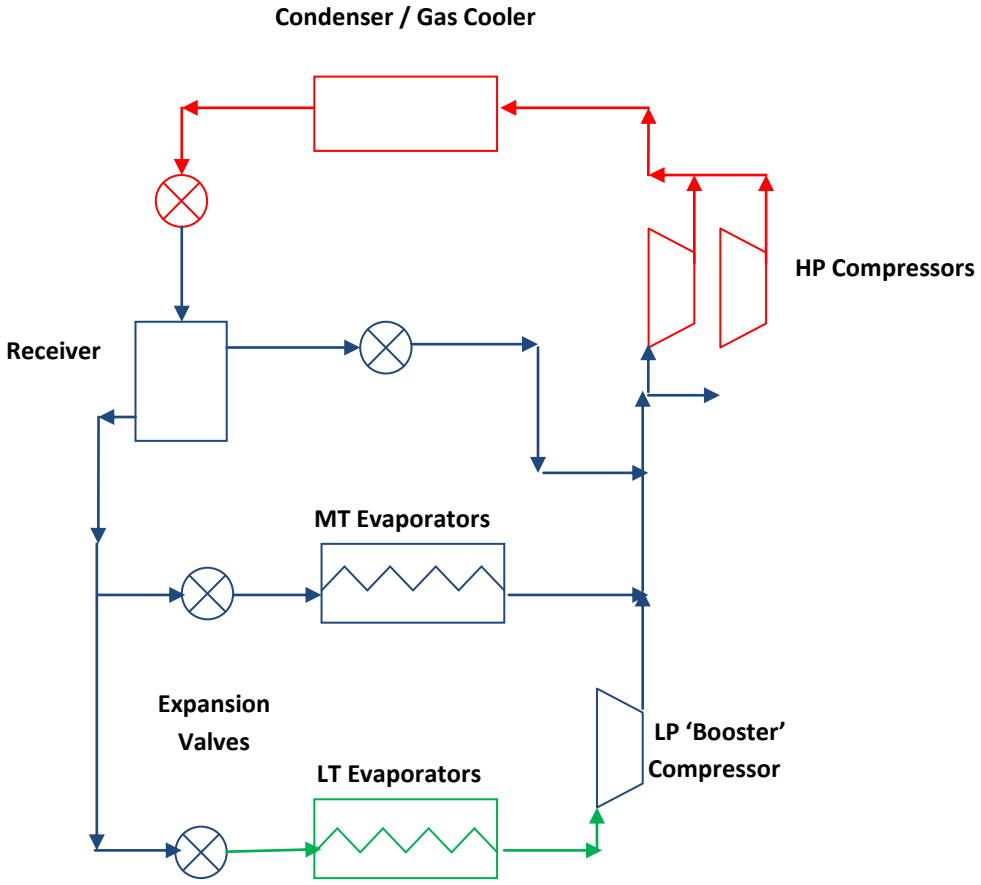

Figure 1.2 Schematic diagram of booster refrigeration cycle

1.3 Research aims and objectives

The objectives of this thesis are:

1. To investigate the practicality, economic viability and environmental benefits from the adoption of an all-CO_2 transcritical cycle in small supermarket applications. Whilst the environmental benefits of using CO_2 as a refrigerant are clear, there is a shortage of both practical and technical knowledge for the

design of these systems. This research will contribute to the development of knowledge to assist in the design and adoption of transcritical CO_2 systems for small supermarket applications.

2. To investigate existing CO_2 simulation models and develop simulation models for the design of transcritical CO_2 systems which will enable components to be selected based on the desired capacity of the system. The models will also facilitate research into the performance of individual components and the cycle as a whole.

3. Use an experimental CO_2 system to validate the numerical models against actual system outputs, such as pressures, temperatures and power consumption. The experimental system will also be used to demonstrate the concept, test components and establish the performance characteristics of the system.

4. To compare the performance of the CO_2 system using validated numerical models with that of a fully operational HFC system in a small supermarket. Historical energy and leakage rates from a small supermarket in Northern Ireland will be analysed and compared to the simulation results of an all CO_2 solution. The benefits of replacing current HFC systems with CO_2 systems in Northern Ireland will be discussed.

1.4 Thesis structure

Chapter 1 Introduction

This chapter of the thesis provides background information relevant to the thesis. The environmental consequences of synthetic refrigerants are reviewed and the historical refrigerant shifts experienced by supermarket operators are discussed. The overall aims and objectives of this research are presented.

Chapter 2 Literature Review

This chapter provides a review of existing published and commercial literature available which has had an influence on this research. Supermarket refrigeration systems are reviewed and operational components and basic governing thermodynamic principles are presented. The motivation behind the use of natural refrigerants is discussed and their performance and chemical properties as refrigerants is compared. The different subcritical and transcritical refrigeration cycles are considered and the wide variety of CO_2 based installations worldwide is presented.

Chapter 3 Simulation Model Design

Based on the conclusions of the literature review this chapter describes the design of a proposed CO_2 system and the benefits of using numerical models to simulate the performance of the system comparatively against systems currently in use. The simulation model is a complex set of mathematical equations written in code, which is used to simulate the thermodynamic performance of a refrigeration system. This chapter presents the underlying mathematical equations used to simulate the refrigeration systems and their components.

Chapter 4 Simulation Procedure and Results

The procedure for simulating each refrigeration system is described, using the models developed in Chapter 3, with the inputs and boundary conditions to each model. The results of the CO_2 and R404A refrigeration system models are analysed and the annual energy performance of each system is discussed and compared. Using the TEWI (Total Equivalent Warming Impact) calculation, the environmental performance of each system, considering direct and indirect emissions, is calculated over the system lifecycle.

Chapter 5 Experimental Design

In this chapter the design of an experimental system used to run tests to validate the simulation models is presented. The components used in the experimental system

and their functions are described with input parameters used to operate the system. The schematic diagram of the controls system used in the tests is also presented.

Chapter 6 Test results and model verification

The results from the tests run on the experimental system are analysed in this chapter and are compared with the simulation model results. Any differences between the actual test results and the simulation model results are explained and the model is optimised using the test data.

Chapter 7 Study of the application of a transcritical CO_2 system in a supermarket

This chapter presents and discusses the application of a transcritical CO_2 system in a real supermarket. A small supermarket in Northern Ireland has been fitted with a monitoring system which records the power consumed by the supermarket's R404A refrigeration system. The monitored results are compared with the simulation results of a CO_2 system. The ambient temperatures of ten different UK locations are used to analyse how the performance of a CO_2 system is affected by different geographical locations.

Chapter 8 Economic investigation

Using the installation costs of the real supermarket studied in Chapter 7 and costs of a CO_2 booster system of equal capacity an economic analysis is performed to assess how costs would affect the future uptake of CO_2 refrigeration systems in small supermarkets.

Conclusions and future work

In this chapter the main conclusions from this research are discussed and suggestions for future work are made.

Chapter 2 Literature review

2.1 Supermarket Refrigeration Systems

Supermarket refrigeration systems are required for the preservation of food for retailing. Whilst there are many different types of systems, there are two distinct temperature levels:

- Medium Temperature (MT) - This is for fresh chilled products at -1°C to 5°C.
- Low Temperature (LT) - This is for frozen products held at -18°C to -23°C.

The chilled food products are typically sold from open fronted multi-deck display cabinets arranged in aisles. The frozen food products are also found in multi-deck display cabinets with glass doors, or they can be stored in open top reach-in cabinets. Supermarkets can generally be classified into four sizes, with average requirements of temperature levels in kW of refrigerating capacity shown below in Table 2.1. The type of refrigeration system used is generally remote systems, where the compressors and condensers are located remotely from the refrigerated aisles in the supermarket. A general layout of a small supermarket is shown in Figure 2.1.

Table 2.1 Capacity of supermarket refrigeration systems (Tassou *et al.*, 2010)

Store Type	Size (m^2)	Medium Temperature (kW)	Low temperature (kW)	Estimated Quantity of refrigerant (kg)
Small Shop	50 - 150	2.5 - 20	1 - 3	3 - 25
Small supermarket (Convenience store and Service Station Forecourt)	150 - 280	20 – 46	3 - 7	25– 70
Supermarket	280 – 1,400	46 - 100	7 – 30	70 – 150
Superstores	1,400 – 5,000	100 - 250	30 - 50	150 – 500
Hypermarkets	5,000 – 10,000+	300+	50+	500

Figure 2.1 Refrigeration layout in a small supermarket

A supermarket refrigeration system operates using the vapour compression cycle, transferring heat from a low temperature region to a high temperature region. The ideal basic single stage vapour compression cycle consists of 4 components, a compressor system, condenser / gas cooler, expansion device and evaporator shown in Figure 2.2, with corresponding ideal pressure – enthalpy chart shown in Figure 2.3.

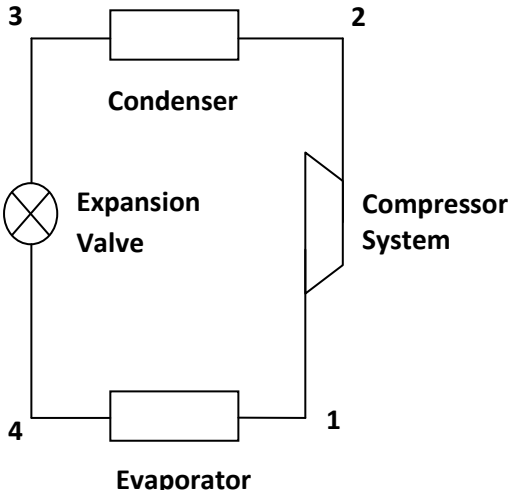

Figure 2.2 Schematic diagram of single stage vapour compression cycle

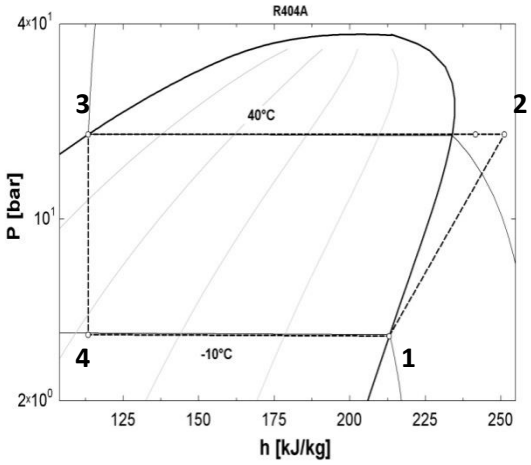

Figure 2.3 Pressure - enthalpy chart of single stage vapour compression cycle

1 – 2: Compression Isentropic compression. The refrigerant enters the compressor as a saturated vapour and is compressed to the condenser pressure. The temperature of the refrigerant increases during the compression process, well above the condensing temperature. It becomes a superheated vapour.

2 – 3: Condensation Isobaric heat rejection. The refrigerant enters the condenser as a superheated vapour and heat is rejected from the refrigerant at a constant pressure. The refrigerant condenses from a superheated vapour to a saturated liquid.

3 – 4: Expansion Isenthalpic. The pressure of the refrigerant is reduced by a throttling process in the expansion valve which reduces the temperature of the refrigerant to the required set point.

4 – 1: Evaporation Isobaric heat absorption. The refrigerant enters the evaporator as a low quality saturated mixture and evaporates to a saturated vapour by absorbing heat from the surroundings. The phase change process enables a high rate of heat transfer.

The actual vapour compression cycle behaves very differently to the ideal cycle presented in Figure 2.3. The actual processes are described below.

1 – 2: Compression The actual compression process is not isentropic. Losses occur in the compressor giving the compressor an isentropic efficiency. Due to these losses the compression process decreases the entropy of the refrigerant.

2 – 3: Condensation The refrigerant heat rejection in the condenser is not isobaric. Pressure drops occur due to frictional effects of the refrigerant travelling though the pipework. The pressure of the refrigerant will reduce during the condensation process.

3 – 4: Expansion Frictional losses during the expansion process mean that the actual expansion process is not isenthalpic. The refrigerant after the expansion process will have a lower enthalpy.

4 – 1: Evaporation A pressure drop occurs as the refrigerant is travelling though the evaporator due to friction occurring at the pipe walls. As the refrigerant is in the saturation curve a temperature drop also occurs.

2.2 Remote refrigeration system

There are two types of remote refrigeration systems, a centralised system and a distributed system, which will be described in the next sections.

2.2.1 Centralised System

Centralised systems use a compressor pack system for all refrigeration at the same temperature. The refrigerant is distributed through the supermarket to each direct expansion evaporator by interconnecting pipework, where the expansion process occurs directly at each evaporator. The compressor systems are located remotely from the refrigerated sections of the supermarket as they generate heat and noise so usually have a dedicated machine room or are located on the roof of the supermarket.

The maximum capacity of the compressor system is matched to the maximum capacity of the refrigeration required in the supermarket. Figure 2.4 shows a schematic diagram of a typical centralised compressor system. The discharge and suction outlets of the compressors are joined into discharge and suction headers enabling the capacity of the system to be modulated to match the load required by the refrigeration system. The compressors are controlled by pressure set points. Individual refrigerated display cabinets control the flow of refrigerant through the evaporators, as less refrigeration is required by the cabinets a reduction in refrigerant flow rate developed by the compressors is required to meet the suction stage pressure set point. This is achieved by modulating the speed of the compressors using frequency inverters or switching compressors off in multi compressor systems. The disadvantage of these systems is that they require a large volume of refrigerant due to the long distances of interconnecting pipe work. Leakage rates are greater in these systems due to the large volume of refrigerant and due to the long distances of pipe work where leaks can occur at joints.

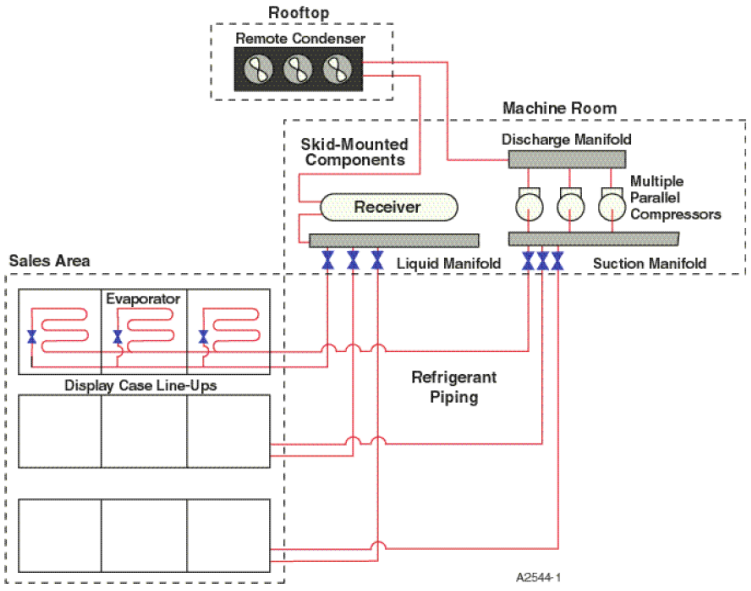

Figure 2.4 Schematic diagram centralised compressor system (Baxter, 2006)

2.2.2 Distributed system

A distributed refrigeration system uses a number of smaller compressor systems distributed throughout the supermarket. These are usually single condensing units which house a compressor and condenser as shown by Figure 2.5, where the condensing unit is connected directly to the direct expansion evaporator. These systems are typically used for smaller supermarkets where there may only be 1 or 2 evaporators per condensing unit. The condensing units usually contain one single speed compressor, so the compressor output cannot be modulated to meet the load requirement of the evaporators, making the system inefficient. Although inverter controlled condensing units which can modulate the output of the compressor are becoming available, they are much more expensive than the single speed units. The advantage of this system is that there is a reduction in the pipe work required and therefore a reduction in the leakage of refrigerant from pipe work joints and components.

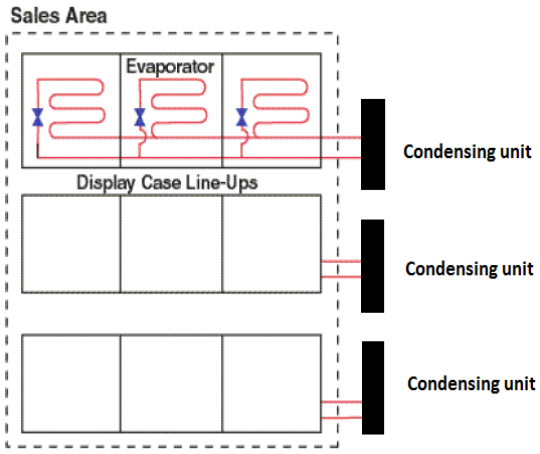

Figure 2.5 Schematic diagram distributed compressor system (Baxter, 2003)

2.3 Condenser

The centralised system uses an air cooled condenser to reject heat and condense the refrigerant. The condenser uses ambient air forced over a coil, distributing the

refrigerant over a large surface area, to reject the heat from the refrigerant to the ambient. The refrigerant enters the condenser as a superheated vapour and leaves as a saturated liquid. Condensers are available in many shapes and sizes to suit the location required. Figure 2.6, shows an image of a typical air cooled condenser.

Figure 2.6 Typical air cooled condenser (Direct industry, 2012)

2.4 Evaporator and expansion device

The refrigerated cabinets house the evaporator which uses the heat from the products blown over the evaporator to change the phase of the refrigerant from a liquid to a saturated vapour. The phase change process enables a high rate of heat transfer to the refrigerant. For a medium temperature display cabinet the evaporator is usually positioned in the bottom of the cabinet, but can be positioned at the back of the cabinet. Fans are used to distribute air over products transferring heat from the products to the evaporator. The fans are also used to create an air curtain for the open display cabinets, creating a barrier of air between the cabinet and the ambient to reduce the influx of ambient air.

The expansion device is a throttling valve, either a thermostatic expansion valve (TEV) or an electronic expansion valve (EEV). Most modern supermarkets use EEVs, as the electronic valve regulation enables better control over the evaporator pressure and condensing temperature due to close superheat control. The EEVs have

also been reported to lead to less ice accumulation on the evaporator and better cabinet product temperature (Tahir and Bansal, 2005).

2.5 Energy Use and Carbon Emissions

Supermarket refrigeration systems are energy intensive systems and can account for up to 60% of the electrical energy used by the supermarket. Lighting can account for up to 25% and HVAC (Heating Ventilation and Air Conditioning) systems and hot water and other systems account for the remaining 15%. A study by Tassou *et al.*, (2011) compared the electrical intensity of 2570 supermarkets of sizes from 80 m^2 to 10,000 m^2 in the UK, Figure 2.7. The study found an exponential drop in electrical energy use up to a sales area of 1400 $m^{2.}$ The smaller stores which are more food dominant use had a greater electrical energy use per m^2 of sales area. The smaller stores use energy intensive refrigeration systems due to an emphasis on fresh produce. The larger supermarkets have a greater range of non-perishable food produce for sale, which does not require the energy intensive refrigeration systems. The larger supermarkets also stock clothing and white goods ranges which only require space with minimum energy usage. A reduction in the electrical energy used by the refrigeration system in the smaller stores would have a significant impact in the reduction of electrical energy used by supermarkets in the UK.

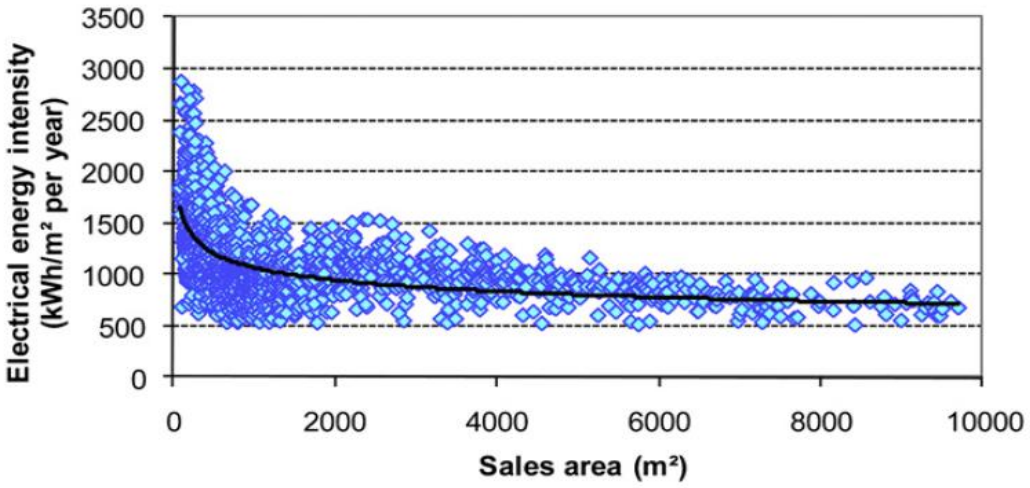

Figure 2.7 Variation of electrical energy intensity of 2570 UK retail stores with sales area from 80m^2 to 10,000m^2 (Tassou *et al.*, 2011)

The indirect carbon emissions are not the only source of greenhouse gas emissions from the supermarkets. Direct emissions of greenhouse gases come from the leakage of refrigerants from refrigeration systems. Most supermarkets now use HFCs with very high GWP values. The most common refrigerant used for supermarket systems is R404A with a GWP of 3780 (BSI, 2010). With reported UK leakage rates of up to 20% (Cowan *et al.*, 2009), this makes the direct emissions due to leakage a significant source of greenhouse gas emissions from supermarkets and a cause for concern highlighted in three reports published by the Environmental Investigation Agency (EIA, 2011; Walravens and Hailes, 2010; Walravens and Hailes, 2009).

2.6 Refrigerants

R11, R12 and R502 were the refrigerants used for early supermarket refrigeration systems but these were CFCs which the Montreal Protocol banned in 1995. Their replacements HCFCs were banned in 2010. The replacement for HCFCs, HFCs are now under strict control due to the Kyoto Protocol in 2006. Supermarket refrigeration systems adopted the use of the HFC R404A as a replacement for the HCFC R22 for new refrigeration systems. After the introduction of the Kyoto protocol in 2006 this refrigerant was under strict control due to the high GWP, Table 2.2, and supermarket operators are under pressure from environmental groups to stop using refrigerants with a high GWP.

Table 2.2 Characteristics of refrigerants (Kim et al., 2004)

	R-12	R-22	R-134a	R-404a	R-717	R-290	R-744
ODP/GWP	1/10600	0.05/1700	0/1300	0/3780	0/0	0/3	0/1
Flammability/toxicity	N/N	N/N	N/N	N/N	Y/Y	Y/ N	N/N
Molecular mass (kg/kmol)	120.9	86.5	102.0	97.6	17.0	44.1	44.0
Normal Boiling Point (°C)	-29.8	-40.8	-26.2	-48.7	-33.3	-42.1	-78.4
Critical Pressure (Mpa)	4.11	4.97	4.07	3.73	11.42	4.25	7.38
Critical Temperature (°C)	112.0	96.0	101.1	72.07	133.0	96.7	31.1
First Commercial Use as a refrigerant	1931	1936	1990	1993	1859	?	1869

2.7 HFC Leakages and Regulatory Control

The inclusion of HFCs as one of the six gases included in the Kyoto Protocol lead to the introduction of the Fluorinated Gas Regulations (F-Gas) or Regulation (EC) No 842/2006 of the European Parliament. The primary objective of this regulation is to reduce the emissions of the fluorinated greenhouse gases covered by the Kyoto Protocol and thus to protect the environment (Defra, 2007). Refrigeration and air conditioning equipment containing HFCs were identified as major sources of HFC emissions due to leakages to the atmosphere. Leakages in a refrigeration system can occur from:

- Installation of equipment
- Maintenance of equipment
- Decommissioning of equipment
- Pipe leakages

It is difficult to place a figure on how much refrigeration systems leak as the information is not widely available due its sensitivity but leaks of up to 20% annually are not uncommon (Cowan *et al.*, 2009). Many factors affect leakage including:

- System design and components used.
- The type of joint and the quality of brazing.
- How pipes are routed, supported and clipped.
- Vibration.
- The quality of pressure and leak testing during commissioning.
- The standard and suitability of service and maintenance.

The EU Fluorinated gas regulations have concentrated on the containment of HFCs within systems by:

- Prevention and minimisation of leakages.
- Mandatory inspections.
- Leakage detection system for large systems.
- Detailed record keeping.

- Recovery of refrigerant.
- Training and certification.

Some countries have placed further restrictions on the use of HFCs. In 2007 Denmark banned the use of HFC refrigerants in refrigeration equipment having a total charge of more than 10 kg of HFCs (Danish Environmental Protection Agency, 2002). Denmark has also placed tax on HCFCs and HFCs. Taxation of F-gases at €20/tCO_2eq is administered by the Danish Tax Authorities (SKAT). The tax act levies a green tax on the import of fluorinated greenhouse gases, to be paid to the Danish Government. The tax on greenhouse gases is differentiated as follows: the gases with the greatest impact on climate are subject to the highest tax level, with a tax level in 2011 set at about €17.5/kg for R134A and €50.7/kg for R404A (Shecco, 2012).

Norway has also enforced a tax on the use of refrigerants similar to Denmark; the gases with the highest GWP have the highest tax. Sweden currently limits the maximum refrigerant charges allowed in a supermarket to 20 kg for MT and 30 kg for LT (Cowan *et al.*, 2009) but the Swedish ministry has issued a proposal of the taxation of HFCs (R744.com, 2009), which is still in the consultation phase.

A paper by (Hekkenberg and Shoot-Uiterkamp, 2007) explored the three strategies currently being pursued in Europe titled 'Exploring policy strategies for mitigating HFC emissions from refrigeration and air conditioning' and has listed the advantages and disadvantages of each, shown in Table 2.3.

Table 2.3 Pros and Cons of different European Strategies (Hekkenberg and Uiterkamp, 2007)

Strategy and Countries	Advantages	Disadvantages
HFC containment (Sweden and Netherlands)	Targets new and existing applications	Requires continuous control stakeholder compliance
	Relatively quick results available	Required education and disposal facilities
		Potential risk of release remains
HFC phase out (Austria and Denmark)	No HFC use no HFC emissions	Availability of replacement options questionable
	Potential risk of release of stocks disappears	Only new application
HFC tax (Norway and Denmark)	Targets both emissions and stocks	Increases purchase costs of applications

Whether it happens immediately or over a period of time, other European countries and adopting policies which all point in the same direction – the phase-out of HFCs. The ban in Denmark has forces the industry to look for alternative refrigerants, namely, natural refrigerants.

2.8 Revival of Natural Refrigerants

Natural refrigerants are not synthetic, but a group of naturally occurring chemicals that have the correct chemical and thermodynamic properties to be used as refrigerants. The idea of natural refrigerants is not a new one, as some of these refrigerants were the original refrigerants used in the first refrigeration machines invented as far back as the 1800's (Kim et al., 2004; Pearson, 2005). CO_2 cannot be used as a direct replacement refrigerant like some HCs can. The unique chemical properties of CO_2 call for a complete redesign of refrigeration components. Of the three alternative choices presented, Ammonia, HCs and CO_2, CO_2 has gained the most attention in recent years for commercial refrigeration applications. This was

initiated by a paper by Lorentzen and Petterson, (1993) titled ‘A new, efficient and environmentally benign system for car air conditioning’ and in a subsequent paper by Lorentzen, (1994) titled ‘Revival of CO_2 as a Refrigerant’, where Lorentzen detailed the possible use of CO_2 in a commercial refrigeration system.

2.8.1 Properties

Synthetic refrigerants are manufactured with thermodynamic properties to maximise the performance of refrigeration systems. They can contain mixtures of various pure synthetic refrigerants to maximise performance for the application.

R22, R404A, R717 and R290 all operate at similar pressures at set evaporating and condensing temperatures, but R744 (CO_2) operates at much higher pressures. Condensation does not occur from points 2 – 3 in the R744 pressure-enthalpy vapour compression cycle. This process occurs at supercritical pressures and temperatures above the critical point of R744. The typical evaporating pressure of CO_2 at -10°C is 26.49 bar, 6 times higher than R404A and condensing at 40°C leads to a gas cooling (no condensation) pressure of 90 bar, 5 times higher than R404A. This high heat rejection pressure is above the safe working pressure of refrigeration grade copper which is 46 bar. Stainless steel pipes must be used for these high pressures.

The pressure difference between the gas cooling/condensing and evaporating pressures are much higher for CO_2 than for the other refrigerants, as shown by the data in Table 2.4. The expansion device requires a minimum pressure differential between the condensing and evaporation processes to operate. For R404A this is usually 6 – 8 bar for a thermostatic expansion valve, therefore the minimum condensing temperature is 20°C. The lower the condensing temperature, the less energy used by the compressor to maintain the pressure differential. A CO_2 expansion device requires a minimum pressure differential of approximately 6 bar to maximise the capacity of the evaporator. The condensing temperature can therefore be dropped to 33 bar or approx 0°C but the expansion valve must be correctly selected due to the large pressure differential it will experience and its impact on the evaporator capacity (Danfoss, 2011a).

Table 2.4 Condensing / gas cooling, evaporating and pressure differentials of refrigerants

Refrigerant	Condensing / Gas Cooling[1] Pressure at 40°C (bar)	Evaporating Pressure at -10°C (bar)	ΔP (bar)
R22	15.34	3.55	11.79
R404A	18.33	4.39	13.94
R744	90.00	26.49	63.51
R290	13.69	3.45	10.24
R717	15.55	2.90	12.65

Figure 2.8 displays the low critical temperature of CO_2 compared to the other refrigerants. A saturation condition cannot exist above this temperature so heat rejection above this temperature operates at supercritical temperatures and pressures where no phase change occurs. A transcritical cycle occurs with subcritical low side and supercritical heat rejection. The high saturation pressure of CO_2 between temperature levels compared to the other refrigerants, results in a high vapour density, shown in Figure 2.9 and high volumetric refrigeration effect, shown in Figure 2.10. This is defined as the product of vapour density and latent heat of vaporisation. The high volumetric refrigeration effect means a lower volume flow of refrigerant is required for a specific cooling capacity resulting is smaller component sizes. CO_2 has some well documented important heat transfer properties. A Low surface tension induces nucleate boiling and two phase flow characteristics (Kim *et al.*, 2004b), shown in Figure 2.11.

[1] CO_2 does not condense but cools at temperatures above the critical temperature

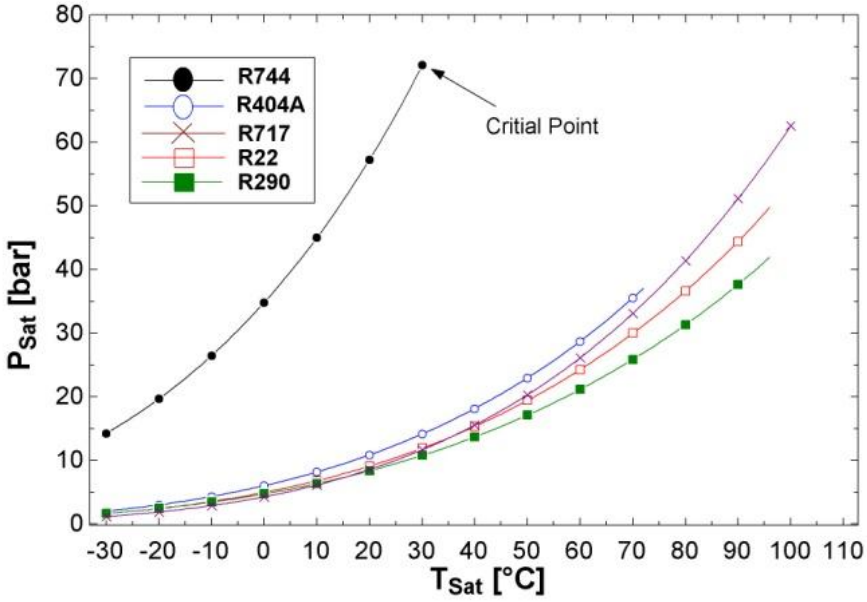

Figure 2.8 Variation of pressure with temperature

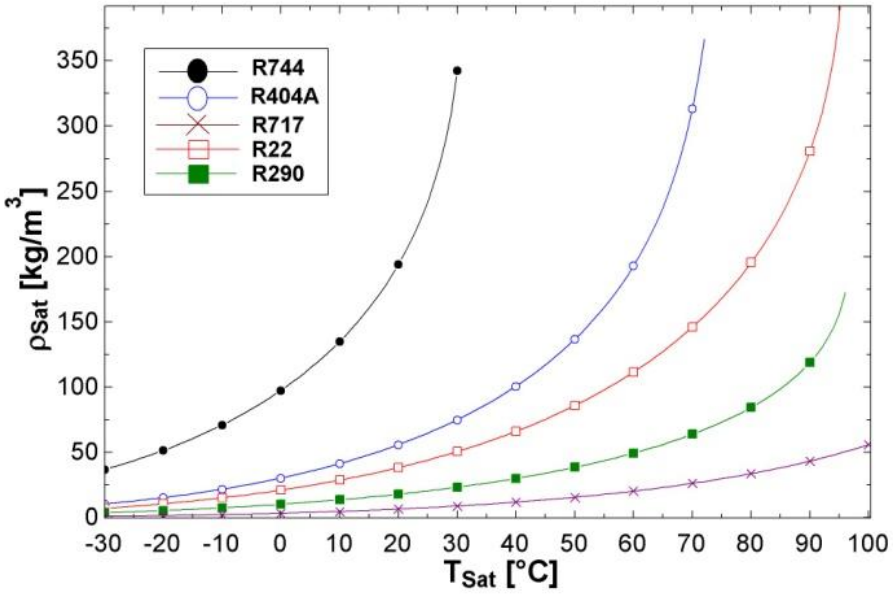

Figure 2.9 Variation of vapour density with temperature

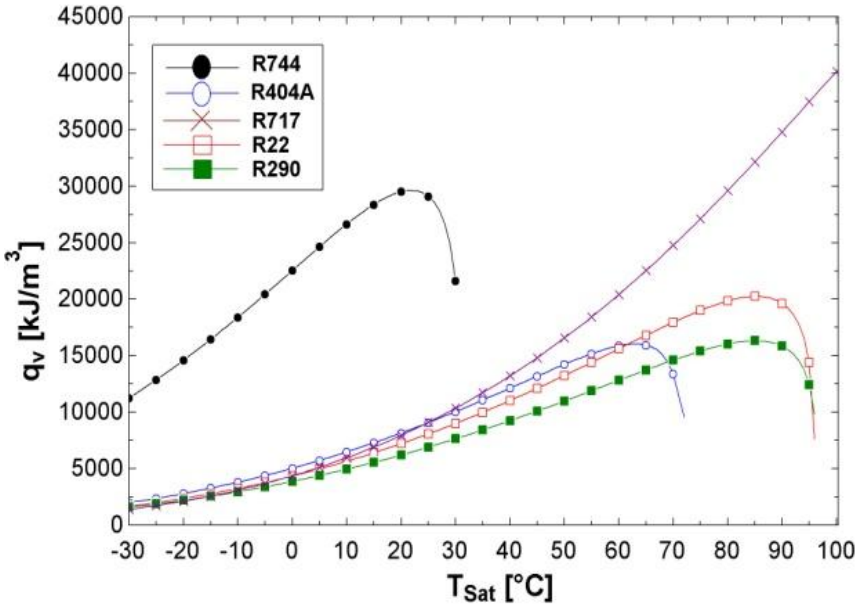

Figure 2.10 Variation of volumetric refrigeration effect with temperature

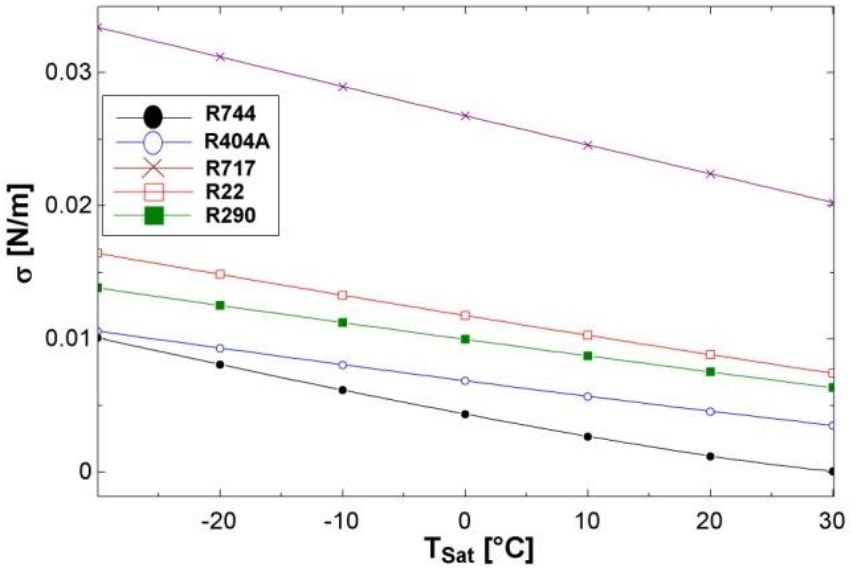

Figure 2.11 Variation of surface tension with temperature

2.8.2 Heat exchange properties

The higher operating pressures result in high vapour densities, very low surface tensions, high vapour viscosities and low liquid viscosities and thus yield flow boiling heat transfer and two-phase flow characteristics that are quite different from those of conventional refrigerants (Cheng *et al.*, 2006). The refrigerant side heat transfer coefficient of CO_2 is greater than that of other refrigerants which is clearly shown in Figure 2.12, from a paper by Choi *et al.*, (2007). Choi compared the boiling heat transfer of R-22, R134a and CO_2 in horizontal mini-channels and reported the mean heat transfer coefficient ratio of R22:R134a:CO_2 was approximately 1.0:0.8:2.0.

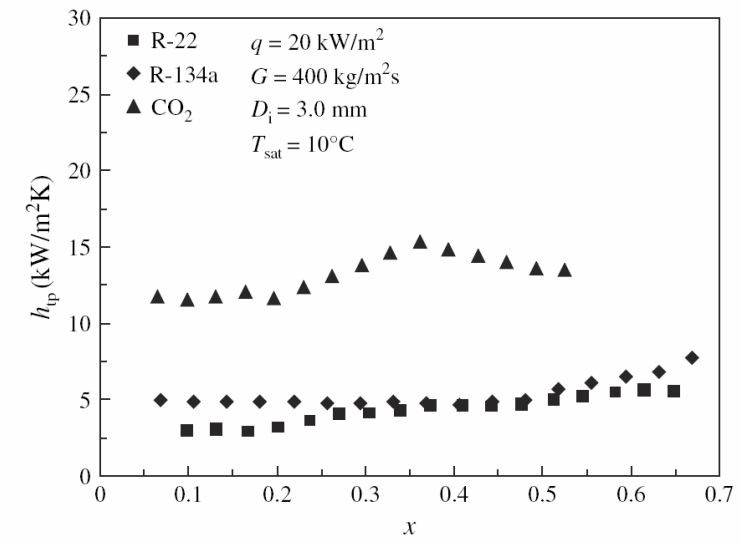

Figure 2.12 Comparison of the heat transfer coefficient for R-22, R-134a and CO_2 (Choi *et al.*, 2007)

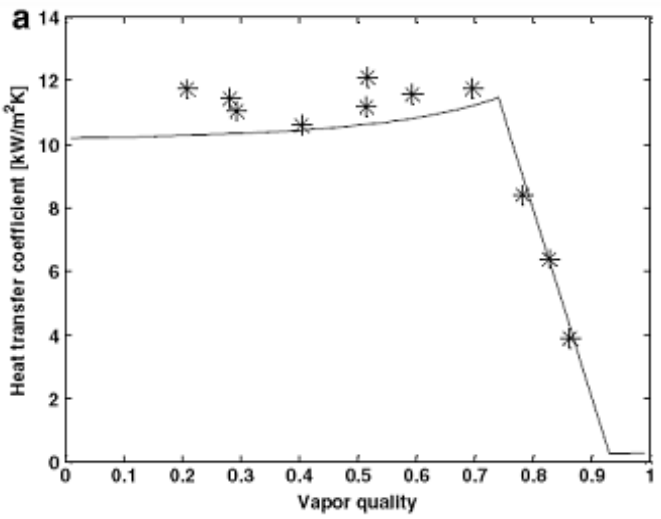

Figure 2.13 Predicted heat transfer coefficients of CO_2 and the corresponding flow pattern map (D_{eq} = 1.15 mm, G = 300 kg/m^2 s, T_{sat} = 10 °C, q = 11 kW/m^2) (Cheng *et al.,* 2008)

There have been numerous studies on the prediction methods for heat transfer and flow boiling of CO_2.The most recent being Cheng *et al.*, (2008) and Yoon *et al.*, (2004). These studies show higher heat transfer coefficients at lower refrigerant qualities with a sharp decline in heat transfer at the onset of dry out. Figure 2.13 shows the predicted heat transfer coefficient using Cheng's correlation. The high heat transfer coefficient at low vapour quality is clearly shown as is the sharp reduction at the onset of dry out. A lower vapour quality at the evaporator inlet could therefore aid heat transfer in a supermarket refrigeration system; this can be achieved by the sub cooling of the refrigerant after condensation / gas cooling. While there have been many developments in new compressor technology, control valves, control strategies and gas coolers, there has not been so much research into evaporator design to utilise the high refrigerant heat transfer coefficients highlighted by many researchers.

Commercial refrigeration installations use finned-tube heat exchangers for heat exchange processes. They have been used for many years to exchange heat between gases and liquids, which can be single or two-phase. The heat exchanger uses extended finned surfaces to enhance the heat transfer performance. Finned-tube heat exchangers are used extensively in supermarket refrigeration applications as forced

air evaporators. Many different extended fin configurations have been researched to further aid heat transfer but the plate fin configuration is mostly used for these applications due to reduced costs and ease of manufacture when compared to the other fin configurations.

Finned-tube heat exchangers using synthetic refrigerants have been extensively investigated numerically and experimentally by many researchers. Horuz *et al.*, (1998) carried out a theoretical and experimental investigation of a plate finned-tube evaporator and found that the main parameters affecting the evaporator cooling capacity and overall heat transfer coefficient were the air velocity, fin spacing, tube diameter, evaporator temperature, refrigerant type and frost height. McQuiston, (1978) and Grey and Webb, (1986) developed some of the earliest heat transfer coefficient correlations for finned-tube heat exchangers. This has been the main focus of most research in this area since, developing reliable correlations that will accurately predict the heat transfer and frictional performance of finned-tube heat exchangers. Wang and Chi, (1999) have published repeatedly in this area experimenting with fin spacing, tube diameter and tube rows and developing more accurate heat transfer correlations. Pettersen *et al.*, (1998) reported on a number of compact heat exchangers for use in CO_2 air conditioning systems. They reported that the number of tubes in a CO_2 evaporator should be increased and the tube diameter reduced for optimum design. Current research on CO_2 evaporators has focused on the use of micro-channels (Kim *et al.*, 2001; Yun *et al.*, 2007), which can offer space, material and weight reductions although these heat exchangers are much more expensive to manufacture. The base of the refrigerated display cabinet has a space which is sufficient for a finned-tube type evaporator, a reduction in the size of the evaporator is not necessary. For these reasons the use of micro-channels has not been investigated in this thesis. Aidoun and Ouzzane, (2009) developed a numerical model to study the circuitry inside CO_2 finned-tube evaporators and concluded that it was possible to use longer circuitry in CO_2 finned-tube coils.

The heat transfer mechanisms in a finned-tube evaporator are characterised by two coefficients, the air side heat transfer coefficient and the refrigerant side heat transfer coefficient. The air side coefficient is unique to each evaporator and is dependent on

the geometry and flow rate of air across the evaporator. The frosting and fouling of the fins can also have and affect on the air side heat transfer. The refrigerant side heat transfer coefficient is dependent on the refrigerant used, the state of the refrigerant and flow rate of the refrigerant. Other factors such as the internal pipe geometry and any resistances such as internal fouling of the pipes also have an effect on the refrigerant side heat transfer.

A typical HFC evaporator splits the mass flow of refrigerant into a number of circuits to reduce the refrigerant pressure and temperature drop across the evaporator. This can cause a mal-distribution of refrigerant across the evaporator. CO_2 has much lower temperature drop per unit of pressure, therefore multiple circuits may not be needed to separate the mass flow of refrigerant to reduce the pressure drop. Further investigation on the impact of the evaporator geometry, tube circuitry and tube diameter on the performance of CO_2 could lead to increased levels of heat transfer.

2.8.3 Performance

The low critical temperature of CO_2 means a transcritical cycle occurs when the refrigerant is unable to reject to a temperature below 31.1°C. It has been reported that this occurs at an ambient temperature above 22°C (Campbell *et al.*, 2007). This assumes a ΔT of 9.1 K across the condenser. By using a condenser which enabled a higher rate of heat rejection to lower the ΔT, subcritical operation could be achieved at higher ambient temperatures.

Figure 2.14 shows a pressure - enthalpy diagram of both a subcritical and transcritical cycle. At supercritical temperatures a gas cooling process occurs as the refrigerant cannot be condensed, temperature is also independent of pressure therefore the high side is controlled rather differently. As the pressure is independent of temperature the enthalpy of expansion valve inlet is calculated from the ‘S’ shaped isotherms on the pressure - enthalpy chart, Figure 2.15. At point 3 the gas cooler outlet temperature can be fixed and the pressure can increased and decreased due to the ‘S’ shaped isotherms. As the pressure is increased or decreased the refrigeration capacity will also increase and decrease, affecting the COP (Coefficient of

Performance) of the cycle and increasing or decreasing the work required by the compressor. An optimum pressure therefore exists for each gas cooler outlet temperature. This is a unique operational characteristic of a transcritical cycle; the high stage pressure must be optimised and is dependent on the temperature of the refrigerant before expansion.

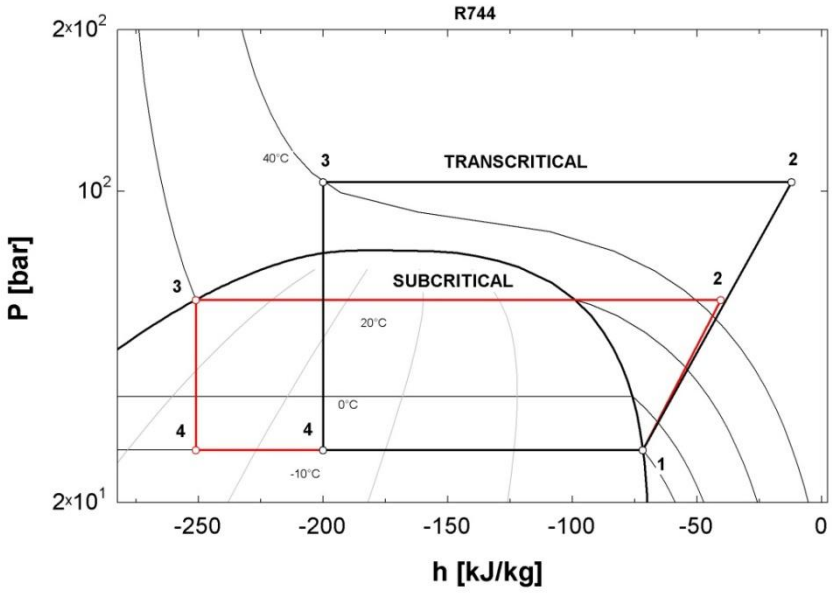

Figure 2.14 Pressure - enthalpy chart showing a Subcritical CO_2 cycle condensing at 20°C and a transcritical cycle gas cooling at 40°C, both evaporating at -10°C

The performance of a refrigerant in a refrigeration cycle can be calculated by the ratio of cooling capacity (Q) to compressor power input (W), both calculated by the change in enthalpy of the refrigerant across the process. The Coefficient of Performance is used for this purpose; it can be calculated from a pressure - enthalpy chart as shown in Figure 2.15 and by using equation 2.1.

$$COP = \frac{Q}{W} = \frac{h_1 - h_4}{h_2 - h_1} \qquad \textbf{(2.1)}$$

Figure 2.15 shows the COP calculated for five refrigerants, evaporating at -10°C and condensing / gas cooling from 20°C to 40°C, in an ideal vapour compression cycle. The figure clearly shows that CO_2 is the worst performing refrigerant when compared to the other refrigerants at high condensing/gas cooling temperatures.

However, the pressure difference between the high stage and low stage is much higher for CO_2 than for any of the other refrigerants. This pressure difference is required across the expansion valve to expand the refrigerant. Generally there is a minimum pressure difference required of 6 – 8 bar required across the expansion valve; a lower pressure difference will reduce the capacity of the evaporator. The minimum condensing temperature of the other refrigerants based on this pressure difference is 20 - 25°C, this is shown on Figure 2.16. CO_2 can condense at much lower temperatures than the other refrigerants. The optimum pressure difference across a CO_2 expansion valve is 18 – 30 bar, based on the Danfoss technical manual for CO_2 electronic expansion valves but the valve will still operated at a reduced capacity at 6 bar (Danfoss, 2011a). The CO_2 condensing temperature can consequently be reduced to 0 – 15°C, when the ambient temperature permits. This affects the COP of the CO_2 cycle at lower ambient temperatures shown by Figure 2.17. The poor performance of CO_2 at high ambient temperatures means it more suited to locations with low ambient temperatures, where the refrigerant can operate in a subcritical cycle with a low head pressure and high COP. Figure 2.18 shows an average annual temperature chart for Belfast with a maximum average temperature in July of 19°C. A CO_2 refrigeration system would be well suited to this climate.

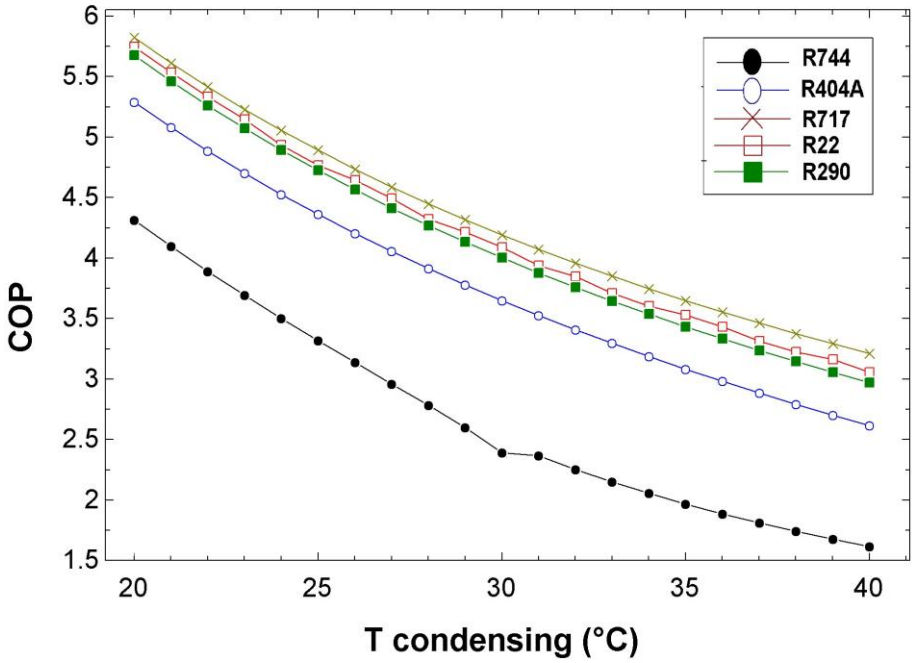

Figure 2.15 Comparison of calculated COPs for an ideal vapour compression cycle with increasing condensing temperature, evaporating at -10°C

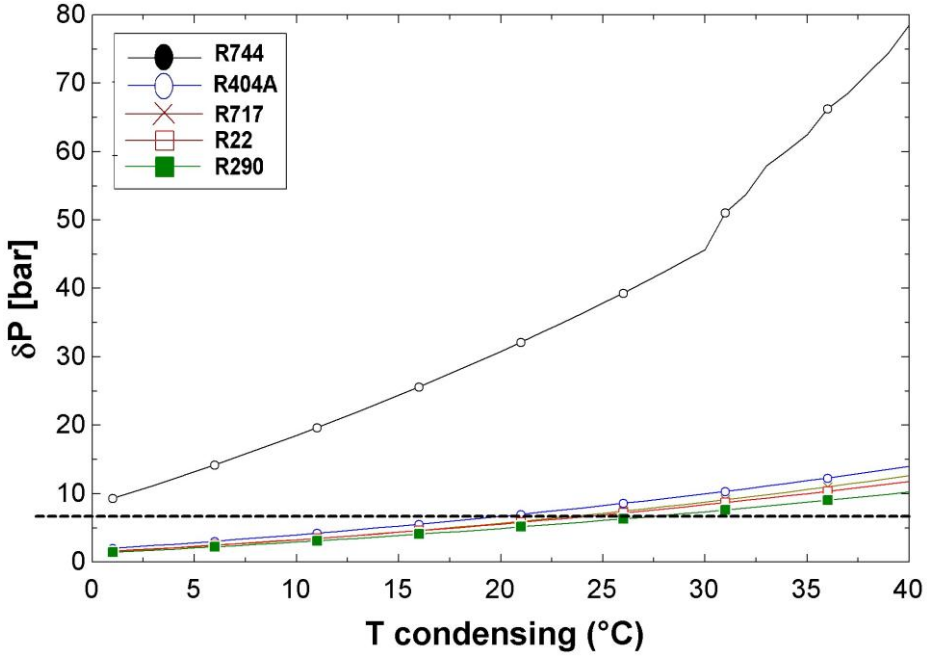

Figure 2.16 Comparison of calculated pressure differences between an increasing condensing temperature and a fixed evaporating temperature of -10°C

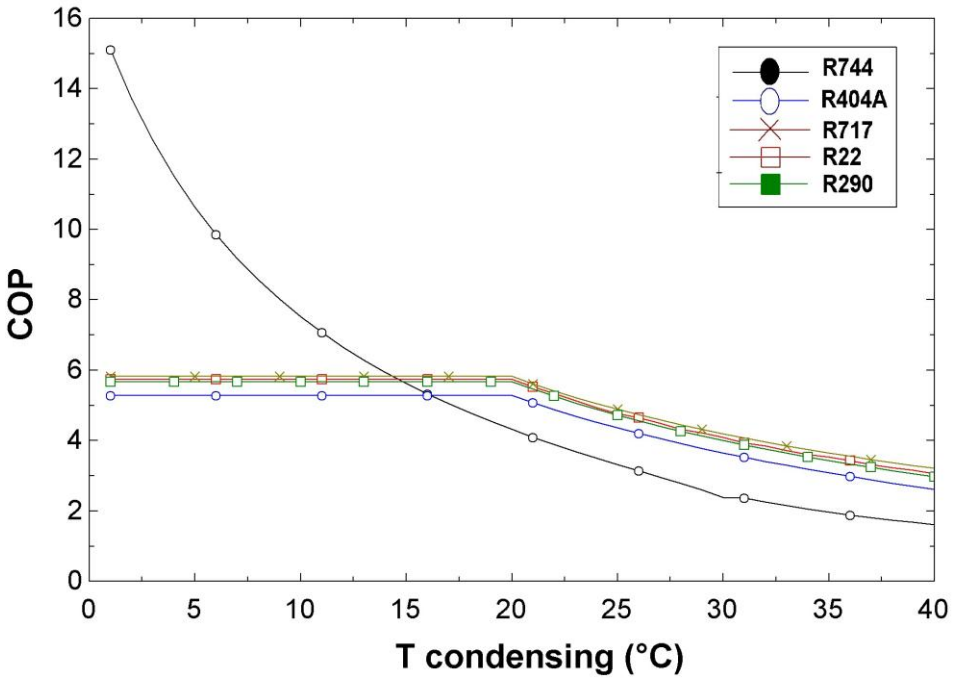

Figure 2.17 Comparison of calculated COP values

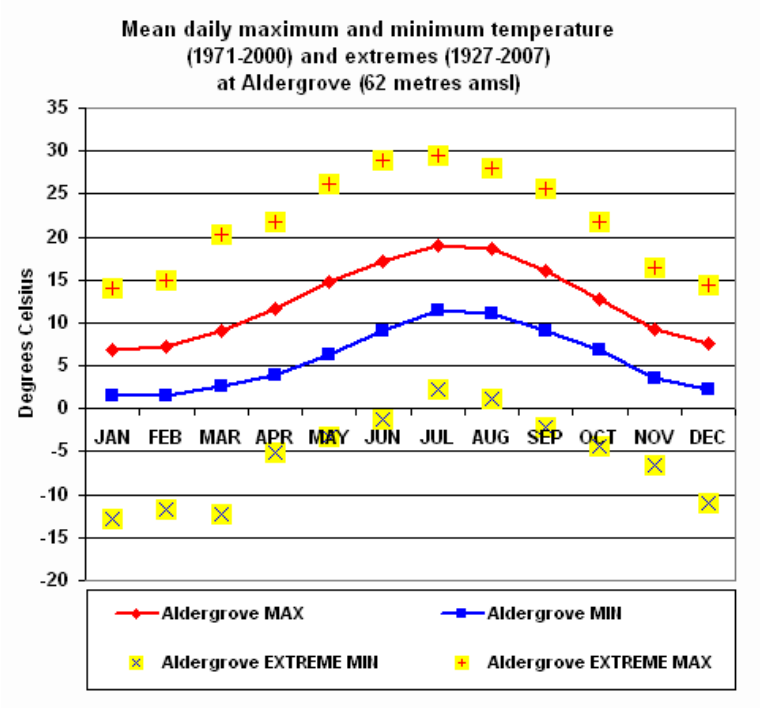

Figure 2.18 Annual average monthly minimum and maximum ambient temperature for Belfast (Met Office, 2012)

2.9 CO_2 Solutions for Supermarkets

Hundreds of thousands of people come into close contact with supermarket refrigeration systems every day. The use of either Ammonia or Hydrocarbons is simply too dangerous due to the high charge of refrigerants in these systems and the risk of refrigerant leakages in the supermarket. One such incident occurred at a cold store facility in Tamahere, New Zealand in 2008. The propane used in the refrigeration system ignited, killing one fire fighter and injuring many workers (New Zealand Fire Service, 2008). Due to the risks associated with these refrigerants and the proximity of the flowing refrigerant to supermarket users, Hydrocarbons or Ammonia are not really options for supermarkets except for use in a cascade system, where the refrigerant would only be located at a safe distance from the users. CO_2 is the only natural refrigerant which can safely be used in a supermarket avoiding the risk from flammable and toxic refrigerant leaks.

As previously explained, the operating thermodynamic properties of CO_2 are different to HFCs, HCs and Ammonia. The low critical temperature of CO_2 and the higher operating pressures have been a challenge to engineers designing systems to utilise the properties of this refrigerant.

There have been two choices for CO_2 refrigeration systems:

- **Subcritical Cascade system**

A subcritical CO_2 cycle maintains the refrigerant below the critical point at all times by the use of a cascade heat exchanger. The system uses another refrigerant as the heat rejection medium in a separate refrigeration system. The cascade condenser acts as an evaporator for the high temperature refrigerant and a condenser for the CO_2. There have been many different refrigerants used for the high temperature refrigerant each with advantages and disadvantages

- **Transcritical system**

The transcritical system operates transcritically at high ambient temperature and subcritical at low ambient temperatures. CO_2 is the only working fluid in the cycle.

The next section is a literature review on the published different systems using either a subcritical cascade CO_2 system or transcritical CO_2 systems.

2.9.1 Subcritical cascade cycles

To use CO_2 in a subcritical cycle the refrigerant must condense through heat rejection, which is not possible at relatively high ambient temperatures due to the low critical temperature of CO_2. The changeover ambient temperature from subcritical to transcritical has been published to be above 22°C (Campbell *et al.*, 2007). This depends on the ability of the condenser reject heat from the refrigerant at these high ambient temperatures. In ambient temperatures approaching the critical temperature of CO_2 ambient air cannot be used as a heat rejection medium, a cascade cycle must be used keep CO_2 below the critical temperature.

A cascade cycle can be used to keep CO_2 running in a subcritical cycle by using another refrigerant as the heat rejection medium. The cycle consists of two separate vapour compression cycles joined by a heat exchanger. The heat exchanger acts as a condenser for the low temperature stage and an evaporator for the high temperature stage. Traditionally cascade cycles were used for low temperature refrigeration systems typically between the range -30°C and -100°C (Bansal and Jain, 2007). At these low temperatures single stage cycles are inefficient due to the high temperature differential and high compression ratios. The cascade cycle splits the compression process into two separate stages utilising the thermodynamic properties of different refrigerants for each stage, whist lowering the overall compression ratio. This cycle has been of particular interest for supermarket refrigeration designers wishing to use CO_2 but not use the transcritical cycle. For supermarket applications CO_2 is used as the LT secondary refrigerant and another refrigerant is used for the primary refrigerant or HT (High Temperature) refrigerant. CO_2 is condensed by rejecting heat to the HT refrigerant which uses the rejected heat to evaporate through a heat exchanger. CO_2 is typically condensed at -10°C which is well under the critical point ensuring subcritical operation. The cascade refrigeration cycle's energy performance

using subcritical CO_2 is therefore not as dependant on the ambient temperature as the transcritical CO_2 cycle making it a more viable option in warmer climates.

There have been many cascade system installations using CO_2 as a LT refrigerant and as a MT refrigerant. However, there as yet not been consensus on which refrigerant to use as the HT heat rejection refrigerant. There have been a number of installations using either a HFC or another natural refrigerant. The thermodynamic performance of two stage cascade refrigeration cycles has been presented by several researchers. Lee *et al.*, (2006) researched the optimal condensing temperature for a CO_2-R717 refrigeration system using a thermodynamic energy and exergy analysis. They found the optimal condensing temperature to be -15°C for the cycle at an evaporating temperature of -50°C, but the optimal condensing temperature increased with an increase evaporating temperature. Getu and Bansal, (2008) presented the thermodynamic analysis of a R744 (CO_2) cascade refrigeration system. They found that the use of ethanol as the high stage refrigerant produced the highest COP followed by R717. The worst performing high stage refrigerant was R404A.

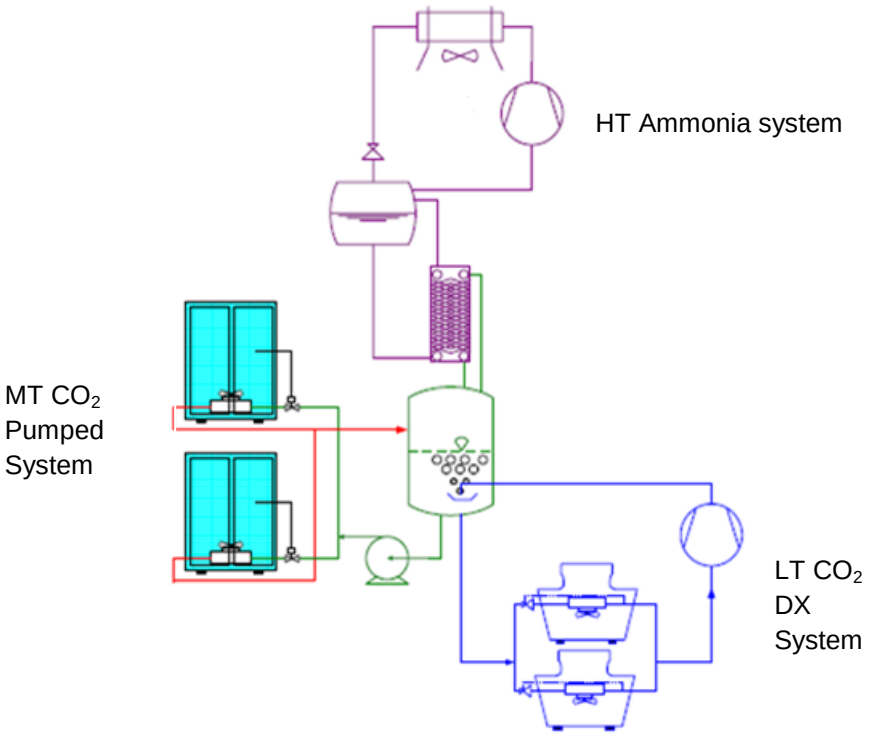

Figure 2.19 Schematic diagram of CO_2 / Ammonia refrigeration system (Sawalha, 2008)

Sawalha, (2008) presented an experimental analysis of a CO_2 / Ammonia cascade system for supermarket refrigeration application, shown in Figure 2.19. For the LT refrigeration the CO_2 was evaporated at -37°C and condensed in the receiver at -8°C. Ammonia was used for the primary HT refrigerant, evaporating at -10°C and condensing at 37°C. Pumped subcritical CO_2 was used for the MT refrigeration, utilising the receiver temperature of -8°C. Sawalha concluded that the COPs for the CO_2 / Ammonia cascade solution were 50 to 60% higher than that of a direct R404A system installed in the same laboratory environment.

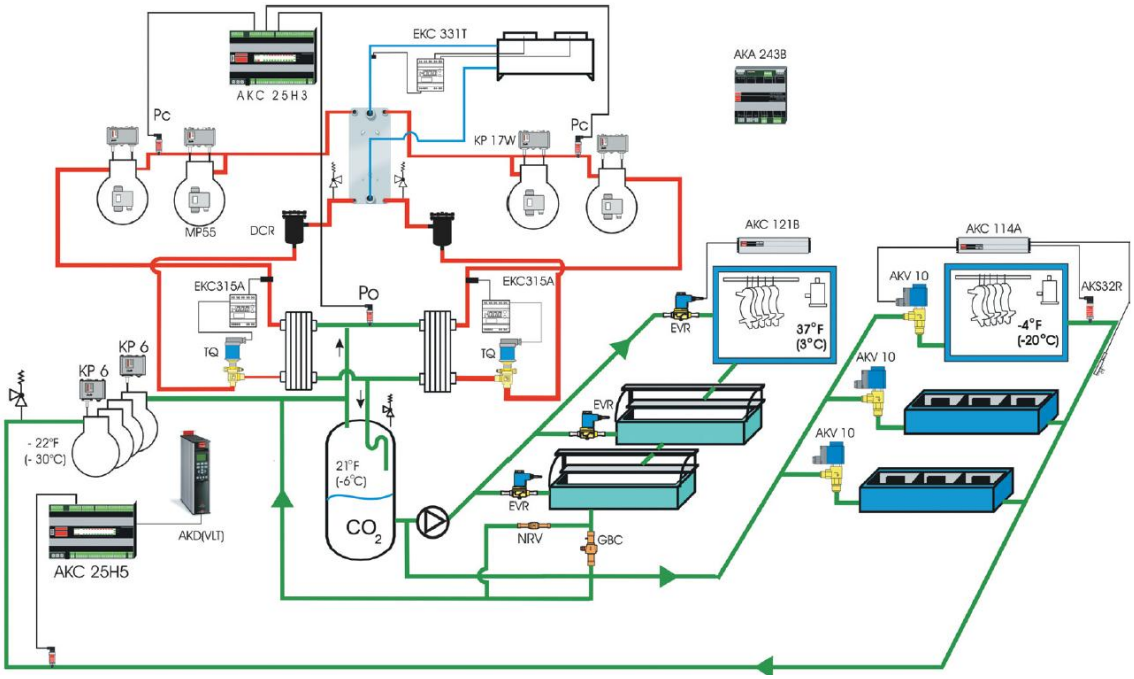

Figure 2.20 Schematic diagram of CO_2 / R404A refrigeration system (Danfoss, 2003)

A publication by Danfoss in 2003 (Danfoss, 2003) described R404A / CO_2 based installation in a 21,500 sqft supermarket in Copenhagen, shown in Figure 2.20. The driving force for this installation was the heavy tax on HFCs by the Danish government. The system used two R404A systems for the high stage. The two systems ensured that if one failed, the refrigeration would continue preventing the CO_2 from reaching high pressures. The medium temperature system was fed by a

pump with liquid CO_2 from a large receiver. The low temperature system used a single group of compressors and two plate heat exchangers connected to the R404A side to condense the refrigerant. The initial cost of the system was higher than for an all HFC system but more recent systems were nearer to the cost of a traditional HFC system. There were no running costs available.

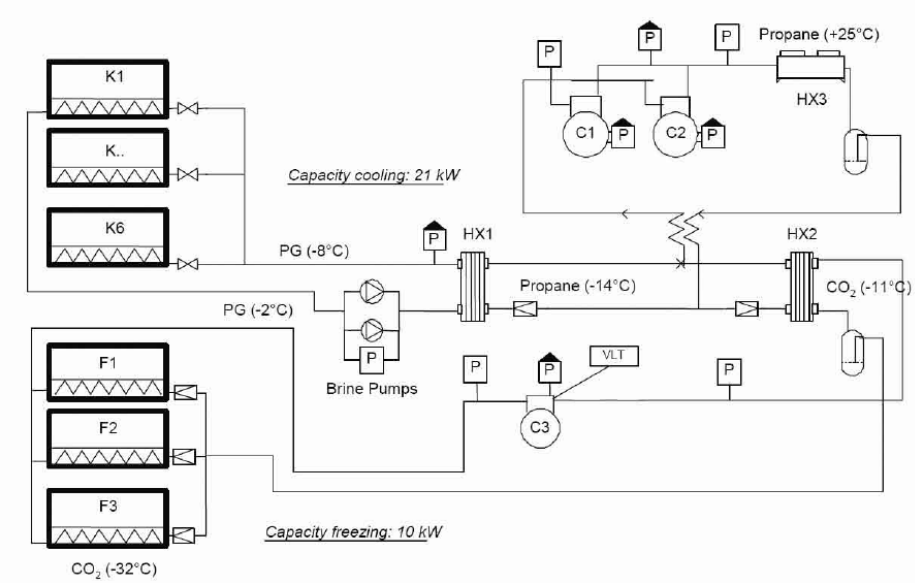

Figure 2.21 Schematic diagram of R290 / CO_2 refrigeration system (Christensen and Bertilsen, 2004)

The Danish supermarket Fakta Beder installed a R290 / CO_2 system. The system design and energy analysis was presented by Christensen and Bertilsen in 2004 (Christensen and Bertilsen, 2004). The system used R290 for the high side, pumped glycol for medium temperature and cascaded CO_2 for the low temperature, shown in Figure 2.21. The size of the system is small, only 21 kW of medium temperature refrigeration and 10 kW of low temperature refrigeration. When compared to eight very similar supermarkets using DX systems with R404A the energy consumption was 5% less than the average of the eight conventional supermarkets. However, the installation required an additional investment of 12–20 % compared to the R404A installation.

The UK supermarket industry has been using CO_2 as a refrigerant in supermarkets since 2005. Of the main UK supermarket retailers, Sainsbury's were the first to use CO_2 as a refrigerant, which was a subcritical cascade system with R404A at its Clapham store in 2005. The system consisted of a high temperature pumped CO_2 system and a low temperature direct expansion subcritical CO_2 cycle. There were no results available for this system.

Hinde, (2009) presented a paper on CO_2 in North American supermarkets. After the laboratory testing of low temperature CO_2 secondary system in 2001 and the first trial installation in 2006, by 2008 nine systems had been installed in the US and Canada. The paper presented an energy analysis which was performed on three different low temperature systems, a DX HFC system, a low temperature cascade pumped CO_2 system and a low temperature cascade DX CO_2 system. The results of the model showed that the low temperature cascade pumped system could save between 0 – 5% of annual energy and the cascade DX system could save between 3 – 5% of annual energy compared to the low temperature DX HFC system. Both the CO_2 systems also offered considerable savings in copper pipe work (Hinde, 2009).

Silva, (2010) presented a paper of the energy efficiency comparison of 3 supermarket refrigeration systems. A conventional R404A system, a conventional R22 system and a subcritical CO_2 cascade system. The cooling capacities were 20 kW for MT and 10 kW for LT. The systems were run week on week off so an accurate comparison could be made. The cascade solution used pumped CO_2 for the MT requirements and direct expansion LT cascaded with R404A. The CO_2 solution outperformed the R404A only solution by 24.67% and the R22 solution by 15.47%, although the initial cost of the CO_2 system was 18.5% higher than the other solutions. The R404A charge of the cascade system was only 15 kg while the conventional R404A system had a charge of 125 kg. The comparison proved that the CO_2 cascade R404A system can provide superior performance and a more environmentally friendly solution. An image of the three systems is shown in Figure 2.22.

Figure 2.22 Image of CO_2/R404A Cascade, R22 and R404 refrigeration systems trailed by Bitzer for supermarket refrigeration (Silva *et al.*, 2010)

2.9.2 Transcritical cycles

As previously explained, the transcritical cycle operates with supercritical heat rejection and subcritical evaporation. The supercritical heat rejection only occurs when CO_2 is unable to reject heat to the ambient due to high ambient temperatures approaching the critical temperature of CO_2. A transcritical system can therefore operate as a subcritical system when ambient temperatures are below the transition temperature. The transition temperature depends on the ability of the condenser to reject heat but has been reported to be above 22°C (Campbell *et al.*, 2007). At temperatures above this supercritical heat rejection take place by gas cooling the refrigerant.

The benefits of the transcritical cycle are the ability to use an all CO_2 system without the need of a cascade condenser and an additional vapour compression cycle with another refrigerant. Using CO_2 for heat rejection is much safer than using cascaded Ammonia or Propane. Both Ammonia and Propane cannot be used when they cannot be located a safe enough distance away from the public. Using CO_2 for heat rejection

is also much more environmentally friendly than using cascaded HFCs, due to their high GWP.

However, the increased indirect CO_2 emissions as a result of the reduced energy performance of CO_2 operating in a transcritical cycle at high ambient temperatures must be taken into account when analysing the overall environmental performance of a transcritical CO_2 system. There are a number of different transcritical cycles which will be explained in the next section.

Tesco in the UK installed a transcritical CO_2 refrigeration system for providing 38.5 kW of MT refrigeration. The cycle operated in a subcritical cycle when the ambient temperature was below 22°C. Campbell *et al.*, (2007) reported improved heat transfer performance in the CO_2 cabinets which also had a build up of ice; this was rectified by increasing the evaporation temperature which increased the performance of the system. A schematic diagram of the system is shown in Figure 2.23.

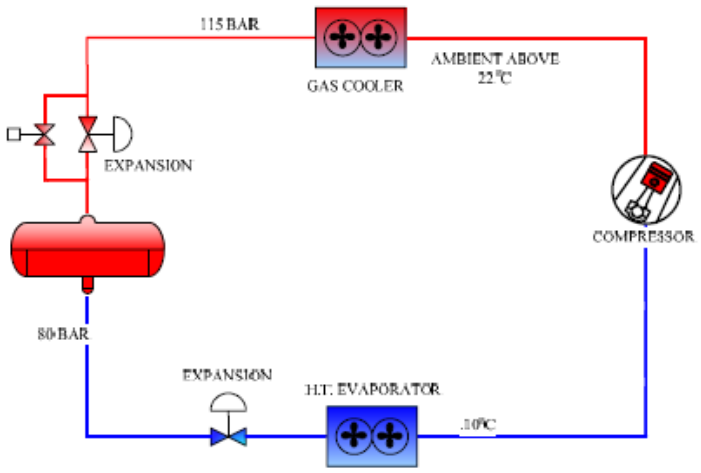

Figure 2.23 Schematic diagram of transcritical system installed at Tesco Swansea (Campbell *et al.*, 2007)

Dual temperature systems use CO_2 for both MT and LT refrigeration. Girotto *et al.*, (2004) presented the results of an all transcritical CO_2 system operating in a 1200 m^2 supermarket in the north of Italy, shown in Figure 2.24. This was a relatively large

system with 120kW of MT refrigeration and 25kW of LT refrigeration. The system operated in a transcritical cycle when the ambient temperature was above 15°C. The energy consumption during one year was estimated to be 10% higher than that of an equivalent R404A system with an additional cost of about 20%. Girotto also identified possible system improvements including flashing gas from an intermediate receiver to get a lower refrigerant quality at the evaporator inlet and higher evaporator capacity and also using a two stage compression system for the MT refrigeration. Laboratory test data for this system including the improvements increased the performance by 27%.

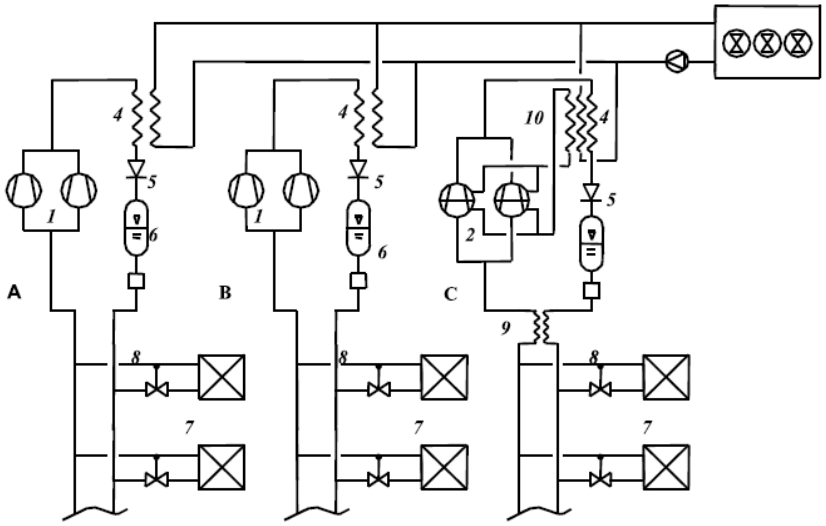

Figure 2.24 Schematic diagram of transcritical system (Girotto, Minetto and Neksa, 2004/11)

Other transcritical systems which have been installed include the Carrier CO2OLTEC™ (Haff *et al.*, 2005). This system uses transcritical CO_2 directly for the MT refrigeration and a cascade subcritical CO_2 system for the LT refrigeration, Figure 2.25. This system has seen a rapid growth of installations in the central and northern European supermarkets and Carrier are now offering a booster version of this system where low temperature compressors are connected directly to the suction side of the medium temperature compressors. Carrier have installed over 300 of these

systems over central and northern Europe and are promoting increased efficiencies of 10% versus a traditional HFC or CO_2 cascade system (Brouwers and Serwas, 2011).

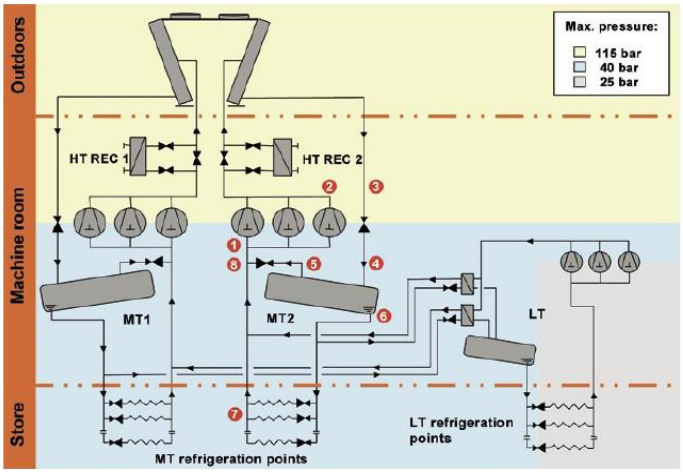

Figure 2.25 Schematic diagram of carrier CO2OLTEC refrigeration system (Haff, *et al.*, 2005)

2.9.2.1 Transcritical booster system

Most transcritical cycles installed follow the principle of using a separate cascade CO_2 cycle for the LT refrigeration. The transcritical booster cycle avoids the use of a separate cascaded cycle by integrating the LT refrigeration requirement into the primary transcritical cycle by the use of an additional 'booster' compressor. The LT compressor increases the pressure of the LT refrigerant to the MT refrigeration pressure whilst providing enough suction to satisfy the LT refrigeration. The avoidance of a separate cascade cycle is an advantage as it makes the system much easier to design and install. Figure 2.26 shows a schematic of the transcritical booster cycle and Figure 2.27 shows a pressure – enthalpy chart of the cycle.

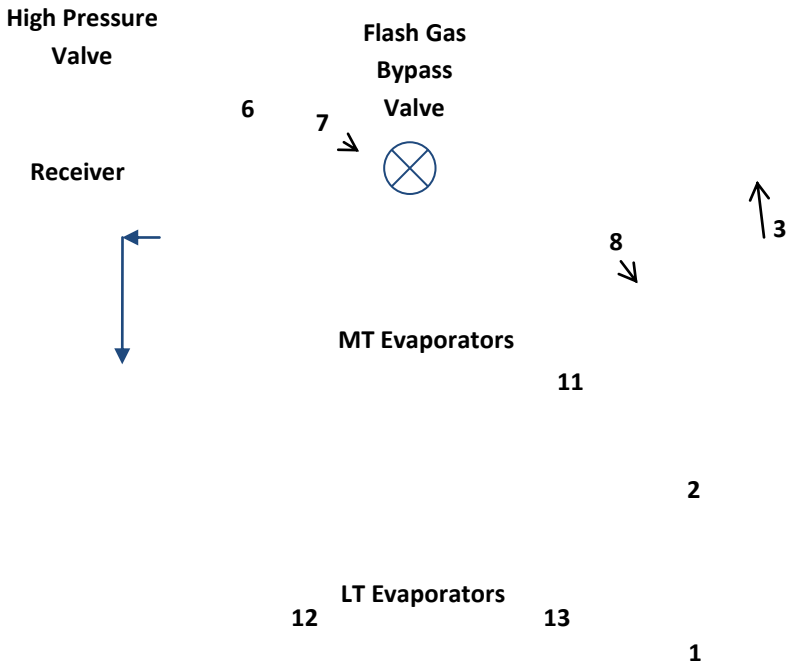

Figure 2.26 Schematic diagram of CO_2 Booster refrigeration cycle

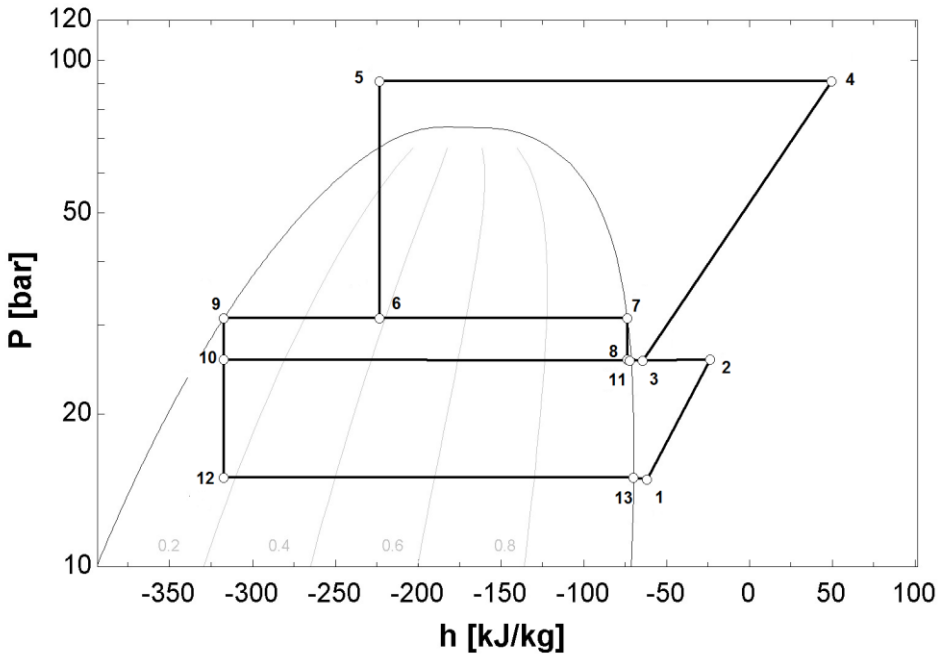

Figure 2.27 Pressure – enthalpy chart of CO_2 booster refrigeration cycle

There have been a number of booster system installations. A trial system was installed in July 2006 by Epta in Juchen, Germany (Austin-Davies and Da Ros, 2007). Their objectives were to provide a practical and reliable system with a single pack to meet both MT and LT refrigeration loads. The performance of the system in the winter months was as good as an equivalent R404A system.

Some results of a transcritical booster CO_2 system were presented by the DTI (Danish Technical Institute) (Madsen, 2007), Figure 2.29. The system was installed in a REMA1000 discount store in Denmark in 2007. The system had MT capacity of 26 kW and a LT capacity of 10 kW, a small convenience store type system. The energy used by the transcritical booster system was 4% less than a conventional R404A system and the reduced the TEWI by 50%. Figure 2.27 shows a schematic diagram of the booster cycle. Overall the system installation was considered to be a success and in the same year approximately 50 similar systems were installed in Denmark.

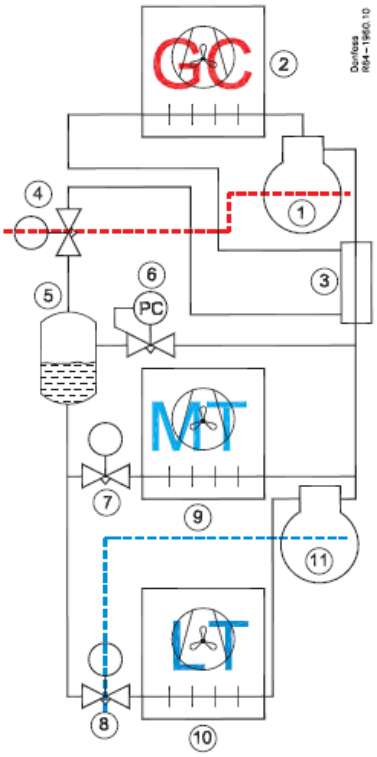

Figure 2.28 Schematic diagram of transcritical Booster CO_2 refrigeration system (Danfoss, 2008)

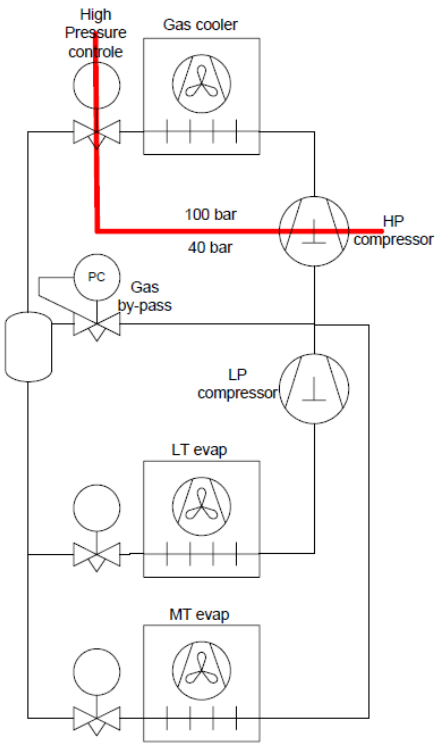

Figure 2.29 Schematic diagram of transcritical booster system (Madsen, 2007).

Danfoss (2008) presented a paper on the design and performance of a booster system installed at a small discount supermarket in Denmark, Figure 2.28 The system was proven to be very efficient and reliable with and energy consumption which was lower than a comparable R404A system. The system did have some problems though, due to the sizing of the high pressure and low pressure compressors. A frequency inverter was installed on the HP compressor which helped but the solution was described as being 'far from perfect'. Danfoss have made improvements to the booster system presented in a paper in 2011 (Danfoss, 2011) promoting their improvements as a 2nd generation system. The 2nd generation CO_2 booster systems are 10% more energy efficient than the R404A system. Improvements were made to control algorithms, part load capacities and smoothing the control of the gas bypass.

2.10 Supermarket review

From the early prototype CO_2 supermarket installations, there has been a rapid growth in the number of installations in supermarkets worldwide. Unlike the conventional separate HT and LT R404A multi compressor systems which have been the UK standard for supermarket refrigeration systems, there has not yet been a standardised design for CO_2. As described in the previous section there are a number of different systems available and each supermarket is taking a different approach. There have been a number of documents published detailing the type and number of systems installed in Europe, of which the following summary has been compiled. Recently Shecco (2012) published a report on the natural refrigerant market growth for Europe. Figure 2.30 is a figure from the report showing the number of transcritical supermarket systems in Europe, reportedly 1331 at the time of the publication with 267 of the systems in the UK. Shecco also published a similar report in 2009 (Shecco, 2009), the estimate at that time was approximately 250 systems in Europe, with over 100 installed in Denmark as of September 2008. This equates to an increase in 1081 CO_2 systems installed from September 2008 to November 201l and indicates European confidence in transcritical CO_2 systems in Europe particularly in Denmark, the United Kingdom, Germany, Switzerland,

Norway and Sweden. These countries all have an average ambient temperature well below the critical point of CO_2, so the systems would only be operating transcritically for a fraction of the year, if at all.

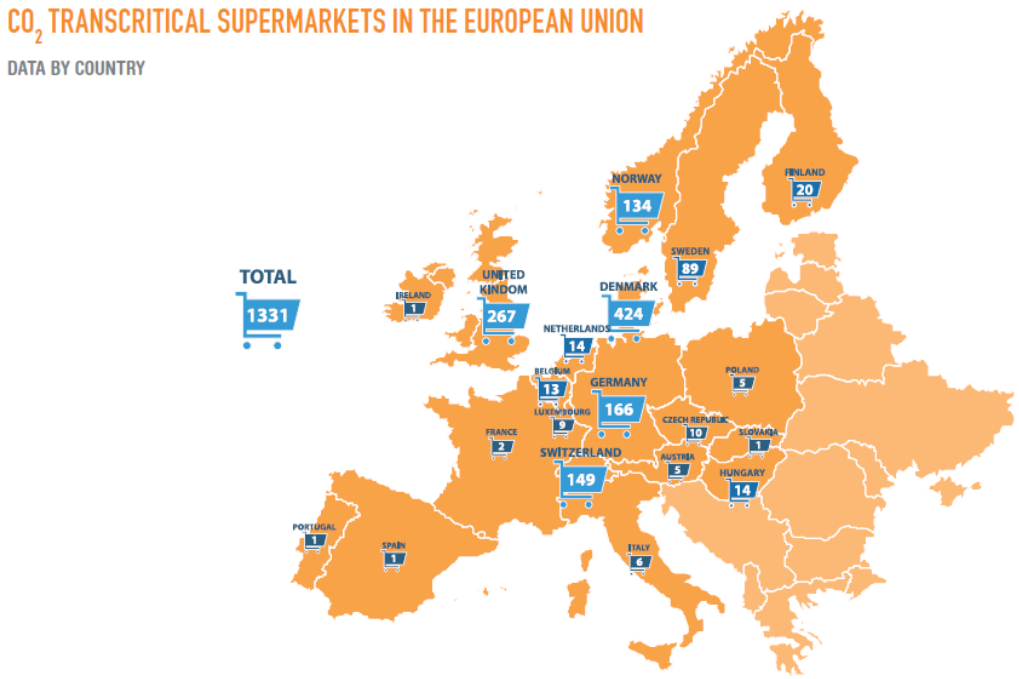

Figure 2.30 Transcritical CO_2 supermarkets in the European Union (Shecco, 2012)

Three published reports by the Environmental Investigation Agency (EIA) (EIA, 2011; Walravens and Hailes, 2010; Walravens and Hailes, 2009) outlined the results of surveys sent to the main supermarket operators in the UK, on their intentions to move away from using HFCs in their refrigeration systems. Figure 2.31 combines the results of the three reports on the number of CO_2 or HC based systems in each of the supermarkets from 2008 – 2011. Waitrose and Marks & Spencer are using combinations of HC, HFC and CO_2 systems (Arthur, 2011). In the UK CO_2 based supermarket installs have increased from a total of 16 in 2009 to 239 in 2011, an increase of 223. The difference in the Shecco and EIA results could be the timing of the publication of each report. This is a large increase in CO_2 based systems and is predominantly due to the transcritical CO_2 systems being installed by Sainsbury's. Sainsbury's opened its 100th CO_2 store (R744, 2012) in early 2012 and has set a

milestone of 250 stores by 2014. Initially, during 2009 – 2010 Tesco was leading the charge with CO_2 refrigeration install projections in the media, quoting 150 installs by 2012 from only 5 installs in 2009 (Walravens and Hailes, 2010). Two explosions inside Tesco supermarkets with CO_2 systems both due to pipe rupture has halted the rate of Tesco CO_2 installs in the UK (Milnes, 2011; Milnes, 2010). What is encouraging about the UK market for CO_2 refrigeration systems is the increase in the number of installs without any government taxes on HFCs being introduced as has happened in Denmark and Norway.

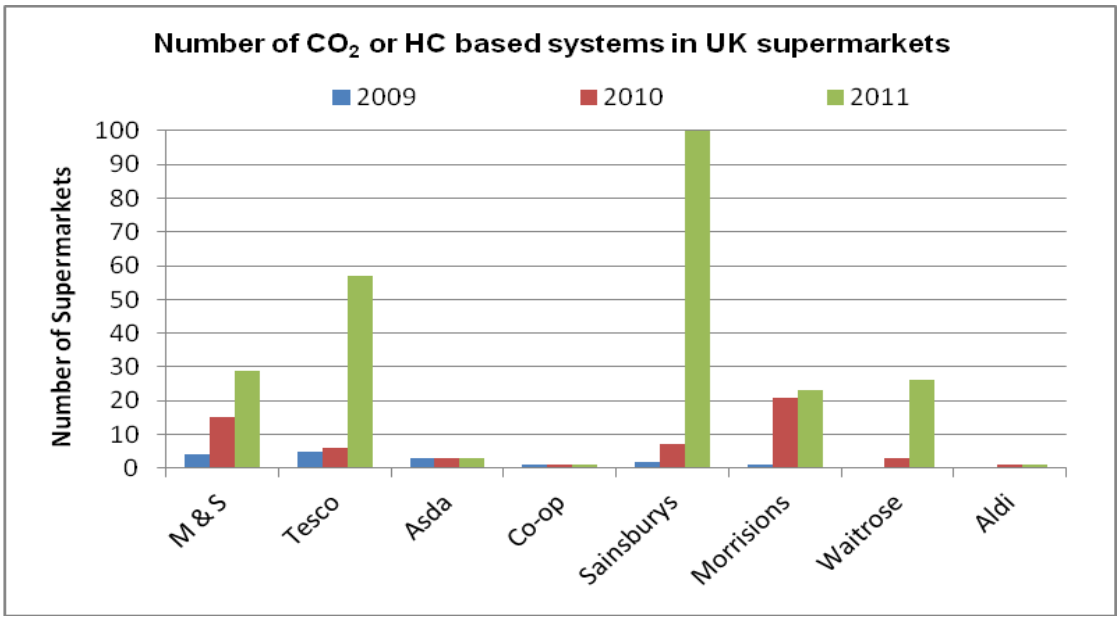

Figure 2.31 Number of CO_2 or HC based systems in UK supermarkets

2.11 Distribution of Supermarkets in Northern Ireland

From a review of available information on the number of supermarkets in Northern Ireland in 2010, Table 2.5 was compiled (Carbon Trust, 2010). The table shows the retailer name and the number of supermarkets including details on the size, category and the total average MT and LT refrigeration capacities. The average capacities were calculated using the average MT and LT capacities from each category in Table 2.1. There are approximately 298 small shops, 615 small supermarkets, 310 larger

supermarkets and 81 superstores. Both the small supermarkets and the superstore numbers are on the rise but the supermarket sized store numbers have fallen. The supermarket sized stores are being bought over and closed down by the superstores, which are relocating to out of town locations. There is a large rural population in Northern Ireland, located too far from the larger superstores so they generally shop in the small shops and small supermarkets for convenience.

Figure 2.32 is a chart showing the total average distributed refrigeration capacity of supermarkets in Northern Ireland. The supermarkets have the largest distributed refrigeration capacities; these stores include City and Town centre supermarkets such as Marks and Spencer, Co-Op and the Northern Ireland based retailers Eurospar and Supervalu. CO_2 refrigeration solutions for this size of supermarket have been installed in the UK. The CO_2 systems for this size of store are similar in design to the superstore sized systems as the same components can be used.

The total average refrigeration capacity for the small supermarkets in Northern Ireland is estimated to be 23,370 kW, only 18% lower than that of the supermarkets. There have been many installations using CO_2 across the UK for the larger supermarkets and superstores but only a small number of installations in small supermarkets. An appropriate CO_2 refrigeration solution for the smaller supermarket sized stores would lead to a significant reduction in the environmental impact of refrigerant leakages.

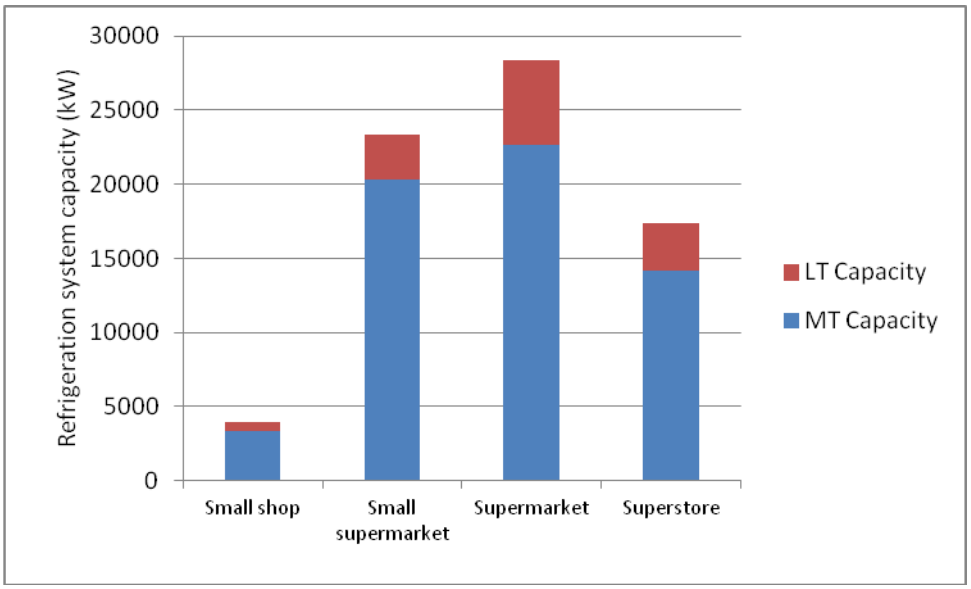

Figure 2.32 Average total distributed refrigeration capacities of supermarkets in Northern Ireland

Table 2.5 Number of Supermarkets in Northern Ireland by retailer (Carbon Trust, 2010)

Retail group	No. Of Stores in NI	Average retail area per store (m^2)	Total retail area per group (m^2)	Store category	Total average MT refrigeration capacity (kW)	Total average LT refrigeration capacity (kW)
Asda	14	2693	37702	Superstore	2450	560
Co-Op	36	431	15516	Supermarket	2628	666
Iceland	31	437	13547	Supermarket	2263	573.5
Lidl	23	929	21367	Supermarket	1679	425.5
Marks and Spencer	20	972	19440	Supermarket	1460	370
Sainsburys	10	3214	32140	Superstore	1750	400
Tesco : Superstore & Metro	34	2360	80240	Superstore	5950	1360
: Express	9	189	1701	Small supermarket	297	45
Costcutter	123	280	34440	Small supermarket	4059	615
Hendersons: Eurospar / Vivo Extra	6	498	2988	Supermarket	438	111
: Spar / Vivo	64	234	14976	Small supermarket	2112	320
: Independents	400	232	92800	Small supermarket	13200	2000
Musgrave : Supervalu	42	1115	46830	Supermarket	3066	777
: Centra	82	465	38130	Supermarket	5986	1517
: Mace	149	139	20711	Small shop	1676.25	298
XL Stop n Shop	53	93	4929	Small Shop	596.25	106
Day Today	96	74	7104	Small shop	1080	192
NISA : Todays	70	465	32550	Supermarket	5110	1295
Dunnes	23	2000	46000	Superstore	4025	920
Shop 4 U	19	242	4598	Small supermarket	627	95
Totals	**1304**	**17062**	**567709**			

2.12 Summary

The impact from the leakage of HFC refrigerants can account for up to 11% of the total carbon emissions from supermarkets. This is due to the high GWP of HFC refrigerants currently used in supermarket refrigeration systems. HFCs were invented as replacements for CFCs and HCFCs before the high GWP of the refrigerants was an issue due to the adoption of the Kyoto Protocol in 2006. The inclusion of HFCs as one of the six gases in Kyoto Protocol has forced member countries to act on reducing the emissions of HFCs. In the UK the focus has been on containment, enforcing regular leak checks of systems and that engineers are suitably qualified to work with HFC systems. These regulations, coupled with environmental pressures, has made supermarket operators search for refrigerants which are environmentally sound and will not adversely affect the energy performance of the systems.

The literature review revealed a lack of research in the utilisation of the high heat transfer properties of CO_2 to increase the efficiency of finned tube evaporators used in refrigerated multi-deck cabinets for supermarkets. An increase in the heat transfer efficiency of the evaporator could lead to a reduced material content, reducing the associated embodied energy and environmental impact of supermarket refrigeration systems.

The review of literature in Chapter 2 has revealed a resurgent interest in the use of CO_2 as a refrigerant in supermarket refrigeration systems. There has been a significant growth of CO_2 based systems in the UK with all of the major supermarkets having trialled systems and most planning a high number of future installations. The large variety of commercial and experimental systems using CO_2 in a subcritical and transcritical cycle was also reviewed; concluding that unlike traditional R404A systems there was no single system design that has been adopted. There have been many installations using CO_2 across the UK for the larger supermarkets and superstores but only a small number of installations in small supermarkets. An appropriate CO_2 refrigeration solution for the smaller supermarket

sized stores would lead to a significant reduction in the environmental impact of refrigerant leakages.

Chapter 3 Simulation models design

3.1 Introduction

This chapter describes the development of numerical simulation models used to simulate the components and the behaviour of a refrigeration system. The simulation models have been used to research the performance of a CO_2 refrigeration system suitable for small supermarkets. A model has also been developed to investigate how the geometry of a finned tube heat exchanger can be redesigned to utilise the reported high heat transfer capabilities of CO_2.

Numerical models enable a thermodynamic analysis of refrigeration cycles and components without the expense and time associated with an experimental facility. A numerical model is also an essential part for the selection of components for an experimental system before manufacture though the simulation of the proposed cycle using mathematical equations and laws of thermodynamics.

3.2 Simulation software and models

The mathematical models of the system have been developed using EES (Klein and Alvardo, 2002). EES (Engineering Equation Solver) is a mathematical based piece of software; its basic function is to provide the numerical solution to a set of algebraic equations, which must be inputted. EES can also be used to solve differential and integral equations, do optimization, provide uncertainty analyses and linear and non-linear regression, convert units and check unit consistency and generate publication-quality plots. EES provides many built-in mathematical and thermo physical property functions for refrigerants, useful for engineering calculations.

The models which have been developed using EES are as follows:

1. **Refrigeration system simulation models**

Two different refrigeration models have been simulated using the EES software. The simulation results of both models have been analysed and compared with the aim of reducing the environmental impact of a small supermarket refrigeration system by reducing the equivalent direct and indirect CO_2 emissions.

- **Transcritical CO_2 booster refrigeration system**
  A supermarket using a CO_2 booster refrigeration system combining the MT and LT refrigeration requirements into a one refrigeration system.

- **R404A refrigeration system**
  A conventional R404A small supermarket using separate refrigeration systems for the LT and MT refrigeration systems.

2. **Evaporator simulation model**

The evaporator is a finned tube type, which is used in refrigerated multi-deck display cabinets used in all supermarkets. The geometry of the evaporator will be altered and the results of the simulations analysed and compared using CO_2 as the refrigerant. The objective of this research is to improve the heat transfer performance of the evaporator with the aim of reducing the environmental impact of the supermarket refrigeration system. The performance of the evaporator is affected by resistances outside the tubes (air side) and inside the tubes (refrigerant side). Both of these will be issues affecting the performance of the evaporator, which will be investigated.

3.3 Refrigeration system models

3.3.1 Transcritical CO_2 booster refrigeration system

This system combines both the MT and LT refrigeration loads into one refrigeration cycle. A schematic diagram of the cycle is shown in Figure 3.1. The design of the system is similar to that presented by Madson (2007). The cycle is basically a transcritical MT refrigeration cycle with a LT 'booster' compressor added to the cycle, making the cycle two stage. The compressed high pressure refrigerant is either condensed or gas cooled if the cycle is operating transcritically. The ICMT valve or high pressure valve (HPV) separates the high pressure (HP) side of the system from the medium pressure (MP) side. The valve maintains the high pressure side of the cycle at the optimum gas cooling pressure, which will be explained in more detail in later sections. From the high pressure valve the receiver is held at the medium pressure by the flash gas bypass valve. The receiver also acts as a separator with liquid refrigerant flowing to the evaporators and vapour refrigerant flowing directly to the HP compressor suction line. Figure 3.2 shows a pressure - enthalpy diagram of the cycle.

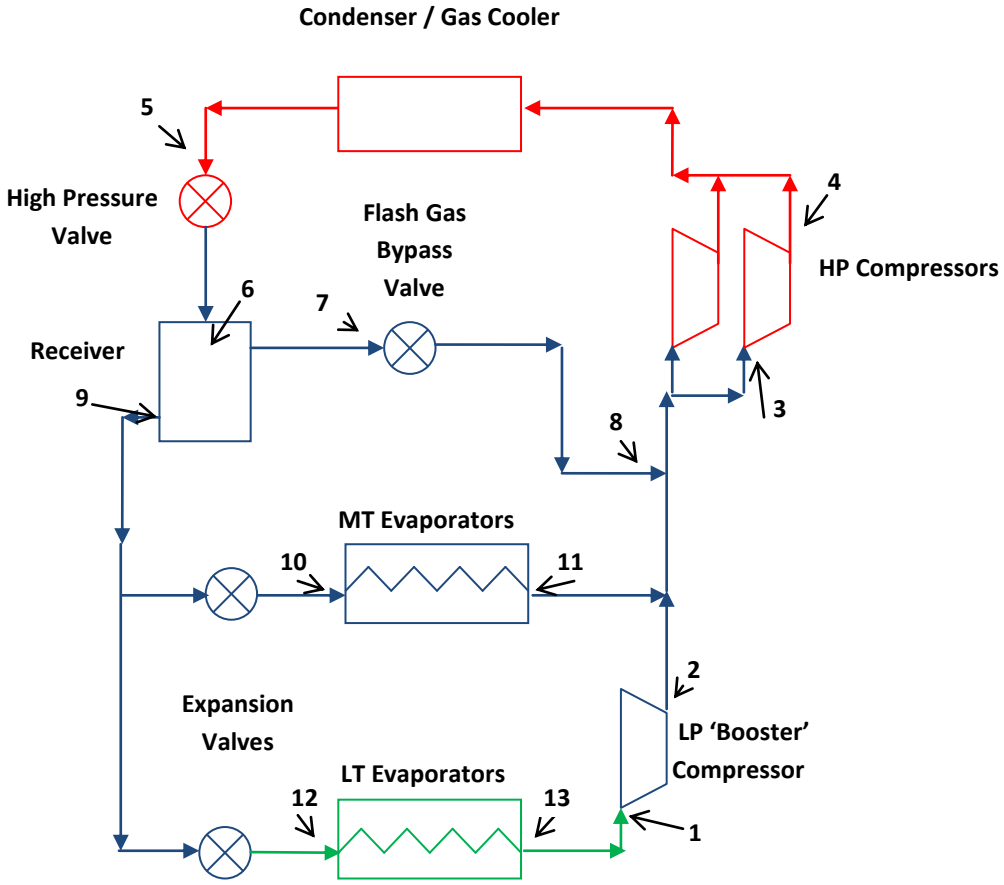

Figure 3.1 Schematic diagram of CO_2 Booster refrigeration cycle

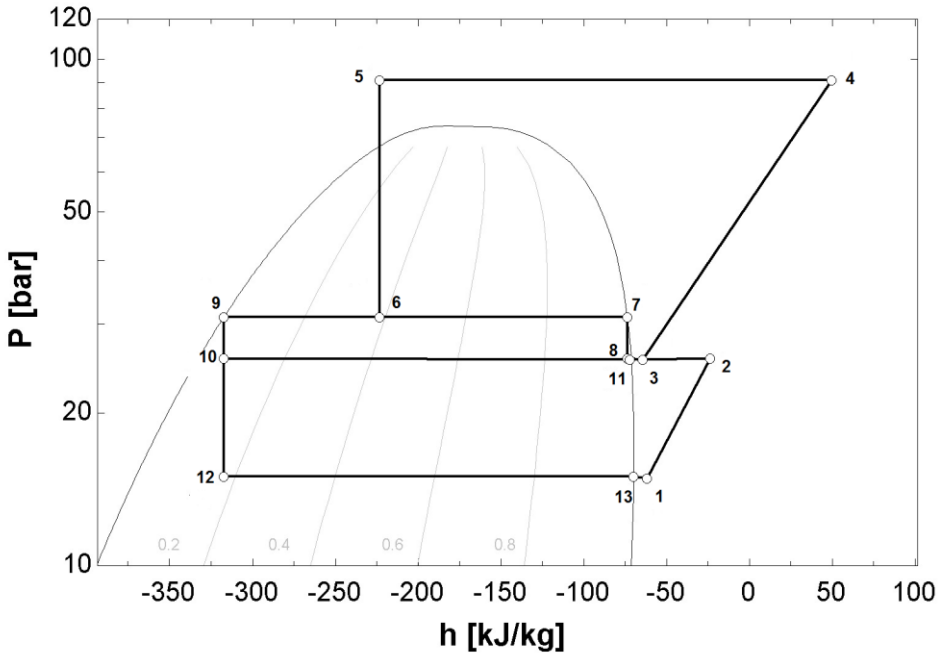

Figure 3.2 Pressure – enthalpy chart of CO_2 booster refrigeration cycle

3.3.2 Compressors

There are two compression points in the cycle, a low pressure (LP) compressor, which compresses the refrigerant from the LT evaporator pressure to the MT evaporator pressure and a HP compressor, which compresses the refrigerant from the MT evaporator pressure to the condensing / gas cooling pressure. The compression processes are shown on the cycle pressure - enthalpy chart in Figure 3.2. The work of the compressors is calculated by equations 3.1 and 3.2.

$$W_{LP} = \dot{m}_{LP} \times (h_2 - h_1) \quad \textbf{(3.1)}$$

$$W_{HP} = \dot{m}_{HP} \times (h_4 - h_3) \quad \textbf{(3.2)}$$

The enthalpy before compression (h_1, h_3) is calculated from the pressure and temperature of the refrigerant at this point. The enthalpy after compression (h_2, h_4) is calculated using the isentropic efficiency (η_{is}), of the compressor as shown in equation 3.3.

$$h_2 = \frac{(h_{2is} - h_1)}{(\eta_{is})} + h_1 \quad \textbf{(3.3)}$$

The actual isentropic efficiency of the MT and LT CO_2 compressors was calculated from preliminary test results from the experimental system at Brunel University using Equation 3.4. The ideal isentropic enthalpy of the refrigerant out of the compressor (h_{2is}) was calculated by assuming isentropic compression. The other points were calculated using the test data.

$$\eta_{is} = \frac{(h_{2is} - h_1)}{(h_2 - h_1)} \quad \textbf{(3.4)}$$

$h_2 = f(t_2, p_2)$ = Refrigerant enthalpy out of compressor **(3.5)**

$h_1 = f(t_1, p_1)$ = Refrigerant enthalpy into compressor **(3.6)**

Figures 3.3 to 3.6 shows the experimental isentropic efficiency of the MT compressor and the experimental data used to calculate the isentropic efficiency.

Figures 3.7 to 3.10 shows the experimental isentropic efficiency of the LT compressor and the experimental data used to calculate the isentropic efficiency. The average results over the test were 0.55 and 0.63 for the high stage and low stage respectively. Hundy (2008) commented that an average to good compressor isentropic efficiency would be approximately 65%.

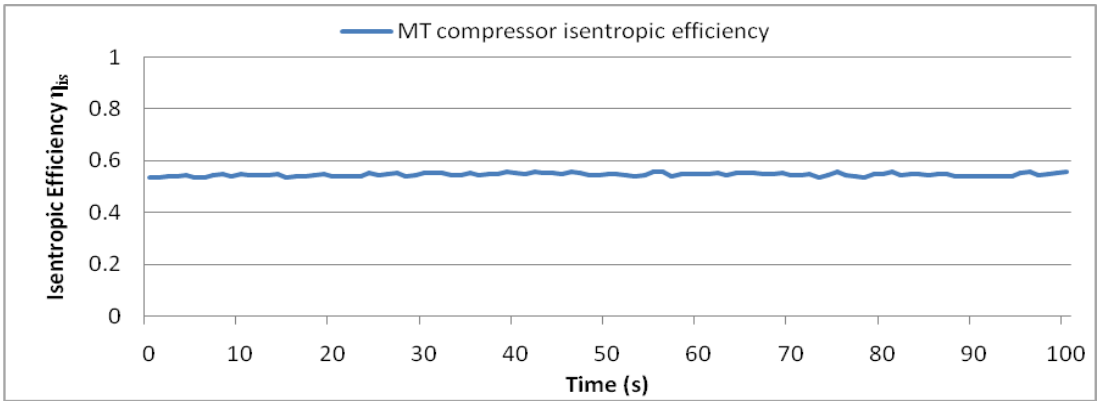

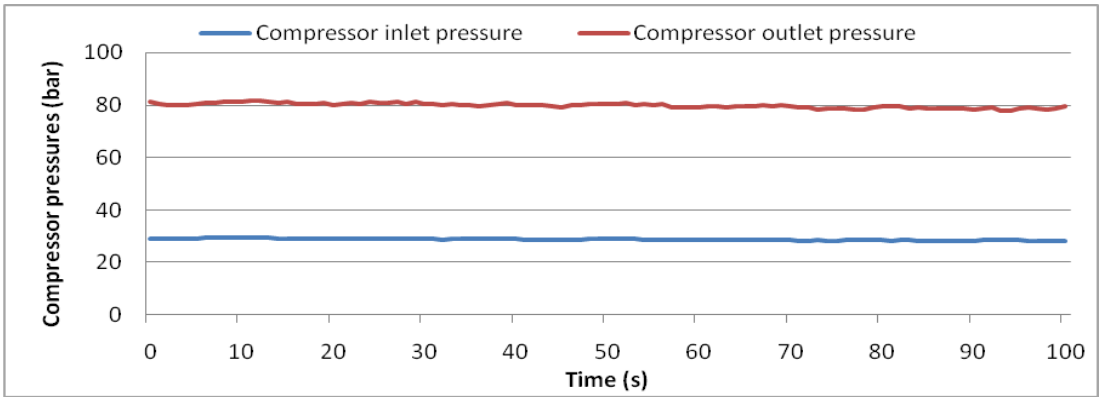

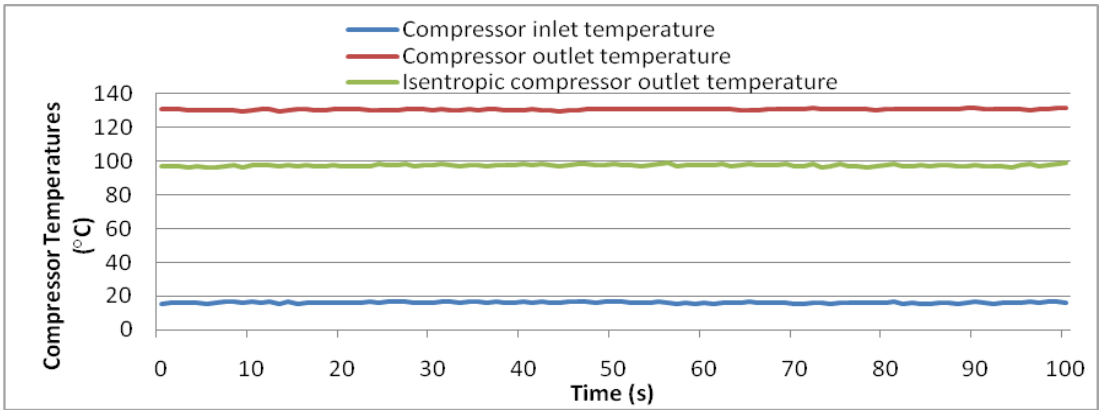

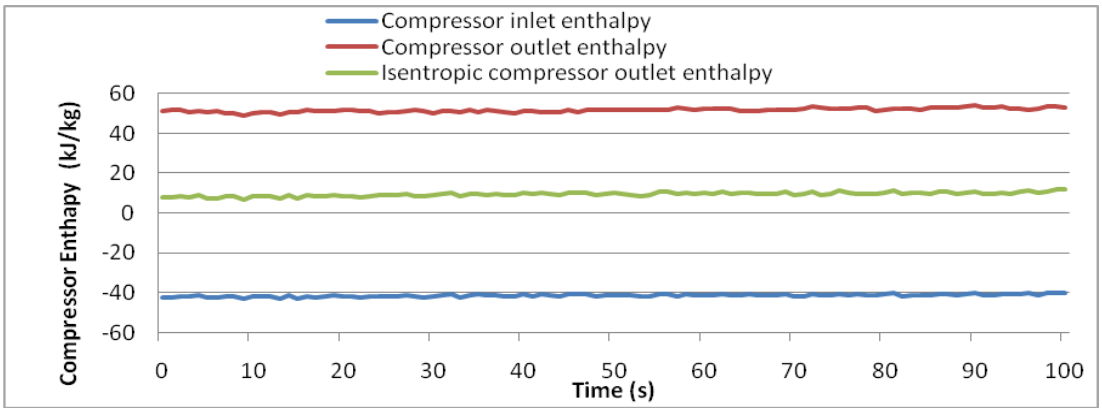

Figures 3.3, 3.4, 3.5, 3.6. Experimental isentropic efficiency of MT compressor calculation values

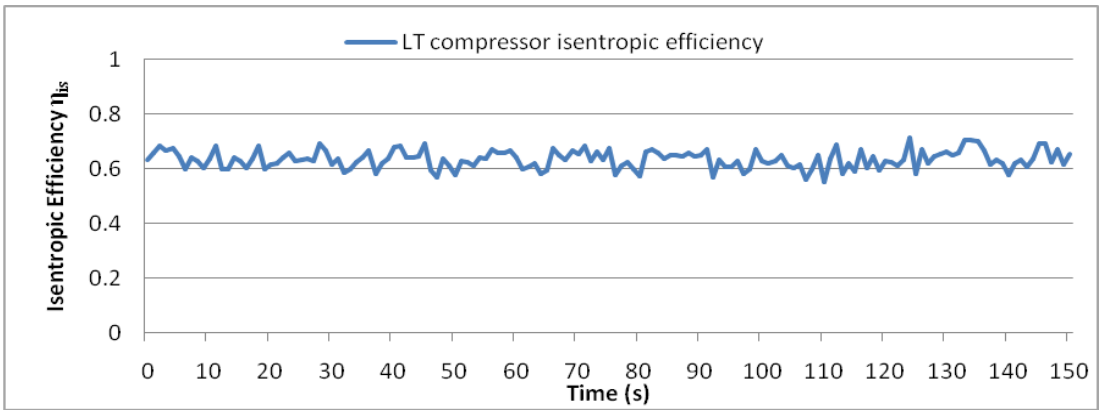

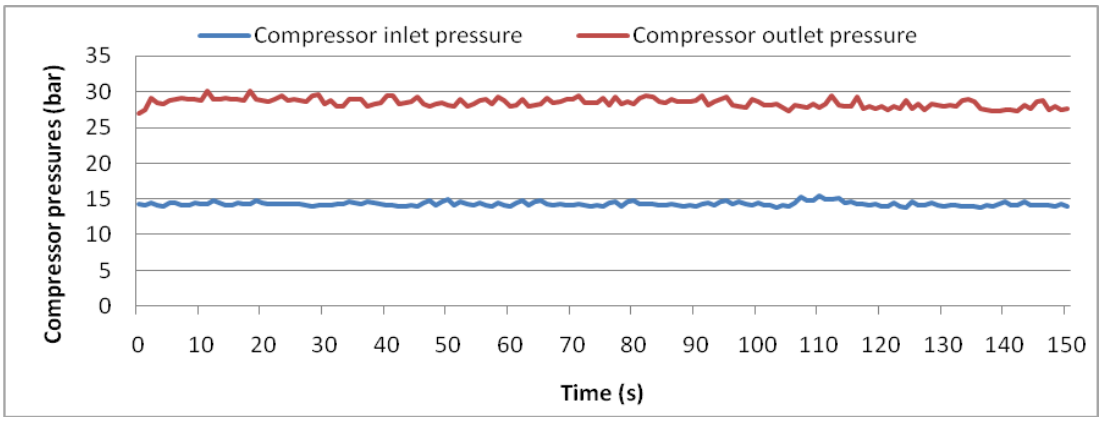

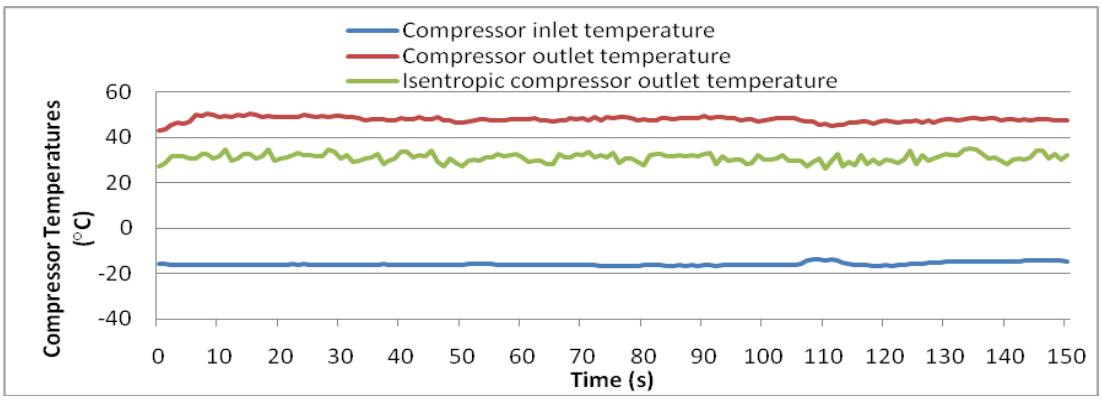

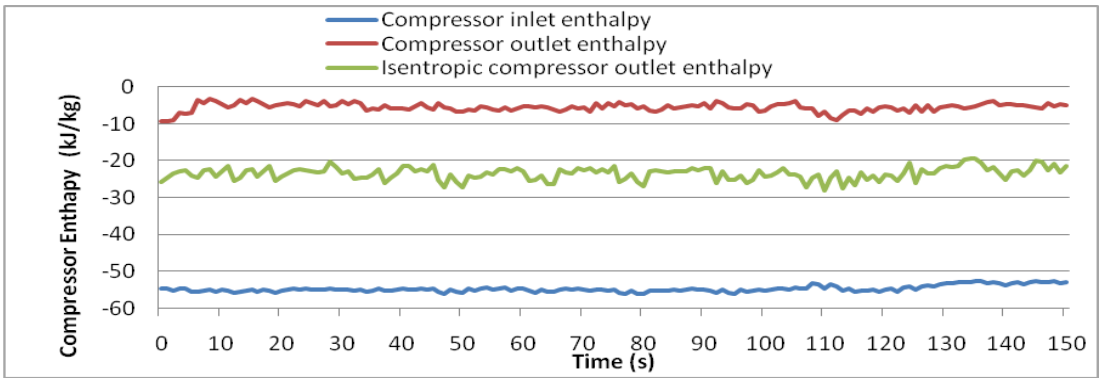

Figures 3.7, 3.8, 3.9, 3.10 Experimental isentropic efficiency of LT compressor calculation values

3.3.3 Condenser / Gas Cooler

When the condenser is unable to reject the heat of the refrigerant to a temperature below 31.1°C, the refrigerant rejects heat in a supercritical state. The refrigerant cannot be condensed as the heat rejection temperature is above the critical point of CO_2, therefore a gas cooling process occurs. At supercritical temperatures the pressure is independent of temperature as shown by Figure 3.11. An optimum gas cooling pressure exists for each gas cooler outlet temperature where the COP is at its maximum. An increase in gas cooler pressure increases the work done by the compressor but due to the 'S' shaped isotherms this also increases the enthalpy difference across the evaporator, increasing the cooling capacity of the evaporator shown in Figure 3.11.

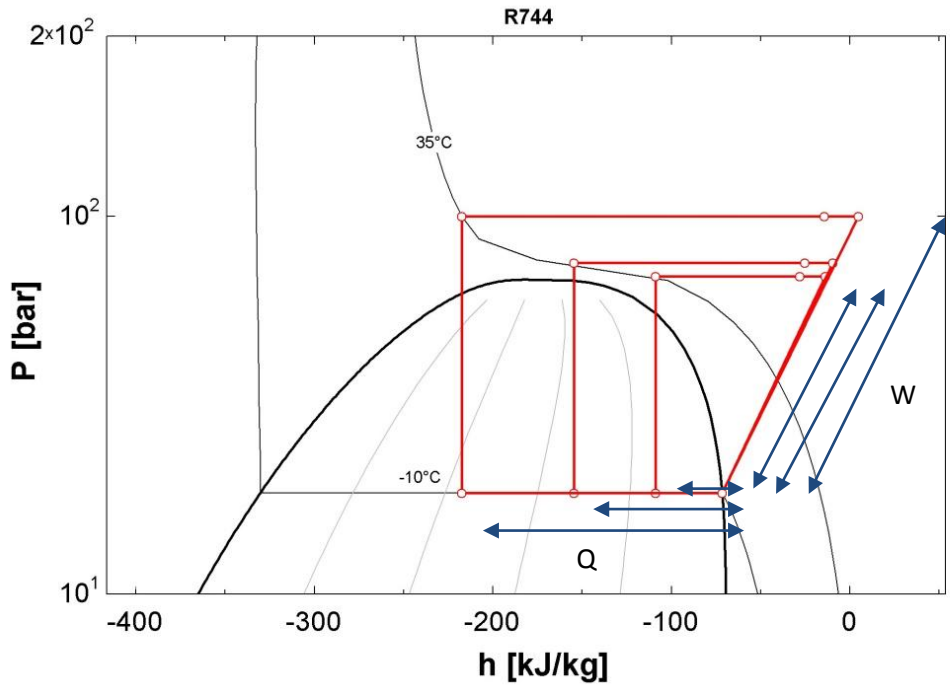

Figure 3.11 CO_2 Pressure – enthalpy chart showing that transcritical temperature, independent of pressure

The optimum gas cooling pressure for a transcritical system has been studied by many researchers. Kauf (1999) and Chen and Gu (2005) both concluded that the evaporating temperature has no significant effect on the optimum pressure. The efficiency of the compressor has a much greater effect on the optimum pressure as

discussed by Sawalha (2008) and more recently by Srinivasan (2010). The CO_2 system was simulated using a range of different gas cooling temperatures shown in Figure 3.12. This figure shows the simulation of five fixed gas cooling temperatures. The evaporation temperatures of MT and LT evaporators were constant for all the simulations. As CO_2 was in a super critical state the refrigerant pressure was independent of the refrigerant temperature. The refrigerant pressure (gas cooler pressure) was increased for each of the five simulations and the COP of the cycle was calculated using Equation 3.7.

$$COP = \frac{Q_{LT} + Q_{MT}}{W_{LT} + W_{MT}} \tag{3.7}$$

Fitting a curve to the peak of each gas cooling temperature lead to the following correlation:

$$P_{GCopt} = T_{GC} \times 2.875 - 1.12 \tag{3.8}$$

This correlation agrees well with those presented by Kauf (1999), Chen and Gu (2005), Sawalha (2008) and Zang *et al.*, (2010) shown in Figure 3.13. This correlation is used in the simulation models in this thesis.

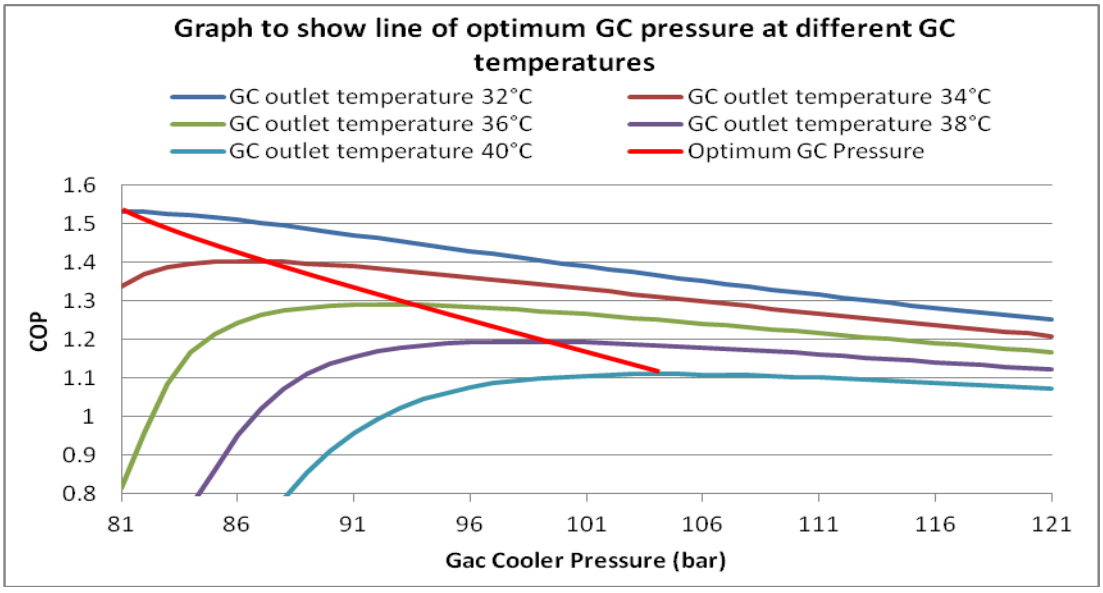

Figure 3.12 Optimum gas cooling pressure at different gas cooling temperatures

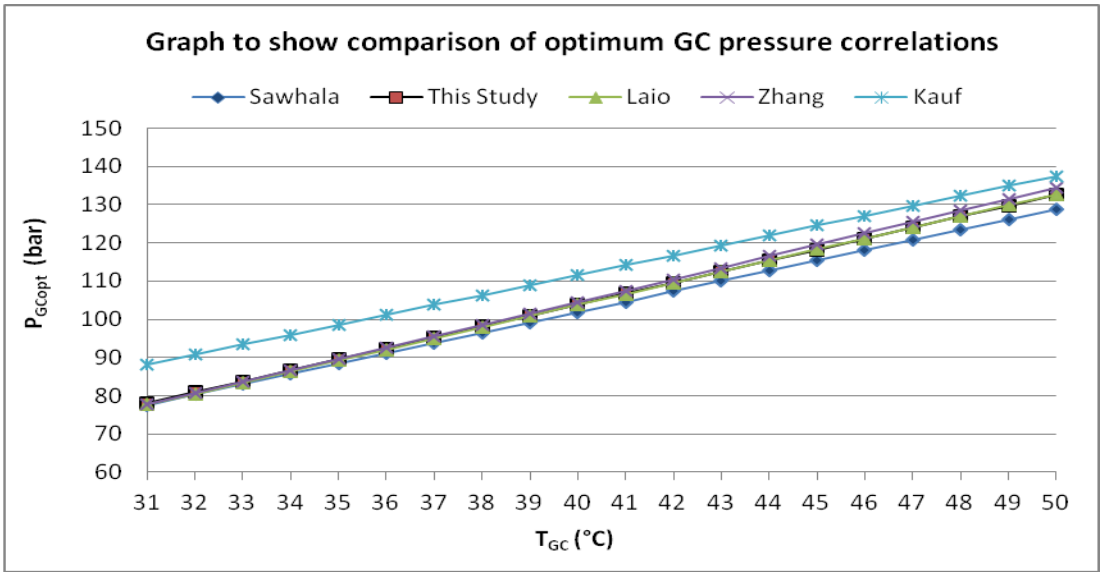

Figure 3.13 Comparison of optimum GC pressure correlations

The temperature difference between the outlet temperature of the gas cooler (T_{GC}) and the ambient temperature (T_{amb}) is the gas cooler approach temperature (T_{GCapr}), Temperature differential (TD) or the ΔT., equation 3.9.

$$T_{GCapr} = T_{GC} - T_{amb} \quad \textbf{(3.9)}$$

This value should be as low as possible and depends on the ability of the condenser / gas cooler to reject the heat. The lower the condenser / gas cooler outlet temperature, the lower the power consumption of the MT compressor, due to a lower compression ratio across the compressor. For these simulations an approach temperature of 10 K will be assumed, equal to that of a R404A system design. If the assumed approach temperature for a CO_2 system is lower than what a real system can achieve the simulation results will simulate a lower power consumption of the compressor than would occur in a real system. The assumed approach temperature value is therefore very important and will be verified with experimental results.

For transcritical operation, gas cooling temperatures above 31.1°C or ambient temperatures above 21.1ºC the gas cooler pressure and compressor discharge pressure is calculated by equation 3.8. For subcritical operation the condenser pressure is controlled by the condensing temperature set point.

3.3.4 High pressure valve

The high pressure valve (HPV) used in the booster system is used to set the optimum gas cooler pressure when the cycle is in transcritical operation. The high pressure valve process is highlighted in the pressure - enthalpy chart in Figure 3.14. This device also separates the high pressure side of the booster system from the medium pressure side and enables standard refrigeration grade copper components to be used for the medium and low pressure sides of the system. Figure 3.8 shows how the high pressure valve holds a pressure differential between the receiver pressure and gas cooler pressure at different gas cooler outlet temperatures. The valve expands the refrigerant from the optimum gas cooler pressure (P_{GCopt}) to the receiver pressure (P_r) when in transcritical mode and from the saturated liquid pressure from the condenser when in subcritical mode. For the simulation model the pressures and enthalpy values in and out of the valve are calculated as follows:

$$P_{HPVin} = P_{GCopt} \quad \textbf{(3.10)}$$

$$P_{HPVout} = P_r \quad \textbf{(3.11)}$$

$$H_{HPVin} = f\left(T_{GC}, P_{GCopt}\right) \quad \textbf{(3.12)}$$

$$H_{HPVout} = H_{HPVin} \quad \textbf{(3.13)}$$

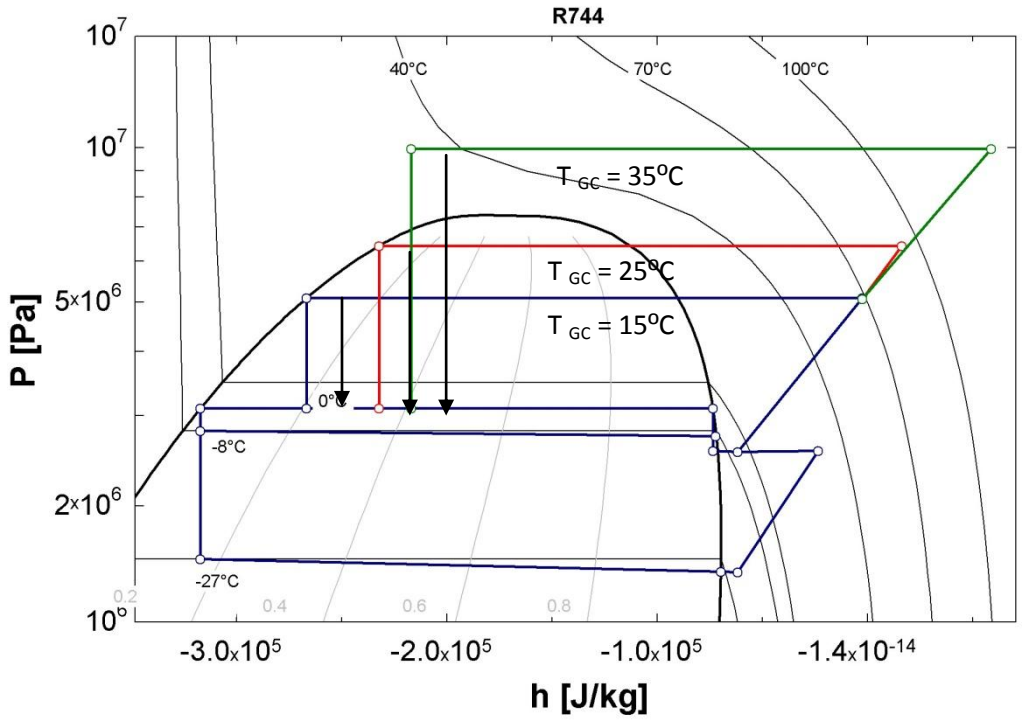

Figure 3.14 CO_2 Pressure – enthalpy chart showing refrigerant expansion from high pressure valve at different gas cooling pressures

3.3.5 Receiver / separator

The receiver in this cycle is used as a reservoir of refrigerant and as a liquid/vapour separator. The liquid refrigerant is sent directly to the evaporators and the vapour refrigerant is bypassed the evaporators and mixed with the evaporated refrigerant from the evaporators before compression, as shown in Figure 3.15. The gas bypass or flashing process also allows the user to alter the pressure the receiver is held at, by the use of a gas bypass valve. Adjusting the valve will release pressure to or from the receiver. The receiver pressure is therefore not dependent on the ambient temperature or the gas cooler temperature. To calculate the mass flow rate of the liquid and flash vapour, a mass – enthalpy balance is used as shown in equations 3.14 and 3.22.

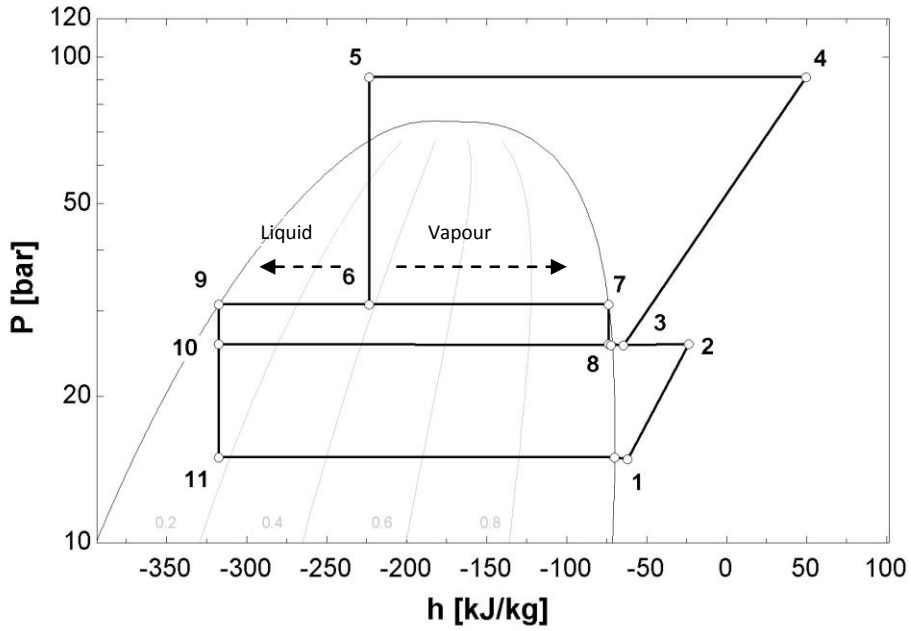

Figure 3.15 CO_2 Pressure – enthalpy chart showing receiver separation of liquid and vapour phases

$$\dot{m}_6 h_6 = \dot{m}_9 h_9 + \dot{m}_7 h_7 \quad \textbf{(3.14)}$$

$$\dot{m}_6 = \dot{m}_9 + \dot{m}_7 \quad \textbf{(3.15)}$$

$$\dot{m}_7 = \dot{m}_6 - \dot{m}_9 \quad \textbf{(3.16)}$$

$$\dot{m}_9 h_9 = \dot{m}_6 h_6 - \dot{m}_7 h_7 \quad \textbf{(3.17)}$$

$$\dot{m}_9 h_9 = \dot{m}_6 h_6 - (\dot{m}_6 - \dot{m}_9) h_7 \quad \textbf{(3.18)}$$

$$\dot{m}_9 h_9 = \dot{m}_6 h_6 - \dot{m}_6 h_7 + \dot{m}_9 h_7 \quad \textbf{(3.19)}$$

$$\dot{m}_9 h_9 - \dot{m}_9 h_7 = \dot{m}_6 h_6 - \dot{m}_6 h_7 \quad \textbf{(3.20)}$$

$$\dot{m}_9 (h_9 - h_7) = \dot{m}_6 (h_6 - h_7) \quad \textbf{(3.21)}$$

$$\dot{m}_9 = \frac{\dot{m}_6 (h_6 - h_7)}{(h_9 - h_7)} \quad \textbf{(3.22)}$$

3.3.6 Receiver pressure

The receiver pressure is a variable which can be varied by adjusting the flash gas bypass valve controller. The pressure must be above the medium temperature evaporator pressure so refrigerant will flow to the evaporators and there is a pressure differential across the expansion valve. The pressure must be below the design pressure of the receiver and if copper pipes are to be used for distribution of the refrigerant to the supermarket evaporators then this pressure must be below the safe working pressure of refrigeration grade copper, which is 46 bar.

Figure 3.16 shows how the performance of the booster cycle varies with the intermediate receiver pressure. At all ambient temperatures the COP of the cycle is higher when the receiver pressure is lower. For the simulations a receiver pressure set point of 34 bar was chosen which is 6 bar above the medium temperature evaporator, enough to maintain a pressure differential across the expansion valve.

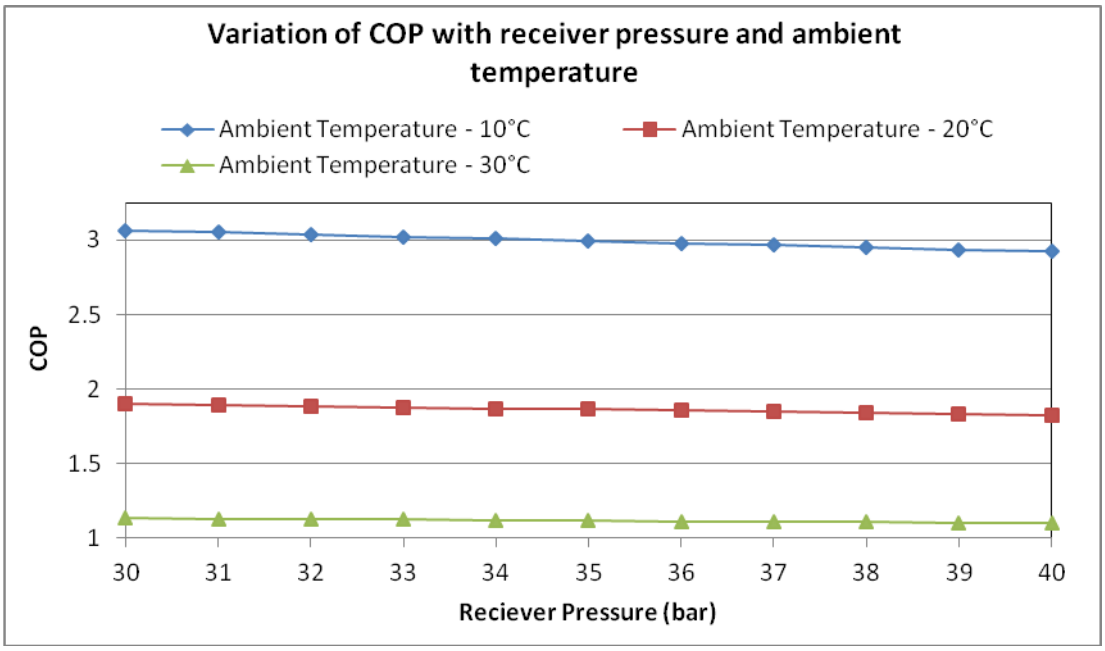

Figure 3.16 Variation of receiver pressure with ambient temperature COP

3.3.7 Gas bypass valve

The gas bypass valve controls the flow of the vapour refrigerant from the receiver to the HP compressor suction line, where it is mixed with the superheated refrigerant from the MT evaporator and the refrigerant from LP compressor discharge. The valve enables the control of the receiver pressure by maintaining a pressure differential across the medium MT pressure and the receiver pressure. The valve expands the vapour refrigerant from the receiver pressure to the MT evaporator pressure as shown in Figure 3.17 from point 7 to 8, using an isenthalpic expansion process.

$$h_7 = h_8 \tag{3.23}$$

The ability to control the pressure of the receiver decouples the temperature of the receiver from the ambient temperature.

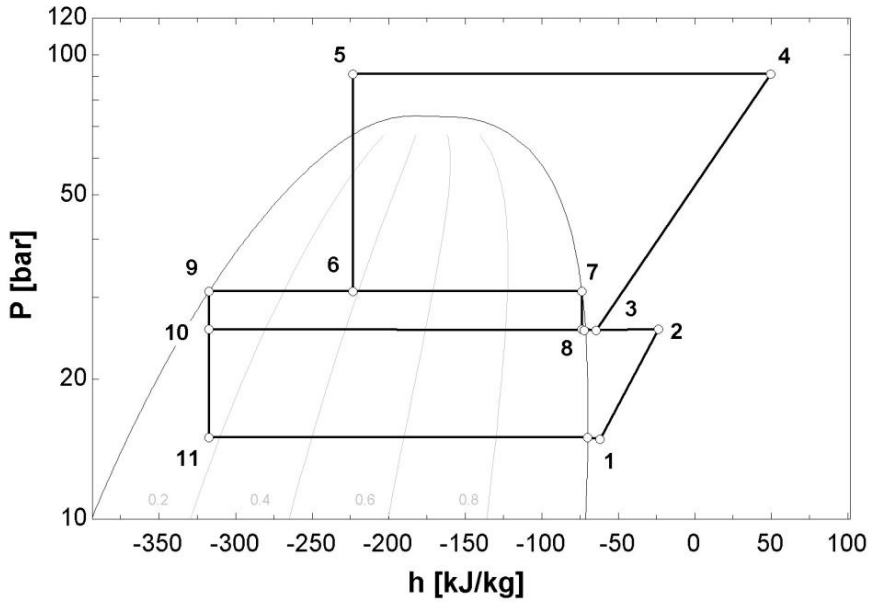

Figure 3.17 CO_2 Pressure – enthalpy chart showing expansion process of gas bypass valve

3.3.8 Refrigerated display cabinets

The refrigerated display cabinets generate the medium temperature and low temperature refrigeration loads for the system. The evaporation process from points 10 to 3 and 11 to 1 on the cycle pressure – enthalpy chart. The simulated small supermarket contains a total medium temperature refrigerated capacity (Q_{MT}) of 36 kW and a low temperature refrigerated capacity (Q_{LT}) of 5 kW. Each cabinet has separate controls which turn the liquid refrigerant flow to the cabinet on and off as the cabinet requires. The cooling capacity provided by the display cabinets is the input for calculating the mass flow rate of refrigerant required to generate the cooling capacity. The overall MT and LT mass flow rate of refrigerant is calculated as follows:

$$\dot{m}_{LT} = \frac{Q_{LT}}{h_1 - h_{11}} \quad \textbf{(3.24)}$$

$$\dot{m}_{MT} = \frac{Q_{MT}}{h_3 - h_{10}} \quad \textbf{(3.25)}$$

An electronic expansion valve acts as a solenoid, controlling the mass flow of refrigerant to the evaporator. The mass flow of refrigerant to the cabinets is interrupted for two reasons.

1. The temperature of the cabinet is controlled by a thermostat which switches the flow of refrigerant off when the required low temperature set point is achieved and switches flow of refrigerant on when the temperature inside the cabinet has reached the high temperature set point.
2. A build up of ice occurs over time on the fins of the evaporator. The evaporator is defrosted at regular intervals by switching off the flow of refrigerant to the evaporator.
3. The flow of refrigerant through the evaporator is modulated by the electronic expansion valve using the superheat for control. The expansion valve opens and closes, modulating the flow of refrigerant to meet the superheat set-point. The refrigerant superheat is calculated using the pressure and

temperature of the refrigerant entering the evaporator and the same parameters after the evaporator.

Although the refrigeration capacity of the system varies as cabinets are switched on and off by controllers, for the purposes of this reseach a constant evaporator load is assumed for each temperature level.

3.3.9 Mixing points

The booster system has two mixing points where refrigerant at different temperatures and flow rates are mixed, these points are unique to the system:

- Common suction mixing point: - Mixing point of sub cooled low temperature compressor discharge and the super heated refrigerant from the medium temperature evaporator.
- Gas bypass mixing point – Mixing point of the common suction line from the evaporators and the gas bypass from the receiver.

3.3.10 Internal heat exchangers

The IHEs (Internal heat exchangers) are used to exchange heat between various positions in the cycle. The method used for calculating the temperatures of the IHE is based on the method by Chen and Gu, (2005). Chen and Gu based the heat exchange calculations on the maximum amount of heat that can be transferred from one fluid to another.

The refrigerant on the hot side of heat exchanger in Figure 3.18, can theoretically be cooled down to $T_{3_{MIN}}$, which is the evaporating temperature. The refrigerant on the cold side of the heat exchanger can theoretically be heated to $T_{1_{MAX}}$. Due to the large property variance of the fluid, the enthalpy difference of $\left(h_3 - h_{3,\min}\right)$ and

$\left(h_{1,\max} - h_1\right)$ are not equal therefore the maximum specific heat transfer that can occur will be the minimum of the two:

$$q_{potn} = \min\left\{h_3 - h_{3,\min}, h_{1,\max} - h_1\right\} \quad \textbf{(3.26)}$$

The calculation of the enthalpy of points $h_{3,IHX}$ and $h_{1,IHX}$ is based on the following equations, using the effectiveness of the heat exchanger η_{IHX} as the input variable:

$$h_{3,IHX} = h_3 - q_{potn}\eta_{IHX} \quad \textbf{(3.27)}$$

$$h_{1,IHX} = q_{potn}\eta_{IHX} + h_1 \quad \textbf{(3.28)}$$

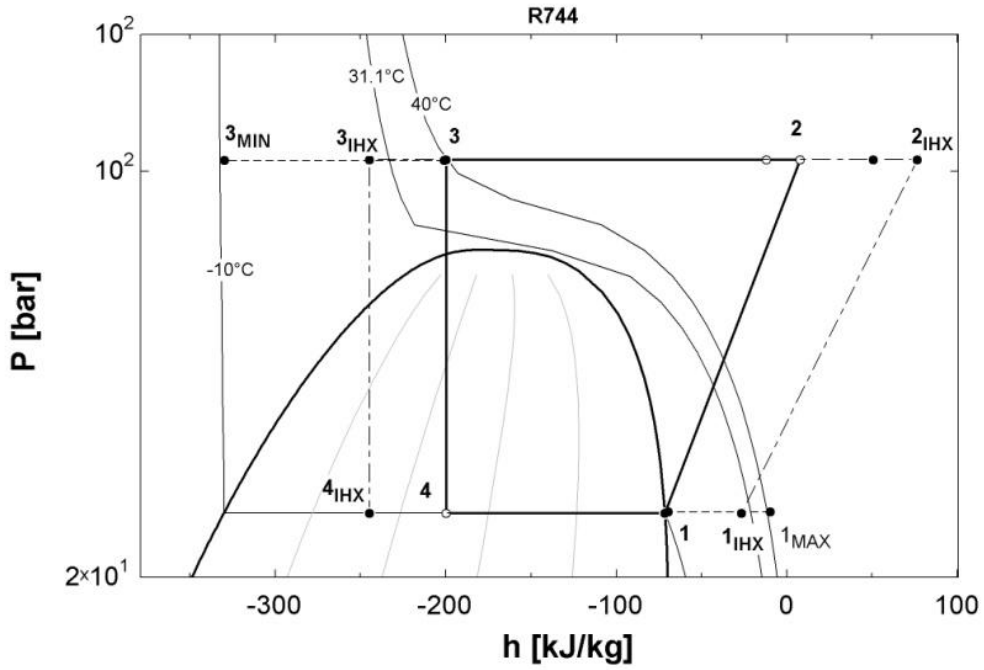

Figure 3.18 Pressure-enthalpy diagram for the Basic SLHX single Stage Cycle refrigeration cycle.

3.3.11 Pressure and temperature drops

Refrigerant pressure drops occur in the refrigeration pipe work between components and also across components. These pressure drops can reduce the pressure at the inlet of the compressor, increasing the power consumed by the compressor. The pressure

drops must be accounted for and included in the simulation model. The pressure drop calculations are also used to select the correct pipe sizes for the distribution pipe work, to minimise the pressure drops. Depending on the phase of the refrigerant either single or two phase flow, the following equations are used to calculate pressure drops.

3.3.11.1 Single Phase Flow

Single phase flow can either be in liquid or vapour phase, outside the refrigerant saturation curve. Equation 3.29 is used to calculate the pressure drop. The associated temperature drop in the line can be calculated using the refrigerant pressure-temperature relationship.

$$\Delta P = f \frac{G^2.L}{2.\rho.D_i} \quad \textbf{(3.29)}$$

The Blasius equation for the friction factor is the most widely used for turbulent flow in smooth pipes and is calculated by equations 3.30 and 3.31 (Kakac and Liu, 2002)

$$f = 0.316.\mathrm{Re}^{-1/4} \text{ for } \mathrm{Re} \leq 2000 \quad \textbf{(3.30)}$$

$$f = 0.316.\mathrm{Re}^{-1/5} \text{ for } \mathrm{Re} \geq 2000 \quad \textbf{(3.31)}$$

3.3.11.2 Two Phase Flow

Ould-Didi, *et al.*, (2002) presented a comparison of the seven most quoted methods in the literature used for calculating two phase pressure drops of refrigerants in horizontal tubes. They concluded that the method developed by Muller-Steinhagen and Heck, (1986) constantly gave the best predictions. For this reason this method was used to calculate the frictional pressure drop across the evaporator. This method is as follows:

The two phase pressure drop inside the tubes is comprised of the sum of three contributions:

$$\Delta P_{TP} = \Delta P_{Static} + \Delta P_{Momentum} + \Delta P_{Friction} \quad \textbf{(3.32)}$$

The evaporator pipes are horizontal apart from the bends but these are neglected for the purposes of this calculation, which omits the static pressure drop. The momentum pressure drop reflects a change in kinetic energy and is calculated by:

$$\Delta P_{Momentum} = \dot{m}^2 \left\{ \left[\frac{(1-X)^2}{\rho_F (1-\varepsilon)} + \frac{X^2}{\rho_V \varepsilon} \right]_{in} - \left[\frac{(1-X)^2}{\rho_F (1-\varepsilon)} + \frac{X^2}{\rho_V \varepsilon} \right]_{out} \right\} \quad \textbf{(3.33)}$$

The two phase frictional pressure drop correlation is given by:

$$\left(\frac{dp}{dz} \right)_{Frictional} = G(1-X)^{1/3} + bX^3 \quad \textbf{(3.34)}$$

$$G = a + 2(b-a)X \quad \textbf{(3.35)}$$

$$a = f_L \frac{2G^2}{D_i \rho_L} \quad \textbf{(3.36)}$$

$$b = f_V \frac{2G^2}{D_i \rho_V} \quad \textbf{(3.37)}$$

3.4 R404A Refrigeration system

Separate direct expansion R404A refrigeration systems for LT and MT requirements are currently by far the most popular refrigeration systems used in small supermarkets. Condensing units containing the compressors, condenser and receiver are very popular due to the reduced installation time and reduced floor space required than a separate compressor system and condenser. The compressor, condenser, receiver and controls are integrally housed as shown in Figure 3.20. These types of units are cheaper to purchase than the individual components. A schematic of the MT and LT R404A refrigeration cycles is shown in Figure 3.19. In Northern Ireland

one of the most abundant systems used for MT requirements in small supermarkets is the Copeland EasyCool Networked condensing units (Emerson, 2012). The condensing units enable a wide variety of refrigeration capacities to be achieved by the modular design. A number of smaller capacity condensing units can be "networked" to get the design capacity for the supermarket. The networked condensing unit system is capacity controlled by switching compressors on and off and by the use of a lead digital scroll compressor, which can reduce the refrigerating capacity down to 10% of its maximum load. Figure 3.20 shows an image of the condensing units which are generally used for MT refrigeration capacities from 15 kW upwards.

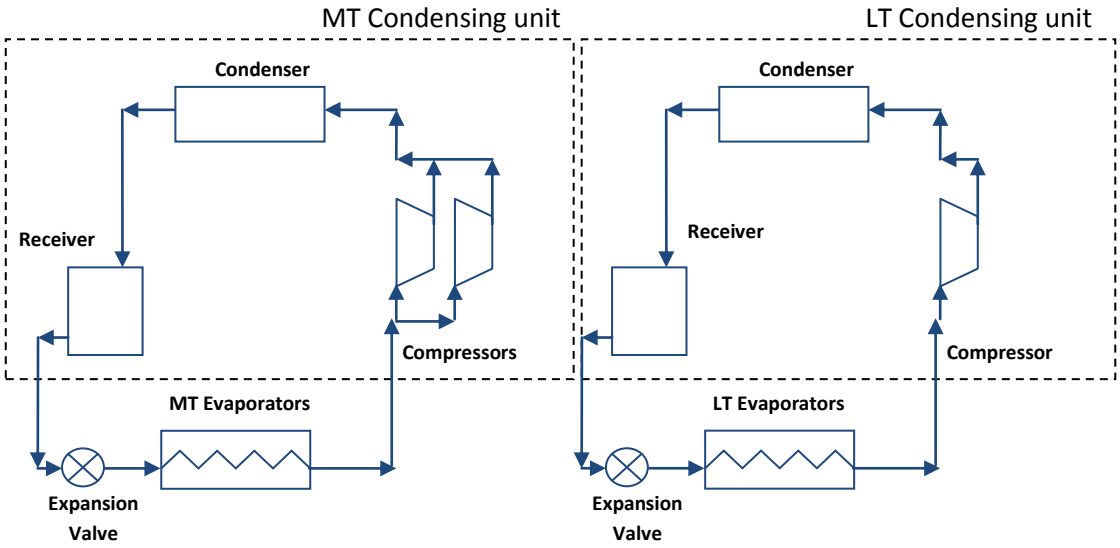

Figure 3.19 Schematic diagrams of MT and LT R404A refrigeration cycles

Figure 3.20 Image of Copeland eazycool condensing units used for small supermarkets (Emerson, 2012).

3.4.1 Compressors

There is one compression point in each R404A refrigeration cycle. The compressors used in the R404A system are Copeland Scroll compressors. No compressor efficiency data for the R404A scroll compressors was available so an assumption of average to good isentropic efficiency of 65% was used for the purposes of the simulation (Hundy *et al.,* 2008). The compressor discharge pressure is a function of the condensing temperature shown by equation 3.38. The compressor discharge properties can be calculated by equation 3.39 using the assumed isentropic efficiency. The work input to the compressor is calculated by equation 3.40. A pressure – enthalpy chart of the R404A cycle is shown in Figure 3.21.

$$P_2 = P_3 = f\left(T_3\right) \quad \textbf{(3.38)}$$

$$h_2 = \left(\frac{\left(h_{2is} - h_1\right)}{\eta_{is}}\right) - h_1 \quad \textbf{(3.39)}$$

$$W = \dot{m}\left(h_2 - h_1\right) \quad \textbf{(3.40)}$$

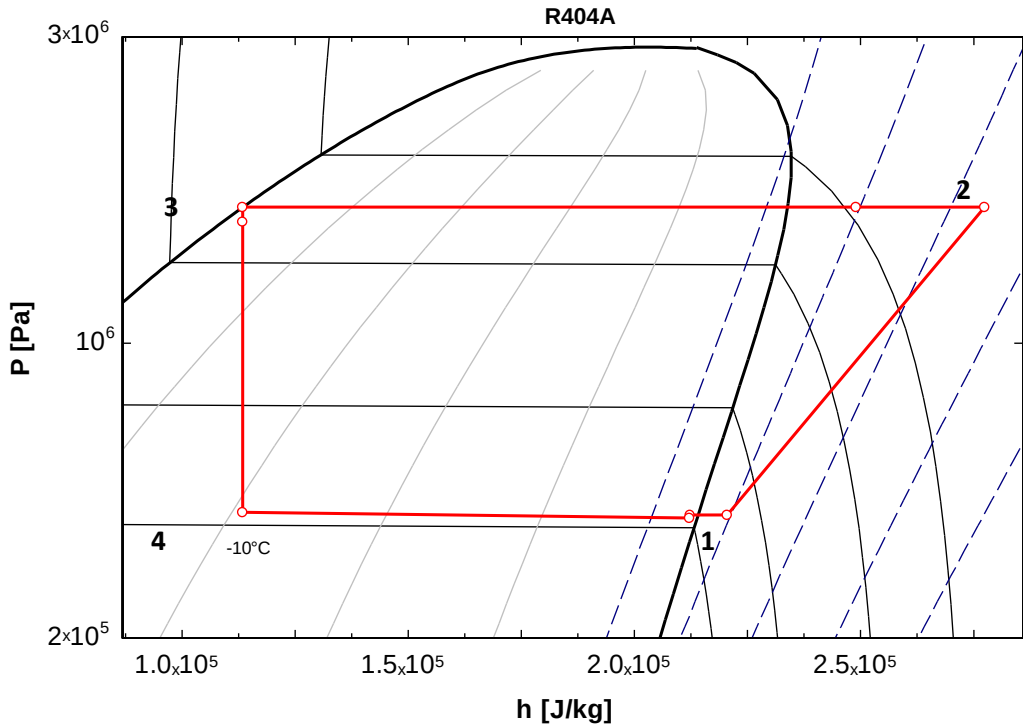

Figure 3.21 R404A Pressure – enthalpy chart compression process

3.4.2 Condenser

Subcritical condensation always occurs as the heat rejection method in a R404A refrigeration cycle. This simplifies the controls required as no high pressure valve is needed to maintain an optimum pressure. The refrigerant is condensed from a superheated vapour to a sub-cooled liquid in the condenser. The condensing temperature of the refrigerant depends on the ability of the condenser to reject heat to the atmosphere and depends on the ambient temperature. Table 3.1 shows the technical selection data of the MT and LT condensing units from the Copeland compressor selection software (Copeland, 2011). As the ambient temperature rises, so does the condensing temperature. The ΔT values in Table 3.1 are used to calculate the condensing temperature of the R404A systems at each ambient temperature.

$$T_3 = T_{amb} + \Delta T \quad \textbf{(3.41)}$$

$$H_3 = f\left(T_3, X_3 = 0\right) \quad \textbf{(3.42)}$$

Table 3.1 MT and LT R404A performance data from Select 7 software

	MT Copeland Easycool 1 x ZBD45KCE + 3 x ZB45KCE					LT Copeland MC-M8-ZF18K4E-TFD				
Amb temp °C	**Q (kW)**	**P (kW)**	**COP**	**Cond Temp (°C)**	**TD (K)**	**Q (kW)**	**P (kW)**	**COP**	**Cond Temp (°C)**	**TD (K)**
32	34.67	20.47	1.69	46.10	14.1	5.1	6.24	0.82	41.3	9.3
31	35.33	20.08	1.76	45.20	14.2	5.29	6.11	0.87	40.3	9.3
30	35.98	19.71	1.83	44.30	14.3	5.47	5.98	0.91	39.4	9.4
29	36.63	19.34	1.89	43.30	14.3	5.65	5.86	0.96	38.4	9.4
28	37.28	18.98	1.96	42.40	14.4	5.83	5.74	1.02	37.5	9.5
27	37.92	18.62	2.04	41.50	14.5	6.01	5.63	1.07	36.6	9.6
26	38.56	18.28	2.11	40.60	14.6	6.18	5.51	1.12	35.6	9.6
25	39.19	17.94	2.18	39.60	14.6	6.35	5.4	1.18	34.7	9.7
24	39.82	17.60	2.26	38.70	14.7	6.52	5.3	1.23	33.7	9.7
23	40.44	17.28	2.34	37.80	14.8	6.68	5.19	1.29	32.8	9.8
22	41.06	16.96	2.42	36.90	14.9	6.85	5.09	1.35	31.9	9.9
21	41.68	16.65	2.50	35.90	14.9	7	4.99	1.40	30.9	9.9
20	42.29	16.34	2.59	35.00	15	7.16	4.9	1.46	30	10
19	42.90	16.04	2.67	34.10	15.1	7.31	4.8	1.52	29	10
18	43.50	15.74	2.76	33.20	15.2	7.46	4.71	1.58	28.1	10.1
17	44.10	15.45	2.85	32.30	15.3	7.61	4.62	1.65	27.1	10.1
16	44.70	15.17	2.95	31.30	15.3	7.75	4.54	1.71	26.2	10.2
15	45.29	14.89	3.04	30.40	15.4	7.9	4.45	1.78	25.2	10.2
14	45.88	14.62	3.14	29.50	15.5	8.04	4.37	1.84	24.4	10.4
13	46.47	14.35	3.24	28.60	15.6	8.17	4.29	1.90	23.4	10.4
12	47.05	14.08	3.34	27.70	15.7	8.31	4.42	1.88	22.4	10.4
11	47.63	13.82	3.45	26.70	15.7	8.44	4.14	2.04	21.5	10.5
10	48.21	13.57	3.55	25.80	15.8	8.57	4.07	2.11	20.5	10.5
9	48.78	13.32	3.66	24.90	15.9	8.69	3.99	2.18	19.6	10.6
8	49.35	13.07	3.78	24.00	16	8.82	3.92	2.25	18.6	10.6
7	49.91	12.83	3.89	23.10	16.1	8.94	3.86	2.32	17.7	10.7
6	50.48	12.60	4.01	22.20	16.2	9.06	3.79	2.39	16.7	10.7
5	51.04	12.36	4.13	21.20	16.2	9.18	3.72	2.47	15.8	10.8
4	51.59	12.13	4.25	20.30	16.3	9.29	3.66	2.54	14.8	10.8

3.4.3 Refrigerated display cabinets

The refrigerated display cabinets generate the MT and LT refrigeration loads for the systems. The evaporation process is the same as that of the CO_2 booster cycle, only each cycle has one evaporation temperature. The cooling capacities are the same for the R404A systems as the CO_2 booster system, 36 kW MT load and 5 kW LT load. The mass flow of refrigerant through the evaporators is calculated using equations 3.24 and 3.25.

3.5 Evaporator simulation model

A numerical model of a plate finned-tube evaporator has been developed to investigate the heat transfer performance of CO_2 evaporators under different circuitry arrangements and tube diameters. The numerical model uses energy and momentum balances to enable the simulation of the finned-tube evaporator under a variety of conditions. Key parameters such as air and refrigerant flow rates and temperatures and the geometry of the heat exchanger can all be varied to investigate the comparative heat transfer performance. This research uses the mathematical software EES.

Figure 3.22 shows the typical circuit arrangement for the finned-tube evaporator used in a 3 door upright frozen food cabinet. Fans push air over the evaporator transferring heat from the produce to the heat exchanger which absorbs the heat, evaporating the refrigerant flowing though the tubes. Typically the tubes are made from copper and the fins are aluminum. Figure 3.23 shows a modified evaporator which uses a single interconnected circuit to distribute the refrigerant. Four different evaporators have been simulated using the numerical model. Further details of each evaporator are given in Table 3.2.

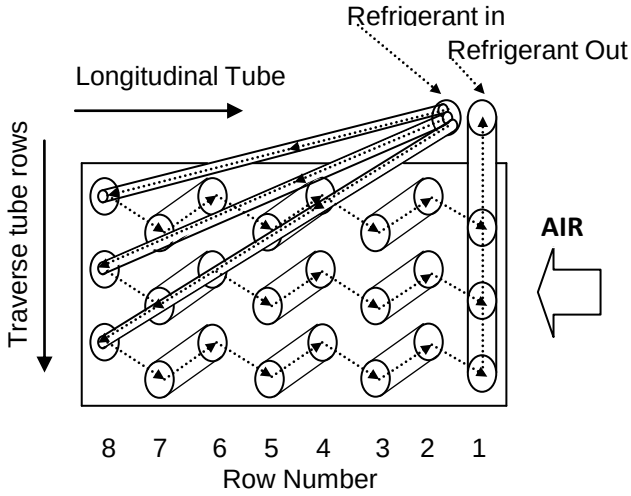

Figure 3.22 Side view of tube arrangement of 3 circuit plate finned tube heat exchanger

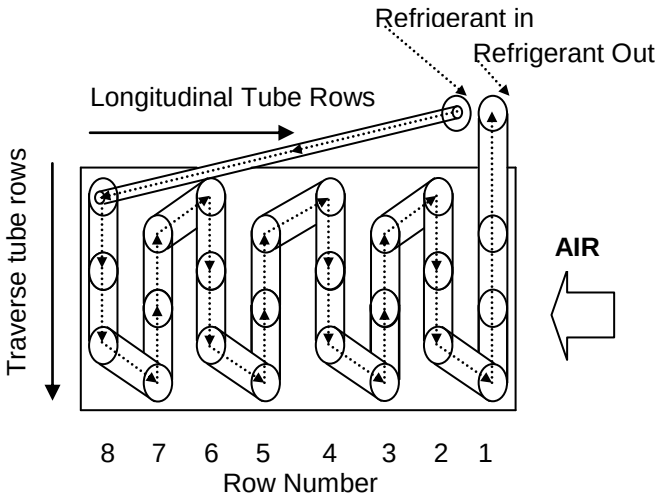

Figure 3.23 Side view of tube arrangement of 1 circuit plate finned tube heat exchanger

Table 3.2 Details of finned-tube evaporators

Parameter	Evaporator 1	Evaporator 2	Evaporator 3	Evaporator 4
Fin material	Aluminum	Aluminum	Aluminum	Aluminum
Fin thickness (mm)	1	1	1	1
Fin pitch (fins/inch)	3	3	3	3
Fin pitch (fins/m)	118	118	118	118
Tube material	Copper	Copper	Copper	Copper
Tube thickness (mm)	2	2	2	2
Tube inside diameter (mm)	**10.920**	**8.010**	**10.920**	**8.010**
Transverse tube pitch (mm)	25	25	25	25
Longitudinal tube pitch (mm)	25	25	25	25
Number of transverse of tube rows	3	3	3	3
Number of longitudinal tube rows	8	8	8	8
Number of circuits	**1**	**1**	**3**	**3**
Evaporator width (m)	2	2	2	2
Evaporator height (m)	0.18	0.18	0.18	0.18
Evaporator depth (m)	0.305	0.305	0.305	0.305
Air temperature (°C)	-20	-20	-20	-20
Air velocity (m/s)	2	2	2	2
Evaporation temperature (°C)	-30	-30	-30	-30
Refrigerant flow rate (kg/s)	0.0069	0.0069	0.0023	0.0023
Evaporator capacity (kW)	2.052	2.052	2.052	2.052

3.5.1.1 Control volume approach

The evaporator was modeled as either one tube or a set of tubes depending on the circuitry arrangement. Each tube was divided up into a number of control volume elements from the inlet quality of X=0, to an exit quality of X=1, with a constant ΔX. The control volumes are connected in series in the direction of refrigerant flow. The simulation model calculated the length of the control volume required to increase the quality of the refrigerant by ΔX, shown in Figure 3.24.

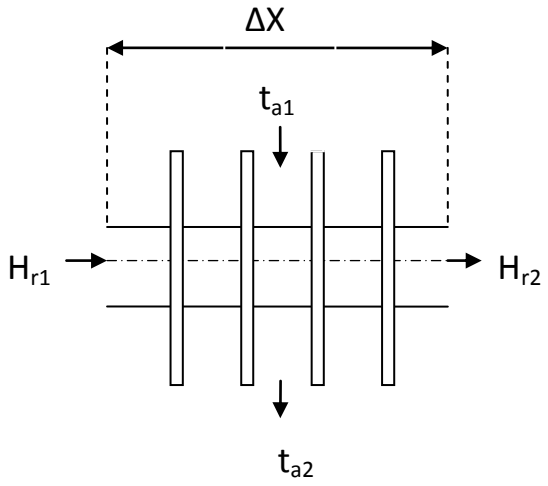

Figure 3.24 Schematic of control volume

3.5.1.2 Energy and mass balances

Mass and energy balances are applied to each control volume as shown in Figure 3.24. The rates of heat transfer for the evaporator are obtained by applying the following mass energy balances, shown in equations (3.43) to (3.50). Latent heat has been neglected for these simulations, the input values for the air temperature, velocity and the refrigerant temperature and flow rate have been held constant for each of the simulations on the each of the evaporators with different tube geometry. The number of tubes and fin pitch has also remained the same so it was assumed that the levels of frosting would be similar. For this reason frosting has not been considered in this work but will be considered in future work.

$$Q = \dot{m}_r \left(H_{r2} - H_{r1} \right) = \dot{m}_a c_{p,a} \left(t_{a1} - t_{a2} \right) \quad \textbf{(3.43)}$$

$$Q = U A_o \Delta T_{lm} \quad \textbf{(3.44)}$$

$$U = \left[\frac{A_o}{\alpha_o A_i} + \frac{A_o LN\left(\frac{D_o}{D_i} \right)}{2\pi \lambda_t \Delta L_i} + \frac{1}{\alpha_o \eta_o} \right]^{-1} \quad \textbf{(3.45)}$$

$$\eta_o = 1 - \frac{A_f}{A_T}(1-\eta) \quad \textbf{(3.46)}$$

$$\eta = \frac{\tanh(mr_{tube}\phi)}{mr_{tube}\phi} \quad \textbf{(3.47)}$$

$$m = \sqrt{\frac{2\alpha_o}{k_f \Delta_{fin}}} \quad \textbf{(3.48)}$$

$$\phi = \frac{R_{eq}}{r_{tube}}\left[1 + \left(\frac{R_{eq}}{r_{tube}}\right)\right] \quad \textbf{(3.49)}$$

$$\frac{R_{eq}}{r_{tube}} = 1.27\frac{X_m}{r_{tube}}\left(\frac{X_L}{X_m} - 0.3\right)^{1/2} \quad \textbf{(3.50)}$$

3.5.1.3 Refrigerant side heat transfer and pressure drop

The heat transfer correlation for the two phase flow of CO_2 was calculated using the correlations developed by Cheng *et al.*, (2008). The correlations were the most recent at the time of this study. The correlation uses the results of an updated flow boiling heat transfer map developed by Cheng *et al.*, (2006), where the flow is separated into different flow regimes of CO_2 evaporation. The refrigerant heat transfer coefficient is calculated for each flow regime which changes as the refrigerant quality increases as the flow moves from intermediate flow to annular flow to the onset of dry-out and finally the mist flow region. Equations (3.51) to (3.53) show how the refrigerant side heat transfer coefficient is calculated based on the quality of the refrigerant and the flow region.

IF $X < X_{di}$ then $\alpha_o = \alpha_{tp}$ **(3.51)**

IF $X < X_{de}$ then $\alpha_o = \alpha_{do}$ **(3.52)**

IF $X \geq X_{de}$ then $\alpha_o = \alpha_{mist}$ **(3.53)**

The full equations for two phase, dry-out and mist flow heat transfer coefficients can be found in Cheng *et al.,* (2008). The two phase refrigerant pressure drop along the tube is calculated from the sum of the static, momentum and frictional pressure drops as shown in Ould-Didi *et al.,* (2002).

$$\Delta P_T = \Delta P_{static} + \Delta P_{mom} + \Delta P_{frict} \quad \textbf{(3.54)}$$

The tubes in the evaporator are mainly horizontal, so for the purposes of this research the static pressure drop can be assumed to be zero. Ould-Didi *et al.,* (2002) compared seven of the most popular correlations for two phase frictional pressure drop. The correlation by Muller-Steinhagan and Heck, (1986) gave the best predictions so it is used for this research.

3.5.1.4 Air side heat transfer and pressure drop

The heat transfer coefficient for air flow through the evaporator is calculated using the Colburn j-factor coefficient described by Kim and Kim, (2005). The j-factor is dependent on the geometry of the evaporator including the fin geometry and number of tube rows. The correlation was developed specifically for flat plate finned-tube heat exchangers for both in line and staggered tube arrangements.

$$\alpha_o = jG_a Cp_a \,\mathrm{Pr}^{-2/3} \quad \textbf{(3.55)}$$

$$j = 0.170 N_{row}^{-0.141} D_o F^{0.394} \,\mathrm{Re}_{Dh}^{-0.349} \quad \textbf{(3.56)}$$

3.6 Summary

This chapter has developed a mathematical model of the proposed CO_2 booster refrigeration system and a R404A refrigeration system in a typical small supermarket. The models use thermodynamic and mass balance principles to calculate operational performance parameters of each refrigeration system. Using the variation of ambient temperature as input, the model determines outputs such as optimum pressures, temperatures, flow rates, pressure drops and power consumption. These results are presented in the next chapter.

A model of a plate-finned tube evaporator used in refrigerated supermarket display cabinets has also been developed. An increase in the heat transfer efficiency of the evaporator could lead to a reduced material content, reducing the associated embodied energy and environmental impact of supermarket refrigeration systems.

Chapter 4 Simulation procedure and results

4.1 Introduction

This chapter presents the procedure used to simulate the CO_2 booster and the R404A refrigeration systems and the evaporator. The chapter also presents and discusses the results of the simulations, comparing the performance of the refrigeration systems and the evaporator models. Each of the systems has a different control strategy and simulation procedure which is explained below:

4.2 Refrigeration systems control strategy and simulation procedure

4.2.1 R404A supermarket

The R404A system is controlled using a floating head pressure strategy. For the MT system an average TD (Temperature differential) of 16 K is maintained between the refrigerant condensing temperature and the ambient temperature, which has been selected based on manufacturer's data in Table 3.1. A TD of 10 K is selected for the LT system using the same data. For the MT system the condensing temperature is allowed to drop to a minimum of 20°C at ambient temperatures of 4°C or lower, which will maintain a sufficient pressure differential across the expansion valve without effecting the capacity of the evaporators. For the LT system the condensing temperature was set at a minimum of 10°C with a TD of 10 K.

4.2.2 CO_2 booster supermarket

The transcritical CO_2 system is sensitive to ambient temperature due to the low critical point of CO_2. A transition temperature from subcritical operation to

transcritical operation of 21ºC was chosen for the system using the same TD as the R404A system. During subcritical operation the system will operate using a floating head control strategy where the condensing temperature will follow the ambient temperature maintaining a TD of 10 K. The condensing temperature will be set to drop to a minimum of 10ºC at ambient temperatures of 0ºC and below. This will still maintain a sufficient pressure differential across the expansion valve to maintain evaporator capacity. During transcritical operation the system is controlled by the refrigerant temperature out of the gas cooler. This is summarised below in a similar method as presented by Ge and Tassou (2010).

$$P_{Cond/GC} = \begin{cases} 45bar & \text{if } t_{amb} \leq 0°C \\ f(t_{Cond}, t_{amb}) & \text{if } 0°C \leq t_{amb} < 21°C \\ 78bar & \text{if } 21°C \geq t_{amb} \leq 22°C \text{ subcritical} \\ 78bar & \text{if } 21°C \geq t_{amb} \leq 22°C \text{ transcritical} \\ 2.75t_{amb} + 20.07 & \text{if } t_{amb} > 22°C \end{cases} \quad \textbf{(4.1)}$$

4.2.3 Refrigeration system simulation flowchart

Figure 4.1 shows a flow chart of the simulation procedure and the inputs used in the simulation.

4.3 Evaporator control strategy and simulation procedure

The output of the model is the calculation of the required length of each control volume required to evaporate the refrigerant through a set ΔX, based on the location of the control volume in the evaporator and heat transfer properties of the air and refrigerant at that location. As the length of the first control volume is unknown the volume flow of air over this control volume is also unknown. An iterative process using a guess for the first and subsequent control volumes is used to calculate the volume flow of air over each control volume.

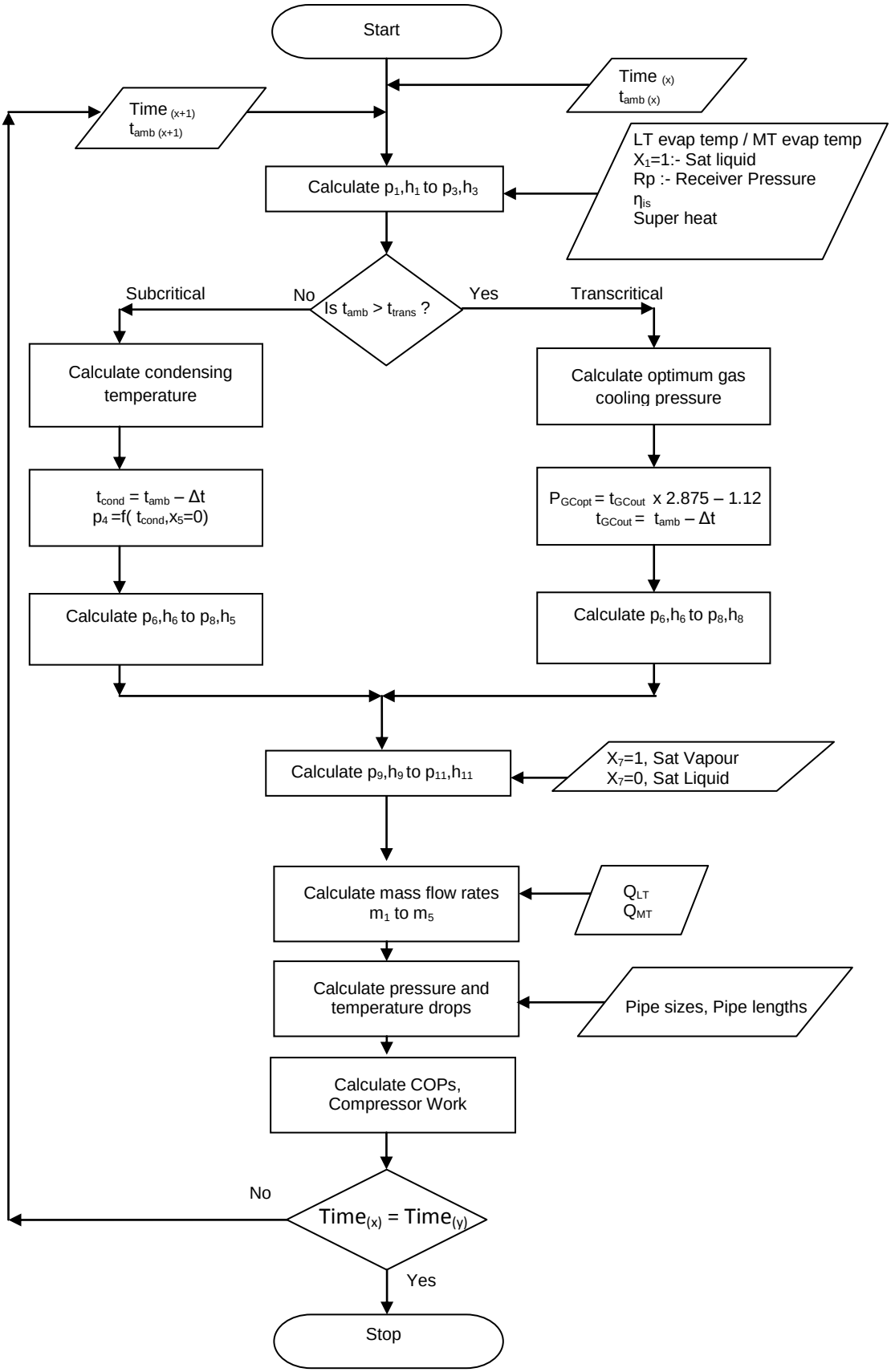

Figure 4.1 Flow chart of simulation procedure

4.4 Refrigeration system simulation results

4.4.1 COP and compressor performance comparison

The variation of the COP of each refrigeration system with ambient temperature is shown in Figure 4.2. The combined COP for the LT and MT R404A systems is also shown to enable comparison with the CO_2 booster system. At ambient temperatures above 3ºC the COP of the R404A system is higher than the COP of the CO_2 booster system but at ambient temperatures below 3ºC the COP of the CO_2 booster system is higher. The booster system is operating in a subcritical cycle at these low ambient temperatures. The MT R404A condensing unit system has the highest COP values over the range of ambient temperatures but when it is combined with the lower LT R404A condensing unit COP values, the overall COP for the R404A supermarket becomes lower.

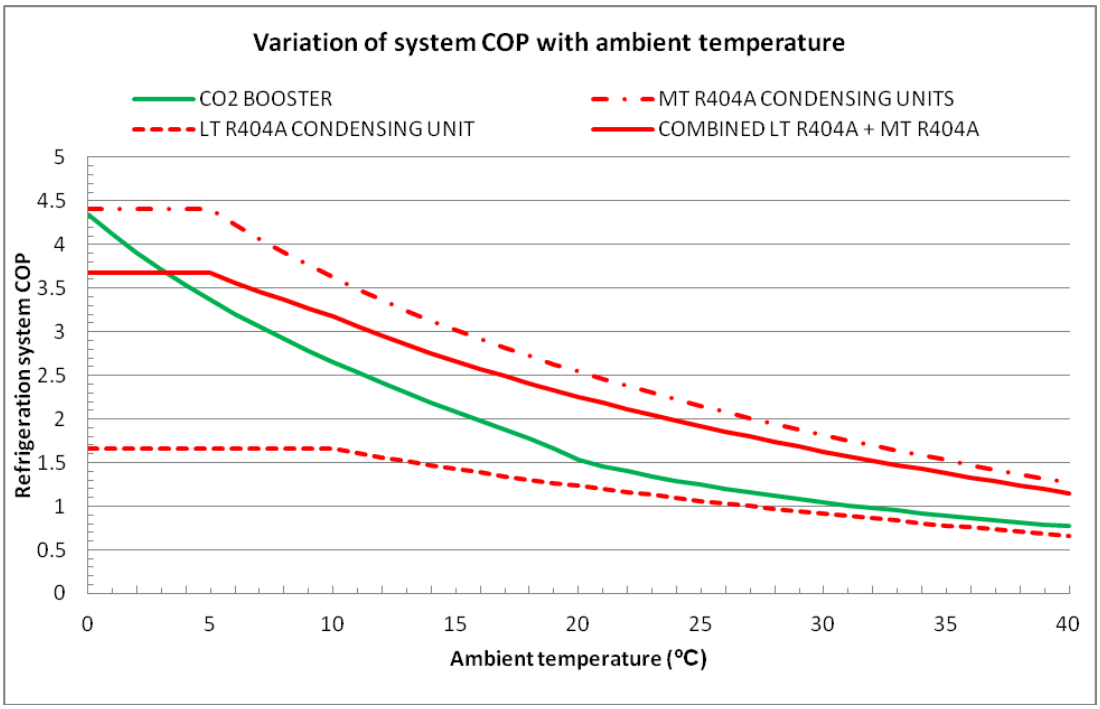

Figure 4.2 Variation of system COP with ambient temperature

Figure 4.3 shows the compressor power consumption for both the CO_2 booster and R404A systems over 24 hours on a warm summer day. The CO_2 booster system has

the highest power consumption throughout the day. The power consumption of this system is mostly influenced by the power consumption of the HP compressors, while the LP compressor power consumption is constant at 0.75 kW throughout the day. From 10:00 – 18:30 the CO_2 system is operating transcritically as the ambient temperature is higher than 21°C. A peak ambient temperature of 25.1°C occurs at 15:00. At this time the power consumption of the CO_2 system is 33.2 kW. This is 55% higher than the power consumption of the R404A system, which was 21.4 kW.

The power consumption of the LP CO_2 compressor was constant throughout the day; it was independent of the ambient temperatures and was lower than the LP R404A compressor power consumption, which did vary slightly with ambient temperature. The constant power consumption of the LT CO_2 compressor was due to the constant compressor discharge pressure or condensing pressure. This 'booster' compressor only had to compress the refrigerant to the MT evaporation pressure as this was the 1st stage of a two stage compression process.

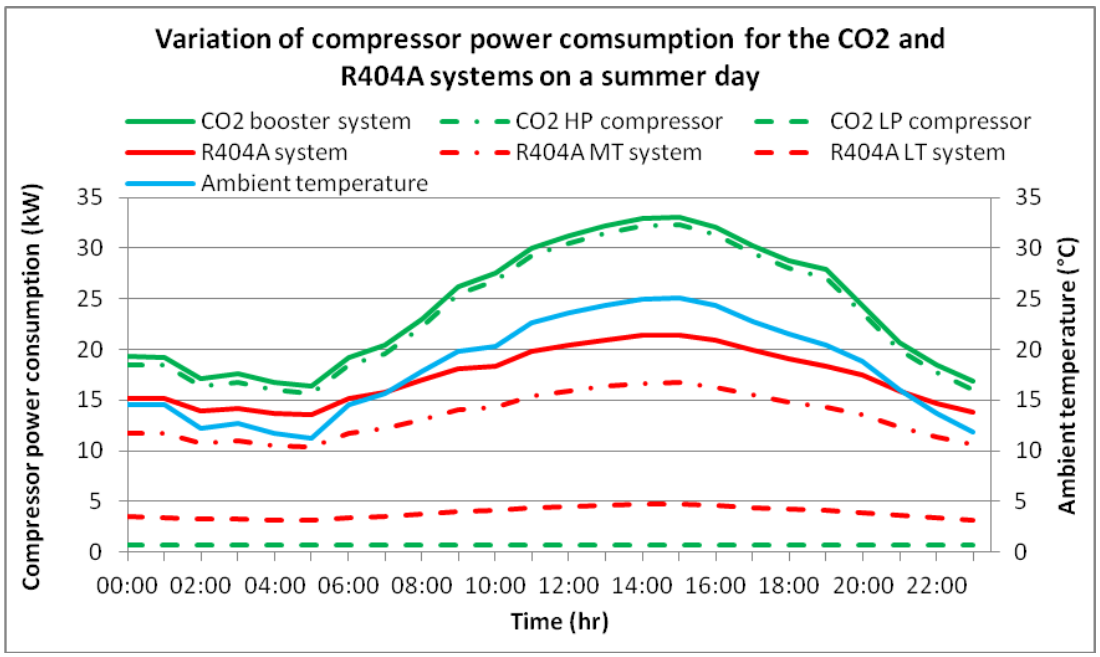

Figure 4.3 Variation of compressor power with ambient temperature on a warm summer day

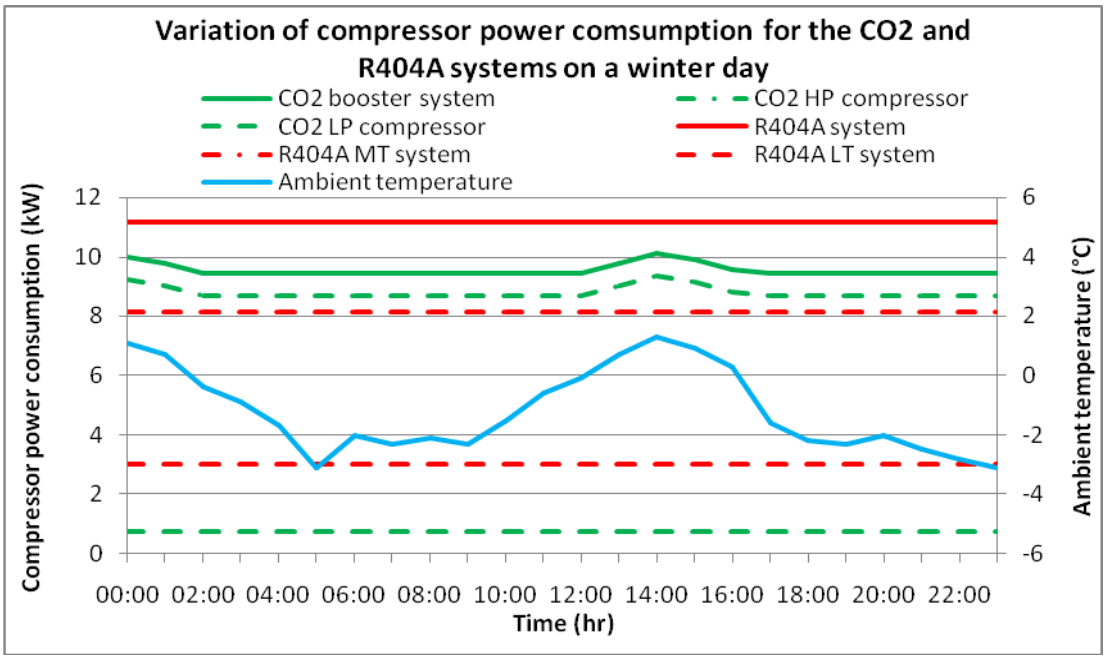

Figure 4.4 Variation of compressor power with ambient temperature on a winter day

Figure 4.4 shows the power consumption of the compressors on a winter day. The ambient temperatures are much lower than the summer day varying from -3.1°C to 1.3°C. The power consumption of the compressors is much steadier due to the systems reaching their minimum condensing temperature set points. The CO_2 system consumes less power than the R404A system throughout the day. The system has a power consumption of 9.4 kW for most of the day apart from when the ambient temperature rises above 0°C. The R404A system consumes 11.2 kW throughout the day, 19% more than the CO_2 system.

The CO_2 system is much more efficient at generating the cooling for the LT evaporators. The CO_2 system consumes a steady 0.75 kW while the R404A system consumes 3.0 kW, four times more power to generate the same 5 kW of LT refrigeration. This is due to the low power consumption of the LT CO_2 'booster' compressor due to its independence from the fluctuating ambient temperature. The LT 'booster' compressor power consumption depends on the evaporating temperature of the LT evaporators and the discharge pressure of the compressor. The discharge pressure of the LP compressor it dependant on the evaporating temperature

of the MT evaporators as the refrigerant discharged from the LP compressor is mixed with the refrigerant leaving the MT evaporators.

Figure 4.5 shows the variation of the compressor swept volume requirements with the rise in ambient temperature. The CO_2 compressors require a much lower compressor swept volume than their R404A counterparts. This enables the compressors to be much smaller for an equivalent cooling capacity. Using a design ambient temperature of 32ºC, the LT CO_2 compressor requires a minimum swept volume of 2.64 m^3/h to generate a cooling capacity of 5 kW. The high stage or MT CO_2 compressor requires a swept volume of 21.45 m^3/h to generate a cooling capacity of 36 kW.

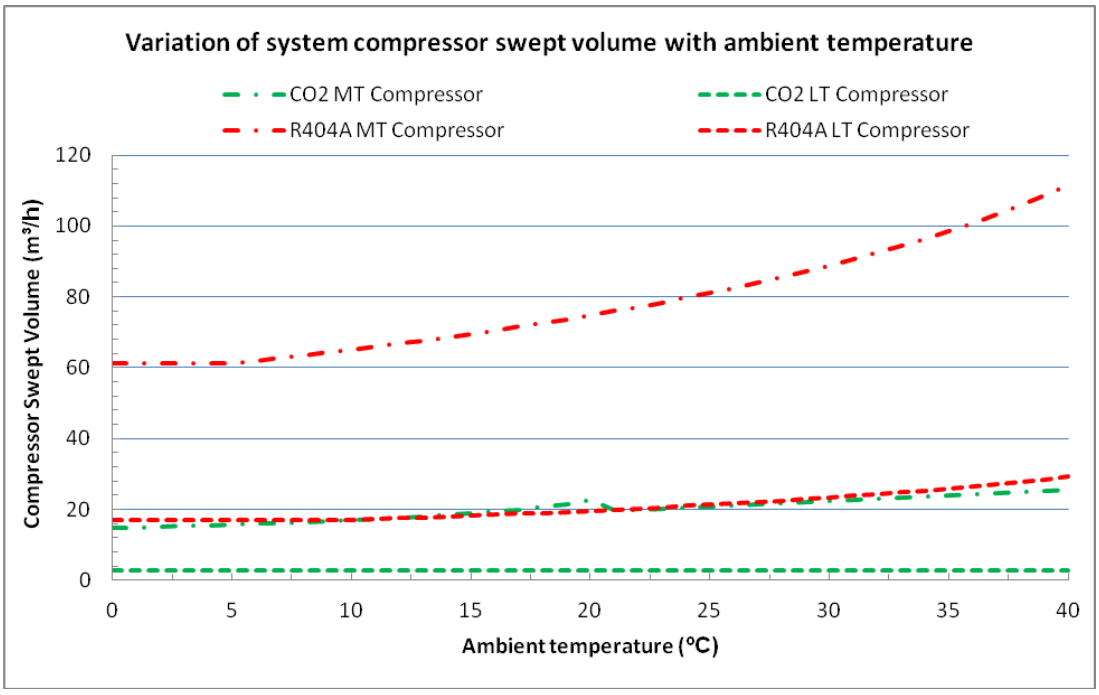

Figure 4.5 Variation of compressor swept volume with ambient temperature

4.4.2 Comparison of operating pressures

The suction and discharge pressures associated with the CO_2 booster system are much greater than that of the R404A systems. Figure 4.6 shows the variation of the

MT CO_2 compressor suction and discharge pressures, with the MT R404A compressor suction and discharge pressures on a summer day. The suction pressures of both compressors are constant throughout the day, 25.4 bar and 4.64 bar for the CO_2 and R404A compressors respectively. The R404A compressor discharge pressure slightly fluctuates from 13.0 bar to 18.3 bar with an increase in ambient temperature. The discharge pressure from the CO_2 compressor fluctuates from 59 bar to a maximum of 92 bar at an ambient temperature of 25ºC, gas cooling at 35ºC. At this ambient temperature both the discharge pressure and gas cooling temperature are above the critical pressure and temperature of CO_2 so the system is operating in the transcritical mode.

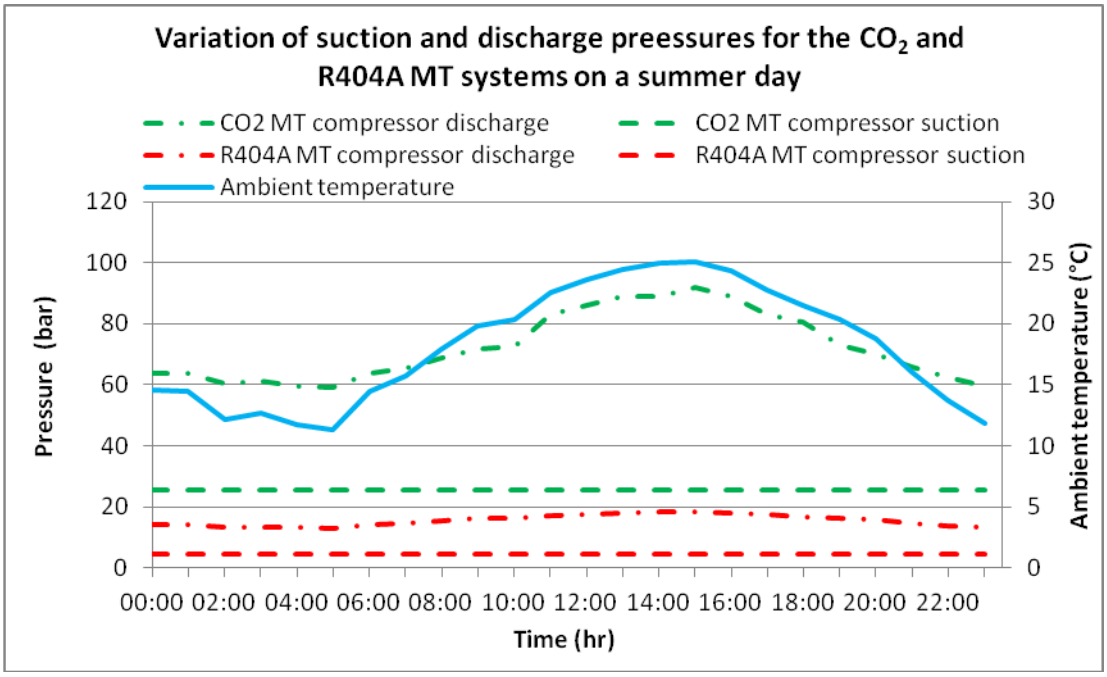

Figure 4.6 Variation of compressor suction and discharge pressures with ambient temperature on a summer day

4.4.3 Annual energy performance comparison

Figure 4.7 displays the hourly power input of each system over one year with variable ambient temperatures. The power consumption peaks of the CO_2 system are much higher than the R404A system throughout the year, especially during the summer months when the ambient temperatures are higher. During the winter

months the power consumption of the CO_2 system is lower than the R404A system, only when the ambient temperature is below 3°C.

The total annual power consumption of the R404A refrigeration system compressors is calculated to be 116,126 kWh. The total annual power consumption of the CO_2 system compressors is calculated to be 137,565 kWh, 18% higher than the traditional R404A system. Using an average price of electricity in Northern Ireland to the small supermarket retailers of £0.14 per kWh, this would lead to a £3,001 annual increase in the retailer's energy bills.

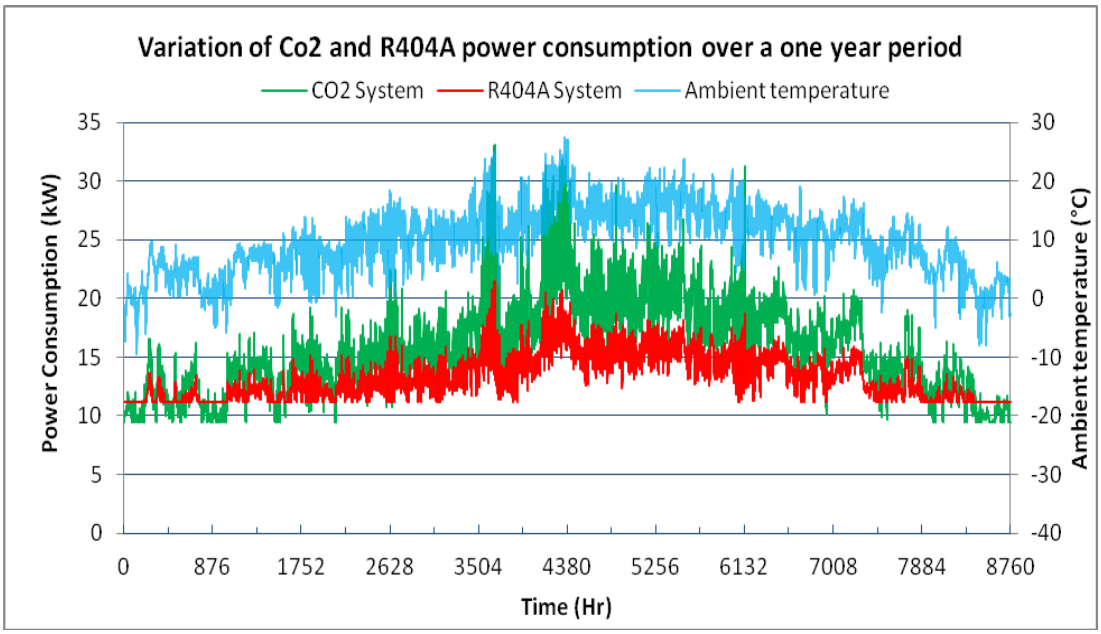

Figure 4.7 Variation of power input of system over one year

Table 4.1 Power consumption of R404A and CO_2 Booster Supermarket refrigeration systems over one year of simulated operation

	Compressor Power Consumption (kWh)		
	MT	**LT**	**TOTAL**
R404A	88,062	28,064	116,126
CO_2 Booster	130,936	6,629	137,565

4.4.4 TEWI Calculation

The environmental impact of a refrigeration system is measured by the direct and indirect carbon dioxide emissions from the operation of the refrigeration system. The direct carbon dioxide emissions are a result of refrigerant leakage from the system. The indirect emissions depend on the electrical power used by the system; the emissions are a result of the power generation at the source. The TEWI (Total Equivalent Warming Impact) equation developed by the British Refrigeration Association (BRA, 2006) can be used to compare and assess the environmental impact of different refrigeration systems due to direct and indirect carbon dioxide emissions. The results are shown in Table 4.2.

$$TEWI = (GWP \times m \times N \times L_1) + (GWP \times m \times (1-\alpha)) + (N \times \beta \times E) \qquad \textbf{(4.2)}$$

The GWP of the refrigerant is used to show the environmental impact of the direct emissions from leakage etc. Table 4.2 shows that R404A has a much higher GWP than CO_2. The N value in Table 4.2 is the number of years that the refrigeration system will be in operation, which is used to calculate the indirect emissions from the power used to run the system. The mass of refrigeration contained within each system is denoted by m and α is the multiplication factor for the amount of refrigerant recovered at the end of the system life. A value of 0.9 is assumed so 0.1 (10%) is leaked into the atmosphere during the refrigerant recovery. An annual leakage rate of 15% is assumed for both systems, this value is considered to be a good estimate of actual refrigerant leakage from supermarket systems, Cowan *et al.*, 2009. The conversion factor of 0.53 kg CO_2 / kWh is taken the Carbon Trust publication CTL153 (Carbon Trust, 2011)

The result in Table 4.2 show that although the indirect emissions of the CO_2 booster system are 18% higher due to the higher annual power consumption, the TEWI of the booster system is 15% lower than the R404A system. This is due to the high GWP of R404A and the leakage rate of 15%. The installation of CO_2 booster refrigeration systems a small supermarket in Northern Ireland instead of a traditional R404A system could reduce the environmental impact of that supermarket by 128,167 kg/CO_2 over the 10 year life span of the refrigeration system.

Table 4.2 Calculated Combined R404A cycles TEWI and CO_2 Booster cycle TEWI

	R404a LT Cycle and MT Cycle	CO_2 Booster Cycle
GWP	3,780	*1*
N (Years)	10	10
m (kg)	40	48
α	0.9	0.9
L_1 (%)	15	15
β (kg Co_2 / kWh)	0.53	0.53
E (kWh)	116,126	137,565
DIRECT (kg Co_2)	241,920	77
INDIRECT (kg Co_2)	615,648	729,095
TEWI (kg Co_2)	857,388	729,171

4.5 Evaporator simulation results

This section presents and discusses the results of the simulation model developed in section 3.5, to research how the high heat transfer properties of CO_2 could be used improve the performance or lower the environmental impact of a plate-finned tube evaporator used in supermarket refrigeration systems. A schematic diagram of the evaporator designs in shown in Figure 4.8 and 4.9.

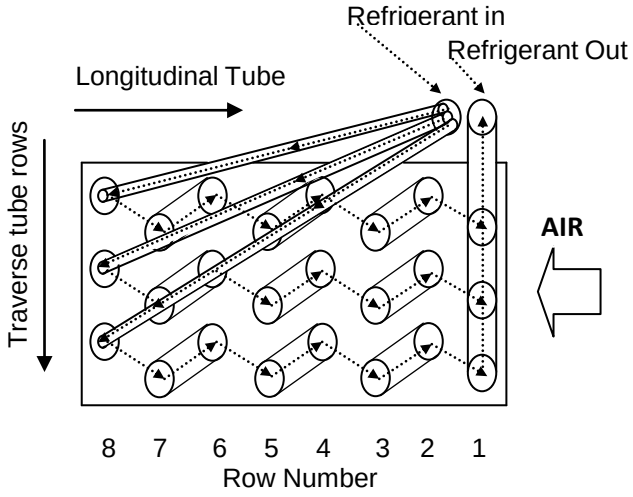

Figure 4.8 Side view of tube arrangement of 3 circuit plate finned tube heat exchanger

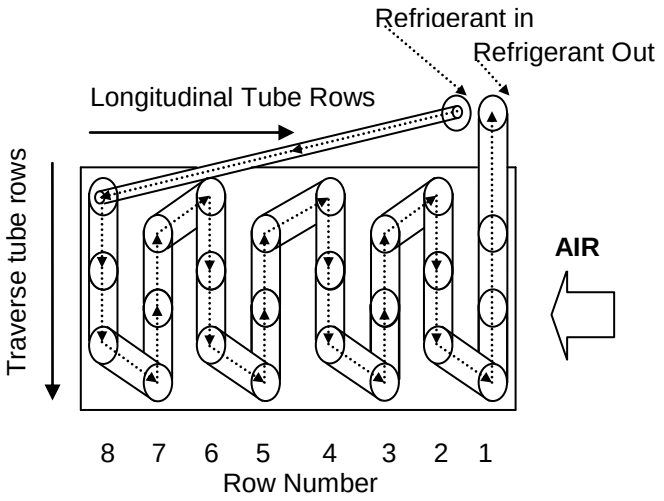

Figure 4.9 Side view of tube arrangement of 1 circuit plate finned tube heat exchanger

Figure 4.10 displays the total two-phase refrigerant pressure drops across the four simulated evaporators. The single circuited evaporator displays much higher pressure drops compared to the traditional three circuited evaporator, due to the longer evaporator tubes and greater mass flow rate. As the quality of the refrigerant increases, the gradient of the pressure drop increases for all circuitry arrangements and tube diameters. Decreasing the tube diameter also increased the pressure drop across the evaporator. This was due to the smaller cross sectional area of the evaporator tubes.

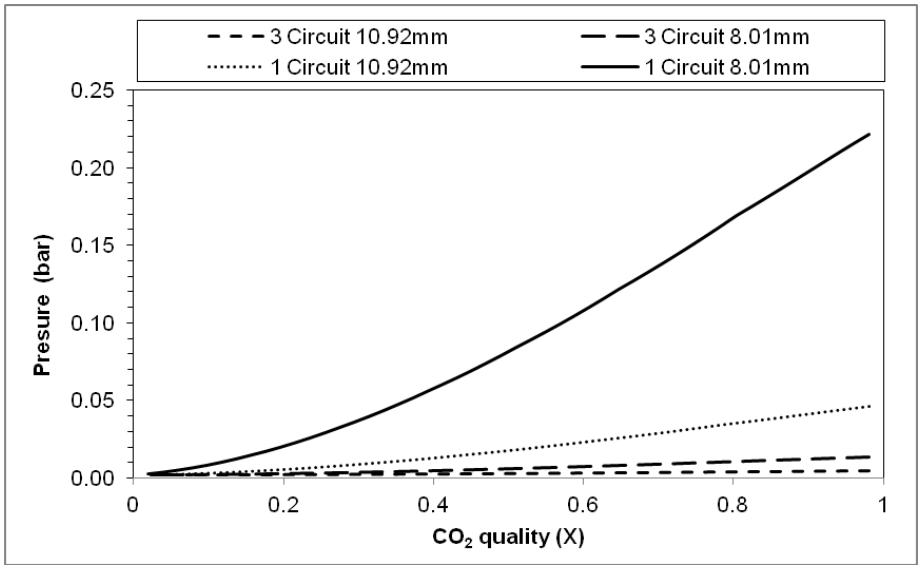

Figure 4.10 CO2 pressure drop across finned tube evaporators with increasing refrigerant quality

Due to the thermodynamic relationships of the refrigerant, an increase in pressure drop results in an increase in the temperature drop. Figure 4.11 displays the corresponding refrigerant temperature drops across the evaporators. As expected the single circuited evaporator with the 8.01mm tube displayed the highest temperature drop of 0.46°C.

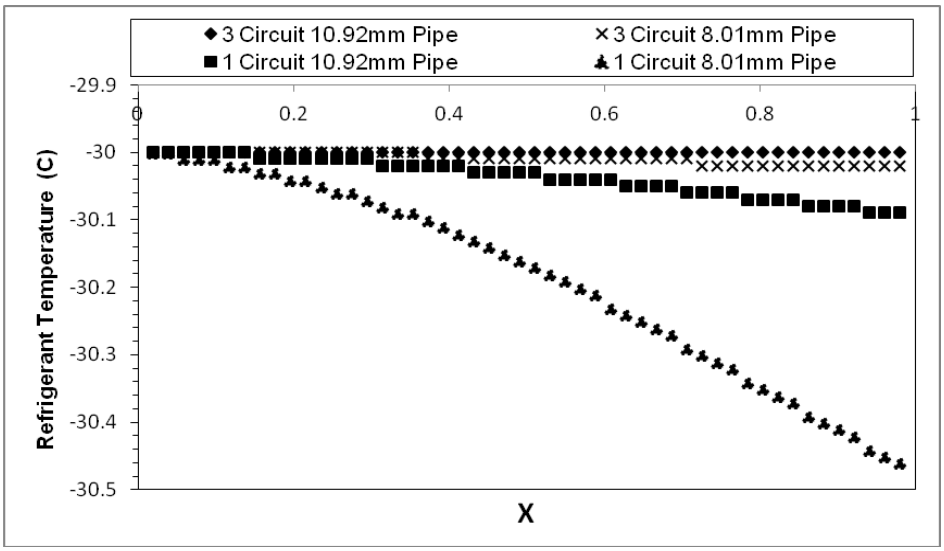

Figure 4.11 CO2 pressure drop across finned tube evaporators with increasing refrigerant quality

The velocities of the refrigerant during evaporation are shown in Figure 4.12 as the refrigerant moves through the evaporator tube. As the quality of the refrigerant increases, the density of the refrigerant decreases due to the refrigerant phase change. The decrease in density increases the velocity of the refrigerant through the evaporator. CO_2 refrigerant velocities are lower than R404A velocities for an equal evaporator cooling capacity and pipe diameter. Using CO_2 in a traditional three circuited 10.92mm evaporator results in very low refrigerant velocities. Oil build up may occur inside the evaporator resulting in the uneven distribution of refrigerant and a reduction in surface heat transfer.

The higher refrigerant mass flow in the single circuited 8.01mm evaporator coupled with the smaller diameter increased the refrigerant velocities. These higher velocities

will keep the oil circulating through the evaporator and reduce the potential for oil build up.

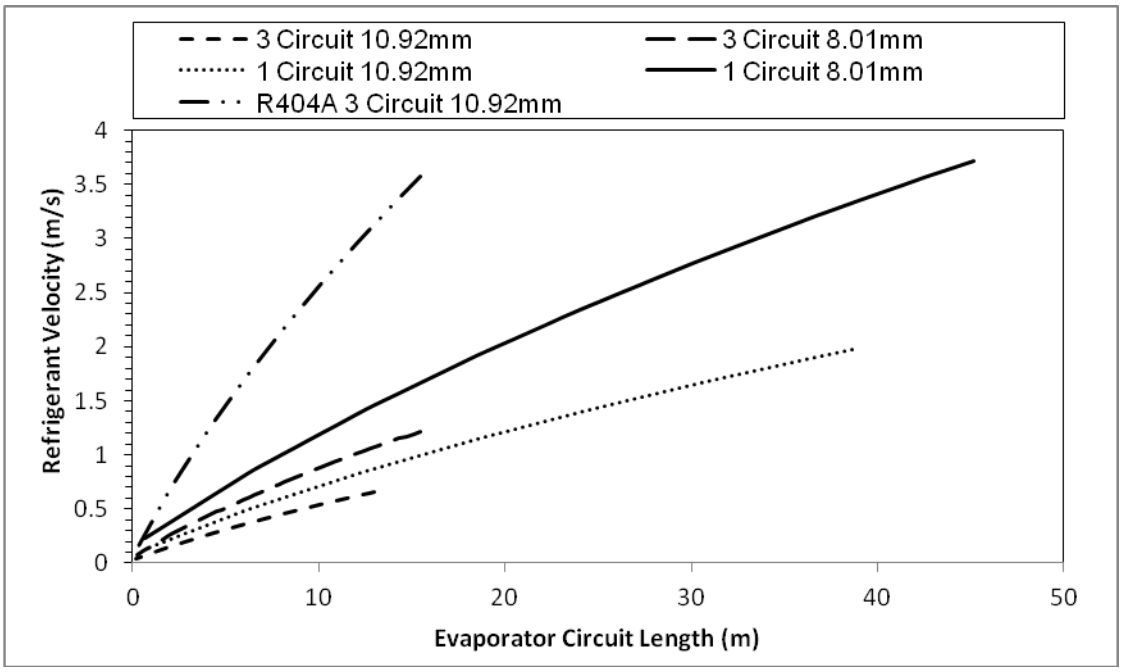

Figure 4.12 CO2 Refrigerant velocities across evaporators varying circuit numbers and tube diameters

The overall heat transfer coefficient for the finned-tube evaporator is calculated using the heat transfer coefficients outside the tube (air side) and the coefficients inside the tube (refrigerant side). To compare two different evaporator designs and calculate the overall heat transfer coefficients, Figure 4.13 shows the air and refrigerant side coefficients as the refrigerant evaporates.

The air side coefficients are very similar, as the refrigerant moves to the front of the evaporator the air side coefficient increases. The maximum air side coefficient was at the front row of the evaporator. The refrigerant side coefficients show very different values. Both coefficients increased as the refrigerant quality increased but the single circuited evaporator had a much greater increase in the refrigerant side coefficient. The increased mass flux of the refrigerant in the single circuited evaporator increased

the convective boiling heat transfer coefficient which increased the two phase flow coefficient.

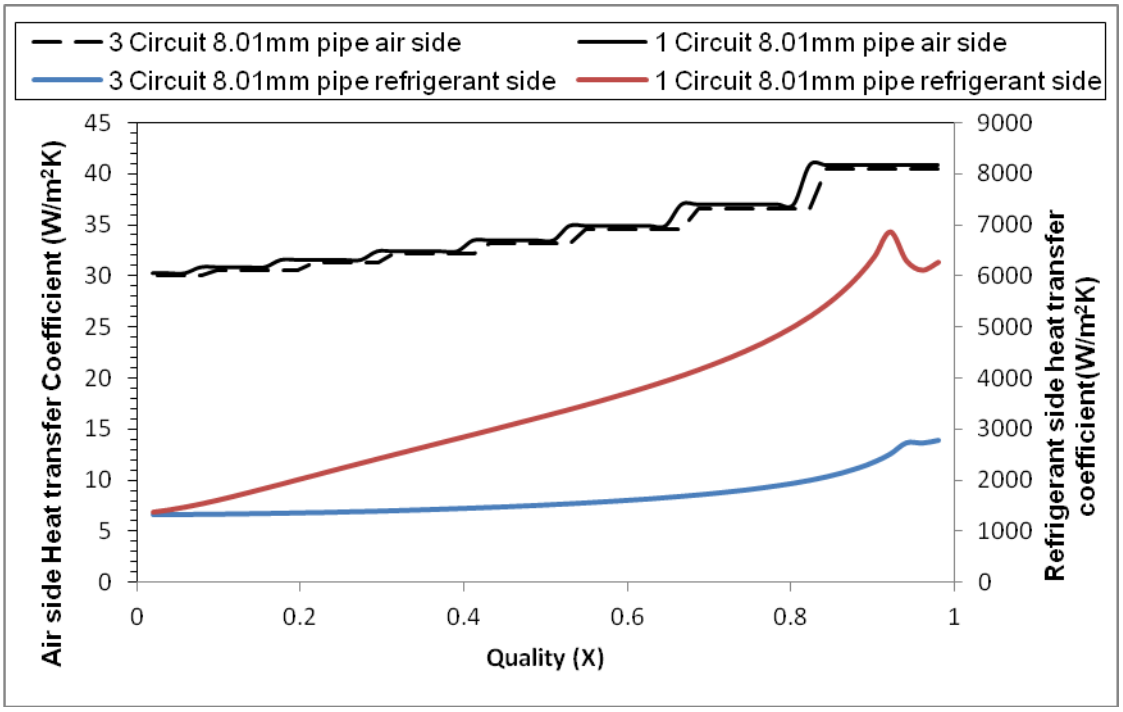

Figure 4.13 8.01mm Tube evaporator air and refrigerant side heat transfer coefficients

The simulation model automatically calculated the length of each control volume required to generate the rate of heat transfer required, ΔX and ΔH were the same for each control volume. Figure 4.14 shows how the length of tube required for each control volume changes as the refrigerant moves from the back of the evaporator, X=0, to the front of the evaporator, X=1. Each point of the figure denotes the length and quality of a control volume. The smaller overall heat transfer coefficient in the back row led to a larger control volume length required for complete evaporation. The single circuited evaporators required much longer control volumes for complete evaporation than the 3 circuited evaporators. The sum population of control volumes in each row enabled the cooling capacity of each row to be calculated. The front row of the evaporator had the greatest population of control volumes for each of the evaporators simulated, therefore had the greatest capacity. As the row number

increased, the number of control volumes per row decreased with a decrease in row capacity. Both of the evaporators with the smaller pipe diameter required an additional row for the complete evaporation of the refrigerant.

The cooling capacity of each row of the evaporator can be calculated by summing the control volumes in each row, as due to each control volume having a constant ΔX, the capacity of each control volume is the same. Figure 4.15 shows the cooling capacity of each row of the different evaporator designs. The single circuit evaporator required a smaller length of pipe to complete the evaporation of the refrigerant than the 3 circuit evaporator for both tube diameters. The 8.01mm tube required 2.5% pipework in the single circuited evaporator than the 3 circuited evaporator. This can be used to reduce the material content of the evaporator or increase the cooling capacity of the evaporator.

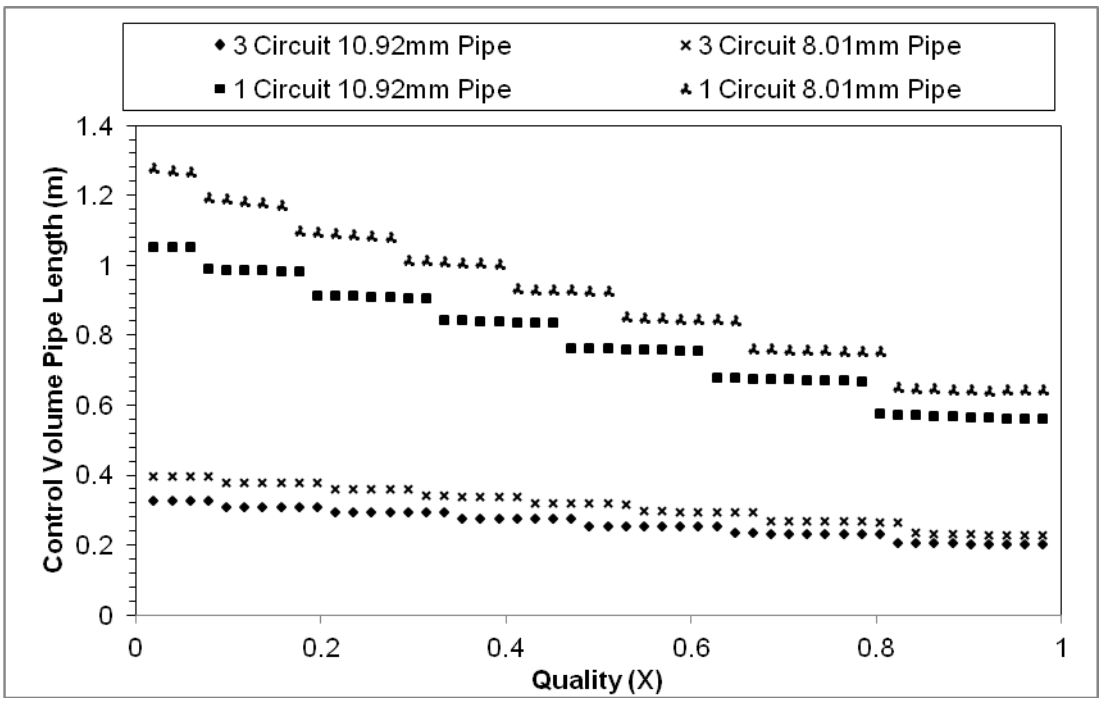

Figure 4.14 Control volume length calculation across the evaporator varying the number of circuits and diameter of tube.

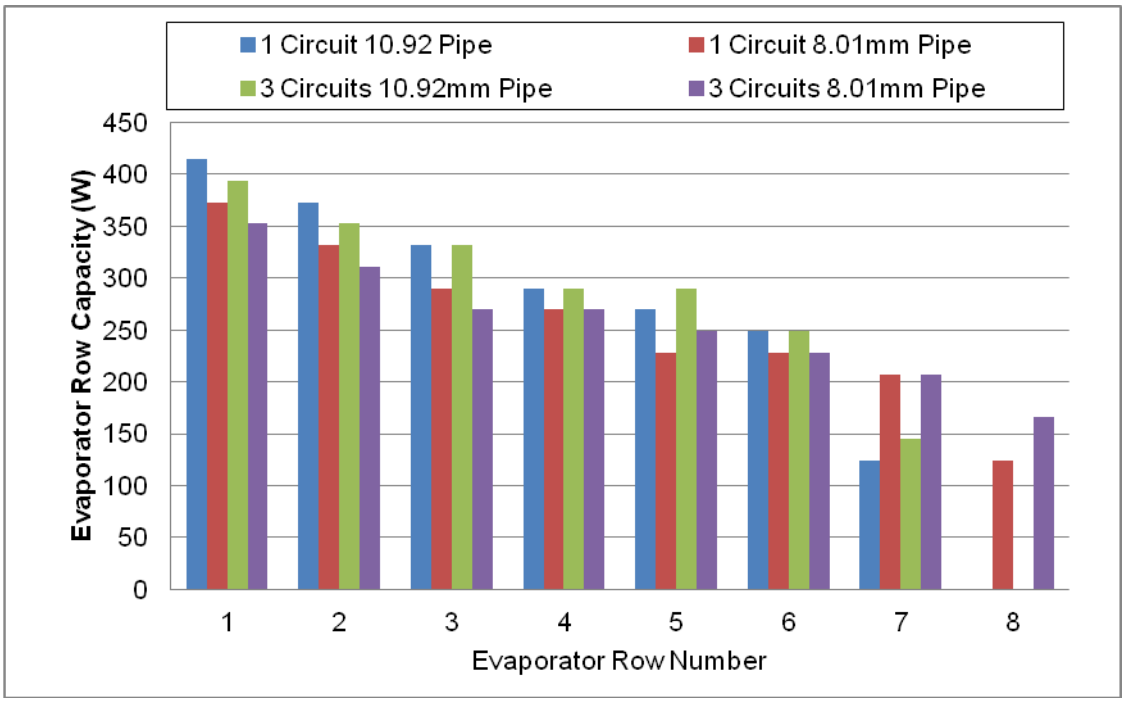

Figure 4.15 Evaporator row capacity calculation varying the number of circuits and diameter of tube.

4.6 Summary

This chapter presented an analysis of the simulation results from the models developed of the CO_2 booster and R404A refrigeration systems and a finned tube evaporator used in supermarket refrigeration systems.

The refrigeration system simulations showed that at ambient temperatures above 3°C the COP of the R404A system was greater than that of the CO_2 system. Over a period of one year the CO_2 refrigeration system consumed 18% more energy than the R404A system. This would increase the indirect emissions from the small supermarket by approximately 40 tCO_2 annually. However, the high GWP of R404A combined with refrigerant leakage resulted in an overall reduction in TEWI for the CO_2 system. Over a 10 year period the CO_2 system could reduce the environmental impact of a small supermarket by 128 tCO_2. While the environmental benefits of the CO_2 booster system are clear, the higher energy consumption costs of

£3,001 annually would be a barrier to future installs. The smaller supermarket retailers would find it difficult to absorb this increase in energy consumption costs. Further research and development is required to reduce the power consumption of the CO_2 booster system.

A numerical model of a plate-finned tube evaporator was developed and different circuitry configurations and tube diameters were simulated using CO_2 as the refrigerant. The investigation found that reducing the number of circuits from 3 to 1 increased the mass flux of the refrigerant which increased the velocity of the refrigerant. The single circuited evaporator reduced the length of pipe needed for complete evaporation. It was also found that reducing the diameter of tubes used in the CO_2 evaporator increased the length of evaporator required for evaporation, but this also increased the velocity of the refrigerant which is a positive feature considering the low velocities of CO_2 compared to other refrigerants. However, the reduction in tube diameter and reducing the number of circuits did increase the refrigerant pressure drop across the evaporator. This pressure drop is small and will have minimal impact on the compressor power consumption.

Chapter 5 Experimental system design

5.1 Introduction

The results of the theoretical simulations concluded that using fixed refrigeration capacities of 36 kW and 5 kW for the MT and LT loads respectively, the CO_2 booster system had annual energy consumption higher than that of a R404A system using transient ambient temperatures from Belfast. However, when simulated over a 10 year lifecycle the CO_2 system could reduce the environmental impact of a small supermarket by up to 128 tCO_2.The results of the theoretical simulations have therefore concluded that the CO_2 booster system could be a good alternative to the traditional R404A refrigeration systems installed in small supermarkets if the annual energy consumption figures where comparable.

An experimental system has been designed and built at Brunel University which has been used to validate the simulation models against actual system outputs, such as pressures, temperatures and energy use. Most of the investigations carried out for CO_2 solutions in commercial refrigeration are based on actual installations, which makes it difficult to perform parametric analyses and modify or optimise the system. It is also hard to draw conclusions on CO_2 system performance in relation to other systems due to the fact that comparisons are usually made between non-identical systems with different boundaries and operating conditions. Therefore, there is a real need for comprehensive laboratory testing of CO_2 systems where it is possible to control the operating conditions and carry out design modifications.

5.2 Experimental system design

A schematic diagram of the experimental system is shown in Figure 5.1. The transcritical booster system consists of two refrigeration temperature levels combined in one refrigeration system; a medium temperature (MT) level and a low temperature (LT) level.

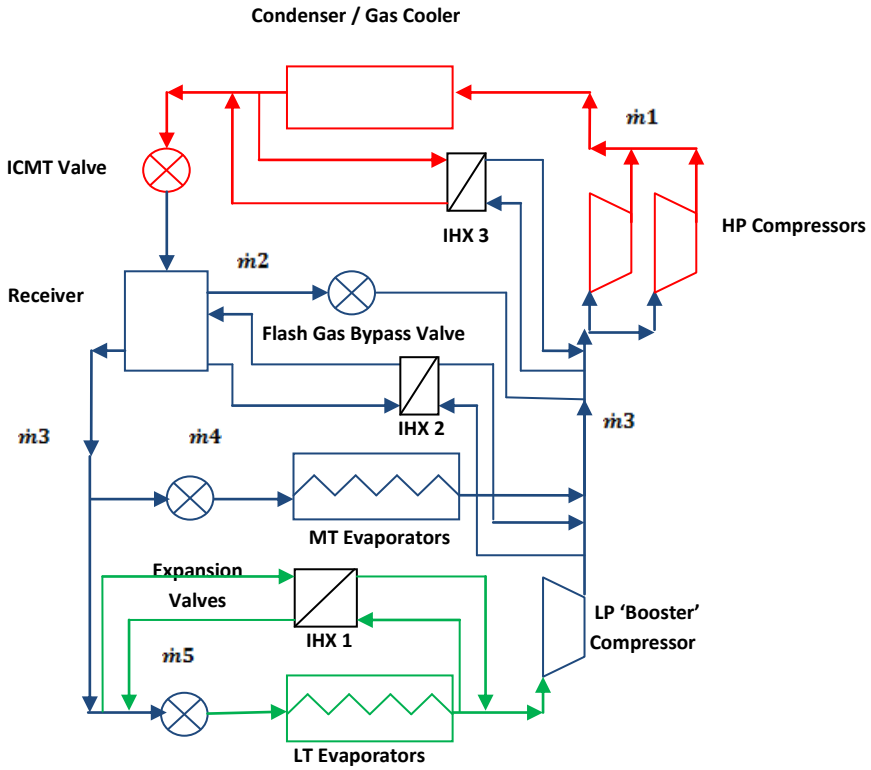

Figure 5.1 Schematic diagram of CO_2 Booster refrigeration cycle

Figure 5.2 Photo of manufactured and installed CO_2 booster system at Brunel University

5.3 Component selection

The selection of components for an experimental system is a critical part of the design process. When the system was being designed there was not a wide variety of components available for CO_2 systems. The selection process for each component in the cycle is detailed in the next sections. The design was based on an ambient temperature of 32ºC. At this temperature the system will be operating transcritically.

5.3.1 Compressors

The capacity of a compressor in a refrigeration system is selected according to the cooling load required. The cooling load requirements for a small supermarket are typically 36 kW for MT refrigeration and 5 kW for LT refrigeration, which were used as input values for the theoretical simulations. The calculation process for the

compressor selection for a booster system is different to that of a single temperature refrigeration system i.e. MT or LT only. The LT booster compressor discharges into the suction line of the MT compressors. This additional mass flow of refrigerant must be accounted for when designing the system. Unlike a single temperature system where there is only one mass flow rate of refrigerant, the booster system has five different mass flow rates of refrigerant, shown in Figure 5.1. The refrigerant mass flow rates are calculated from the required evaporator cooling capacity and the enthalpy difference across the respective evaporator, Equation 5.1. The calculated refrigerant mass flow is used to calculate the swept volume flow rate of the compressor required to generate the cooling capacity using the refrigerant inlet suction density and the volumetric efficiency of the compressor, Equation 5.2. Table 5.1 shows the calculation values for the required compressor swept volumes based on the cooling load requirements for a small supermarket. It must be noted that the mass flow rate for the medium temperature is mass flow $\dot{m}1$ shown in Figure 5.1. This has been calculated by the simulation model as it is a combination of mass flows due to the Booster system design with the flash gas bypass.

$$\dot{m} = \frac{Q_{MT}}{\Delta H} \tag{5.1}$$

$$\dot{V}_{swept} = \frac{\dot{m}}{\rho_{suc}\eta_{vol}} \tag{5.2}$$

Table 5.1 Properties of Compressors

	Cooling Load (kW)	ΔH (kg/kJ)	Mass Flow Rate (kg/s)	Refrigerant suction density (m^3/kg)	Volumetric efficiency (%)	Compressor swept volume (m^3/s)	(m^3/h)
Medium Temperature	36	242.4	0.315	69.81	76	0.0059	21.24
Low Temperature	6	243.7	0.024	36.79	76	0.0008	2.38

For the experimental system, it was not necessary to design the system for the full cooling capacities required in a small supermarket. A smaller system using the same design could be used to prove the concept and to generate the results required to verify the theoretical simulations. Two CO_2 compressors were made available from the manufacturer Bock for the purposes of the experimental system. Bock supplied two of RKX 26/31-2 for the high pressure side and one HGX12P/30-4 for the low pressure side of the experimental system. Table 5.2 shows the technical data of each compressor. The RKX compressor was a new design from Bock, specifically developed for Transcritical CO_2 applications. The mass flow rate of refrigerant available from each compressor was calculated using equation 5.2.

Table 5.2 Properties of Compressors

Model	No Cylinders	Swept Volume (m^3/h)	Suction Density (kg/m^3)	Suction Pressure (bar)	Suction Temp (ºC)	Mass flow available (kg/s)
RKX 26/31-2	6	5.40	69.81	27.80	-0.56	0.08
HGX 12P/30-4	2	2.80	36.79	14.89	-22.09	0.02

The simulation model was used to calculate the cooling capacity which would be generated by the installation of two RKX 26/31-2 high stage compressors and one HGX 12P/30-4 low stage compressor. The LT refrigeration capacity would be 5.2 kW and the MT cooling capacity would be 9.4 kW. This system would be unbalanced so it was necessary to install inverters to regulate the speed of the compressors and therefore the capacity of the system.

5.3.2 Valves

The valves in the refrigeration system are used to control the flow of refrigerant around the system, expand the refrigerant and maintain a pressure differential across the various components in the system.

High pressure valve - ICMT

This valve is only required for a transcritical system. Its function is to maintain the gas cooling pressure at an optimum value, explained in section 3.22 of this thesis. The valve maintains a pressure differential between the high stage pressure stage and medium pressure stage of the booster system, opening and closing from 100 – 0 % as required.

At the time of the system being designed and built there was only one commercially available valve, the Danfoss ICMT 20 valve with an ICAD 600S actuator, controlled by a Danfoss EKC 326 controller. An optimum high stage pressure is kept by the EKC 326 by controlling the ICMT valve. The optimum pressure is based on temperature and pressure readings from a pressure transducer and temperature sensor at the exit of the gas cooler.

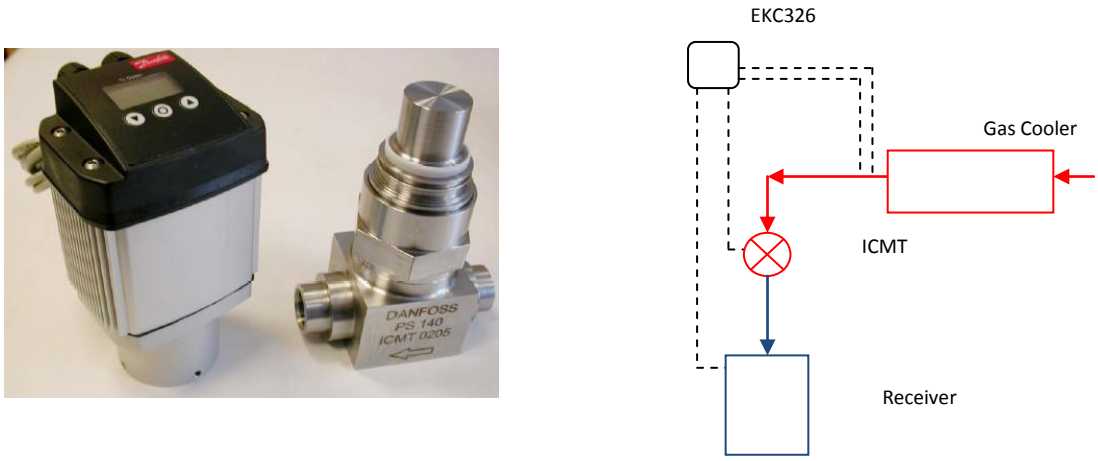

Figure 5.3 Image and controls schematic for ICMT valve

Gas bypass valve - ICM

The function of the gas bypass valve is to control flow of the vapour refrigerant from the receiver. The refrigerant is separated into liquid and vapour phases in the receiver and the gas is sent to the gas bypass valve at the top of the receiver. The pressure in the receiver is controlled by maintaining a pressure differential across the valve which separates the receiver pressure from the suction pressure. This also decouples

the receiver pressure from the ambient temperature. An analysis of the optimum receiver pressure is shown in section 3.25 of this thesis. The ambient temperature will therefore not affect the pressure inside the receiver and the flow of refrigerant to the evaporators.

The model is a Danfoss ICM 20 valve with an ICAD 600S actuator and is controlled by a Danfoss EKC 347 controller. A pressure transducer senses the pressure in the receiver and the EKC347 controller adjusts the opening of the ICM valve to maintain the receiver set pressure.

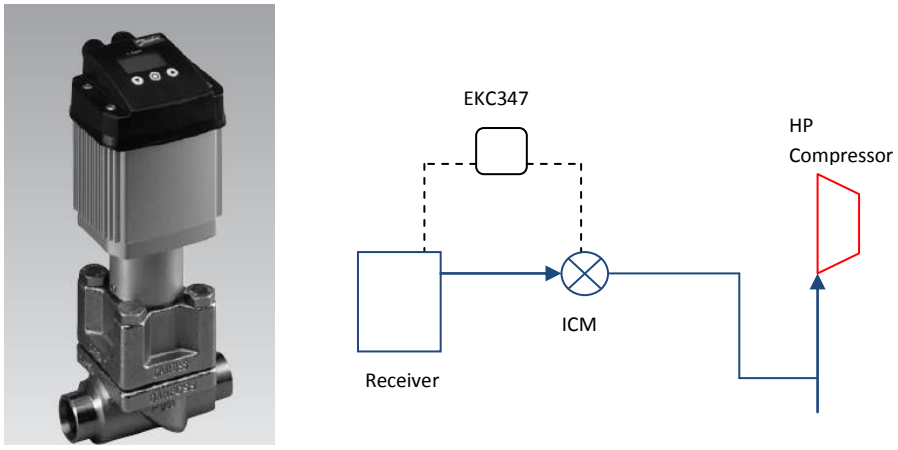

Figure 5.4 Image and controls schematic for ICM valve

Electronic expansion valves

The electronic expansion valves are positioned before the evaporator and are used to expand the refrigerant at the receiver pressure to the pressure / temperature required at the MT and LT evaporators. Danfoss AKVH electronic expansion valves were selected; these are specifically designed for the higher pressures associated with CO_2 systems. Danfoss AK-CC 550A controllers were used to control the refrigerant through the expansion valves.

The valve maintains a set superheat value at the evaporator exit by opening and closing 100 – 0%. A Danfoss AK-CC 550A controller is used to adjust the valve to

maintain the superheat. The controller uses data from a pressure transducer and temperature sensor at the exit of the evaporator and calculates the superheat.

The temperature inside the MT and LT cabinets are controlled by two temperature sensors, air temperature off the evaporator and air temperature onto the evaporator. The AKVH valve also acts as a solenoid, so when the cabinet reaches the desired temperature set point, the valve closes.

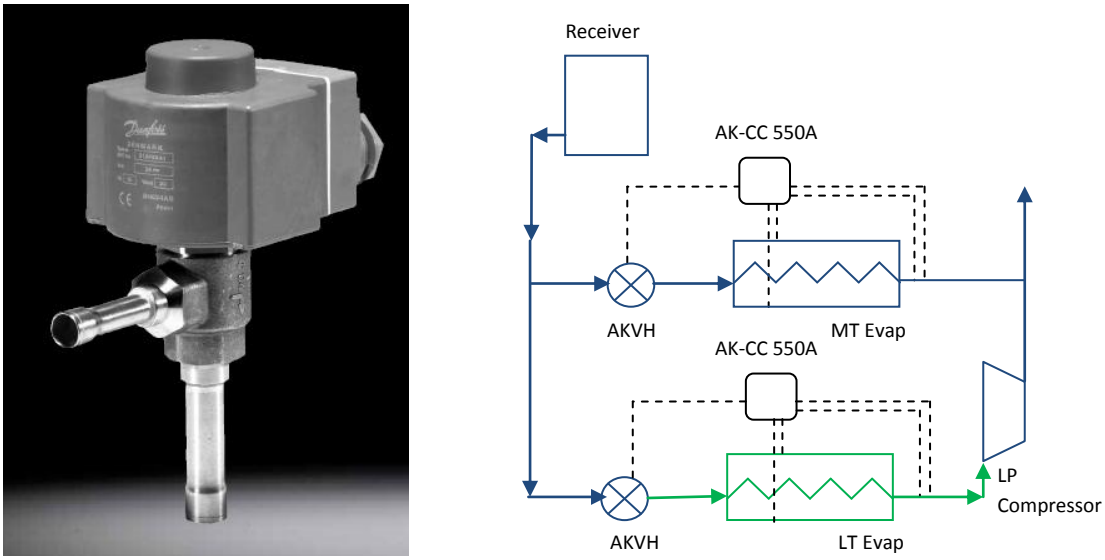

Figure 5.5 Image and controls schematic for AKVH valve

5.3.3 Gas cooler / condenser

The gas cooler is used to reject the heat from the supercritical refrigerant when the system is operating transcritically. When the system is operating subcritically the gas cooler acts as a condenser, condensing the subcritical refrigerant into a liquid phase before expansion. The selection parameters for the gas cooler are shown in Table 5.3. The gas cooler must be able to withstand the high gas cooling pressures of CO_2.

Figure 5.6 Image of gas cooler / condenser

Table 5.3 Design parameters for experimental gas cooler selection

Design Condition	
Refrigerant flow rate	0.15 kg/s
Refrigerant inlet temperature	107.0 ºC
Refrigerant outlet temperature	42.0 ºC
Ambient temperature	32.0 ºC
Gas cooling pressure	107.0 bar
Max design pressure	130.0 bar
Bock RKX 26/31-2 Gas cooler heat rejection	14.3 kW per compressor
Total Design Heat Rejection	28.6 kW

5.3.4 Receiver

The liquid receiver also acts as a liquid separator in the CO_2 booster system. Liquid refrigerant is transferred to the evaporators from the liquid receiver and the vapour refrigerant is bypassed around the evaporators. The following design points were used to determine the size of the receiver.

- The receiver should be sized to enable full pump down of the system, holding the full refrigerant charge.
- The gas bypass outlet should be high enough on the receiver so it is not submersed by liquid refrigerant.

- A maximum internal diameter of 0.3m was chosen so the receiver could fit inside the rack for the compressors; the receiver would be positioned vertically to enable this.

An estimate of the volume of liquid inside the system is calculated in Table 5.3.

Table 5.4 Calculation of estimated liquid volume

Component	Length (m)	Internal Pipe Diameter (m)	Internal Pipe Volume (m^3)	Liquid %	Liquid Volume (m^3)	Gas Volume (m^3)
Liquid Line	15	0.0139	0.0023	100	0.0023	0.0000
MT Evap	15	0.0107	0.0013	50	0.0007	0.0007
LT Evap	15	0.0107	0.0013	50	0.0007	0.0007
Extra Evap	15	0.0107	0.0013	50	0.0007	0.0007
Condenser	20	0.0107	0.0018	60	0.0011	0.0007
				Total Volume	**0.0054**	**0.0027**

While the pressure of the receiver will be maintained at approx 31 bar, the receiver must be designed to withstand a maximum design pressure of 80 bar.

5.3.5 Internal Heat exchangers

The internal heat exchangers are used to transfer heat between different processes in the system:

1. **IHX 1 – Protection for LT compressor**

   This internal heat exchanger acts as a protection device for the LT compressor to prevent liquid from entering the suction of the LT compressor. Any remaining liquid that has not been evaporated in the LT evaporator will be evaporated in this internal heat exchanger. The use of this heat exchanger will increase the suction temperature of the LP compressor, increasing the

discharge temperature and total enthalpy difference across the LP compression process. The increase in enthalpy difference across the LP compressor will increase the total work input to the compressor. This heat exchanger should not be used unless necessary for further compressor protection.

2. **IHX 2 – Inter-cooling from receiver**

   This heat exchanger uses the flow of liquid refrigerant from the receiver to intercool the refrigerant between compression stages. The inter-cooling between stages is a positive effect that decreases the refrigerant suction temperature of the HP compressors and therefore the discharge temperature. This decreases the total enthalpy difference across the total two stage compression process and therefore the total work input by the compressors.

   This heat exchanger could also have the negative effect of increasing the temperature of the receiver or evaporating refrigerant in the receiver. Both effects must be experimentally analysed.

3. **IHX 3 – Suction line internal heat exchanger**

   This internal heat exchanger provides sub-cooling of the refrigerant after gas cooling. This can provide an increase in cooling capacity for a transcritical system with no flash gas bypass but due to the separation of the liquid and vapour in the receiver in the booster system, this device does not increase the capacity but can be used as a protection device for the high stage compressors.

5.3.6 Evaporators

For the experimental system, two supermarket refrigeration cabinets will be used as the evaporators, one 2.5m MT multi-deck cabinet and one 3 door multi-deck LT cabinet with doors. Both cabinets are shown as installed in Figure 5.7. The cabinets are housed inside a test chamber shown in Figure 5.8, which maintains the internal

environmental to ISO (International Organisation for Standardisation) standards, BS EN ISO 23953-2:2005 Refrigerated display cabinets – Classification, requirements and test conditions, (BSI, 2005). The indoor climate was maintained at Climate Class 3, throughout the tests. To simulate product in the cabinets and apply a load to the cabinets each cabinet was filled with M-packs in containers as shown in Figure 5.7. The M-packs were placed on the base of each cabinet and on the shelves. The M-packs contained a mixture of hydroxyethylmethyl cellulose (Tylose), sodium chloride (salt), 4-chloro-m-cresol (anti-bacteria), with boiling water as specified by the supplier (Sigma-Aldrich company, Ltd). To monitor and record the temperature of the cabinets a total 36 thermocouples were installed in to the M-packs on each cabinet. The thermocouples were installed into the top, middle and bottom shelves at locations on the left, middle and right of each shelf. This gives a good spread of the temperatures inside the cabinets to show the cooling performance of the CO_2 booster system.

Figure 5.7 Photos of MT and LT multi-deck cabinets in the test chamber

Figure 5.8 External photo of the test chamber

5.4 Piping design

The higher operational pressures of CO_2 compared to traditional HFCs means further consideration must be given to the materials used for the distribution pipe work. The internal dimensions of the pipe work depend on refrigerant pressure drop and the velocity of refrigerant inside the pipe work. Internal pipe diameters are selected to be large enough to reduce the pressure drop across the section of pipe work but must also maintain the refrigerant at a high enough velocity so that oil distributes around the circuit efficiently, carried by the refrigerant. The recommended pipe sizes and materials are shown in Table 5.5. (BSI, 2002; BSI, 2006; BSI, 2009)

Table 5.5 Calculated properties of recommended distribution pipe work

Pipe work	P_{Max} (bar)	L (m)	D_{int} (mm)	Pipe ΔT (mm)	Pipe ΔP (bar)	Vel (m/s)	Material	P_{Burst} (bar)
Common HP Suction	52	5	13.9	1	0.3	16.4	5/8 Copper Drawn 19 SWG	49
Common HP Discharge	130	10	12.5	2.3	0.4	7.5	3/8 Stainless Steel A312 40	1430
After Gas Cooler	130	10	12.5	2.3			3/8 Stainless Steel A312 40	1430
After Internal Heat Exchanger	130	1	12.5	2.3			3/8 Stainless Steel A312 40	1430
Common Liquid Line	52	10	13.7	1	0.02	0.6	5/8 Copper Drawn 19 SWG	49
MT Liquid Line	52	25	10.7	1	0.07	0.55	1/2 Copper Drawn 19 SWG	53
MT Suction Line	52	25	10.7	1	0.58	7.5	1/2 Copper Drawn 19 SWG	53
LT Liquid	52	10	7.52	1	0.1	0.7	3/8 Copper Drawn 19 SWG	62
LT Suction	52	10	10.7	1	0.3	12.3	1/2 Copper Drawn 19 SWG	53

5.5 Controls

Figure 5.9 shows a schematic diagram of the controls system for the CO_2 booster refrigeration system. Danfoss controls were the only controls available for this system at the time of manufacture. All of the controllers communicate using the Danfoss ADAP-Kool control system. All of the controllers can be set from the Danfoss AK-SC255 system controller located in the test chamber; Figure 5.10 shows an image of the system controller.

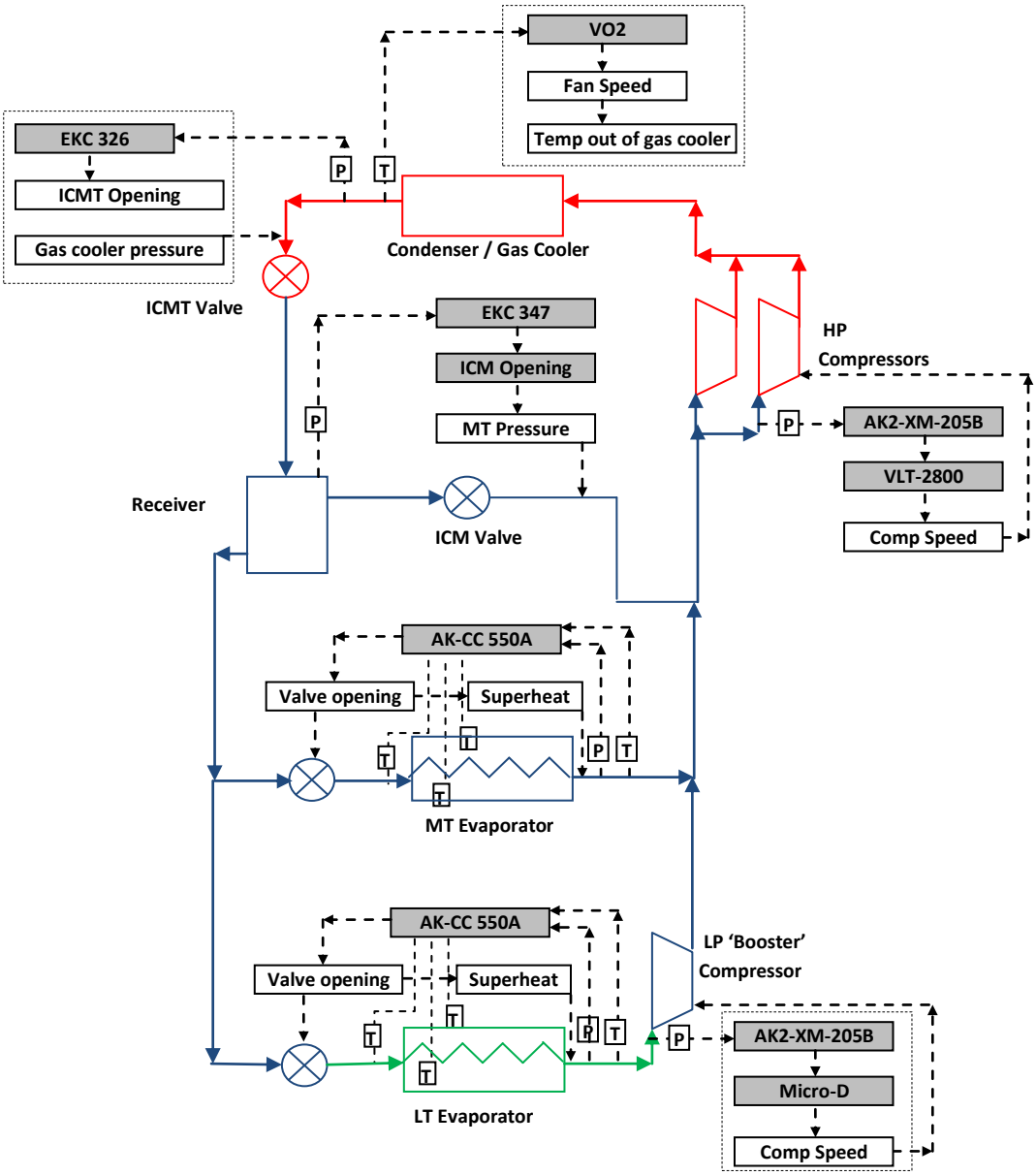

Figure 5.9 CO_2 booster refrigeration system controls schematic

Figure 5.10 Photo of the Danfoss system controller

5.6 Monitoring

Monitoring software is used to monitor and record pressures, temperatures and flow rates at various locations on the test system. Table 5.6 lists the number of sensors used for the system as well as their location and type. The thermocouples and pressure transducers in the compressor system are used to record the pressures and temperatures of the refrigerant when the system is running. These will be used to verify the simulation models.

The flow rate of the refrigerant in the MT and LT liquid lines is monitored by two coriolis flow meters. This will enable the calculation of the cooling capacity of the MT and LT cabinets. The relative humidity of the test chamber is being recorded to ensure the ISO conditions are being adhered to. Two other relative humidity sensors are placed in the MT cabinet and the LT cabinet. These will be used to calculate the air side refrigeration capacity of each cabinet.

All of the sensors are connected to Datascan modules and Labtech software, which shows the sensor output live on a computer screen and also records the outputs every 20 seconds. Figure 5.11 shows the screen view of the Labtech software.

Table 5.6 Test system sensor numbers, types and locations.

Sensor Type	Sensor records	Sensor Location	Number of Sensors
Thermocouple	Temperature	MT Cabinet	36
Thermocouple	Temperature	LT Cabinet	36
Thermocouple	Temperature	Compressor system	37
Pressure transducers	Pressure	Compressor system	11
Thermocouple	Temperature	Roof	1
Coriolis flow meter	Refrigerant flow rate	On MT liquid line	1
Coriolis flow meter	Refrigerant flow rate	On LT liquid line	1
Relative humidity sensor	Relative humidity	Test chamber, MT cabinet, LT cabinet	3

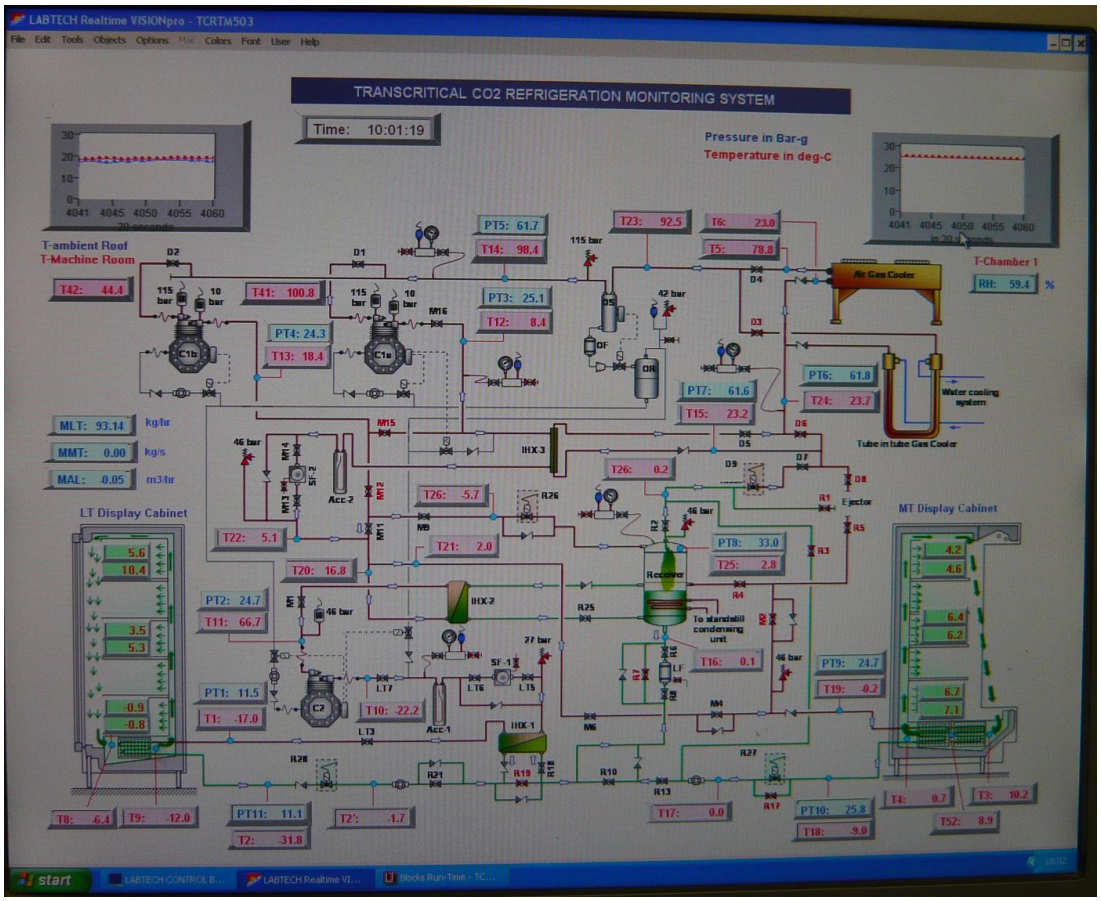

Figure 5.11 Labtech software screen

5.7 Summary

This chapter has described the experimental system at Brunel University which was used to run tests to validate and optimise the simulation models developed in Chapter 3 of this thesis. The components have been sized and selected according to the capacity of the system. The component selection also depended on what components were available for the CO_2 system from manufacturers at the time of construction of the system. The controls used for the system have also been described. The input parameters for the controls are presented in the next chapter.

Chapter 6 Test results and model verification

6.1 Introduction

This chapter presents and discusses the results of tests performed on the CO_2 booster refrigeration system in a laboratory environment. The design of the refrigeration system was presented in detail in Chapter 5. The test results will enable the validation of the numerical simulation model, developed and presented in Chapters 3 and 4. Firstly, the set points, assumptions and controls used for the test system are discussed then the test results are presented. The simulation model is then used to simulate the experimental system using the evaporator capacities calculated from the test results and the recorded ambient temperature during the tests. The results from the simulation model are then presented and compared with the test results. Any differences between the actual test results and the simulation model results will be explained and the model will then be optimised using the test data.

6.2 Set points and controls

The booster CO_2 refrigeration system consists of both the high stage and low stage compressors for MT and LT refrigeration temperatures in a single refrigeration circuit. Traditionally these two temperature levels are used in separate refrigeration circuits in smaller supermarket refrigeration systems. A schematic diagram of the system and the associated controls are shown in Figure 5.9. The control parameters and set points used for the tests are discussed in the next sections.

6.2.1 Compressor controls

The compressors are controlled by the suction pressure of each respective compressor using a target suction pressure set point with a set pressure differential. A Danfoss AKS pressure transducer measures the suction pressure and the AK2-XM-205B controller varies the speed of the compressor through the VLT or Micro –D inverter to meet the target suction pressure. The controller uses a PI (proportional integral) control loop to control the speed of the compressor to reach the suction pressure settings.

Table 6.1 Compressor settings

Set Points	HP Compressor	LP Compressor
Target suction pressure (bar)	26	12
Target suction temperature (°C)	-10	-32
Pressure differential (bar)	2	2

6.2.2 High pressure valve (ICMT)

The ICMT valve controls the high stage pressure in the refrigeration system, separating the gas cooling pressure from the receiver pressure and therefore evaporating pressures. The valve is controlled by a Danfoss EKC326A controller, specifically designed to regulate the gas cooler pressure for a transcritical CO_2 refrigeration system. CO_2 has an optimum gas cooling pressure when operating transcritically as discussed in section 3.33 of this thesis. The EKC326A controller uses a temperature transducer to measure the temperature of the refrigerant exiting the gas cooler and a pressure transducer to measure the gas cooling pressure as shown in Figure 5.9. The optimum gas cooling pressure is a function of the temperature of the refrigerant exiting the gas cooler. When the system is moving from subcritical to transcritical operation or vice versa the controller uses a transition zone control theory. Figure 6.1 shows the transition zone and Table 6.2 shows the input parameters for the EKC326A controller. When the temperature of the

refrigerant exiting the gas cooler approaches 26°C the system moves from subcritical to a transition subcritical operation then the refrigerant reaches 29°C transcritical operation occurs. The ICMT valve automatically optimises the gas cooler pressure throughout the transition zone and the transcritical operation of the system.

In previous simulations the transition temperature from subcritical operation to transcritical operation was assumed to be 31°C, which is the critical temperature of CO_2. Through experience of transcritical systems Danfoss has factory set the EKC326A controller with the settings in Table 6.2. For the tests, the Danfoss factory settings will be used and the simulation models will be altered for validating, using the Danfoss settings.

Table 6.2 EKC 326A Controller Settings

Parameter	Description	Setpoint
T_{SC} Max (°C)	Maximum gas cooler outlet temperature for sub critical operation	26
T_{tc} Min (°C)	Minimum gas cooler outlet temperature for transcritical operation	29

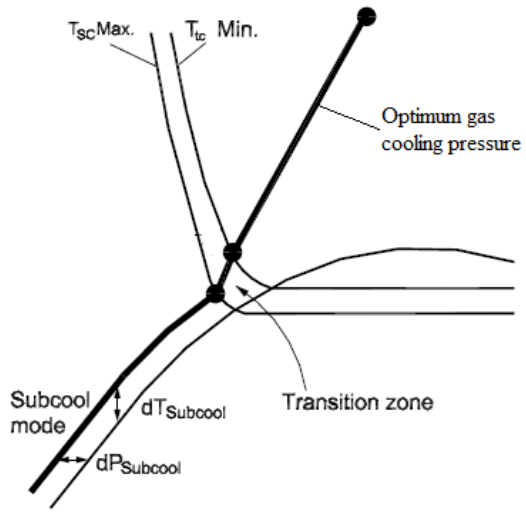

Figure 6.1 Transition zone and optimum gas cooling control of EKC326A controller on CO_2 pressure – enthalpy chart (Danfoss, 2008b)

6.2.3 ICM Valve

The ICM valve controls the pressure in the receiver which also acts as a liquid separator. The liquid refrigerant flows to the evaporators from the bottom of the receiver and the vapour refrigerant is bypassed directly to the HP compressor suction line. The ICM valve controls the flow of vapour refrigerant from the receiver resulting in the control of receiver pressure. This decouples the pressure in the receiver from the ambient temperature, which is beneficial due to the low critical temperature of CO_2. The ICM valve is controlled by an EKC 347 controller. This controller uses a pressure transducer to sense the receiver pressure and adjusts the ICM valve to meet the required set points, shown in Table 6.3. The EKC 347 is a liquid level controller, for regulating the liquid level in a vessel. Although this system required the receiver to be held at a set pressure, not contain a percentage of refrigerant liquid, the EKC 347 was the only controller available at this time. By experimenting with the controller the target liquid refrigerant quality of 65% was found to hold the receiver at the required pressure of 33 bar.

Table 6.3 EKC347 Set points

Parameter	Description	Set point
Liquid level set point (%)	Set point of liquid level required in the vessel	65

6.2.4 Evaporator controls

The MT and LT evaporators are controlled by Danfoss AK-CC-550A controllers. The controller controls the flow of refrigerant to the evaporator by opening and closing the electronic expansion valve to maintain a superheat set point. The superheat is calculated by temperature measurements of the refrigerant from temperature sensors before and after the evaporator and a pressure transducer after the evaporator. This regulates the cooling capacity of the evaporator.

The temperature of the MT and LT cabinets are also controlled by the controller. The desired temperature set point is set on the controller with a temperature differential. Once the temperature inside the cabinet reaches the desired set point the controller closes the electronic expansion valve, stopping the flow of refrigerant through the evaporator. The valve opens again when the temperature in the cabinet exceeds the set point plus the differential. The set points are shown in Table 6.4.

Table 6.4 Evaporator settings

Set Points	MT Evaporator	LT Evaporator
Temperature set point (°C)	-8	-18
Temperature differential (°C)	2	2
Superheat (K)	7	7

6.3 CO_2 refrigeration system test results

The test results of the refrigeration system are presented and discussed in the following sections.

6.3.1 Compressor and gas cooler performance

The system was operated using one HP compressor and one LP compressor. The temperature of the refrigerant through the compression stages is shown in Figure 6.2 when the system was running transcritically due to high ambient temperature. The HP compressor discharge temperature was approximately 118°C and the HP compressor suction temperature averaged 8°C leading to a 110K temperature difference. This was a very high temperature difference compared to that of a R404A compressor, where at the same conditions the temperature difference would be

approximately 65K. The high discharge temperature at high ambient temperatures is a unique feature of CO_2 which could be utilised for heat recovery purposes as discussed by Ge and Tassou, (2011) and Colombo, (2011).

The LP compressor suction temperature averaged -18°C and the discharge temperature was approximately 80°C. The refrigerant discharge temperature for the LP compressor was very high for a refrigerant condensing at the inter-stage pressure of 26 bar or a saturated vapour temperature of -10°C. This result is investigated and discussed in the next section with the simulation model results.

The temperature of the refrigerant exiting the gas cooler averaged 29°C, just below the critical temperature of CO_2. The ambient temperature averaged 27°C, only 2K below the temperature of the refrigerant exiting the gas cooler. In previous simulations the ΔT between the condensing/gas cooling temperature and the ambient temperature was assumed to be 10K, which is used for R404A systems. The low ΔT meant the gas cooler preformed very well at rejecting the heat from CO_2 at these conditions, demonstrating the good heat transfer capabilities of the refrigerant. This will lead to considerable energy savings; the lower condensing/gas cooling temperatures will reduce the pressure differential across the HP compressor lowering the power consumption of the compressor.

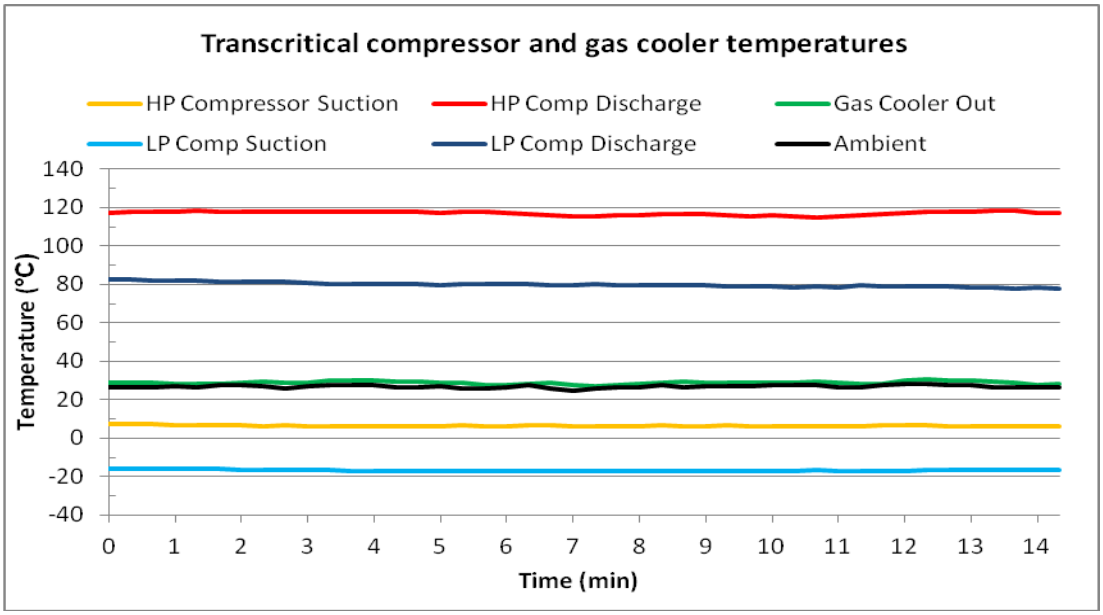

Figure 6.2 System temperatures under transcritical operation

Figure 6.3 shows the system pressures when operating transcritically over the same period shown for the system temperatures in Figure 6.2. The LP compressor suction pressure was around 12 bar, which was approximately the same as the pressure of the LT evaporator. The pressure of the liquid refrigerant feeding the LT evaporator expansion valve was held at a fairly constant 32 – 34 bar in the receiver. This confirmed the ICM valve controller (EKC 347) was functioning well holding the receiver at a set pressure. The liquid receiver also feeds liquid to the MT evaporator. This was at the same pressure as the HP compressor suction. The refrigerant at these stages of the cycle was at approximately 26 bar, which is the target suction pressure of the HP compressor.

All the refrigerant pressures discussed so far have been well below the critical pressure of the refrigerant, but the discharge pressure of the refrigerant shown in Figure 6.3 is fluctuating at the critical pressure of the refrigerant at 73.8 bar. This pressure is very high compared to HFC discharge pressures. R404A would have a maximum discharge pressure of 28 bar at very high ambient temperatures. Stainless steel pipes and components are required on the discharge line to resist the high pressures.

Although the gas cooling temperature of the refrigerant is 27°C (shown in Figure 6.2), which is below the critical temperature of the refrigerant, the gas cooler pressure is fluctuating at the critical pressure. The EKC 326A has decoupled the pressure temperature relationship of the refrigerant, optimising the gas cooler pressure. This proves that the EKC 326A controller is operating using the control theory discussed.

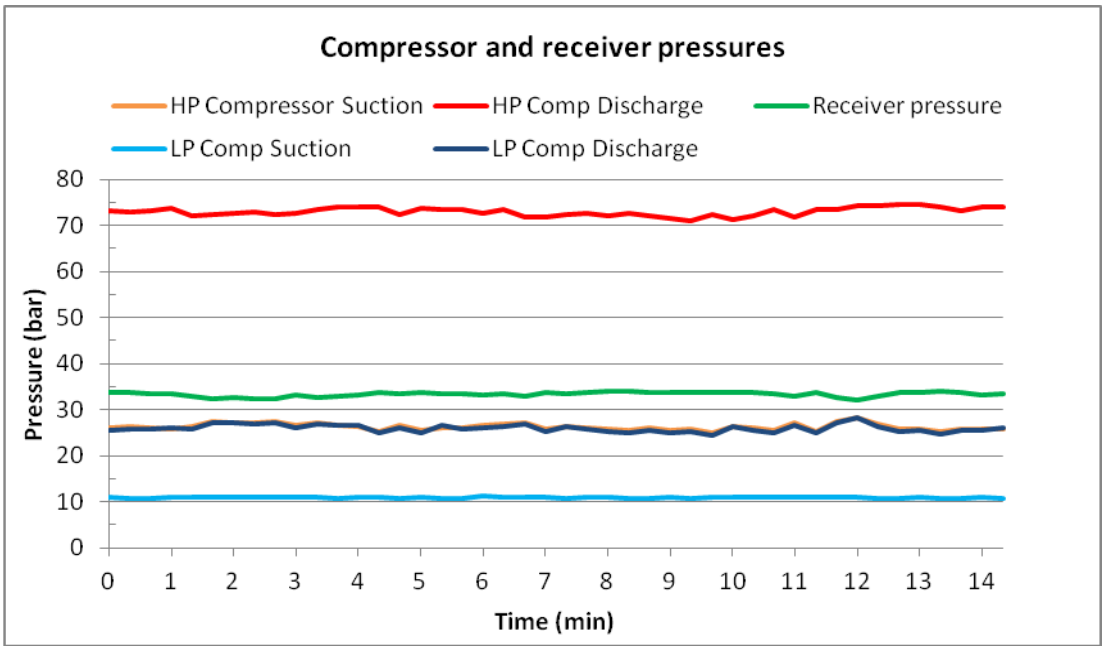

Figure 6.3 System pressures under transcritical operation

6.4 Evaporator performance

The LT evaporator pressure and temperatures are shown in Figure 6.4. The LT evaporating temperature was approximately -33°C. The temperature of the refrigerant exiting evaporator fluctuated, providing superheat up to 15K. These fluctuations can be reduced by tuning the expansion valve. During the test, liquid refrigerant was generally present in the liquid line sight glass so the enthalpy of the refrigerant could be calculated using the liquid properties at this point. The refrigerant was fully evaporated at the exit of the evaporator due to the presence of superheat so the enthalpy of the refrigerant could be calculated using the superheated vapour properties at this point. The capacity of the LT evaporator was calculated by multiplying the refrigerant flow rate measured with a coriolis flow meter with the enthalpy difference of the refrigerant at the inlet and outlet of the evaporator coil. The presence of vapour bubbles in the refrigerant flow in the liquid line caused fluctuations in the measured refrigerant flow rate. This was problematic causing large fluctuations in the refrigerant side capacity calculation of the evaporator, shown in Figure 6.5. To get a more accurate indication of the test capacity of the evaporator

the average refrigerant flow rate through the flow meter was calculated and used to calculate the evaporator capacity, shown in Figure 6.5. The capacity of the evaporator was also calculated using the air side heat exchange, shown in Figure 6.5 using equation 6.1.

The refrigerant side LT evaporator capacity using the average refrigerant flow rate averaged 4.1 kW and the calculation using the air side properties were similar averaging 3.8 kW. The test capacity of the LT evaporator was calculated to be 4.0 kW.

$$Q = m_r(\Delta H_r) = m_a(\Delta H_a) \quad \textbf{(6.1)}$$

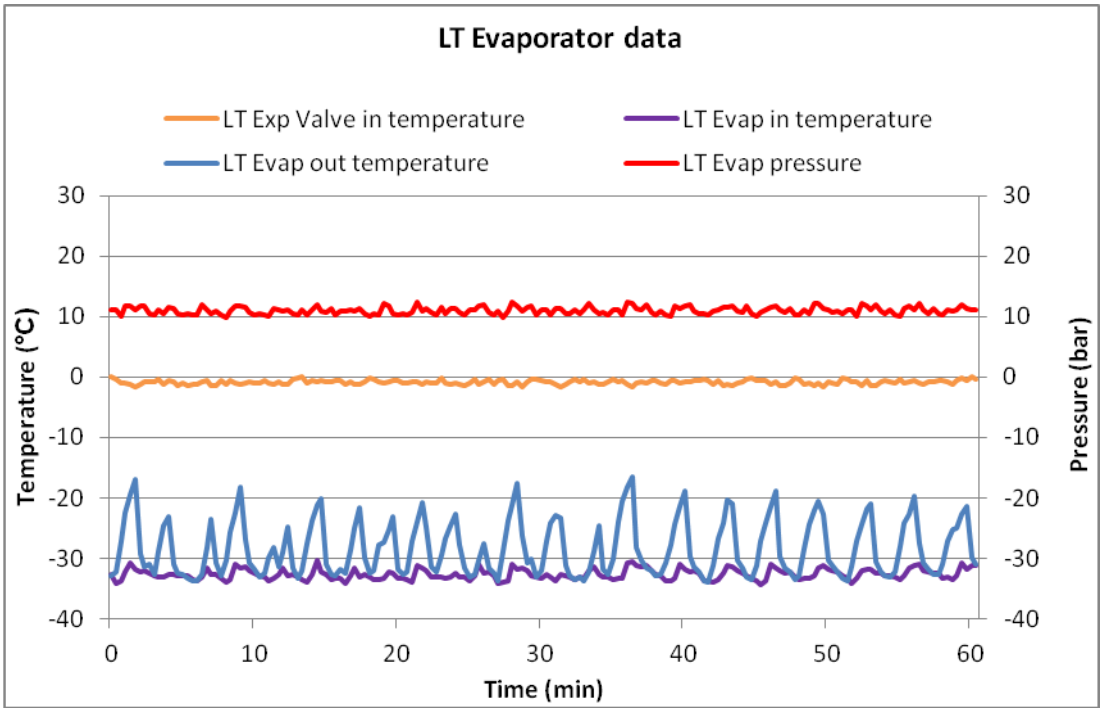

Figure 6.4 LT evaporator performance

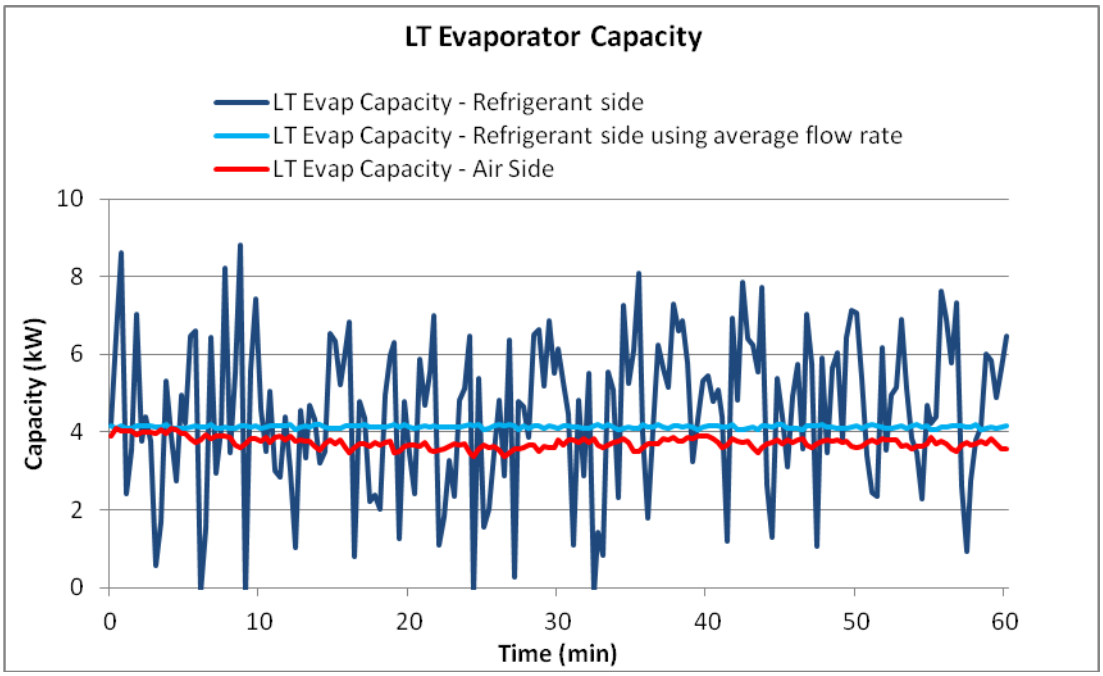

Figure 6.5 LT evaporator capacity calculation

The MT evaporator pressure and temperatures are shown in Figure 6.6. The MT evaporating temperature was approximately was -8°C. The superheat for the MT evaporator was much more closely controlled by the expansion valve as there were fewer fluctuations. The superheat was on average 6K. Liquid was a problem for this evaporator. For most of the experiment there was little liquid present in the liquid line from the compressor system to the evaporator. The liquid had evaporated in the pipes before getting to the sight glass which was unexpected. The absence of liquid could have also been for the following reasons.

- **Insufficient refrigerant charge**

  During the charging of the system the receiver was charged fully with liquid refrigerant. There are two sight glasses on the side of the receiver to indicate the volume of liquid in the system. When initially charged the top sight glass was full of liquid. This level decreased to the lower sight glass when the system was started as the refrigerant was being fed to the MT and LT evaporators. Liquid was present in both the LT and MT sight glasses at the

start, but the MT sight glass became dry after a period of approximately 2 hours.

Due to the high heat transfer properties of CO_2 some of the liquid refrigerant could have been evaporated. The refrigerant could have been evaporated in the receiver/separator and exist as vapour in the receiver during operation, reducing the flow of liquid to the evaporators. A further charge of refrigerant in the system could have helped, allowing for the evaporation of some liquid. The receiver would then be too small to hold all the liquid in the system when shutting down which would be dangerous.

- **High rate of heat transfer and layout of system**

  The compact layout of the experimental system coupled with high ambient temperatures and the high heat transfer properties of CO_2 could have caused the evaporation of liquid refrigerant in the pipes before reaching the MT sight glass.

This problem could have been resolved by increasing the size of the receiver, increasing the insulation on the liquid line pipes or installing a sub-cooling circuit before the MT expansion valve. Unfortunately this could not be completed within the time limitations of this project. A commercial system would not have been so compact and a bigger receiver could easily be installed. The presence of liquid before expansion affects the calculation of enthalpy difference across the evaporator and ultimately the capacity of the evaporator. For the purposes of this research it was assumed that the refrigerant had a quality of 80% liquid available for expansion.

Figure 6.7 shows the capacity of the MT evaporator calculated in the same way as the LT evaporator using a coriolis flow meter to record the flow rate of refrigerant to the evaporator. The large fluctuations are due to the presence of vapour bubbles in the liquid line causing fluctuations in the measured liquid flow rate. Due to the large variation in the measured refrigerant flow rate the refrigerant side MT evaporator capacity was also calculated using the average refrigerant flow rate shown in Figure 6.7. The MT evaporator capacity was also calculated using the air side method used previously for the LT evaporator and the average refrigerant flow rate for the refrigerant side capacity calculation. Using the refrigerant side method with the

average flow rate calculated a MT evaporator capacity of approximately 6.6 kW, the air side method also calculated an average capacity of 6.6 kW.

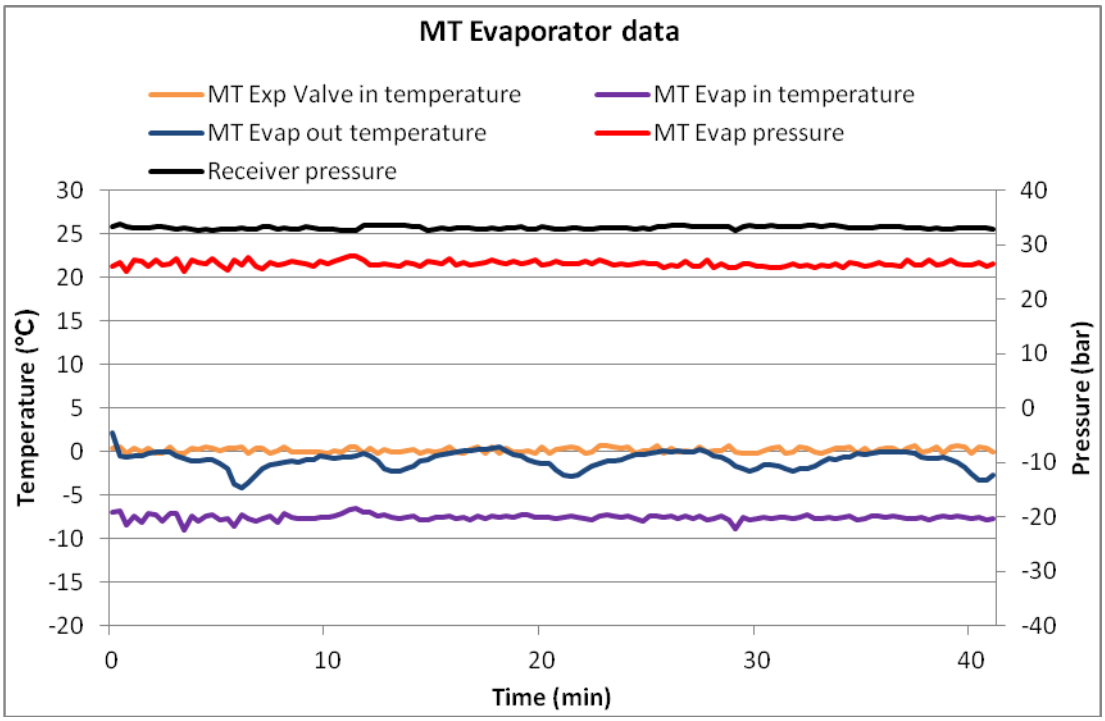

Figure 6.6 MT evaporator performance

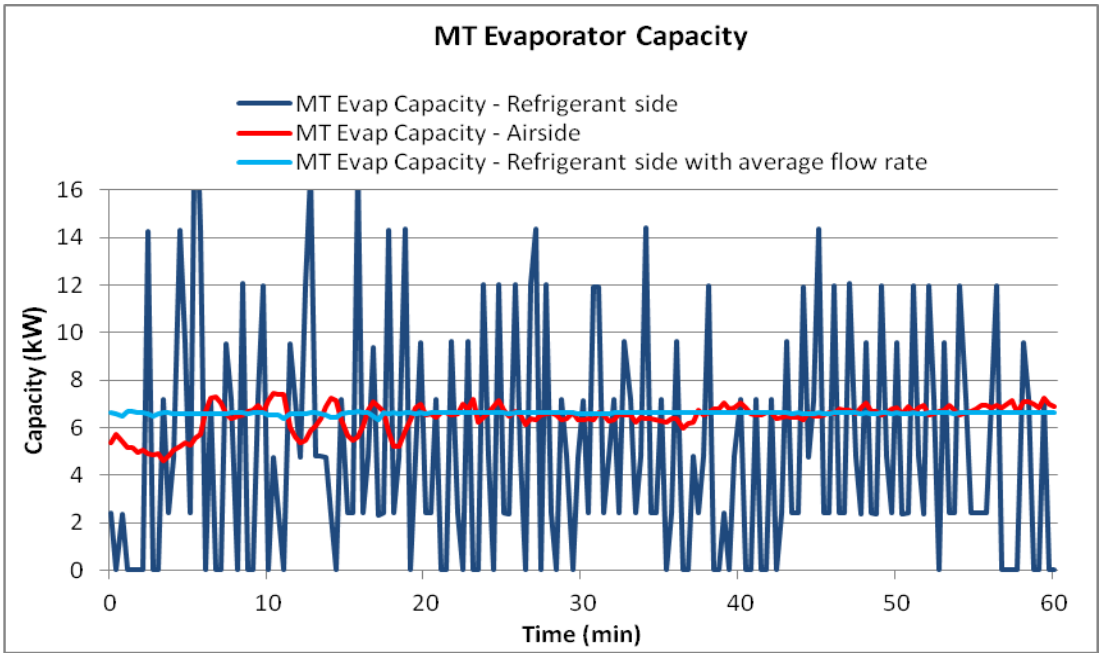

Figure 6.7 MT evaporator capacity calculation

6.5 Energy performance

The electricity consumed by the complete system was recorded using a Voltech PM300 three phase power analyser coupled with recording software on a local PC. The power meter recorded the instantaneous electricity consumed by the complete system. Manufacturer power consumption data for power consuming components are shown in Table 6.5. The standstill condensing unit is a safety feature of the system. The condensing unit is connected to an additional safety cooling circuit inside the receiver. If the system was to fail the condensing unit switches on, preventing the CO_2 inside the receiver dangerously high pressures above the design pressure of the receiver.

Table 6.5 Manufacturer power consumption data of system components.

	Frequency Range / RPM	Power Consumption (kW)
HP Compressor	35 Hz – 50Hz	4.01 – 7.65
LP Compressor	50Hz	1.33
Controls	50Hz	0.38
Standstill Condensing unit	50Hz	2.40
Condenser / Gas Cooler fan	1110 – 1450 RPM	0.44 – 1.00

The power consumption of the compressors when the system was running subcritically and transcritically for a period of one hour is shown in Figures 6.8 and 6.9 respectively. The power consumption of the LP compressor is very steady during both operational periods. This compressor has a fixed suction pressure set point and a fixed condensing pressure, which is the HP compressor suction pressure. Unlike the HP compressor this compressor is not linked to the ambient temperature so the energy consumption is steady, only switching off when the LP the suction pressure set point has been met. The power consumption of this compressor was approximately 1.2 kW during both the subcritical and transcritical periods.

The HP compressor power consumption was much more variable than the LP compressor due to the power consumption being a function of the ambient

temperature and the inverter speed. During the subcritical operation in Figure 6.8 the power consumption was above 4 kW but this was increasing with the ambient temperature, increasing the pressure ratio across the compressor. The HP compressor was cycling on and off to maintain the target suction pressure. Figure 6.9 shows a one hour period of transcritical operation due to the high ambient temperatures and therefore high gas cooler outlet temperatures. The gas cooler outlet temperatures were above the transition zone temperature of 26°C, so the EKC726A controller was optimising the gas cooler pressure. The power consumption of the HP compressor was generally above 6 kW when running at full speed but this reduced to 4 kW when running at slower speeds.

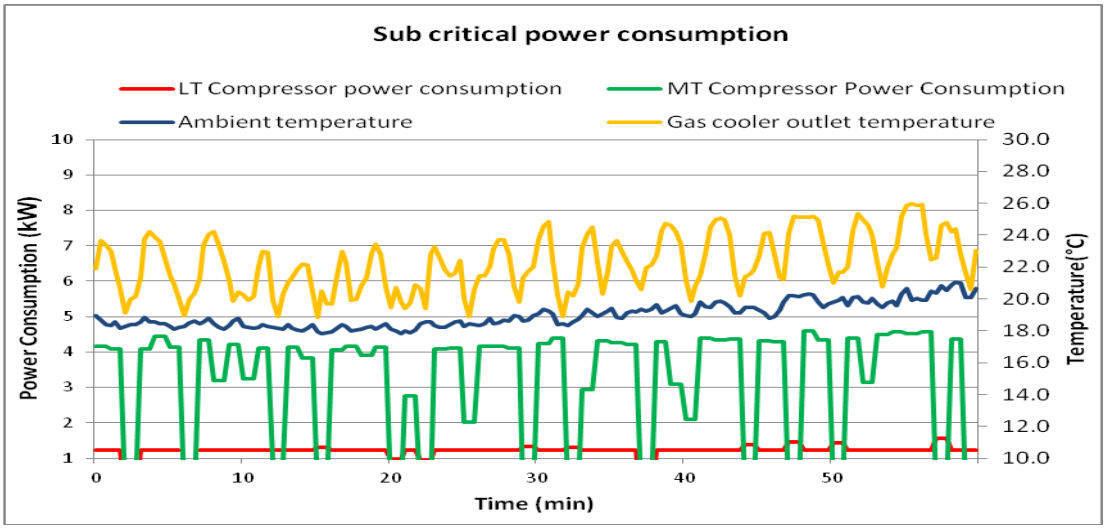

Figure 6.8 Compressors power consumption

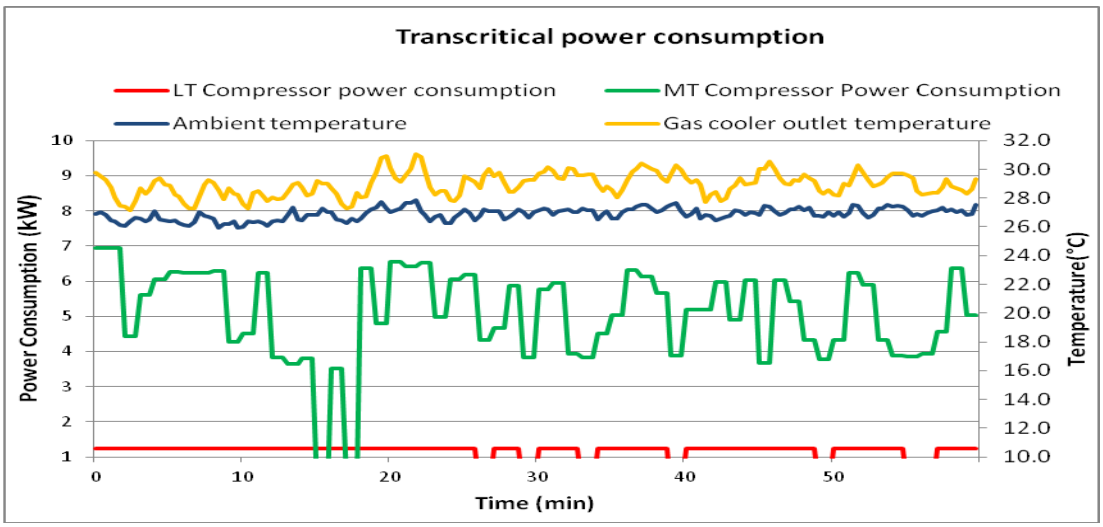

Figure 6.9 Compressors power consumption

The operational properties unique to this dual compression stage cycle are also visible from the power consumption figures. The HP compressor must also compress the refrigerant from the LP compressor discharge as well at the MT evaporator and bypass flash gas. This makes the power consumption of the HP compressor dependent on the LP compressor and the LP suction pressure. If the LP compressor switches off due to the LP target suction pressure being met, the HP compressor suction pressure can drop very quickly due to the reduced flow rate of refrigerant in the HP compressor suction line. This unique feature means careful consideration of the LP and HP compressor capacities must occur during the design stages of the booster refrigeration system.

Figure 6.10 shows the overall performance of the CO_2 refrigeration system using the COP, which is defined as the total cooling capacity divided by the total input power. Figure 6.10 also shows a polynomial line of best fit for the test results. The results show a decrease in COP from 1.80 to 1.35 with an increase in ambient temperature from 18.5°C to 29°C. The decrease in system COP is due to an increase in compressor power consumption at higher ambient temperatures.

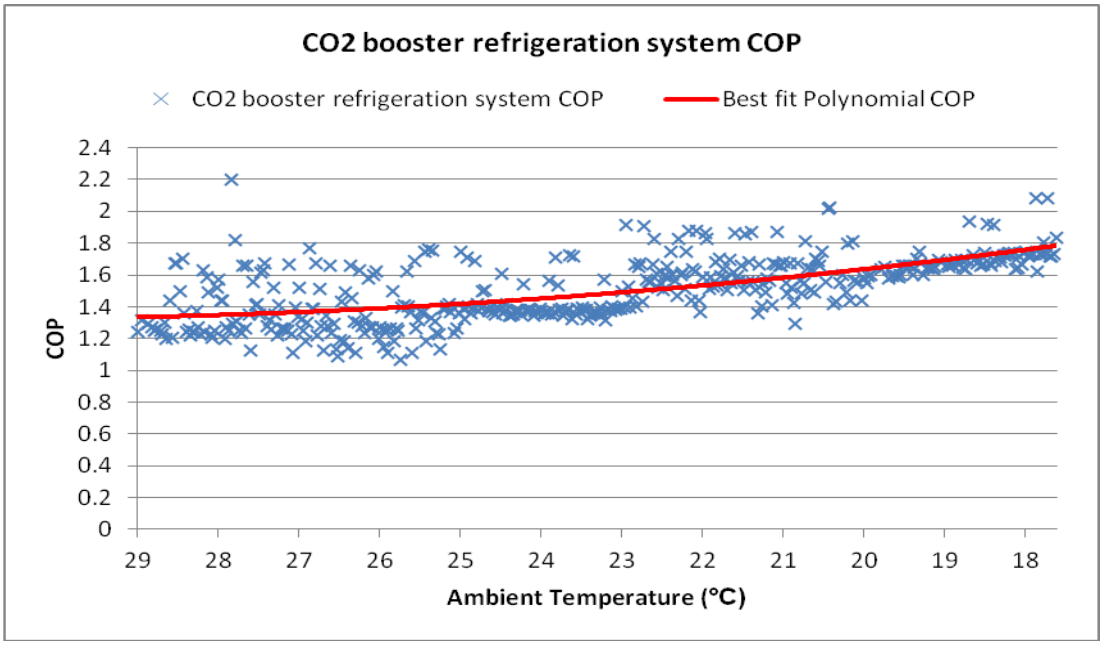

Figure 6.10 Refrigeration system COP

6.6 Verification of the simulation model

In this section the results from the simulation models are compared to the test results. The simulation models already discussed in Chapter 5 of this thesis were developed to simulate the performance of a small supermarket refrigeration system with capacities of 36 kW for MT and 5 kW for LT. The test system refrigeration capacities were smaller, as it was not necessary to replicate a full scale supermarket refrigeration system in the laboratory. In order to verify the results of the test system the simulation model was revised using the test system refrigeration capacities of 6.6 kW for the MT system and 4.0 kW for the LT system. The ambient temperatures recorded during the tests were also used as inputs for the simulation model. A further explanation of equations and simulation procedure used by the simulation model are detailed in Chapters 3 and 4 respectively.

6.6.1 Verification of system pressures

Figure 6.11 shows a comparison between the test and the simulation results for the system pressures. The simulation model results for the LP compressor suction pressures match up well with the actual test results. The simulation result was a constant 12.6 bar which was equivalent to an evaporating temperature set point of -32°C. The slight differences in the results are due to the pulsating of the electronic expansion valve restricting flow and causing fluctuations in the LP compressor suction line. The simulation results for the LP compressor discharge pressures agree well with the actual test results shown in Figure 6.11. The sharp deviations for the actual LP compressor discharge pressures were due to cycling of the LP compressor. This behaviour was not included in the simulation model so these fluctuations can be disregarded. The LP compressor discharge pressure is dependent on the HP compressor suction pressure. Both are at the same pressure due to the single circuit design of the booster refrigeration system. In the test, the HP compressor suction pressure was set at 24.5 bar, so the simulation model was also set at this.

The simulated HP compressor discharge pressures are up to 58% higher than the test results. This was due to the gas cooler performing much better than expected during

the test at rejecting heat from the high pressure CO_2. A temperature differential of 10 K above ambient temperature for the gas cooling temperature was used for the simulation model. The test results achieved a much lower temperature differential of 2 K above ambient temperature. This would reduce the deviation between the test and simulation results for the HP compressor discharge pressure. The model was simulated using the temperature differential of 2 K and is shown in Figure 6.11. This simulation HP discharge pressure agrees well with the test results using a temperature differential of 2 K.

A lower gas cooling temperature results in a lower gas cooling pressure which lowers the HP compressor discharge pressure. Any large fluctuations appearing in both the LP and HP discharge test results are due to the cycling of the LP compressor. The simulation model also reacts instantly to a change in ambient temperature, where the test has a time lag due to heat transfer. This could explain any further deviations.

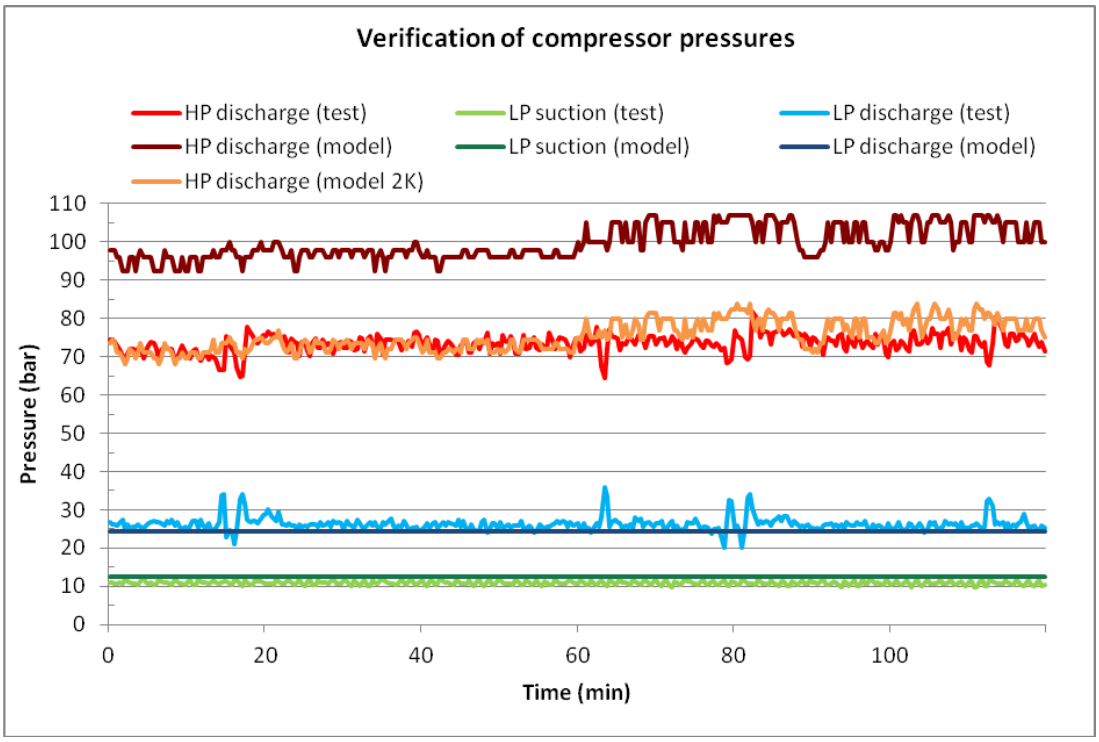

Figure 6.11 Test and simulation compressor pressures

6.6.2 Verification of system temperatures

The simulation model used evaporating temperatures for the LT and MT evaporators as inputs, -32°C and -8°C respectively. The refrigerant temperature at the compressor suction also includes the rise in refrigerant temperature due to superheat, which was assumed to be 7K, equal to the evaporator controller settings. It must be noted that the CO_2 refrigeration system has been modelled as a closed system, only adjusting the discharge pressure to suit the transient ambient temperature. The external influence heat transfer from the ambient to the pipe work and other refrigeration components has not been included in the model.

Figure 6.12 shows the test and simulated compressor temperatures. The test LP compressor suction temperature is on average 15 K higher than the simulated suction temperature. This was due to a temperature rise in the suction line from the LT cabinet to the compressor, shown in more detail by the test results in Figure 6.13. The control of superheat by the LT evaporator electronic expansion valve is clearly visible in Figure 6.13 from the refrigerant temperature fluctuations at the LT evaporator outlet. The superheat varied up to 16 K higher than the evaporating temperature of the evaporator, shown as the LT evaporator in temperature in Figure 6.13. It was expected that the temperature of the refrigerant at the LP compressor suction would not be higher than the superheat peaks shown in Figure 6.13, but this Figure clearly shows a further temperature rise up to 15 K. This temperature rise must have come from another source of heat.

After investigation it was decided that this was due to a high level of heat transfer from the ambient air to the suction line of the LP compressor, and from radiant and conductive heat transfer from high temperature refrigeration pipes that were situated next to the low temperature pipes. The pipe had been insulated but the compact layout of the test system meant high temperature refrigeration lines were situated next to low temperature pipes. This could be avoided by a different piping layout but was unavoidable for these tests. Again the heat transfer capabilities of CO_2 were underestimated in the design of the test system.

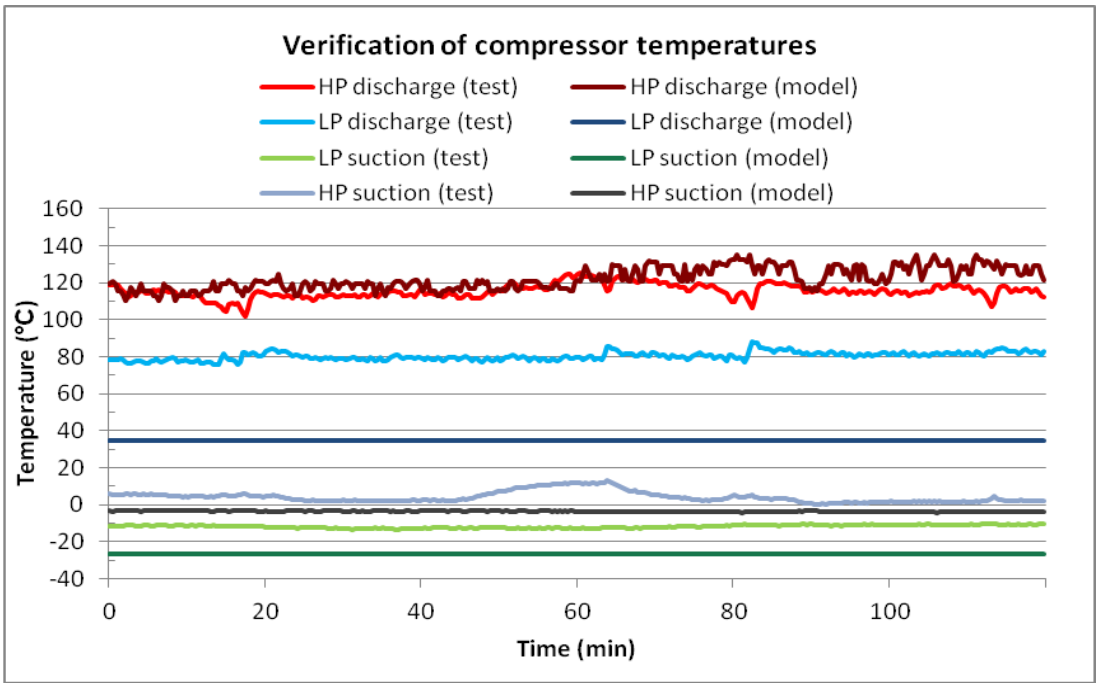

Figure 6.12 Test and simulated compressor temperatures

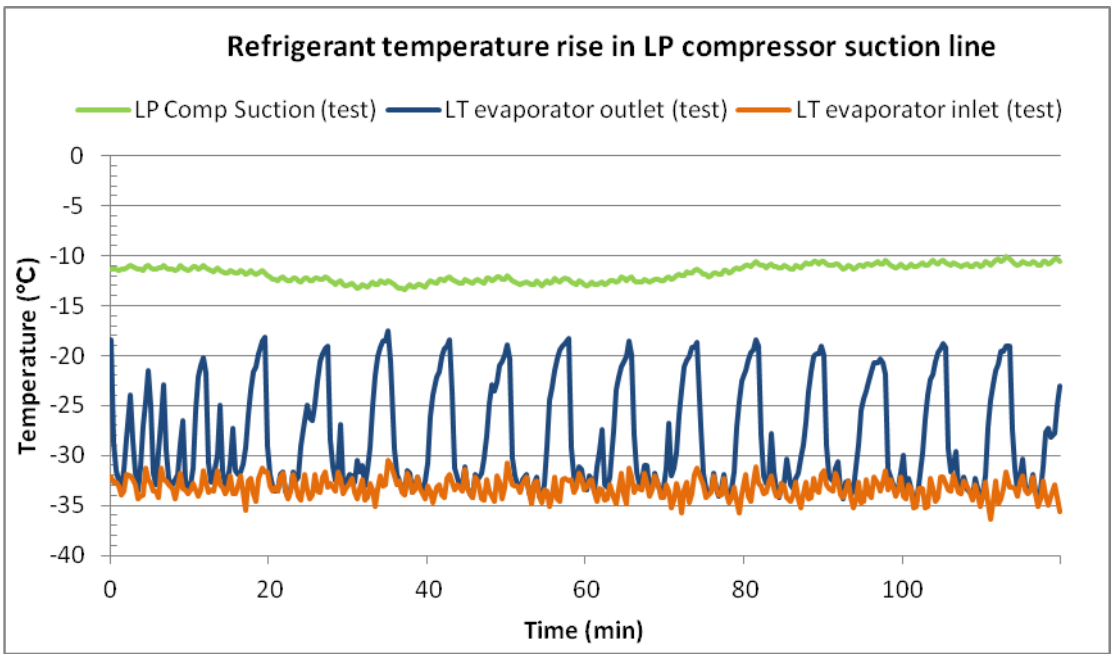

Figure 6.13 LP compressor suction line temperatures

The increase in the refrigerant suction temperature before the LP compressor generated a knock-on effect for the discharge temperature of the LP compressor. The

test results were approximately 39K higher than the model results as shown in Figure 6.14. The LP compressor was a Bock HGX12P/30-4, which was a suction gas cooled compressor so the increase in suction temperature due to the heat exchange in the suction line could have been making the compressor overheat and underperform, reducing the overall efficiency of the compressor and therefore the isentropic efficiency. A reduction in the isentropic efficiency of the compressor would increase the refrigerant discharge temperature. To prove this result the model was simulated using an LP suction temperature of -11°C instead of the original suction temperature of -26°C. The increase in LP compressor discharge temperature from simulating a -11°C suction temperature is shown in Figure 6.14. This did not increase the discharge temperature to the test result average discharge temperature of 80°C. To get this high discharge temperature the model was simulated decreasing the isentropic efficiency of the LP compressor from 61% to 40%. Due to the compressor being suction gas cooled, the high suction gas temperature of -11°C combined low flow of refrigerant through the compressor, due to compressor cycling, could have reduced the efficiency of the compressor to 40%. It can be concluded that the error between the initial simulation result and the test result was not due to an error in the calculation model but due to the heat transfer from external sources that was outside the closed circuit of the simulation model.

Both the test and simulation results for the HP compressor discharge temperature agree well, shown in Figure 6.14. The fluctuations in the test results are due to the cycling of the HP compressor on and off as well as variations in the ambient temperature controlling the HP compressor discharge.

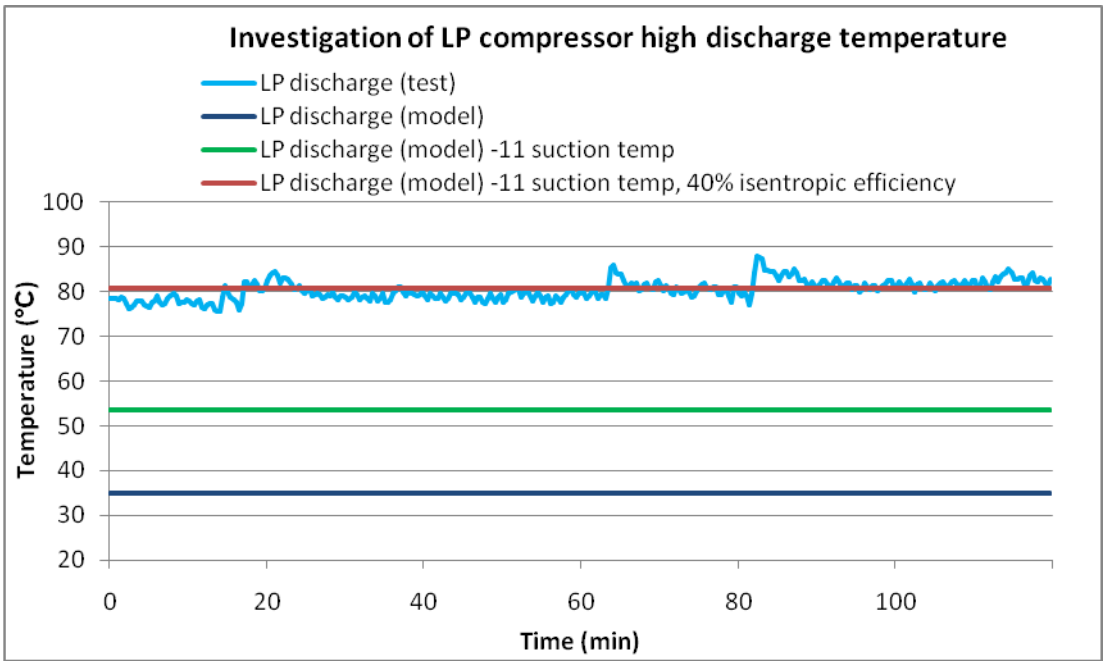

Figure 6.14 High LP compressor discharge temperature test results explanation

6.6.3 Compressor sizing validation

One of the features of the simulation model is the ability to calculate compressor capacities for a proposed system based on the required MT and LT design cooling capacities. The cooling capacities can simply be an input to the model and the model calculates the compressor displacements required to run that system. The sizing of compressors for the CO_2 booster system is more complex than a single temperature system due to the presence of two temperature levels and many different flow rates in one system. The LP compressor condensing temperature is much lower than a single temperature system and the HP compressor has to compress both the refrigerant from the MT evaporators and the refrigerant from the LP compressor discharge. Sizing the compressors using simply the evaporator capacity would overestimate the size of compressor required for the LP compressor and underestimate the size of compressor required for the HP compressor. This is why a simulation model is necessary for accurately calculating the correct compressor sizes.

This simulation model was validated by comparing the actual test compressor displacements against that of the simulation results. The capacities used for this

system were 6.6 kW for MT and 4.0 kW for LT. These results are shown in Table 6.5.

MT Evaporating temperature: -8°C

LT Evaporating temperature: -32°C

Ambient temperature: 32°C

Table 6.6 Design and simulation compressor displacement results

Compressor	Refrigeration capacities (kW)	Design system compressor displacement (m^3/h)	Simulation results compressor displacement (m^3/h)	Error
LP	4.0	2.7	2.5	-7.4%
HP	6.6	5.4	5.9	9.2%

The LP compressor displacement was underestimated by 7.4% by the simulation model. This result was successful as the nearest compressor with a displacement of 2.5 m^3/h, would be the compressor used in the experiment. The HP compressor displacement was overestimated by 9.2%, this result was also successful as the inverter used on the HP compressor varied the compressor displacement from 2.7 m^3/h to 9.3 m^3/h by varying the electrical frequency to the compressor. The simulation result within these compressor displacement figures. This concludes that the simulation model can be successfully used for compressor selection based on the input of specific supermarket refrigeration capacities.

6.6.4 System energy performance validation

The energy consumption of the CO_2 system was simulated over a 50 minute period using the ambient temperatures recorded during the tests. Figure 6.15 shows the simulation results and the actual monitored instantaneous power consumption over the same period. The power consumption calculated by the simulation model is fairly

steady, only fluctuating due to ambient temperature. The system was transcritical for the 50 minutes of simulation and monitoring.

The fluctuations in the actual monitored results are due to the HP compressor inverter adjusting the speed of the compressor and therefore the power consumed by the compressor. Inverter control was not included in the HP compressor simulation model for the test system. A fixed refrigeration load was assumed for this simulation. The peaks of the actual monitored results show when the compressor were running at full speed, this can be used to verify the simulation results as the compressor was modelled at full speed. The actual monitored total compressor power consumption peaked at 7.79 kW; the simulated total compressor power at this time was 7.76 kW. For the simulation results the optimised 2 K results were used, if the original 10 K results were used the total simulated compressor power would have been 10.68 kW. This original result over estimated the actual compression power by 2.89 kW. It can therefore be concluded that the results of the optimised 2 K simulation model agree well with the actual monitored results.

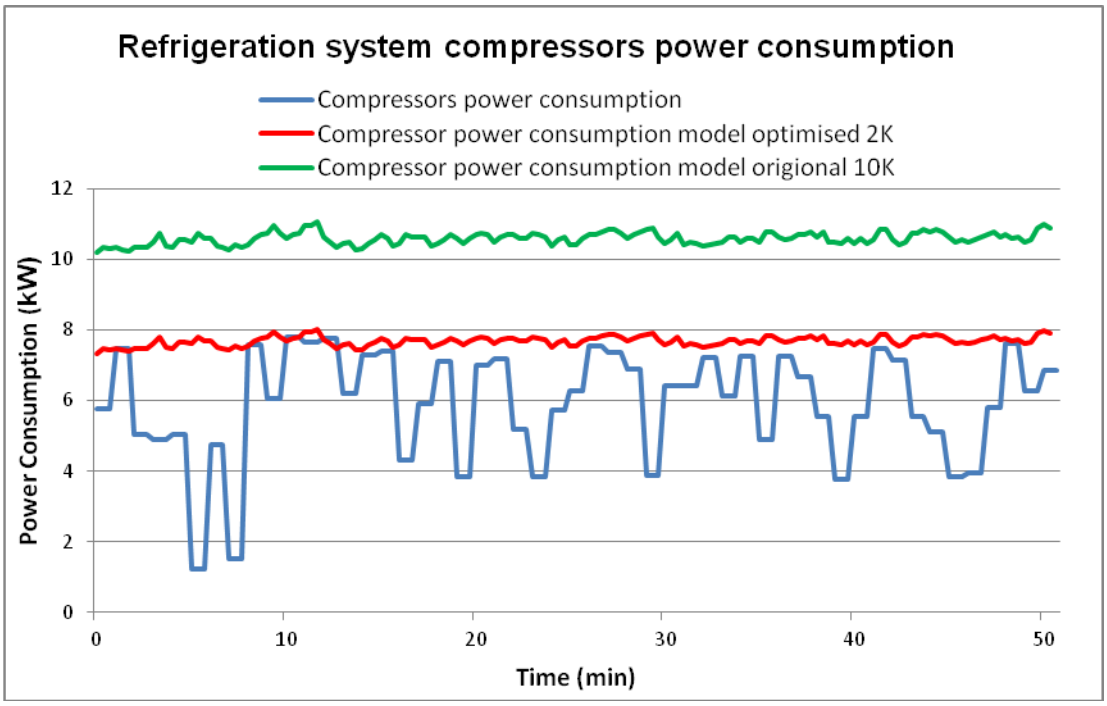

Figure 6.15 Test and simulated refrigeration system power consumption

6.7 Summary

This chapter presented the results from tests performed on an experimental CO_2 refrigeration system. The results of the tests have been used to verify and optimise a simulation model developed to simulate the performance of a CO_2 refrigeration system suitable for a small supermarket.

The test results validated the simulation results for the design compressor displacements. This proves that the simulation model can be used as a compressor selection tool for calculating the correct compressors to be installed in a commercial CO_2 booster system given the MT and LT refrigeration capacities.

Chapter 7 Study of the application of a CO_2 transcritical system in a supermarket

7.1 Introduction

This chapter presents and discusses the application of a transcritical CO_2 booster system in a real supermarket. A small supermarket in Northern Ireland has been fitted with a monitoring system which records the power consumed by the supermarket's R404A refrigeration system. The monitoring system also monitors the cooling demand from each piece of refrigeration equipment by recording the state of the electronic expansion valves. The recorded cooling demand for the MT and LT refrigeration fixtures and the ambient temperature are used as inputs to the CO_2 refrigeration simulation model presented in Chapter 3 and verified in Chapter 6 of this thesis. The model is used to simulate the annual energy consumption of the CO_2 refrigeration system and is compared to the results of the system in the R404A supermarket.

7.2 R404A Supermarket

The supermarket is located in Ballynahinch, Northern Ireland. It has a shop floor area of approximately 450 m^2. The supermarket also has a petrol station forecourt and is located on a main road approximately 2 miles outside Ballynahinch town centre. The refrigeration system has recently been replaced with a more modern and efficient refrigeration system which uses the HFC R404A. The internal layout of the supermarket is shown in Figure 7.1. The opening hours of the supermarket are from 7:00 to 23:00, 7 days per week.

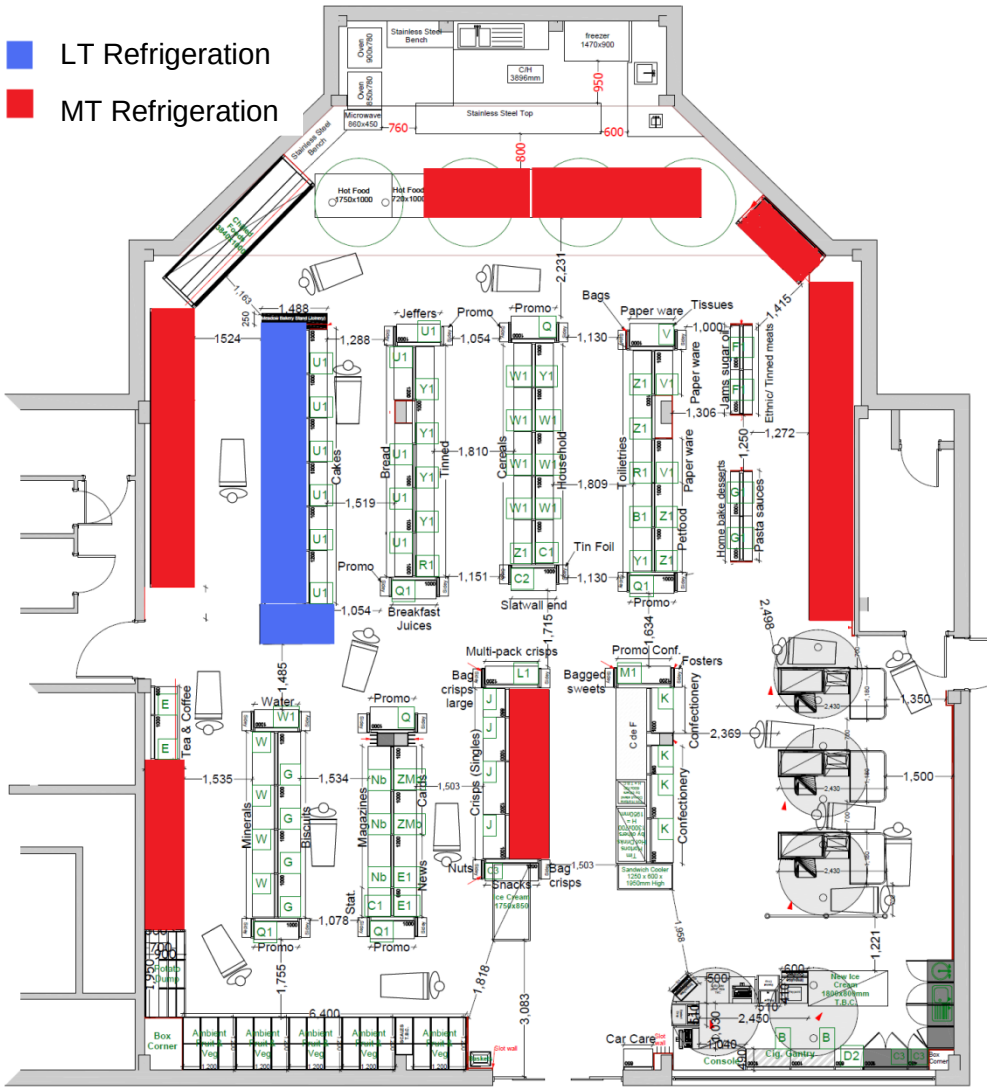

Figure 7.1 Refrigeration system layout of case study supermarket

7.2.1 Refrigeration capacities

The refrigeration requirements of the supermarket are 46 kW MT refrigeration for chilled produce such as dairy products, meat products, fruit and vegetables and for chilled drinks. The LT refrigeration requirement is 6 kW for frozen products. The chilled products are displayed in remote multi-deck cabinets and delicatessen serve-over cabinets as shown in Figures 7.2 and 7.3. There is also a chill room located on the first floor of the supermarket; this is used for storing chilled produce. The frozen products are displayed in wall and well (half glass door) freezer cabinets shown in

Figure 7.4 and an upright glass door cabinet. The refrigeration capacity required for each of the different types of refrigeration cabinet discussed is shown in Table 7.1.

Table 7.1 Supermarket refrigeration capacities

Cabinet type	Temperature	Number	Total length / Area (m)	Refrigeration capacity (kW)
Multi-deck	MT	8	26.8	40.3
Serveover	MT	1	3.75	1.5
Chill room	MT	1	16 (m^2)	4
Total MT				**45.8**
Wall and Well	LT	2	6.25	4.7
Upright Glass Door	LT	1	1.5	1.3
Total LT				**6**

Figure 7.2 MT chilled produce multi-deck display cabinet

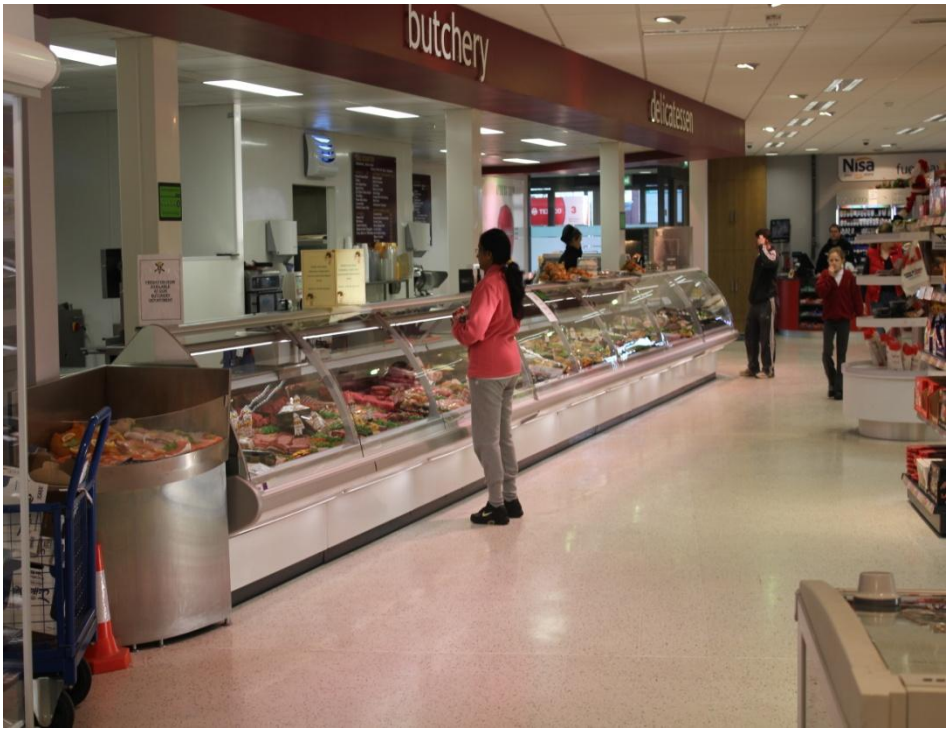

Figure 7.3 MT chilled produce serve-over cabinet

Figure 7.4 LT frozen produce wall and well cabinet

7.2.2 Refrigeration equipment

The refrigeration equipment installed for the MT refrigeration is a four compressor Bitzer pack system using three 4DC-5.2Y compressors and one lead 4EC-6.F1Y inverter compressor (Bitzer, 2012). This is connected to a Centauro ACP-EC156/280 3 EC fan condenser mounted on the roof of the supermarket (Centauro, 2012). The condenser is sized to enable the refrigerant condensing temperature to be reduced to 10K above the ambient temperature, with a minimum condensing temperature of 20°C at 10°C ambient. An image of the pack system is shown in Figure 7.5. The MT compressor system was controlled using a RDM PRO600 pack system and condenser controller (RDM, 2012a). The controller was set up using floating head condenser pressure control. The floating head control floats the condensing pressure with a rise / fall in ambient temperature, maintaining a temperature differential of 10K between the condensing temperature and ambient temperature. The minimum condensing temperature is set to 20°C which is equivalent to 10 bar for R404A. This minimum pressure has been chosen as a pressure differential and must be maintained across the electronic expansion valves to maintain a cooling capacity in the evaporators. The evaporating temperature of -8°C is equivalent to an evaporating pressure of approximately 3.7 bar. This leads to a minimum pressure differential across the expansion valve of 6.3 bar, which is sufficient to maintain a cooling capacity in the cabinets.

The LT refrigeration equipment installed has three separate LT condensing units. One HZF13 and one HZF15 from Hubbard refrigeration was used for the 6.25m wall and well cabinet and one CML34 from Electrolux was used for the upright glass door cabinet (Hubbard, 2012). Figure 7.6 shows an image of this type of condensing unit. The evaporating temperature of the LT systems is controlled at -30°C. The power consumption of the refrigeration system was monitored using a Socomec A20 power analyser (Socomec, 2012); this was connected to the RDM data manager system which stored the data from the A20 power analyser every 15s (RDM, 2012b).

Figure 7.5 MT refrigeration multi-compressor pack system

Figure 7.6 LT refrigeration condensing units

7.2.3 Daily refrigeration load and power consumption

The MT and LT refrigeration capacity profile over a 24 hour period on the 11th November 2011 is shown in Figure 7.7. This was calculated using the data from the

controllers of the MT and LT cabinets. Each cabinet controller sends information on the state of the expansion valve; if the expansion valve is open, for the purposes of the load profile calculation, the evaporator is using the rated cooling capacity. The electronic expansion valve actually modulates the load, opening and closing the valve in steps, to maintain a superheat set-point. Adding up the cabinet capacities based on the state of the expansion valve gave a good indication of the refrigeration being provided by the MT pack system and the LT condensing units. Both the MT and LT profiles show a similar pattern, peak refrigeration capacity occurred during the daytime hours when the ambient temperatures were highest and the shop was open. At 6.00am the night blinds in the MT multi-deck cabinets were raised, increasing the cooling required by the cabinets shown in Figure 7.7.

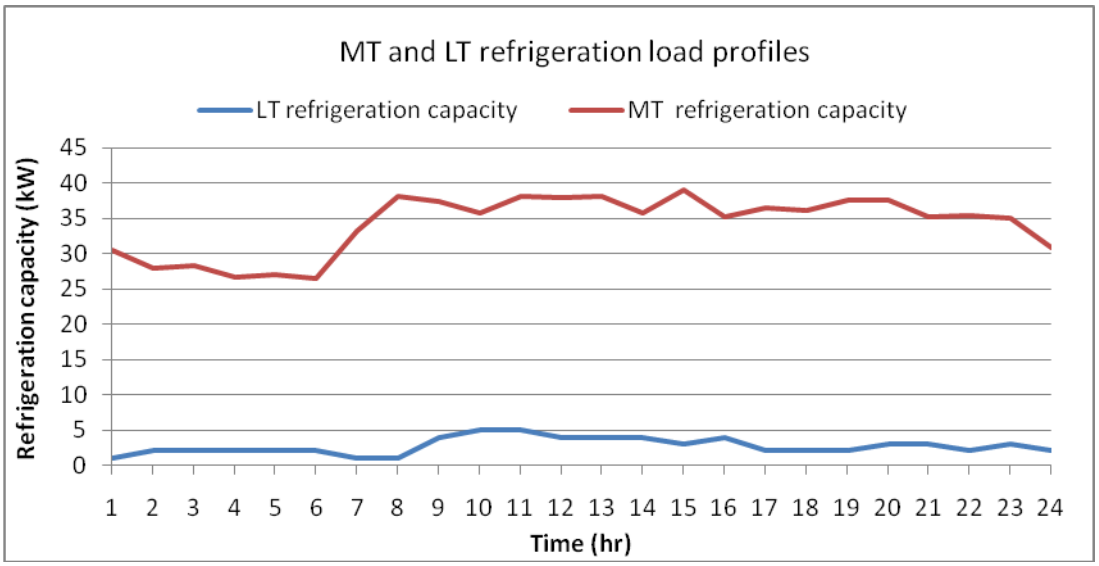

Figure 7.7 Case study supermarket MT and LT refrigeration load profiles, November 2011

Over the 24 hour period the average daily MT load was 36 kW, which was 78% of the total system design load of 46 kW. This lower result is due to the MT systems not running for 24 hours; they switch on and off due to defrosting and temperature controls. The average daily load for the LT system was 2.7 kW; this was 45% of the total design load. The LT system had a lower average load over the 24 hour period than the MT system load due to the freezer cabinets in the supermarket having lids

and doors. This reduced the infiltration of air into the cabinets reducing the time the compressors were on.

The internal environmental conditions inside the supermarket could affect the refrigeration load profiles seasonally. Most supermarkets have their internal environment controlled by air conditioning systems, maintaining a constant internal temperature throughout the year. The monitored load profiles shown in Figure 7.7 were used as the daily load profile for both the R404A system and the CO_2 system. As the load profiles were the same for both simulations any effects due to seasonal variations could be neglected for the purposes of the simulations.

The power consumption of the refrigeration plant over a 24 hour period is shown in Figure 7.8. The total power consumption of the total MT and LT system was taken directly from the monitored data as the Socomec energy meter recorded the total power consumed. To separate the MT and LT system power consumption a combination of the monitored results and the Bitzer compressor selection software package was used (Bitzer, 2011). The software package enables the user to input the compressor model, evaporating and condensing temperatures and the software calculates the power consumption and COP of the compressor.

By using the calculated COP values from the software for the MT refrigeration system compressors (Bitzer, 2011) and the refrigeration loads shown in Figure 7.7, the power consumption of the total refrigeration system was simulated and the results are shown in Figure 7.8. The hourly power consumption figures do vary slightly throughout the day. The greatest differences occur between 0600 – 0900 and 1600 – 2000, when the actual monitored results are greater than the simulation results. This could have occurred due to the actual refrigeration system having other parameters affecting the total system power consumption that have not been simulated, such as the variable isentropic efficiency of the MT and LT compressors. The total daily power consumption figures only vary by 3 %, so overall the simulation results agreed well with the actual monitored results. This method will be used to calculate the total annual compressor power consumption of the case study R404A supermarket using the daily refrigeration loads in Figure 7.7 and the annual hourly ambient temperature for Belfast as inputs.

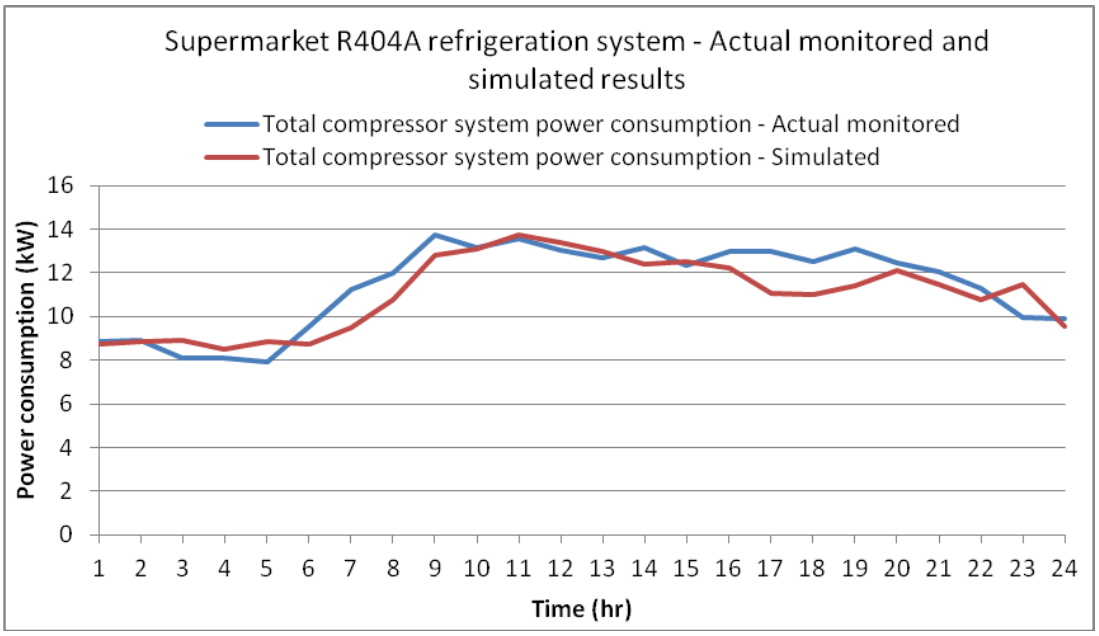

Figure 7.8 Supermarket refrigeration system power consumption

Figure 7.9 shows the separated MT and LT system power consumption and the recorded ambient temperature over the 24 hour period. The power consumption of the MT system averaged 10 kW throughout the day and peaked at 10.5 kW at midday. During the night the MT system power consumption reduced to approximately 7 kW. This was due to the multi-deck cabinets having their night blinds down and the heating in the supermarket being switched off, both factors reducing the cooling capacity required by the cabinets. The power consumption of the LT cabinets averaged 2.5 kW throughout the day and peaked at 3.8 kW at 10.00am. All LT cabinets had doors or lids installed reducing the influx of warm air but at peak business periods the doors were opened more often, increasing the cooling requirement and therefore power consumption of the LT refrigeration system.

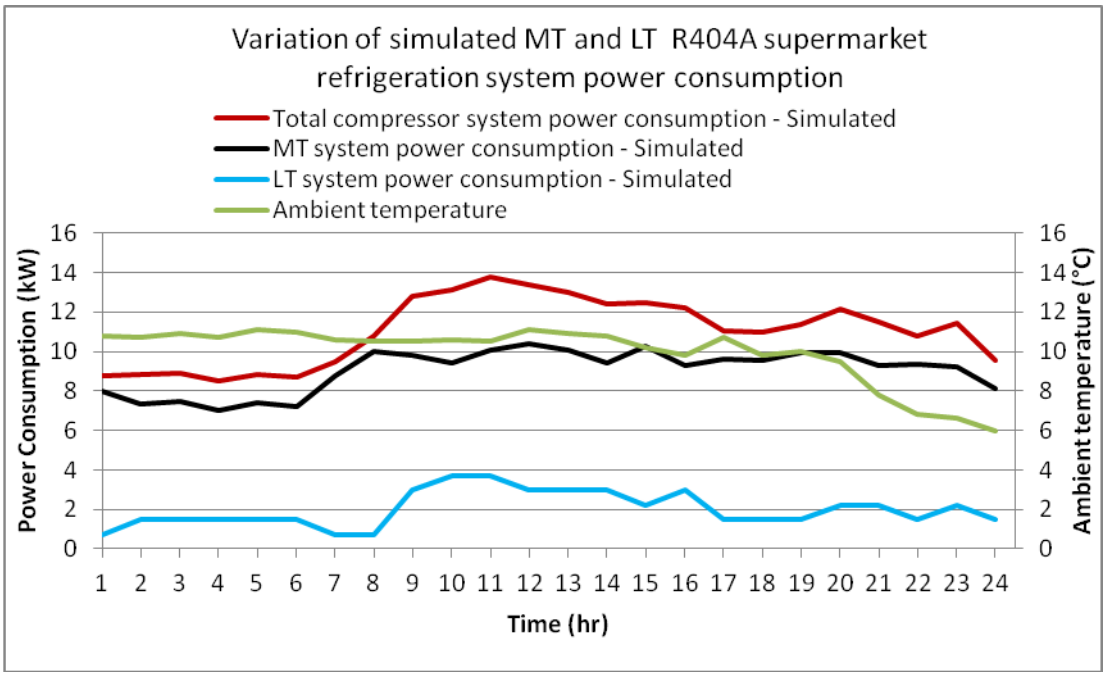

Figure 7.9 Power consumption of supermarket refrigeration systems

7.2.4 R404A system annual energy consumption

Using a combination of actual load profile and power consumption recordings from the site and manufacturer software, the total annual energy consumption for the site was simulated using annual hourly weather data from the Met Office for Belfast. The simulation was run for every day of the year using the ambient temperature and the refrigeration load profile in Figure 7.7 as inputs to the simulation model. Both the R404A and CO_2 models used the same load profile.

Figure 7.10 shows the annual simulated energy consumption of the supermarket and the ambient temperature for Belfast from the Met office. The energy consumption of the system peaked at 22.0kW for the highest ambient temperature of 25.1°C. When the ambient temperature was 10°C or below the energy consumption of the system peaked at 13.5kW. The total simulated annual energy consumption for the MT and LT refrigeration system was determined to be 103,540 kWh.

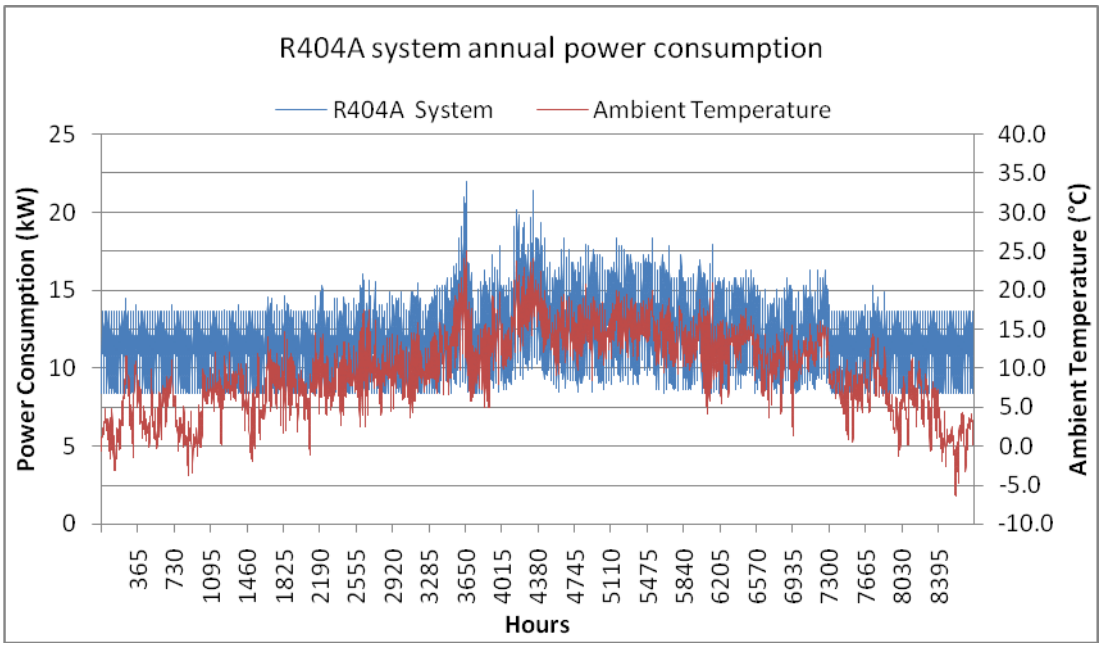

Figure 7.10 Total Annual power consumption of supermarket refrigeration system

7.3 CO_2 booster system

The refrigeration load profiles and power consumption data from the R404A supermarket was used to simulate the CO_2 booster refrigeration system, which is described in detail in Chapter 5. The evaporating temperatures for the model were assumed to be the same as for the R404A system. The MT evaporating was -8°C and the LT evaporating temperature was -32°C.

A floating head pressure control was used in the simulation of the CO_2 system. However CO_2 systems can operate at much lower condensing pressures than R404A without affecting the performance of the expansion valves. The greater operating pressures of CO_2 enable a sufficient pressure differential across the expansion valve to maintain evaporator capacity at lower condensing pressures. The heat exchange performance is also much better for CO_2 than for R404A, this enables the condensing temperature / pressure to be much lower without a significant rise in condenser fan power. The condensing temperature for CO_2 is floated down to 12°C, which is 8 K

lower than what is used in the R404A supermarket presented in section 4.2. CO_2 system annual electrical energy consumption

The simulated energy consumption of the CO_2 system is shown in Figure 7.11 together with the variation in ambient temperature. The compressor power of the CO_2 system increased with ambient temperature reaching 30 kW at the maximum summer temperature of 25.4°C. For ambient temperatures below 12°C the power consumption remained constant at 12.5 kW due to the head pressure control. The annual energy consumption of the system was determined to be 103,941 kWh.

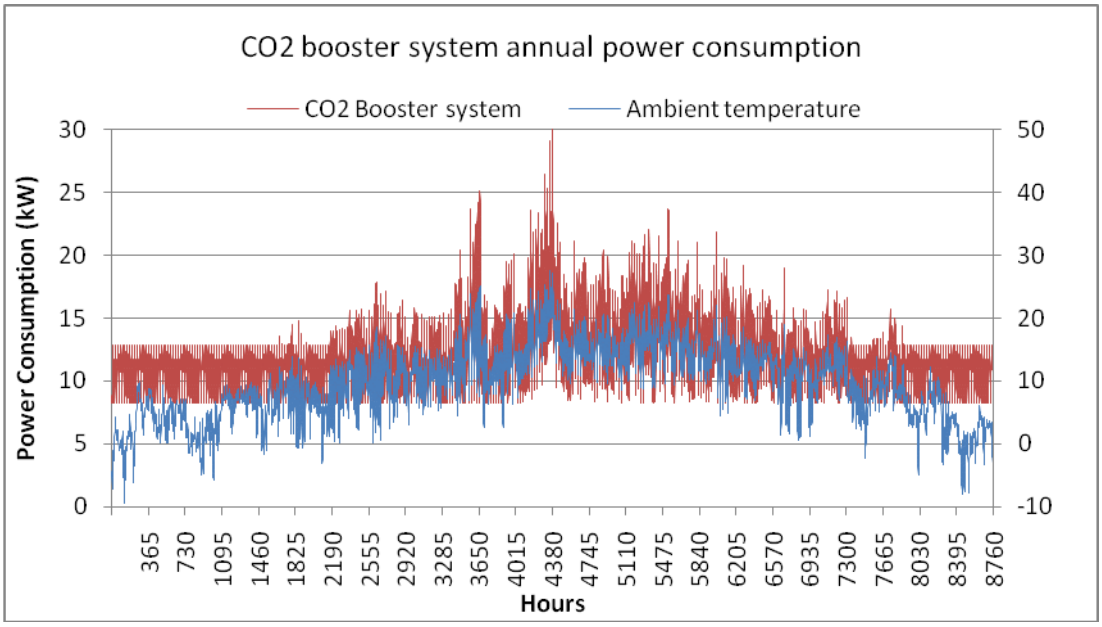

Figure 7.11 Total annual power consumption of CO_2 system

7.4 Comparison and discussion of results

Comparing the simulated annual power consumption of the refrigeration systems the CO_2 booster system consumed 401 kWh more electrical energy than the R404A system. This result was unexpected given the early simulation results in Chapter 3, estimating an 18% annual power increase for a CO_2 booster system. These results only show a 0.4 % increase. The difference is predominantly due to the CO_2 system

being able to reject heat in the condenser better than expected. This lowered the temperature difference between the ambient and condensing temperature to 2 K from an initial simulation of 10 K.

The CO_2 system consumed more energy during the summer months than the R404A system but less energy than the R404A system when the ambient temperatures were lower during the winter months. Figure 7.12 shows the power consumed by both refrigeration systems during a typical summer day with ambient temperatures ranging from 9°C to 23°C. The CO_2 system consumed more power than the R404A system for most of the day but Figure 7.12 clearly shows that the ambient temperature was not the only factor to affect the performance of the CO_2 system. At 07.00 the ambient temperature was approx 16°C and the power consumption of the CO_2 and R404A systems were 15 kW and 11 kW respectively. At 19:30 the ambient temperature again was 16°C but the power consumption of both systems was approximately 15 kW each. As the refrigeration loads were the same for both systems, makeup or ratio of the refrigeration loads was either increasing the performance of the CO_2 system or decreasing the performance of the R404A system.

Figure 7.12 shows the ratio line of MT refrigeration load to LT refrigeration load. The ratio peaks at 7.00 – 8.00 when there is 35 to 38 times more MT refrigeration load then LT refrigeration load, this is due to the blinds of the MT multideck cabinet being opened increasing the MT refrigerant load and the ratio of MT to LT refrigeration. The largest difference in power consumption between the two systems occurred at this time when the ratio was highest, not when the ambient temperature was highest. Over the 24 hour period of the summer day the R404A system consumed 339 kWh and the CO_2 system consumed 365 kWh, 8% more than the R404A system.

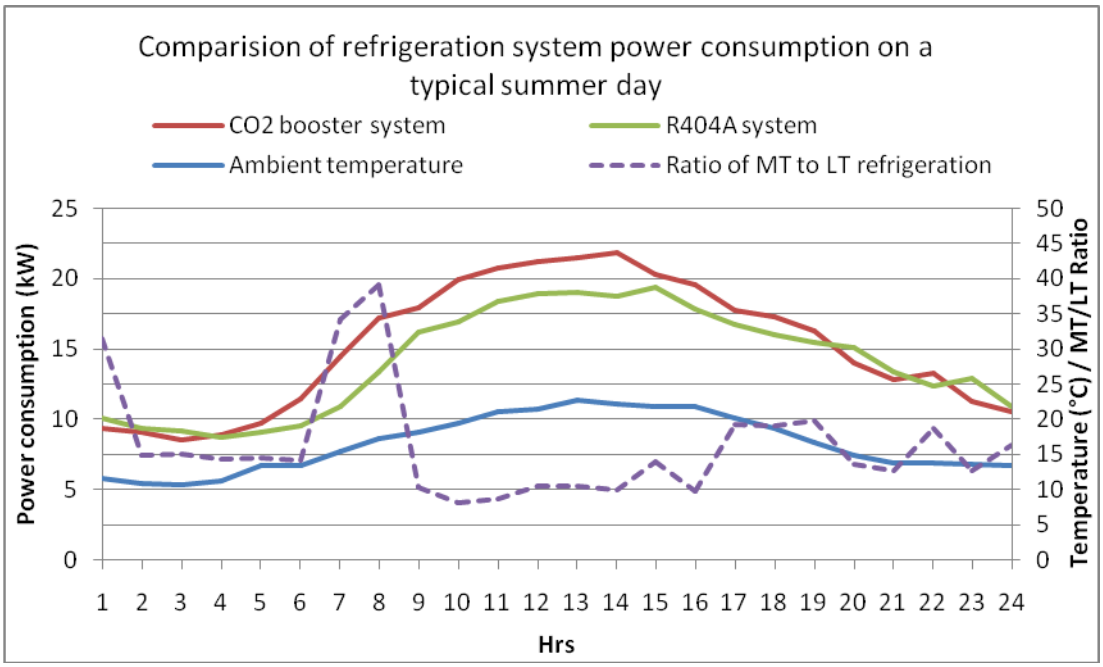

Figure 7.12 Comparison of power consumption of refrigeration systems during a typical summer day

Figure 7.13 shows a comparison of the power consumption of the two refrigeration systems over a 24 hour period on a typical winter day. The ambient temperature varied from -2°C to 7°C. The R404A system consumed more power than the CO_2 system but there were only slight increases for most parts of the day. The total power consumed by the CO_2 system was 254 kWh compared to 264 kWh for the R404A system, a 4% increase. The ratio line of MT to LT refrigeration is also shown in Figure 7.13. Even though the ambient temperature was approx 0°C at 08.00 the CO_2 system consumed more power than the R404A system due to the very high ratio of MT refrigeration to LT refrigeration. It was expected that the CO_2 system would consume less energy than the R404A system at low ambient temperatures. The refrigeration ratios for the CO_2 system will be investigated and discussed in the next section.

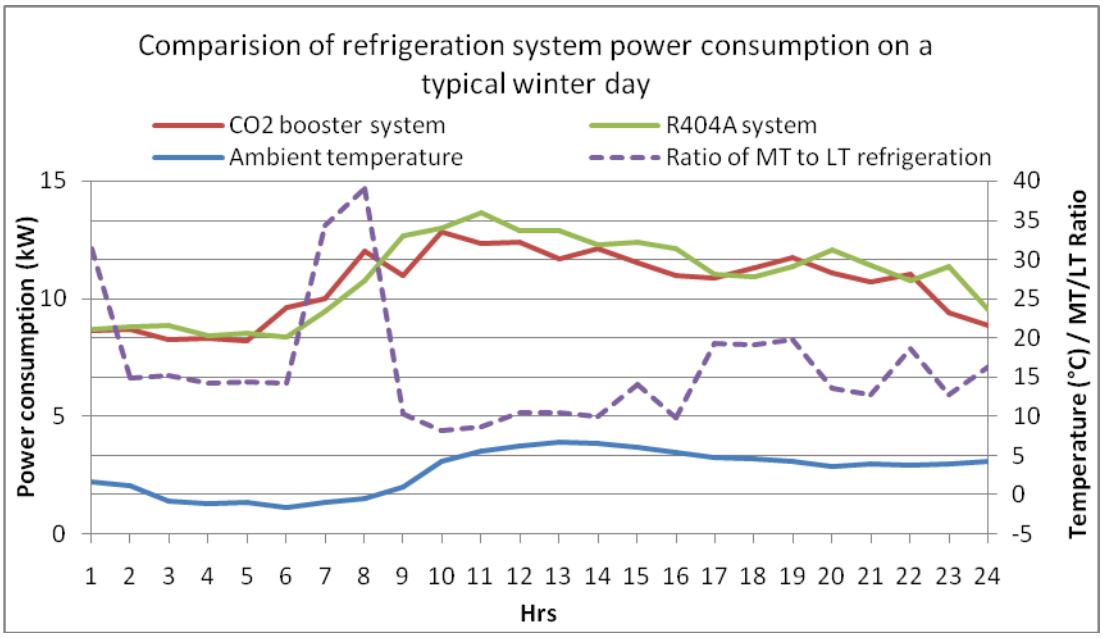

Figure 7.13 Comparison of power consumption of refrigeration systems during a typical winter day

Figure 7.14 shows a comparison of the calculated COP for the R404A supermarket refrigeration system and the simulated CO_2 booster system. At the lower ambient temperatures both refrigeration system COPs are at their highest, 3.4 for the CO_2 system and 3.2 for the R404A system. As the ambient temperature increased to 10°C a change in COP occurs for both systems, this is due to the set points of the condensing temperature for both systems. The R404A has a condensing set point of 20°C with a design ΔT of 10 K leading to an increase in condensing temperature / pressure at ambient temperatures above 10°C. This increases the work input required by the compressor due to the higher condensing pressure required and therefore reduces the system COP. The CO_2 system had a condensing temperature set point of 12°C and a design ΔT of 2 K so a similar process occurs for this system at ambient temperatures above 10°C.

The COP of the CO_2 system drops more rapidly than the R404A system, crossing at an ambient of approximately 13°C. Below this temperature the CO_2 system is more efficient and above this temperature the R404A system is more efficient. At an ambient of 24°C the CO_2 system begins to operate transcritically in the transition

zone until 27°C when the Danfoss EKC 326A controller begins to maintain the gas cooling pressure to optimise the system COP.

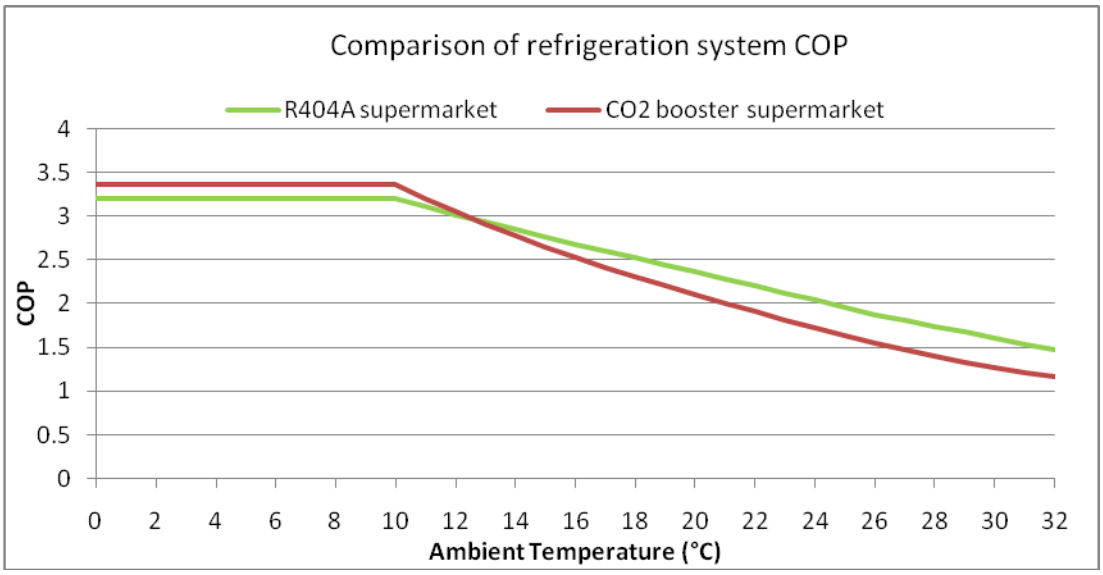

Figure 7.14 Comparison of R404A and CO_2 refrigeration systems COP with increasing ambient temperature

7.5 Booster system refrigeration ratios

By analysing the power consumption of the CO_2 booster system throughout a 24 hr period and comparing this to the R404A system, it was discovered that reducing the ratio of MT refrigeration to LT refrigeration increased the performance of the booster system comparatively to the R404A system. The increase in performance of the booster system is due to the single circuit design of the system combining two refrigeration temperatures into one circuit. The CO_2 system is more efficient than the R404A system at LT. The higher the LT load in proportion to the total load, the higher the COP of the CO_2 system.

The simulation model was used to simulate a range of refrigeration ratios for the R404A system and the CO_2 booster system. Figure 7.15 shows results of annual energy consumption for different refrigeration ratios of MT and LT refrigeration capacities with a total refrigeration load of 50 kW. As the ratio is decreased from 9:1 (45 kW MT: 5 kW LT) to 1:1 (25 kW MT to 25 kW LT) the total power consumed

by the CO_2 system does not change much, only increasing by 1%. This result is very different for the R404A system whose annual energy consumption increases by 22%. The dual compression stages with inter-cooling makes the CO_2 system much more efficient than the R404A system when a lower ratio of MT refrigeration to LT refrigeration is used. For applications where there are equal MT and LT refrigeration requirements the CO_2 booster system can produce savings of up to 16.2% over an R404A system. This could lead to emissions reductions of 10.6 tonnes of CO_2 annually as shown in Table 7.2

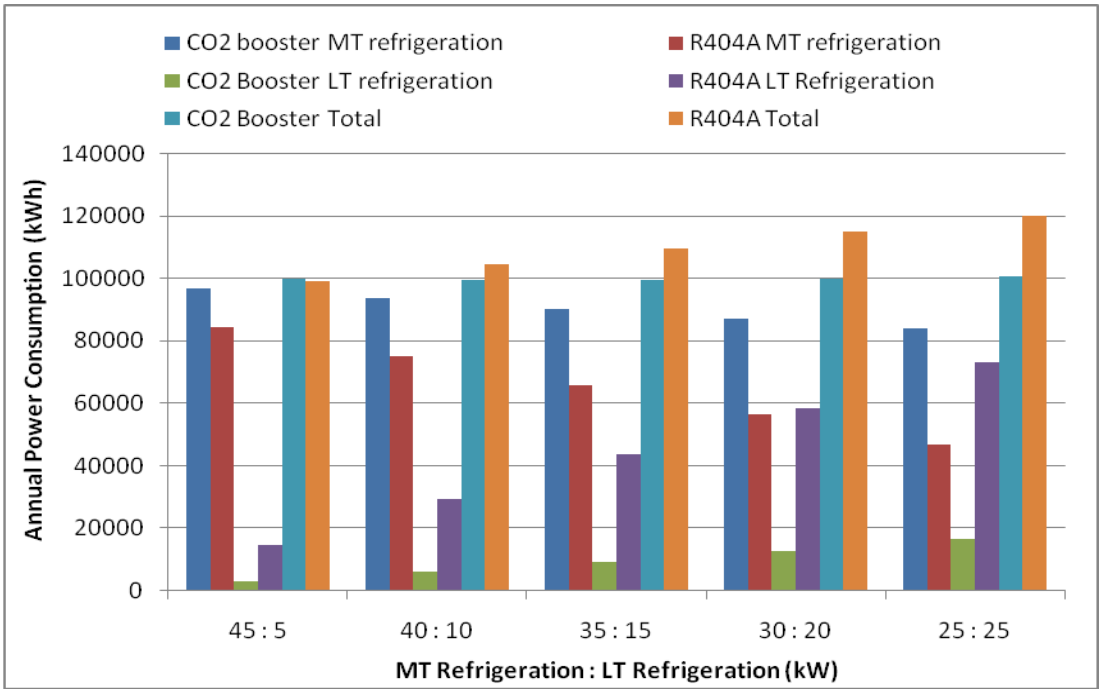

Figure 7.15 Comparison of the total annual power consumption of a CO_2 booster system and a R404A system for five different refrigeration ratio capacities

Table 7.2 Comparison of CO_2 booster system and R404A system power consumption

	Total Annual Power Consumption		Comparison of CO_2 booster with R404A system			
MT:LT (kW)	CO_2 Booster (kWh)	R404A (kWh)	Energy (kWh)	Energy (%)	Emissions (tCO2)	Electricity cost (14p/kWh) (£)
45 : 5	99967	99342	+626	+0.6	+0.3	+88
40 : 10	99783	104594	-4811	-4.6	-2.6	-674
35 : 15	99819	109853	-10034	-9.1	-5.5	-1405
30 : 20	100148	115108	-14960	-13.0	-8.1	-2094
25 : 25	100858	120368	-19510	-16.2	-10.6	-2731

7.6 Optimum ratio of MT and LT refrigeration for CO_2 Booster system

The potential of CO_2 booster systems saving energy depends on the ratio of MT refrigeration to LT refrigeration in the supermarket. Reducing the amount of MT refrigeration in the supermarket and increasing the amount of LT refrigeration leads to savings in annual energy costs and indirect CO_2 emissions compared to a R404A system. As the LT capacity is increased the savings increase but the ratio of MT to LT refrigeration in a supermarket is a function of merchandising consideration rather than energy consumption.

The case study supermarket is a convenience store selling fresh and frozen produce but there is more of an emphasis on the fresh produce than the frozen produce. 46kW of MT to 6kW of LT equates to a ratio of 7.6 to 1. Iceland is another large supermarket retailer but with an emphasis on frozen produce. A typical Iceland store would have approximately 40kW of LT refrigeration and 20kW of MT refrigeration. This equates to a ratio of 0.5 to 1, where considerable savings could be achieved using a CO_2 booster system compared to R404A systems.

7.7 Ambient temperatures in UK

The location of a supermarket in the UK will have an effect on the annual energy consumption of a refrigeration system. Using a floating condensing temperature control, the power consumption of the refrigeration system will follow the change in ambient temperature in a particular location. The higher the condensing temperature the higher the compressor power input required. The ambient temperature has more impact on the CO_2 booster system than the R404A system because of poor performance of the system at higher ambient temperatures and the transcritical cycle occurring above an ambient temperature of 24°C. However, the CO_2 system has less power than an R404A system at lower ambient temperatures as discussed in section 7.4. At ambient temperatures below 13°C the CO_2 booster system outperforms the R404A system. The local ambient temperature has therefore a critical part to play in determining the performance and savings available from a CO_2 booster system.

To investigate the effect of the ambient temperature, hourly ambient temperature data recorded in 2009 for 10 sites spread across the UK was used (Met Office, 2012). The geographical locations of the weather stations are shown in Figure 7.16. Table 7.3 shows for each location the number of hours a CO_2 booster system would be operating transcritically and the number of hours the ambient temperature would be above and below 13°C. The locations have been arranged in order of latitude, moving from the north to the south. The total number of hours that the locations are below 13°C generally follows the same pattern, decreasing as the locations move more southerly apart from. Heathrow is the warmest location with the lowest number of hours under 13°C and the highest number of hours over 13°C. Heathrow was the location with the greatest number of hours over 24°C when the system will be operating transcritically.

Figure 7.16 Locations of UK sites

Table 7.3 Annual hourly temperature data from 10 UK locations

		Average annual temp	No. hours temperature >24°C		No. of hours temperature <13°C		No. hours temperature >13°C	
Site	Location	(°C)	(°C)	%	(°C)	%	(°C)	%
1	Lerwick	8.2	0	0.0	7724	88.2	1036	11.8
2	Edinburgh	9.3	20	0.2	6328	72.2	2432	27.8
3	Aldergrove	9.6	6	0.1	6227	71.1	2533	28.9
4	Durham	9.2	11	0.1	6380	72.8	2380	27.2
5	Hawarden	10.1	42	0.5	5851	66.8	2909	33.2
6	Colesshill	10	47	0.5	5979	68.3	2781	31.7
7	Filton	10.6	59	0.7	5477	62.5	3283	37.5
8	Heathrow	11.5	160	1.8	5023	57.3	3737	42.7
9	Manston	10.9	42	0.5	5422	61.9	3338	38.1
10	Plymouth	10.9	1	0.0	5532	63.2	3228	36.8

Table 7.4 shows the total annual electrical energy consumption of the R404A supermarket and the CO_2 booster system at 10 different locations around the UK. Lerwick has clearly the lowest annual energy consumption for both the R404A and CO_2 systems but the CO_2 system consumes 1.4% less power annually than the R404A system. Heathrow has the highest annual power consumption for both refrigeration systems. The CO_2 system consumed 3.9% more energy than the R404A system. This is due to the higher ambient temperatures at Heathrow and the higher number of hours of transcritical operation. Table 7.4 also shows the simulation results for a different MT:LT refrigeration capacity ratio of 40:10 kW. For all the locations the CO_2 system actually used less energy annually with the decrease in the ratio, while the R404A system showed an increase in annual energy consumption. For each location the minimum MT:LT ratio that would result in energy savings for the CO_2 was calculated and listed in Table 7.4

Using MT:LT ratio load analysis, maximum ratios have been calculated for each of the 10 UK locations. Small supermarkets installing CO_2 booster systems with refrigeration load ratios lower than the maximum ratios presented, would have a lower annual electricity cost than with a traditional R404A system.

Table 7.4 Annual power consumption and max ratios for 10 UK locations

	Case Study Ratio			Trial Ratio			
	46:6 kW			40:10 kW			Max Ratio
	CO_2 booster (kWh)	R404A (kWh)	CO_2 system energy increase / decrease	CO_2 booster (kWh)	R404A (kWh)	CO_2 system energy increase / decrease	
Lerwick	97851	99224	-1.4%	94129	100837	-6.7%	10.0 : 1
Edinburgh	104052	103582	0.5%	99911	104642	-4.5%	8.3 : 1
Aldergrove	103941	103540	0.4%	99783	104594	-4.6%	8.4 : 1
Durham	104172	103648	0.5%	100036	104704	-4.5%	8.2 : 1
Hawarden	106992	105631	1.3%	102663	106459	-3.6%	7.5 : 1
Colesshill	106930	105567	1.3%	102604	106405	-3.6%	7.5 : 1
Filton	108451	106681	1.7%	104056	107368	-3.1%	7.1 : 1
Heathrow	113277	108985	3.9%	108531	110367	-1.7%	5.7 : 1
Manston	106713	105545	1.1%	102395	106341	-3.7%	7.7 : 1
Plymouth	109938	107664	2.1%	105517	108285	-2.6%	6.6 : 1

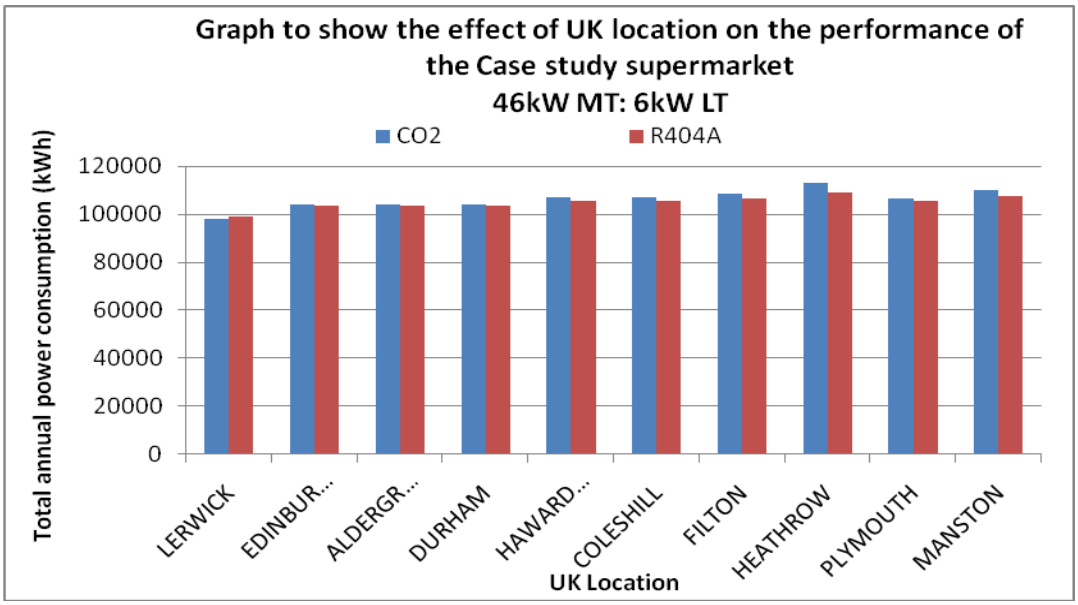

Figure 7.17 Graph of annual power consumption of refrigeration systems in different UK locations

7.8 Environmental Impact

The environmental impact of a refrigeration system is measured by the direct and indirect carbon dioxide emissions from its operation. The direct carbon dioxide emissions are a result of refrigerant leakage from the system. The indirect emissions depend on the electrical energy used by the system. The TEWI (Total Equivalent Warming Impact) equation developed by the British Refrigeration Association can be used to compare and assess the environmental impact of different refrigeration systems due to direct and indirect carbon dioxide emissions (BRA, 2006). The conversion factor of 0.53 kg CO_2 / kWh is taken the Carbon Trust publication CTL153 (Carbon Trust, 2011)

$$TEWI = (GWP \times m \times N \times L_{annual}) + (GWP \times m \times (1-\alpha)) + (N \times \beta \times E) \quad \textbf{(7.1)}$$

7.8.1 Environmental impact of R404A and CO_2 refrigeration systems

The inputs to calculate the TEWI for the case study supermarket R404A system and for the proposed CO_2 booster system using Aldergrove weather data are shown in Table 7.5. The systems were assumed to have a 10 year operating lifetime and 90% of the refrigerant was assumed to be recovered and recycled at the end of the system life cycle. An annual refrigerant leakage rate of 15% has been used for this analysis (Cowan *et al.*, 2009). Over a 10 year operational period the R404A system has a TEWI of 912 tCO_2, with direct emissions due to refrigerant leakage equivalent to 363 tCO_2. The CO_2 system generated a TEWI of 551 tCO_2 over the 10 year operational period which was 361 tCO_2 lower emissions than the R404A system, a 40% reduction in the environmental impact due to refrigerant leakage.

This result shows the high environmental impact due to the high GWP of R404A and the high rate of refrigerant leakage.

Table 7.5 Calculated R404A system TEWI and CO_2 Booster system TEWI

	R404A System	CO_2 Booster System
GWP	3,780	1
N (Years)	10	10
m (kg)	60	75
α (%)	90	90
L_1 (%)	15	15
β (kg Co_2 / kWh)	0.53	0.53
E (kWh)	103,540	103,941
DIRECT (tCO_2)	363	0.12
INDIRECT (tCO_2)	549	550.8
TEWI (tCO_2)	912	551

7.8.2 UK environmental Impact

Section 7.8 of this thesis indicated that if a CO_2 booster system was installed at a supermarket near Heathrow it would consume 3.9% more energy annually than a

R404A system. This would result in an increase in indirect emissions of 22 tCO_2 over a 10 year life cycle. However, installation of a CO_2 booster system at this location would result in a reduction of direct CO_2 emissions of 302 tCO_2 over the system life cycle. Figures 7.18 and 7.19 show the TEWI of both supermarket refrigeration systems at 10 UK locations. This shows that a CO_2 booster system can reduce the environmental impact of a supermarket at any location in the UK. The reduction of direct CO_2 emissions due to the lower GWP of CO_2 compared to R404A has a much greater effect in the reduction of the environmental impact than the increase in indirect emissions due to the higher power consumption of the CO_2 booster system.

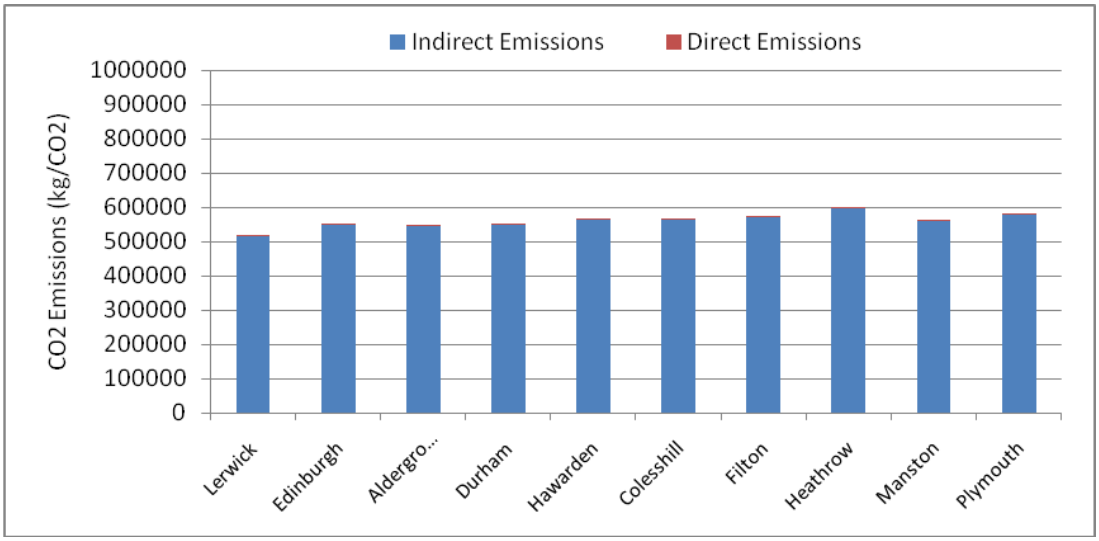

Figure 7.18 CO_2 emissions over 10 years for a supermarket CO_2 Booster refrigeration system at 10 UK Locations

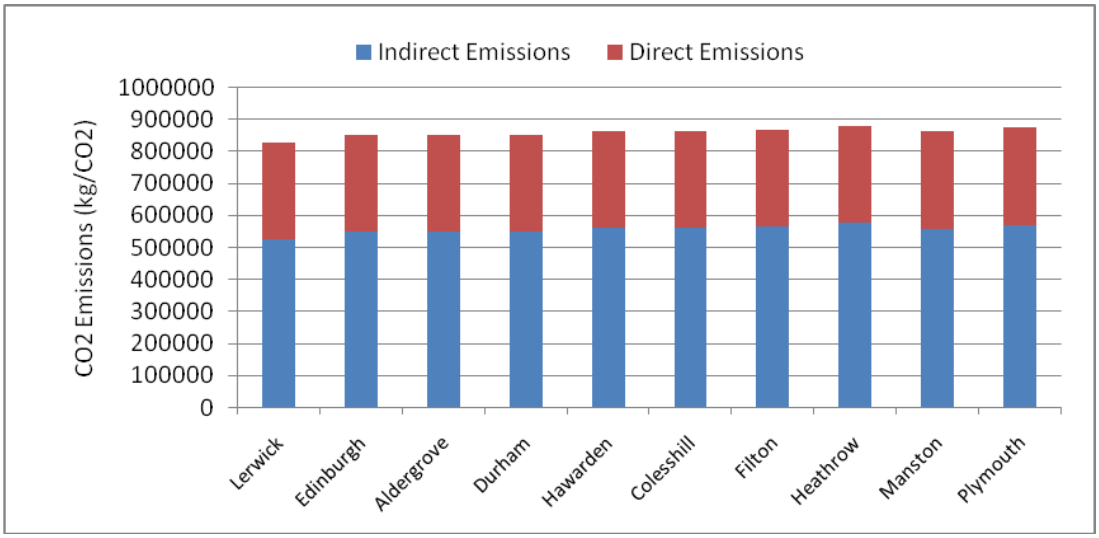

Figure 7.19 CO_2 emissions over 10 years for a supermarket R404A refrigeration system at 10 UK Locations

7.8.3 Environmental impact of small supermarkets in Northern Ireland

Section 2.12 of this thesis highlighted the large total refrigeration capacity of small supermarkets in Northern Ireland. The CO_2 booster system tested in this research has been designed and developed for this size of supermarket, 150 – 280 m^2. The simulation models developed enables the environmental impact of supermarket refrigeration systems due to indirect and direct CO_2 emissions to be estimated. Using the simulation models developed the environmental impact of replacing existing R404A refrigeration systems in small supermarkets with the CO_2 booster system presented in this thesis is calculated. There are approximately 615 small supermarkets in Northern Ireland with MT refrigeration capacities ranging from 20 – 46 kW and LT refrigeration capacities from 3 – 7 kW. Using an average MT refrigeration capacity of 33 kW and an average LT refrigeration capacity of 5 kW for a small supermarket the annual electrical energy consumption of a R404A system and a CO_2 booster system is shown in Table 7.7. Replacing current R404A refrigeration systems in small supermarkets in Northern Ireland with CO_2 booster systems could reduce the TEWI by 188,753 tCO_2 over a 10 year period.

Table 7.6 TEWI analyses of R404A and CO_2 booster systems installed in small supermarkets in Northern Ireland with 33kW of MT and 5kW of LT refrigeration

	R404A System	CO_2 Booster System
GWP	3,780	1
N (Years)	10	10
m (kg)	60	75
α (%)	90	90
L_1 (%)	15	15
β (kg Co_2 / kWh)	0.53	0.53
E (kWh)	76,761	75,894
Number of small supermarkets	615	615
DIRECT (tCO_2)	185,976	49
INDIRECT (tCO_2)	250,202	247,376
TEWI (tCO_2)	436,178	247,425

7.9 Summary

This chapter presented a study of the application of CO_2 booster refrigeration system in a real supermarket using monitored data from a small supermarket located in Northern Ireland. The supermarket has a traditional R404A refrigeration system which has been recently installed. The simulation model was adjusted and optimised, using the input variables of the case study R404A supermarket refrigeration system. The simulation results were then verified using the recorded ambient temperatures, power consumption figures and recorded MT/LT refrigeration loads over a 24 hour period. Using hourly ambient temperatures the case study R404A refrigeration was simulated over a one year period so that the annual power consumption of the system could be calculated. The same ambient temperatures and MT/LT refrigeration loads were used as inputs to the simulation of a CO_2 booster system.

The results of these annual simulations showed that the CO_2 system did consume more power than the R404A at high ambient temperatures but consumed less power at lower ambient temperatures below 13°C. The lower the ratio of LT to LT refrigeration capacities the higher the efficiency of the booster CO_2 system compared

to R404A. This would be beneficial for supermarkets that sell higher volumes of frozen foods compared to chilled foods.

The TEWI calculation was used to measure and compare the environmental impact of both the R404A and CO_2 refrigeration systems. For the supermarket studied, a CO_2 booster refrigeration system would have reduced the environmental impact due to the refrigeration system by 50%, over a ten year lifecycle. This equates to a reduction in direct emissions equivalent to 363 tCO_2. The simulation model was used to calculate the environmental impact of replacing existing R404A refrigeration systems in Northern Ireland with the CO_2 booster system presented in this thesis. Replacing current R404A refrigeration systems in small supermarkets in Northern Ireland with CO_2 booster systems could reduce the TEWI by 188,753 tCO_2 over a 10 year period.

Chapter 8 Economic investigation

8.1 Introduction

This chapter investigates the economics of the CO_2 booster system compared to the R404A counterpart. Capital costs, installation costs and energy costs are considered and compared.

8.2 Capital equipment cost

The capital equipment cost of a CO_2 system has been reported by a number of researchers to be higher than that of an equivalent R404A system. Girotto (2004) reported an increase in capital cost of 20% for a transcritical CO_2 system compared to a R404A system, although this system was relatively large with 120 kW of MT refrigeration and 25 kW of LT refrigeration. De Ono, (2008) also reported a 20% increase in costs for a CO_2 refrigeration system compared to an R404A system. Emerson (2010) compiled a report comparing the energy use, TEWI and investment costs for 14 different solutions commercial refrigeration systems. The CO_2 booster system had an investment cost 48% higher than that of a R404A system but the booster system reduced the TEWI by 42%.

Tables 8.1 and 8.2 show the approximate component costs of the capital refrigeration equipment for a 46 kW MT: 6 kW LT supermarket using either a CO_2 booster or a R404A refrigeration system. The retail costs have been provided by the sponsor company Shilliday Refrigeration. The cost for the capital refrigeration equipment of the CO_2 system costs 63% more than the R404A system. The compressors for the CO_2 system cost £4937 more than for the R404A system, 24% of the additional cost.

This is due to the high price of the HP CO_2 compressors, which are required to withstand much higher pressures due to transcritical operation. The LT CO_2 compressor costs are comparable to the R404A compressors. Other mechanical components for the refrigeration system such as safety valves, ball valves, receiver and the oil system are more expensive for the CO_2 system. These components must withstand the high pressures associated with CO_2 so are more expensive but the system also has more valves due to the dual compression stages and also an extended oil return system due to the booster compressor which is not required for the R404A system. The condenser is more expensive as it must withstand the high gas cooling pressures. Supercritical gas cooling is unique to a transcritical CO_2 refrigeration system which requires the ICMT valve and the associated controls to optimise the gas cooling pressure. The CCM valve is another additional valve which is not required for the R404A system. Its function is to maintain the receiver pressure. These valves increase the cost of the CO_2 system by £4,086 and account for 20% of the additional costs.

The controls for the CO_2 system are higher as the controls required for the LP compressor on the booster system are much more expensive than the basic controllers required for the three smaller condensing units on the R404A system. The electrical panel on the CO_2 system is more expensive as additional contactors and a larger panel is required due to the LP compressor controller and the additional EKC 326A controller which is required to operate the ICMT valve and the CCM valve. Additional pressure and temperature transducers are also required on the CO_2 system because of the ICMT and CCM valves. The more expensive controls account for 23% of the additional costs.

Table 8.1 Capital equipment costs for CO_2 Booster refrigeration system

Component	Model	Cost	Number	Total Cost
Compressors				
HP Compressors	4FTC-20K	7420	2	14840
LP Compressors Includes: Crankcase heater, oil switch, protection, HP/LP switch	2KSL-1K	1746	1	1746
Frame				
Includes frame, oil system, safety valves, pressure valves, ball valves, accumulators, filters, housing		14000	1	14000
Condenser / gas cooler				
Includes EC fans		6300	1	6300
Controls				
Compressor Controllers	AK-PC-740	1732	2	3464
Pressure transducers	AKS2020	171	6	1026
Temperature Transducers	AKS11	140	5	700
Electrical panel		5600	1	5600
Back up controller		700	2	1400
Additional booster system valves				
ICMTS + Actuator + controller		3392	1	3392
CCM Valve		693	1	693
Total Cost				**53161**

Table 8.2 Capital equipment costs for R404A refrigeration system

Component	Model	Cost	Number	Total Cost
Compressors				
MT Compressor	4FC 3.2Y	1977	3	5931
MT Compressor	4FC 5.F1Y	2999	1	2999
LP Compressor (on Condensing unit)	ZF 13	1142	1	1142
LP Compressor (on Condensing unit)	ZF 15	1202	1	1202
LP Compressor (on Condensing unit)	CMP 34	375	1	375
Includes: Crankcase heater, oil switch, protection, HP/LP switch				
Frame				
Pack System		7125	1	7125
LP Condensing units		1009.5	1	1009.5
Includes frame, oil system, safety valves, pressure valves, ball valves, accumulators, filters, housing				
Condenser / gas cooler				
Pack system - Includes EC fans		4500	1	4500
LP Condensing units		1010	1	1010
Controls				
Compressor Controllers	AK-PC-740	1732	1	1732
Pressure transducers		171	3	513
Temperature Transducers		140	3	420
Electrical panel		3000	1	3000
Back up controller		700	1	700
LT condensing units controls		1010	1	1010
Total Cost				**32669**

8.3 Installation costs

The installation costs of a refrigeration system consist of the material costs of installing the distribution pipe work and inline components which connect the central refrigeration system to the refrigerated cabinets. The installation costs also include labour costs. The high volumetric capacity of CO_2 results in a reduction in pipe sizes. Table 8.3 shows the reduction in the liquid and suction pipe size selection for the CO_2 booster system and the R404A system MT refrigeration system. The reduced

sizes will reduce the cost of the copper pipe work but only by approximately £10.34 per meter of combined suction and discharge line. Other mechanical valves such as ball valves, expansion valves and safety valves will also be cheaper due to reduced sizes. On larger systems this would help to reduce the overall cost of the CO_2 installation but the small supermarket systems have a small number of valves so the savings would be minimal.

Table 8.3 Comparison of copper pipe sizes for common liquid and suction lines of CO_2 booster system and MT R404A system, 25m Suction and Liquid lines

		R404A	CO_2
Suction line	Size	41.28mm, 1 5/8”	28.58mm, 1 1/8”
	Temperature drop	0.2°C	0.2°C
	Velocity	11.9 m/s	7.4 m/s
	Cost per meter	£20.40	£13.83
Liquid Line	Size	22mm, 7/8”	0.15mm, 5/8”
	Velocity	0.6 m/s	1.1 m/s
	Cost per m	£8.07	£4.30

The researchers also reported increased labour costs for CO_2 systems compared to R404A systems (Girrotto, 2004; Emerson, 2010). From the practical knowledge gained from the building of the experimental system during this research, actual labour to install the systems will be comparable. Any additional costs due to installation labour for the CO_2 system will be due to the training costs of engineers on how to work with CO_2. Additional training will be required on the charging procedures of CO_2 and safety aspects when installing and maintaining.

Table 8.4 shows a cost refrigerant comparison of the cost of R404A and CO_2. Assuming a 15% refrigerant leakage rate for the supermarket studied in the TEWI analysis, section 7.9.1, over a 10 year life cycle, the cost of the replacement 90 kg of R404A refrigerant would be £1368.00. The replacement cost of refrigerant for the CO_2 system would be £381, a £987 saving over 10 years of operation.

Table 8.4 Comparison refrigerant costs

	R404A	CO_2
Refrigerant Cost per Kg	15.20	4.24

8.4 Running costs

Using an average electricity price of 14p per kWh of electricity in Northern Ireland, Table 8.3 shows the annual operational costs for the R404A and CO_2 refrigeration systems, researched in section 7.2.4 and 7.31. The electricity used by the compressors is only considered because the energy consumed by the other refrigeration components such as fans and lights are assumed to be the same.

Table 8.5 Small supermarket refrigeration compressor system electricity costs

	R404A	CO_2
Annual electricity consumption (kWh)	103,540	103,941
Annual electricity cost (£)	£14,495.60	£14,551.74

8.5 Discussion and summary

This economic study has showed that a CO_2 booster refrigeration system for MT capacity of 46 kW and LT capacity of 6 kW has a capital cost 63% more than a typical R404A system used in small supermarkets. The CO_2 high pressure compressors make up most of the 24% of the additional cost. Compressor manufacturers do expect these costs to decrease with an increase in production volume (Pisano, 2010). The additional valves on the CO_2 system are unavoidable due to the transcritical operation and it is not expected that these costs would reduce that much with larger production volumes. The installation costs of both systems will be similar apart from any engineer training required for CO_2 systems. The refrigerant costs for the CO_2 system are lower and won't be as susceptible to market price fluctuations. Energy costs for the CO_2 system are similar to the R404A system. The high capital cost of the CO_2 solution for small supermarkets presented in this thesis

will act as a barrier to the uptake of the technology. Without a significant saving in operating costs it will be difficult to convince small retailers to invest in a CO_2 booster system on its TEWI alone.

Denmark has banned the use of HFCs in new systems over 10 kg and placed a Tax on use of HFCs, as discussed in section 2.7. This would add an additional cost of approximately £44 per kg of R404A, which would add premium of £3960 due to leakage over a 10 year life cycle in an existing R404A system. These tax savings have worked in Denmark in assisting the uptake of CO_2 refrigeration technology. A similar 'Green' Tax could help with the growth of CO_2 systems in small supermarkets in the UK and save considerable direct emissions due to the high GWP of R404A.

Chapter 9 Conclusions and further work

9.1 Conclusions

Existing HFCs leaked from supermarket refrigeration systems have a detrimental effect on the environment due to their high GWP. This research contributes to the overall aim of reducing this environmental impact by investigating the practicality, economic viability and environmental benefits achievable from the application of the low GWP refrigerant CO_2, to small supermarket refrigeration systems. To investigate this, this research has developed numerical models which have been experimentally validated and used to replicate the operational parameters of a real system and used to calculate and analyse the refrigeration systems energy performance.

Main conclusions

1. This research had shown that the annual energy consumption of a CO_2 booster refrigeration system applied to a small supermarket located in Northern Ireland would be equivalent to that of a traditional R404A refrigeration system. The CO_2 booster system would reduce the environmental impact of the small supermarket due to direct and indirect CO_2 emissions by 363 tCO_2 over a 10 year lifecycle.

2. The efficiency of a CO_2 booster system was found to be dependent on the ambient temperature. The system was proved to be more efficient than a R404A system at temperatures below 13°C. The booster system would therefore operate most efficiently at locations in the UK with ambient temperatures below 13°C for a high proportion of the year.

3. The efficiency of the CO_2 booster system was also discovered to be dependant of the ratio of MT and LT refrigeration loads. The lower the ratio

of MT to LT refrigeration loads in the supermarket, the more efficient the CO_2 booster system when compared to a R404A system of equal capacity. Lowering the MT:LT ratio to 1:1 made the CO_2 booster system 16% more efficient than the R404A system.

4. The dependency of the efficiency of the CO_2 booster system on ambient temperature and refrigeration load ratios meant that the power consumption would vary at different locations around the UK. By simulating a range of different refrigeration ratios at each location, maximum CO_2 booster efficiency ratios were created. CO_2 booster systems designed for each location using these ratios would equal the performance of a R404A system but have a significant reduction in direct CO_2 emissions. If ratios lower than the maximum ratios were used, the CO_2 booster system would outperform a R404A system. These ratios can be used by supermarket operators when developing strategies in the eventual phase-out of HFC refrigerants.

5. It was found that CO_2 has a greater heat transfer performance than R404A. This resulted in a much lower temperature differential between the condensing/gas cooling temperature and the ambient temperature than for a R404A refrigeration system. This increased the efficiency of the CO_2 system by lowering the compression ratio.

6. The performance of the CO_2 system was affected by heat transfer from the surroundings. An insulated receiver should be specified on all CO_2 booster system receivers and high levels of pipework insulation should be specified for all CO_2 refrigeration systems to reduce the high rate of heat transfer and enable CO_2 refrigeration systems to operate as efficiently as possible.

7. By comparing the capital and installation costs of the CO_2 with that of an equivalent HFC system it has been found that the cost of the CO_2 system would be over 60% higher than that of a R404A system. This cost premium could be prohibitive for the widespread application of CO_2 systems to small supermarkets despite of the significant environmental advantages over R404A systems.

9.2 Further work

This research has developed numerical models of a CO_2 booster refrigeration system which have been verified using test data from and experimental test rig. The models have been used to investigate the impact of weather conditions and refrigeration loads on the performance of the CO_2 booster system and comparisons have been made against the performance of a traditional R404A refrigeration system in a small supermarket. This research has also highlighted areas of further work which are discussed in this section.

The numerical model of the evaporator developed in this thesis has highlighted that by redesigning a supermarket refrigerated cabinet evaporator coil specifically for CO_2, would lead to an increase in evaporator capacity or a decrease in the size of coil required for a specific capacity. Since the publication of this research (Shilliday and Tassou, 2010) other researchers (Suamir and Tassou, 2011; Ge and Tassou, 2012) have highlighted that this redesign enables the evaporation temperature of the coil to be raised from -10.0°C to -5.5°C, while maintaining constant cooling capacity. This would decrease the work input required by the compressor and decrease the energy consumed by the refrigeration system. Further numerical modelling and testing of the CO_2 booster system is required to validate the energy savings achievable by the increase in evaporation temperature.

The high rate of heat transferred from the ambient to the LP compressor suction line decreased the performance of the compressor and overall system. Further research is required to establish optimum insulation levels to the piping between components to minimize heat transfer to and from the ambient and between components to increase system performance. More detailed simulation of the individual components of the system will enable greater insight of the effect of individual component geometric parameters and performance characteristics on system performance.

A decrease in the annual electricity consumption of a small supermarket CO_2 booster system by the successful implementation of any of the further research areas detailed above will not alone be enough to increase the attractiveness of these systems to potential users. The main barrier to the widespread application of CO_2 booster

systems in small supermarkets is the high cost of the capital equipment compared to that of a traditional HFC system. More research into individual system component design and control should lead to cheaper and more efficiency components in the future.

References

Aidoun, Z. and Ouzzane, M. (2009) 'A model application to study circuiting and operation in CO2 refrigeration coils', *Applied Thermal Engineering,* 29 pp. 2544-2553.

Arthur, B. (2011) *Marks and Spencer's PLAN A and experience with alternative refrigerants,* Atmosphere Europe 2011 Conference Brussels. Available at: http://www.atmo.org/media.presentation.php?id=82 [Accessed: 7th February 2012]

Austin-Davies, J. and Da Ros, S. (2006) 'Transcritical CO2 Systems: A Case Study Into The Latest Evolution', *Cooling with Carbon Dioxide Conference – Harnessing the potential of CO_2 for mainstream cooling, London WC1, 17th January 2006,* RAC – Refrigeration and air conditioning magazine.

Bansal, P.K. and Jain, S. (2007) 'Cascade systems: Past Present and Future', *ASHRAE Transactions,* 113, pp. 245-252.

Baxter, V.D. (2003) *IEA Annex 26: Advanced Supermarket Refrigeration/Heat Recovery Systems. Final Report Volume 1 – Executive Summary*, Oak Ridge National Laboratory. Available at: http://www.ornl.gov/~webworks/cppr/y2003/rpt/117000.pdf [Accessed 5th October 2007].

Bell, K.J. and Mueller, A.C. (2001) *Wolverine Engineering Data Book II,* Wolverine Tube, Inc. Available at: http://www.wlv.com/products/databook/db3/DataBookIII.pdf [Accessed 7th March 2009].

Bitzer (2011) *Bitzer Software 5.3.2.* Available at: https://www.bitzer.de/eng/productservice/software/1 [Accessed 7th March 2011].

Bitzer (2012) *Bitzer piston compressors: Semi-hermetic reciprocating compressors* Available at: http://bitzer.de/eng/productservice/p2/1 [Accessed 15th April 2012].

BRA (2006) *Guideline Methods of Calculating TEWI,* Issue 2. British Refrigeration Association, Reading, Berks, UK, 36 pgs.

Brouwers, C. And Serwas. L. (2011) *Carrier CO2OLtec. The ultimate CO_2 refrigeraetion system for every food retail store format. Market developments for CO_2 in commercial refrigeration,* Atmosphere Europe 2011 Conference Brussels. Available at: http://www.r744.com/web/assets/paper/file/pdf_791.pdf, [Accessed: 7th February 2012]

BSI (2002) *BS EN 13480-1:2002 +A2:2008 Metallic industrial piping. Part 1: General*. London: British Standards Institute.

BSI (2005) *BS EN ISO 23953-2:2005 Refrigerated display cabinets. Part 2: Classification, requirements and test conditions*. London: British Standards Institute.

BSI (2006) *BS EN 14276-1:2006 Pressure equipment for refrigerating system and heat pumps. Part 1: Vessels – General requirements.* London: British Standards Institute.

BSI (2009) *BS EN 378-2:2005+A1:2009 Refrigerating systems and heat pumps – Safety and environmental requirements. Part 2: Design, construction, testing, marking and documentation*. London: British Standards Institute.

BSI (2010) *BS EN 378-1:2008 + A1:2010 Refrigerating systems and heat pumps - Safety and environmental requirements. Part 1: Basic requirements, definitions, classification and selection criteria*. London: British Standards Institute.

Campbell, A., Missenden, J.F., Maidment, G.G. (2007) 'Carbon Dioxide for Supermarkets', *Proceedings of the Institute of Refrigeration*, London: 5th April 2007.

Carbon Trust (2010) *Retail Refrigeration Sector NI: Energy & Carbon Reduction Opportunities in the Retail Refrigeration Sector in Northern Ireland,* Available at: http://www.carbontrust.co.uk/events/events-resources/Documents/2010-09-refrig-external-slide-pack.pdf [Accessed 3rd March 2011].

Carbon Trust (2011) *Carbon Trust Conversion factors: Energy and carbon conversions 2011 update,* Available at: http://www.carbontrust.com/media/18259/ctl153_conversion_factors.pdf [Accessed 13th October 2012].

Direct industry (2012) *Heatcraft Europe,* Available at: http://www.directindustry.com/prod/heatcraft-europe-friga-bohn-hk-refrigeration/air-cooled-condensers-8259-394029.html, [Accessed: 7th March 2012]

Haff, S., Heinbokel, B. and Gernemann, A. (2005) *First CO_2 Refrigeration System for Medium and Low-Temperature Refrigeration at Swiss Megastore,* KK Die Kalte & Klimatechnik, 2, Available at: http://www.linde-kaeltetechnik.de/uploads/media/CO2_Sonderdruck_deutsch.pdf [Accessed 9th May 2008]

Cengel, Y.A. and Boles, M.A. (2002) *Thermodynamics: An engineering approach*. Fourth Edition. New York: McGraw-Hill

Centauro (2012) *Condensadores* Available at: http://www.centauro.pt/ [Accessed 15th April 2012].

Chen, Y. and Gu, J. (2005) 'The optimum high pressure for CO2 transcritical refrigeration systems with internal heat exchangers', *International Journal of Refrigeration,* 28 (8) pp. 1238-1249.

Cheng, L., Ribatski, G., Wojtan, L. and Thome, J.R. (2006) ' New flow boiling heat transfer model and flow pattern map for carbon dioxide evaporating inside horizontal tubes', *International Journal of Heat and Mass Transfer*, 49(21-22) pp. 4082-4094.

Cheng, L., Ribatski, G. and Thome, J.R. (2008) 'New prediction methods for CO2 evaporation inside tubes: Part II—An updated general flow boiling heat transfer model based on flow patterns', *International Journal of Heat and Mass Transfer,* 51 (1-2) pp. 125-135.

Cho, J.M. and Kim, M.S. (2007) 'Experimental studies on the evaporative heat transfer and pressure drop of CO2 in smooth and micro-fin tubes of the diameters of 5 and 9.52 mm', *International Journal of Refrigeration,* 30 (6) pp. 986-994.

Choi, K., Pamitran, A.S., Oh, C. and Oh, J. (2007) 'Boiling heat transfer of R-22, R-134a, and CO2 in horizontal smooth minichannels', *International Journal of Refrigeration*, 30, (8) pp. 1336-1346.

Christensen, K. and Bertilsen, P. (2004) *Refrigeration systems in supermarkets with propane and CO2 - Energy consumption and economy*. Available at: http://www.r744.com/knowledge/papersView/21 [Accessed 9th March 2008].

Colombo, I., Johal, P., Jordan, L., Chaer, I., Missanden, J.F., and Maidment, G.G. (2011) *Carbon dioxide refrigeration with heat recovery for retail applications*. Proceedings of the Institute of Refrigeration. London 3rd March 2011.

Copeland (2011), *Copeland Select V. 7.5.* Available at: http://www.emersonclimate.com/europe/en-eu/resources/software_tools/Pages/product_selection_software.aspx [Accessed 7th March 2011].

Cowan, D., Gartshore, J., Chear, I., Francis, C. and Maidment, G. (2009) *Real Zero - Reducing refrigerant emissions & leakage*, Proceedings of the Institute of Refrigeration, 7 (1).

Danfoss (2003) *CO_2 is keeping supermarkets cool*. Available at: ww.ra.danfoss.com/TechnicalInfo/Approvals/Files/RAPIDFiles/01/Article/CO2Supe/CO2_superm.pdf [Accessed 10th August 2009]

Danfoss (2008) *Transcritical CO_2 system in a small supermarket.* Available at: http://www.danfoss.com/NewsAndEvents/Archive/Refrigeration+News/2008/Transcritical-CO2-System-in-a-Small-Supermarket/60BF7B78-2E17-4800-B163-F43298D51CDF.html [Accessed 10th August 2009]

Danfoss (2011a) *Technical brochure. Electronically operated valves for CO_2 type AKVH 10.* Available at: http://www.danfoss.com/Products/Categories/Group/RA/Electronically-Operated-Valves/AKVH-Expansion-Valves-for-high-pressure-refrigerants/ef2b92e1-f4d3-4c0c-849d-adc36b242240.html. [Accessed: 12th February 2012]

Danfoss (2011b) *Save energy in your supermarket with a CO_2 refrigeration system. Benchmarking energy optimised HFC stores with transcritical CO_2 booster systems*.

Available at:
http://www.danfoss.com/BusinessAreas/RefrigerationAndAirConditioning/Articles/Save+Energy+in+your+Supermarket+with+a+CO2+Refrigeration+System.htm. [Accessed: 12th February 2012]

Danish Environmental Protection Agency (2002) *Statutory Order no. 552 of 2 July 2002 Regulating Certain Industrial Greenhouse Gases.* Available at: http://www.mst.dk/NR/rdonlyres/4D9C695D-771F-4541-B19E-6AED27057FF2/0/StatutoryOrderno552of2July2002RegulatingCertainIndustrialGreenhouseGases.pdf [Accessed: 10th March 2012].

De Ono, A. (2008) *Transcritical CO_2 (R744) Supermarket Refrigeration in Australia. By the Australian Green Cooling Council,* International meeting on HCFC phase out, European Commission: Montreal, 5-6th April 2008

DECC (2012) *Statistical Release. 2011 UK greenhouse gas emissions, provisional figures and 2010 UK greenhouse gas emissions, final figures by fuel type and end user.* Available at: http://www.decc.gov.uk/en/content/cms/statistics/climate_stats/gg_emissions/uk_emissions/uk_emissions.aspx [Accessed: 15th July 2012]

Defra (2007) *EC Regulation No 842/2006 on certain fluorinated greenhouse gases: Supplementary Guidance for stationary refrigeration air-conditioning and heat pump user*s.

Dossat, R.J. (1996) *Principles of refrigeration*. 5th Edition. Pearson. Ohio: Prentice Hall

EIA (2011) *Chilling Facts III. Supermarkets are reducing the climate change impact of refrigeration*
Available at: http://chillingfacts.org.uk/uploads/chillingfacts3.pdf [Accessed: 12th July 2011].

Emerson (2010) *Refrigerant choices for commercial refrigeration. Finding the right balance*, Available at: http://www.emersonclimate.com/europe/Documents/Resources/Refrigerant_Report_PRINT.pdf [Accessed 14th April 2012]

Emerson (2012) *Scroll Outdoor Units Digital Modulation – R404A,* Available at: http://www.emersonclimate.com/europe/en-eu/Products/Condensing_Units/Scroll_Outdoor_Condensing_Units/EazyCool_Line_Up/Pages/default.aspx?what=list&prod_pic=5&prod=u&bra=1&fam=23&ref=5&Ar=MT&title=Scroll%20Outdoor%20Units%20Digital%20Modulation%20-%20R404A [Accessed 7th April 2012]

Ge, Y.T. and Tassou, S.A. (2011) 'Performance Evaluation and Optimal Design of Supermarket Refrigeration Systems with Supermarket Model "SuperSim", Part II: Model Applications', *International Journal of Refrigeration,* 34 (2) pp. 540-549.

Ge, Y.T. and Tassou, S.A. (2012) 'The impact of geometric structure and flow arrangement on the performance of CO_2 evaporators in multi-deck medium

temperature display cabinets', *International Journal of Refrigeration,* 32 pp. 124-149.

Getu, H.M. and Bansal, P.K. (2008) 'Thermodynamic analysis of an R744–R717 cascade refrigeration system', *International Journal of Refrigeration,* 31 (1) pp. 45-54.

Girotto, S., Minetto, S. and Neksa, P. (2004) 'Commercial refrigeration system using CO2 as the refrigerant', *International Journal of Refrigeration,* 27 (7) pp. 717-723.

Grey, D.L. and Webb, R.L.(1986) ' Heat transfer and friction correlations for plate finned tube heat exchangers having plain fins', *In Proceedings of Eighth International Heat transfer Conference, USA, San Francisco,* 2745-2750.

Hekkenberg, M. and Schoot Uiterkamp, A.J.M. (2007) 'Exploring policy strategies for mitigating HFC emissions from refrigeration and air conditioning', *International Journal of Greenhouse Gas Control,* 1 (3) pp. 298-308.

Hinde, D. (2009) 'Carbon Dioxide in North American Supermarkets', *ASHRAE Transactions,* 51 pp. 18-26.

Horuz, I., Kurem, E. and Yamankaradeniz, R. (1998) 'Experimental and theoretical performance analysis of air-cooled plate-finned-tube evaporators', *International Communications in Heat and Mass Transfer,* 25(6) pp. 787-798.

Hubbard (2012) *HZS Hubbard Zenith Scroll Packaged Condensing Units* Available at: http://www.hubbard.co.uk/commercial/hzs-zenith-scroll.php [Accessed: 7th April 2012]

Hundy, G.F., Trott, A. R., Velch, T. (2008) Refrigeration and Air-Conditioning. Fourth edition, Oxford: Elsever Ltd.

Kakac, S. and Liu, H. (2002) *Heat exchangers: Selection, rating and thermal design.* Second edition. Florida: CRC Press

Kauf, F. (1999) 'Determination of the optimum high pressure for transcritical CO2-refrigeration cycles', *International Journal of Thermal Sciences,* 38 (4) pp. 325-330.

Kim, M. and Bullard, C.W. (2001) 'Development of a micro channel evaporator model for a CO2 air-conditioning system' *Energy,* 26(10) pp. 931-948.

Kim, M., Pettersen, J. and Bullard, C.W. (2004) 'Fundamental process and system design issues in CO2 vapour compression systems', *Progress in Energy and Combustion Science,* 30 (2) pp. 119-174.

Kim, Y. and Kim, Y. (2005) 'Heat transfer characteristics of flat plate finned-tube heat exchangers with large fin pitch' *International Journal of Refrigeration,* 28(6) pp. 851-858.

Klein, S.A. and Alvardo, F.L.E. (2002) *EES - Engineering Equation Solve*r, F-Chart Software LLC, Available at: http://www.fchart.com/ees/

Lacros and Enviros (2007) *UK Implementation of fluorinated gases and ozone depleting substances regulations. Market intelligence and risk-bases Implementation model,* DEFRA. Available at: http://archive.defra.gov.uk/environment/quality/air/fgas/documents/fgas-report-1107.pdf [Accessed: 20th June 2008]

Lee, T., Liu, C. and Chen, T. (2006/11) 'Thermodynamic analysis of optimal condensing temperature of cascade-condenser in CO_2/NH_3 cascade refrigeration systems', *International Journal of Refrigeration,* (29) 7 pp.1100-1108.

Lorentzen, G. (1994) 'Revival of carbon dioxide as a refrigerant', *International Journal of Refrigeration,* 17 (5) pp.292-301.

Lorentzen, G. and Pettersen, J. (1993) 'A new, efficient and environmentally benign system for car air-conditioning', *International Journal of Refrigeration,* 16 (1) pp. 4-12.

Madsen, K.B. (2007) *An International View of Progress in CO_2 cooling. Cooling with Carbon Dioxide Conference – Harnessing the potential of CO_2 for mainstream cooling, London WC1, 17th January 2006,* RAC – Refrigeration and air conditioning magazine.

Menon, E.S. (2004) *Piping calculations manual*. McGraw Hill

Met Office (2012) *Northern Ireland Climate.* Available at: http://www.metoffice.gov.uk/climate/uk/ni/print.html [Accessed: 20th February 2012]

Midgley, T.J. and Henne, A.L. (1930) 'Organic fluorides as refrigerants', *Industrial and engineering Chemistry,* 22 pp. 542-545.

Milnes, J. (2011*) Tesco suffers second CO_2 blast*. Available at: http://www.racplus.com/news/tesco-suffers-second-co2-blast/8609639.article [Accessed: 9th March 2012]

Milnes, J. (2010*) Explosion reported at Tesco store*. Available at: http://www.racplus.com/news/explosion-reported-at-tesco-store/8609112.article [Accessed: 9th March 2012]

McQuiston, F.C. (1978) Correlation of heat mass and momentum transport coefficients for plate-fin-tube heat transfer, *ASHRAE Transactions,* 84 (1) pp.294-308.

Molina, M.J. and Rowland, F.S. (1974) 'Stratospheric sink for chlorofluoromethanes: Chlorine atom catalysed destruction of Ozone', *Nature,* 249 pp.810-812.

Müller-Steinhagen, H. and Heck, K. (1986) 'A simple friction pressure drop correlation for two-phase flow in pipes', *Chemical Engineering and Processing: Process Intensification,* 20 (6) pp. 297-308.

New Zealand Fire Service (2008) *Inquiry into the explosion and fire at the icepak coldstores, Tamaherem on 5th April 200*8. Available at: http://www.fire.org.nz/Media/News/2008/Documents/ca44cf33fe580cebba4ab6a7648e75c0.pdf [Accessed: 7th October 2010]

Ould Didi, M.B., Kattan, N. and Thome, J.R. (2002) 'Prediction of two-phase pressure gradients of refrigerants in horizontal tubes', *International Journal of Refrigeration,* 25 (7) pp. 935-947.

Pearson, A. (2004) 'Carbon Dioxide – New uses for an old refrigerant, *International Journal of Refrigeration,* 28 (8) pp. 1140-1148.

Pearson, S.F. (1993) Development of Improved secondary refrigerants, *The Proceedings of the Institute of Refrigeration,* IIR:72-77.

Pettersen, J., Hafner, A., Skaugen, G. and Rekstad, H. (1998) 'Development of compact heat exchangers for CO2 air-conditioning systems' *International Journal of Refrigeration,* 21 (3) pp.180-193.

Pisano, G. (2010) The compressor role in the Roadmap to viable CO_2 refrigeration equipment, Atmosphere Europe 2010 Conference. Available at: http://www.r744.com/web/assets/paper/file/pdf_698.pdf [Accessed: 7th February 2012]

Proklima International (2008) *Natural refrigerants.* Sustainable ozone and climate friendly alternatives, Frankfurt: German Federal Ministry for Economic Cooperation and Development

R744.com (2009*) Swedish ministry issues HFC tax proposa*l. Available at: http://www.r744.com/articles/2009-07-14-swedish-ministry-issues-hfc-tax-proposal.php [Accessed: October 9th 2010]

R744.com (2012*) Sainsbury's opens its 100th CO_2-equipped store*. Available at: http://www.r744.com/news/view/1614 [Accessed: March 4th 2012]

RDM (2012a) *PRO 600 Pack controller* Available at: http://www.resourcedm.com/docs/Intuitive%20&%20Plant%20Pack%20Controller%20User%20Guide%20V2.9A.pdf [Accessed: 7th April 2012]

RDM (2012b) *RDM Data manager* Available at: http://www.resourcedm.com/ProductDataSheet.aspx?pfid=2&cid=3 [Accessed: 7th April 2012]

Riffat, S.B., Afonso, C.F., Oliveira, A.C. and Reay, D.A. (1997) 'Natural refrigerants for refrigeration and air-conditioning systems', *Applied Thermal Engineering,* 17 (1) pp. 33-42.

Sawalha, S. (2008) 'Theoretical evaluation of trans-critical CO2 systems in supermarket refrigeration. Part I: Modelling, simulation and optimization of two system solutions', *International Journal of Refrigeration,* 31 (3) pp. 516-524.

Shecco (2012) *Guide Shecco Publications. 2012 Natural refrigerants market growth for Europe,* Available at: http://guide.shecco.com/ [Accessed: 2nd March 2012].

Shecco (2009) *shecco Marketing Report. CO_2 Commercial Refrigeration. The Eurpoean Market 2009*
Available at: http://www.shecco.com/files/news/marketing-reportfinal-small.pdf [Accessed: 2nd March 2012].

Shilliday, J.A., Tassou, S.A., (2010) 'Numerical analysis of a fin and tube evaporator using the natural refrigerant CO_2', *1st IIR Conference on sustainability and the cold chain*, Cambridge, UK, March 2010.

Silva, A., Almeida, E. and Bandarra Filho, E.P. (2010) 'Energy Efficiency Comparison of the CO2 Cascade and the R404A and R22 Conventional System for Supermarkets', *9th IIR Gustav Lorentzen Conference 2010, Sydney, Australia.*

Socomec (2012) Socomec Diris A20 Available at:
http://www.socomec.com/presentation-diris-a20_en.html [Accessed: 7th April 2012]

Srinivasan, K., Sheahen, P. and Sarathy, C.S.P. (2010) 'Optimum thermodynamic conditions for upper pressure limits of transcritical carbon dioxide refrigeration cycle', *International Journal of Refrigeration,* 33 (7) pp. 1395-1401.

Suamir, IN., Tassou, S.A., (2011) 'Modelling and performance analyses of CO_2 evaporator coils for chilled and frozen food diaplay cabinets in supermarket applications, *ICR*, Prague, Czech Republic, August 2011.

Tahir, A. and Bansal, P.K. (2005) 'MEPR versus EEPR valves in open supermarket refrigerated display cabinets', *Applied Thermal Engineering,* 25 (2-3) pp. 191-203.

Tassou, S.A., Ge, Y., Hadawey, A. and Marriott, D. (2011) 'Energy consumption and conservation in food retailing', *Applied Thermal Engineering,* 31 (2-3) pp. 147-156.

Tassou, S.A., Lewis, J.S., Ge, Y.T., Hadawey, A. and Chaer, I. (2010) 'A review of emerging technologies for food refrigeration applications', *Applied Thermal Engineering,* 30 (4) pp. 263-276.

Thevenot, R. (1979) *A History of refrigeration throughout the world,* International Institute of Refrigeration.

Thome, J.R. (2010) Engineering Data Book III. Wolverine Tube, Inc. Available at: http://www.wlv.com/products/databook/db3/DataBookIII.pdf [7 March 2009]

UNEP (1987) *The Montreal Protocol on Substances that Deplete the Ozone Layer: Final Act*

Walravens, F. and Hailes, J. (2010) *Chilling Facts II. The supermarket refrigeration scandal continues*
Available at: http://chillingfacts.org.uk/uploads/chillingfacts2.pdf [Accessed: 7th March 2010].

Walravens, F. and Hailes, J. (2009) *Chilling Facts: The big supermarket refrigeration scandal*
Available at: http://www.chillingfacts.org.uk/uploads/chillingfacts.pdf [Accessed: 12th November 2009].

Wang, C., Tao, W. and Chang, C. (1999) 'An investigation of the airside performance of the slit fin-and-tube heat exchangers', *International Journal of Refrigeration*, 22 (8) pp.595-603.

Wang, C., Lin, Y. and Lee, C. (2000) 'Heat and momentum transfer for compact louvered fin-and-tube heat exchangers in wet conditions', *International Journal of Heat and Mass Transfer*, 43 (18) pp. 3443-3452.

Yoon, S.H., Cho, E.S., Hwang, Y.W., Kim, M.S., Min, K. and Kim, Y. (2004) 'Characteristics of evaporative heat transfer and pressure drop of carbon dioxide and correlation development', *International Journal of Refrigeration*, 27 (2) pp.111-119.

Yun, R., Kim, Y. and Park, C. (2007) 'Numerical analysis on a micro channel evaporator designed for CO2 air-conditioning systems'. *Applied Thermal Engineering*, 27(8-9) pp.1320-1326.

Zhang, X.P., Fan, X.W., Wang, F.K. and Shen, H.G. (2010) 'Theoretical and experimental studies on optimum heat rejection pressure for a CO2 heat pump system', *Applied Thermal Engineering*, 30 (16) pp.2537-2544.